POWER FREQUENCY AND TRANSIENT PERFORMANCE OF VERY LONG MULTICONDUCTOR TRANSMISSION LINES.

A Thesis Submitted

to

THE VICTORIA UNIVERSITY OF MANCHESTER

for

THE DEGREE OF DOCTOR OF PHILOSOPHY

by

SULEIMAN EL TAYEB MOHAMED

Power Systems Centre

University of Manchester Institute of Science and Technology

Manchester

JULY 1968

ABOUT THE CANDIDATE.

He graduated from the University of Khartoum - Sudan, in April 1964 with B.Sc. (Eng.), First Class Honours. He was then selected to the post of demonstrator in the Department of Electrical Engineering and continued in this post till December of the same year, when he was granted a scholarship to carry out post-graduate studies in the U.K. at the University of Manchester Institute of Science and Technology Power Systems Centre.

He registered for the degree of Master of Science in January 1965 and carried out work on a project, the results of which were successfully presented in January 1966 in a thesis for the M.Sc. degree.

In April 1966 he started work on the present Ph.D. research project, the findings of which are reported in this thesis.

The candidate is joint author of the following papers:

1. "A negative Impedance Unit for Direct Analogue a.c. Network Analysers," Int.J.Elect.Eng.Educ., No. 2, April 1966, p. 249.
2. "Impedances seen by Distance Relays for Faults on Very Long Lines," Inst.Elect.Engrs, Publication on Present-day Protection Problems, May 1968, p. 208.

SUMMARY.

In countries where economic remote sources of power are available, long distance transmission is always a possibility. At present and possibly for several years to come the case for HVAC as a preferable form of transmission in many situations, as opposed to HVDC, is regarded strong enough. This consideration has formed a reasonable justification for conducting the present work on properties of high voltage a.c. transmission lines with special emphasis on some of the longer lines basic operational problems.

The work presented in this thesis is introduced in chapter one and is clearly shown to cover two major areas. In the first part of the thesis some steady-state properties of long distance lines are examined in the light of the theory of natural modes put forward by WEDEPOHL; this theory is adequately explained in chapter two. In the second, comprehensive analysis to the problem of propagation of switching surges in multiconductor lines is widely covered. System studies are carried out on Atlas Digital Computer.

Distance protection characteristics of long multiconductor lines are dealt with in chapters three and four where the method of analysis and computational results are presented. The work on distance protection is preceded by essential fundamental studies on the performance of faulted long multi-conductor lines where apparent impedance loci properties "seen" on these lines are taken as criterion. In this respect system peculiarities have been revealed; in particular that power frequency resonance phenomenon occurs at an eigth wavelength instead of a quarter wavelength as predicted by classical smooth line theory, and that classical impedance loci are only approached for balanced type faults. Protection characteristics presented have pointed out to the need for a change in the philosophy of popular distance protection schemes to cope with long line problems.

The limitations set on the power capability by line lengths has long been recognized and the problem of capacitive generation of the longer line is not unknown. In the present investigation a fresh approach to the problem of reactive compensation has been introduced; this approach has recognized the asymmetrical nature of the conductors of non-transposed lines and as such has formed a solid basis for a better understanding on the performance of long untransposed lines in relation to series and shunt compensation. The restriction placed on the maximum possible degree of series compensation due to the unbalanced nature of the phases is clearly defined. These problems have formed the topic of chapter five.

The second part of the thesis has been concerned with the propagation properties of switching surges on multiconductor lines because the insulation

levels of these lines and their apparatus become directly related to these surges owing to the continued implementation of higher voltages. The review given in chapter six of past methods of approach to the solution of the transient problem has pointed out the major drawbacks of these methods and the need for a more thorough method of analysis is shown to be met by the method of modal analysis and Fourier transform technique.

In chapter seven, the theory of the modified Fourier transform technique put forward by MULLINEUX and others for numerical transient problems has been discussed and some practical limitations have been raised; these are connected primarily, on the one hand, with the limits of observation of the transient response and, on the other, with computational efficiencies. The reasons for these are given and a new theoretical method of approach to overcome the limitations is proposed. This is based on the analytical formulation of the frequency function and its tremendous scope in extending the limits of observation without impairing "rise time" together with improvement in computational efficiency is evinced. In this area it is pointed out that further work in applications problems is necessary.

In a recent paper the modified Fourier transform methods have been applied for the study of linear transient problems. The present work has discussed these problems; it has, however, extended the field of application of the transform technique to the analysis of non-linear problems, outstanding among which is the problem of sequential energisation of multiconductor lines. The theoretical basis of a new method to deal with non-linear problems is fully discussed in chapter eight.

Chapter nine is a systematic presentation of computational studies on the transient response of multiconductor lines. These studies have yielded very well to interpretations from the theory of natural modes, have shown close agreement with lattice diagram solutions and in general have been known and confirmed from field measurements. Over-voltages of long unloaded lines are reported and the effect of reactive compensation for their restriction is shown. Restriking voltage calculations are also dealt with. The studies of chapter nine are further extended in chapter ten for more practical systems where source and line trapped charge effects are dealt with in detail. Two methods of source representation are proposed and the merits of both methods in retaining the distributed nature of the source and in saving computational costs are demonstrated.

The thesis is finally concluded in chapter eleven where proposals for further investigations are given.

CONTENTS

	Page
CONTENTS	i
LIST OF SYMBOLS	vi
1. INTRODUCTION	1
2. PRESENTATION OF THE BASIC METHOD OF ANALYSIS	14
2.1 Introduction	14
2.2 Multiconductor Line Wave Equations	15
2.2.1 Derivation of Equations	15
2.2.2 Eigenvalues and Eigenvectors	18
2.2.3 Solution of Wave-Equations	20
2.3 Boundary Conditions	24
2.4 Basic System Parameters	27
2.4.1 Series Impedance Matrix	28
2.4.2 Shunt Admittance Matrix	29
2.4.3 Elimination of Earth Wires	29
2.4.4 Computation of System Parameters	30
2.5 General Consideration	30
3. APPARENT IMPEDANCES SEEN BY DISTANCE RELAYS ON VERY LONG UNTRANSPOSED LINES	31
3.1 Introduction	31
3.2 Method of Analysis	33
3.2.1 Nodal Analysis Method	33
3.2.2 Fault Simulation	34
3.2.3 Boundary Conditions	36
3.2.4 Mathematical Models for Fault Calculations	37
3.2.4.1 Single-Ended System	37
3.2.4.2 Double-Ended System	41
3.3 Considerations on Application of Distance Protection to Long Multi-conductor Lines	42
3.3.1 General	42
3.3.2 Characteristics of Distance Relays	42
3.3.3 Relaying Quantities and Principles of Sound-Phase and Residual Compensation	44
3.3.4 Distance Protection Applied to Long Lines	46
4. COMPUTATIONAL RESULTS OF IMPEDANCE LOCI AND APPARENT IMPEDANCES SEEN BY DISTANCE RELAYS ON VERY LONG LINES	47
4.1 Introduction	47
4.2 Description of Computer Program for Evaluation of Short-Circuit Impedance Loci	48
4.3 Lines for Studies	50
4.4 Results of Studies	51

4.4.1 Line Energised by Pure Modes 51
4.4.2 Line Energised from Balanced Three-Phase System 52
4.4.2.1 Three Phase-to-Ground Faults 52
4.4.2.2 Single Line-to-Ground Faults 53
4.4.2.3 Double Line-to-Ground Faults 54
4.4.2.4 Phase-to-Phase Faults 55
4.5 Compensated Impedances Seen by Distance Relays for Faults on Very Long Lines 57
4.5.1 General 57
4.5.2 Computer Program for Evaluation of Apparent Impedances Seen by Distance Relays 58
4.5.3 Three-phase-to-Earth Faults 60
4.5.3.1 200-mile Line 60
4.5.3.2 450-mile Line 60
4.5.3.3 800-mile Line 61
4.5.4 Single Line-to-Earth Faults 62
4.5.6 Line-to-Line Faults 62
4.5.7 Distance Protection of Long Loaded Lines 63
4.5.8 Effect of Fault Impedance 64
4.6 Discussion and Interpretation of Results 65
4.7 Conclusions 70

5. STEADY-STATE PERFORMANCE OF LONG UNTRANSPOSED LINES WITH REFERENCE TO REACTIVE COMPENSATION 72

5.1 Introduction 72
5.2 Method of Analysis 77
5.2.1 Objectives 77
5.2.2 Analysis for Basic Studies 78
5.2.2.1 Voltage Profiles and Reactive Power Requirements of Long Lines 78
5.2.2.2 Power Charts and Long Line Capabilities 82
5.2.3 Analysis for Series and Shunt Compensation 82
5.2.3.1 General 82
5.2.3.2 Series and Shunt Compensation for Untransposed Lines 85
5.2.3.3 Compensation for Transposed Line 87
5.2.4 Source Effects 87
5.3 Digital Computer Program 88
5.3.1 General Considerations 88
5.3.2 Description of Computer Program 88
5.4 Basic Long Line Properties 89
5.5 Effects of Series Compensation 92
5.6 Effect of Series and Shunt Compensation 96
5.6.1 Two Capacitor/reactor Stations 96
5.6.2 Three Capacitor/reactor Stations 97
5.7 Non-transposed Line Unbalance Studies 97
5.7.1 General 97
5.7.2 Horizontal and Vertical Line Unbalances 98
5.8 Conclusions 100

6. GENERAL SURVEY OF SOLUTION OF TRANSMISSION LINE SWITCHING TRANSIENTS 102

6.1 Introduction 102
6.2 Methods of Assessing Transmission Line Transient Performance 103
6.2.1 Transient Analysers 103
6.2.2 Field Tests 104
6.2.3 Analytical Methods of Study 106
6.2.3.1 Lattice Diagram Solution 107
6.2.3.2 Laplace Transform Methods 112
6.2.3.3 Modal Theory and Fourier Transform Method 114
6.3 General Considerations 116

7. APPLICATION OF THE THEORY OF MODAL PROPAGATION AND FOURIER TRANSFORM TECHNIQUE FOR THE ANALYSIS OF MULTICONDUCTOR LINE TRANSIENTS 115

7.1 Introduction 118
7.2 The Modified Fourier Inversion Integral 119
7.3 Physical Interpretation of the Fourier Transform Method 120
7.4 Gibbs Oscillations and the Sigma Factor 122
7.5 The Modified Fourier Transform 124
7.6 Practical Considerations 126
7.7 Analytical Formulation of the Fourier Inversion Integral 128
7.7.1 General 128
7.7.2 Theoretical Basis of the Method 129
7.7.3 Shift Constant 132
7.7.4 Application 133
7.8 Procedure for Numerical Evaluation of Transient Response 137

8. ANALYTICAL METHOD FOR OBTAINING TRANSIENT RESPONSE OF SYSTEMS WITH NON-ANALYTIC FORCING FUNCTIONS 140

8.1 Introduction 140
8.2 Physical Illustration 140
8.3 Digital Simulation of Non-Simultaneous Switching Operations 142
8.4 Fourier Transform of Numeric Functions 143
8.4.1 Criticism of Classical Approach 143
8.4.2 Piecewise Synthesis Approach 147
8.4.2.1 Theory 147
8.4.2.2 Fourier Coefficients Using the Concept of Complex Frequency 150
8.4.2.3 Examples on Synthesis Method 152
8.4.3 Applications of Synthesis Method 154

9. COMPUTATIONAL RESULTS OF TRANSIENT VOLTAGES ON MULTICONDUCTOR LINES 156

9.1 Introduction 156
9.2 Mathematical Models 157
9.3 Boundary Conditions 160
9.3.1 Simultaneous Pole Closure 160
9.3.2 First Pole Closure 161
9.3.3 General Sequential Pole Closure 161
9.4 Description of Digital Computer Programs 163
9.4.1 Simultaneous Energisation Program 164
9.4.2 Sequential Energisation Program 165
9.5 Line Data 167
9.6 Studies Relating to First Pole Closure of 120-mile Line 167
9.7 Studies Relating to First Pole Closure of 600-mile Line 172
9.7.1 Uncompensated Line 172
9.7.2 Compensated Line 173
9.8 Simultaneous Pole Closure Transients Study 174
9.9 Sequential Pole Closure Transients Study 174
9.10 Recovery Voltage Transients Calculations 177
9.10.1 General 177
9.10.2 Theoretical Developments 178
9.10.3 Mathematical Models 182
9.10.4 Digital Computer Program 183
9.10.5 Computational Results 184

10. SOURCE SIMULATION 186

10.1 Introduction 186
10.2 Method of Analysis 187
10.2.1 Simulation of Pole Closure 187
10.2.2 Source Representation by Lumped Parameters 190
10.2.3 Source Representation by Distributed Parameter Networks 192
10.2.3.1 Simplified Representation 193
10.2.3.2 Representation by Symmetrical Circuit 195
10.2.4 Proceudre for Calculation of Sequential Transients with Precharge 197
10.3 Description of Digital Computer Program 198
10.4 Computational Results 199
10.4.1 First Pole Closure Transients 200
10.4.1.1 Simplified Source Representation 200
10.4.1.2 Source Representation by Symmetrical Model 204
10.4.2 Sequential Transients with Precharge and Source Simulation 206
10.4.2.1 Comparative Study with Bewley Lattice Technique 206
10.4.2.2 Source and Line Trapped Charge Studies 208

11. CONCLUSIONS 212

11.1 General 212
11.2 Steady-State Long Line Response 214
11.3 Multiconductor Line Transient Response 218
11.4 Comment 224

APPENDIX 2. Formulation of Series Impedence and Shunt Admittance Matrixes 225

APPENDIX 3. Sound-Phase and Zero-Sequence Compensation Principles of Distance Protection 230

APPENDIX 7. Analytical Formulation of Time Response using Sine and Cosine Transforms 235

APPENDIX 9.1. Determination of Time for Circuit Interruption 238

APPENDIX 9.2. Fourier Transform of Injected Current for Restriking Transients Calculations 240

APPENDIX 9.3. Fourier Transform of Energising Voltages 242

APPENDIX 10. Eigenvalues and Eigenvectors of Symmetrical Circuit 243

APPENDIX 11. Procedure for Handling Resistance Switching and Lightning Arrester Operation 246

BIBLIOGRAPHY 251

ACKNOWLEDGEMENTS 256

LIST OF SYMBOLS

The following nomenclature defines the principal symbols generally used. There are instances where the symbol is used locally for a different quantity where it will be defined accordingly.

Z, Y = series impedance and shunt admittance matrixes per unit length

Z_0, Y_0 = characteristic impedance and characteristic admittance matrixes

Q, S = voltage and current eigenvector matrixes

λ = matrix eigenvalue of ZY

γ = diagonal propagation constant matrix

α, β = attenuation constant and phase shift factor

I_s, I_r = sending and receiving end current column vectors

V_s, V_r = high terminal side sending and receiving end voltage column vectors

Y_s = source admittance matrix

Y_f = fault admittance matrix

Z_s = apparent impedance seen by distance relay

Z_1, Z_0 = positive sequence and zero sequence impedance per unit length

ω = angular frequency

ω_0 = fundamental angular frequency

f_s = supply frequency

a = shift constant

$f(\omega)$ = Fourier transform of $f(t)$

$f(\omega - ja)$ = modified Fourier transform of $f(t)$

T_0 = observation time

t_0 = time step or time interval

N = number of harmonics used in transient analysis

W = truncation frequency

σ = sigma factor

$\bar{V}, \bar{I}$ = voltage and current transforms

v = instantaneous value of voltage

$\hat{V}$ = peak value of voltage

$Z_{\ell s}, Z_{ss}$ = line-side and source-side impedance matrixes

L_s = lumped source inductance

C_s = lumped capacitance at switching station bus-bar

ϕ_1, ϕ_2, ϕ_3 = phase angle displacements

τ = delay time

E_d = trapped charge voltage

ℓ_s = source infeed circuit length

ℓ = main circuit length

non-linearity: means that within a certain time interval f(t) can be represented as being piece-wise linear

CHAPTER ONE

INTRODUCTION

The transportation of remote sources of energy whether coal, oil or gas is a basic requirement for their utilization by centres of load. Rough estimates[1] have indicated that it is cheaper to transport some forms of energy like oil or gas through pipe line though in general the lack of means of energy transportation may provid a hindrance. The alternative is to produce electrical energy out of these various sources and then transmit over long distances; hence the need for long-distance transmission. The remoteness of economic hydro-sources in a country which may be coupled with lack of fuels in that country is also a good justification for the establishment of long-distance point-to-point transmission. The development of an energy source remote from the centres of load would therefore require an energy line to connect up with these centres of consumption. Studies carried out in the United States[2] have shown that the establishment of nuclear plants located near load centres will provide a sound alternative to the transmission of electrical energy generated hundreds of miles away from these centres. This will no doubt take some time before it can be put into practice and even then will be confined to countries which own and have enough experience with nuclear energy.

Although the need for long-distance transmission has long been recognized the problem of whether to use HVAC or HVDC has not yet been completely resolved. HVDC can yield considerable technical and economic advantages[3,4]

over its counterpart whenever long-distance transmission is considered; the absence of the need for costly compensating equipment or power flow control equipment make HVDC more favourable. But HVDC is not without its limitations. Although research work is in progress in many parts of the world to solve the problem of current interruption the lack of the HVDC circuit breaker may still be a fact for several years to come[5]. Tapping off at intermediate points along a high voltage a.c. power line is not a problem but the possibility of doing the same without the need for a costly converting station points out to the limitation of HVDC in this direction. Manufacturing and operating experience with HVDC systems are very limited. It was only in 1950 that results of research and development on an experimental d.c. cable system between Kashira hydro-electric power station and Moscow[6] were available, these provided the major experimental ground for the 294-mile Volgagrad - Donbass projected installation which was brought into full operation in 1964. Prior to this scheme the Gotland - Sweden HVDC cable system (1954) and the Cross - Channel link (1960) between the English and French Grid Systems were brought into service.

Although interest in D.C. transmission problems is growing very rapidly in some countries, the question arises as to what extent can HVDC be relied upon to form the basis on which future power systems are built in a country which has had no past experience either in development or operation of HVDC - assuming its limitations and drawbacks are ignored. The answer to this, no doubt, lies in the inevitable choice of a.c. long-distance transmission.

There are several points to be resolved regarding transmission over long distances by A.C. means. Whereas for HVDC the distance barrier is thought to be 2000 miles[7], in the case of a.c. as the line length approaches a quarter wavelength, about 930 miles at 50 Hz, Ferranti effect and line reactive power requirements increase very rapidly beyond any practical limit while its real power transfer ability is greatly enhanced. The quarter-wave point therefore sets the distance barrier of long-distance a.c. transmission.

In 1965, HUBERT and GENT[8] drew attention to the significance of long-distance transmission and proposed a scheme whereby extra-long-distance transmission (ELD) difficulties may be resolved. The scheme takes advantage of the stable performance of power lines whose electrical lengths lie in the region of 180 - 270 electrical degrees. It introduces a concept of tuned-circuit lines in which a physical power frequency quarter-wave-length line could be extended just beyond the half-wave power point where it will eventually become stable. Basic studies carried out on these half-wave tuned circuit lines showed the possibility of application of this principle for future extra-long-distance transmission (ELD). In view of some major technical and economic limitations, however, the suitability of this method needs further examination before it is accepted as a practical proposition.

Prior to the concept of tuned half-wave power lines, problems of very long lines in the region of quarter- to half-wavelengths have been shown to be managable if their electrical lengths are reduced until they fell in the region

of 0-90 electrical degrees;[9,10,11] in this respect such inordinate long lines are made to behave like ordinary short or medium length lines. To achieve this and bring about steady-state operation, reactive compensation has been employed. Shunt reactors are required to compensate part of the line capacitance in order to limit the line internal voltages and voltage rises due to Ferranti effect owing to the large capacitive power generated by the line under open-circuit or low transmission conditions. Series capacitors are required to compensate for the line inductive reactance and thereby help to increase the line power transfer ability.

Over the years supply authorities concerned with long-distance lines have been carrying out studies relating to reactive compensation as an effective way of increasing transmission distances. The studies, however, have been approached from the view-point of classical transmission theory where system studies have been carried on conventional equivalent single phase circuits on the assumption that the three-phase systems are perfectly balanced. The implications of this approach on an actual untransposed line are not known. It is therefore intended to carry out here further studies on the problem of reactive compensation of long untransposed lines on a three-phase basis and to show the significance of this on the limits of the degree of series compensation believed to be 100% on previous basis[2]. Studies on the number and types of compensating arrangement carried out here have indicated that one compensating station per 200 miles of line provides a design optimum from power transfer, reactive power requirements and voltage profiles

points of view.

Besides problems of reactive compensation of long untransposed lines, these experience certain degrees of unbalance appearing in the form of negative-sequence and zero-sequence currents, which from system operating considerations are undesirable. Precise estimations of untransposed circuit unbalances have been considered in the present investigation and will be illustrated.

An important aspect of very long lines is their behaviour under fault conditions. With the increase in line length the fault current decreases reaching a minimum at the quarter-wave point which has been widely accepted as the safe margin of long-distance transmission. The conventional quarter-wave point is arrived at from a consideration of a balanced line with a balanced type of fault. Extensive fault studies on long untransposed lines have been carried out in the thesis to show that in fact the safe margin is the eighth-wavelength point and not the quarter-wave point. Conventional known loci of short-circuited long lines will be shown to be limiting cases only when balanced type systems are approached.

The apparent impedances seen on faulted long-distance lines are not only of interest from investigating short-circuit resonance phenomena on these lines, but also for purposes of their protection. The satisfactory operation of distance-type protective equipment for short lengths of lines has long been established and the long practical experience with these schemes of system protection has rendered them very popular. It has, therefore, been considered

necessary to approach the problem of protection of very long multiconductor lines from the view-point of distance protection principles for cases of isolated and earth faults. The digital studies presented in the thesis point out in the main towards the need of a change in the philosophy of distance protection for adaptation to long line problems; the results of studies will, however, require field tests confirmation.

The solution of these steady-state long line problems will be dealt with through a new analytical technique where the effect of non-transpositons and unbalanced modes of operation have been considered, and use will be made of an automatic digital computer to carry out numerical studies.

Since the earliest days of electrical power systems miniature system models have been used to solve problems relating to parts of a power system[12]. These miniature circuits which represented, in true proportion, the electrical system used either one phase (to neutral) of a three-phase balanced system or three phases for problems involving unequal current division among the phases and unbalanced line voltages. A further development of these miniature systems was realized owing to the introduction of the principles of symmetrical components[13]. The solution of polyphase transmission network problems by single-phase representation gave rise to new aids whereby analogue methods of representation were adopted. Network analysers or analogue computers have for long played an important role in the design of power system networks and will probably continue

to do so for small simple and moderate size networks as regards their 'day-to-day' operating conditions. With the growth and complexity of power systems and owing to the limitations of the network analyser, the solution of transmission line problems has been carried out through the use of an automatic digital computer.

Advantage has thus been taken of the automatic digital computer in forming fairly accurate mathematical models of power system components which represent their true nature as opposed to the necessary simplifications carried out in the models of the analogue form of representation. In these mathematical models effects such as the continuously distributed nature of transmission lines parameters and asymmetry of the line conductors in case of untransposed line could be well represented.

Some investigators[14,15,16] used matrix transformation techniques to arrive to solutions of transmission line problems in the field of high frequency communication engineering. The solution of the line basic differential equations has been carried out in terms of components or natural modes. The resolution of the system phase voltages and currents into these modes (aerial and ground) has thus enabled the propagation problem between two points of a three-phase line to be analysed in terms of independent uncoupled lines corresponding with the natural modes. Some of these methods, however, have been derived for idealized systems where conductor and ground losses have been ignored. Others have assumed symmetry in which

differences in the properties of aerial modes have been neglected. These assumptions make these methods of approach fall short of a true representation for an actual line.

BOWMAN and McNAMEE[17] developed in 1964 T- and π- equivalent circuits for the analysis of transmission line problems in terms of separate component quantities using matrix transformation methods for the solution of the line differential equations. In their method the distributed nature of the system parameters has been recognized and system losses have been represented. The approach is general and is suited for the analysis of power frequency problems of untransposed lines as well as high frequency problems.

A generalization to the solution of polyphase multi-conductor line problems in the power frequency as well as high frequency ranges was introduced in 1963 by WEDEPOHL[18]. In his approach the concept of eigenvalue analysis has been used to derive the solution to the system differential equations in terms of natural modes of propagation. This powerful method which has formed the basis of studies for the steady-state properties of long untransposed lines will be the subject of discussion in the following chapter.

The knowledge about transient operational problems associated with power systems is of primary importance in defining the design requirements of these systems. In particular, the determination of insulation levels of very high voltage transmission lines together with apparatus connected to them is largely governed by the magnitude and wave-shapes of switching surges travelling on these systems.

The need for a study of the effects of switching surges on the performance of long-distance lines has formed an incentive for carrying out digital computer studies on energisation transients associated with switching operations of multiconductor lines.

A general survey on the solution of switching surge problems of multiconductor lines is provided in Chapter Six. In the survey, the discussion presented has revealed the drawbacks of the transient analyser approach particularly its limitation in dealing with complex multiple systems. Field test methods for investigations on transient disturbances are very effective and with proper measuring techniques can be very precise in reproducing the system performance properties. Field test methods generally tend to be expensive and since they disrupt the continuity of supply they are not favoured. The theoretical approach for the solution of the transient problem of transmission system has for long been recognized. Various analytical methods have been suggested and with the advent of the digital computer numerical solutions have been obtained.

The various methods of approach to the solution of transmission line transients problem have been discussed and their various limitations pointed out in the survey section. The arguments have been put forward for adopting the method of modal analysis[18] and the modified Fourier transform technique[19,20] in the study of the propagation of switching surges in untransposed multiconductor lines. The Fourier transform technique has the advantage of taking

into consideration the frequency dependence of the system parameters and earth return path that has been ignored in previous methods. The Fourier transform technique resolves the transient problem into a steady-state calculation problem. This has its advantages since the same sub-routines used in the calculation of the transmission line steady-state properties can again be used to derive the line transient properties.

The transient work presented in this thesis has not only been concerned with problems of application of the modified Fourier transform technique to the solution of the switching surge problem through the use of the new modal analysis approach. The main object, however, has been to proceed beyond existing work which uses the transform technique[21] in order to lay the foundation for the analysis of outstanding practical problems associated with switching operations of multiconductor lines. The case of analyzing the problem of sequential phase energisation of a transmission line has been resolved. A powerful analytical technique has been presented for the formulation of the system equations and digital studies carried out on practical systems have demonstrated the effectiveness of the approach. The method is rather general and has been shown to be valid for the analysis of the problems of sequential pole tripping.

Restriking transients calculations have been carried out using this new method too and it will be seen that the method is applicable to the general problem of non-linearities in transmission systems, where the non-linearity can be

represented as being piece-wise linear.

The Fourier transform technique used in the present investigation has been based on a Fourier series method of representation and as a result the maximum possible observation time in the study has been limited to half the periodic time of the repetitive Fourier series and due to practical limitations only 80%-90% of this observation is possible. Some of the fundamental problems associated with the Fourier transform method have been considered and a new possible approach has been presented on the basis of a Fourier series representation of f(w). It is shown that this method is capable of yielding greater extensions in the observation time and hence greater efficiencies in computation. The theoretical basis of the method has been laid down and its potential demonstrated by a relevant example. It is claimed that the method provides great possibilities for the solution of transmission system transients though further investigation will be needed before it substitutes the method adopted for the practical calculations of switching transients; these are problems in application.

Transient studies have been carried out on three-phase open-circuited lines and particular attention has been given to the problem of sequential pole closure. With all poles closing at voltage peak from an infinite bus source, it has been found that the severest transient occurs on the second phase energised. Sequential transient calculations with precharge on the line energised have been dealt with,

in this respect comparative studies have been carried out and presented together with calculations arrived at from a Bewley lattice method. Although these comparative studies have not yielded exactly identical results there has generally been close agreement and the general pattern has been known from field tests data. The computational results presented in the thesis for transient received voltages on multiconductor lines have revealed "kick-back" effects on the response of unenergised phases; these properties have also been recognized from practical field tests.

The complexity of source representation has generally been recognized. The tendency was to represent the switching station in question with an infinite-bus source in series with an inductance calculated on the basis of the station's MVA fault level and system voltage. This approach has been reconsidered here and source side representation has been further extended to represent the effect of various feeders terminating at the switching station from which the main line is energised. Two such schemes of representation have been provided. System studies on the role of the source side representation on the magnitude and shape of energisation transients have been presented in Chapter Ten.

Transient calculations and the long line effects have been dealt with briefly and methods of reactive compensation on the control of the tremendous magnitudes of transient overvoltages of a 600-mile line energised from an infinite bus source have also been considered.

It is believed that the principles have been laid down and that particular detailed long line studies can be carried out in the light of these principles.

The sequence of studies in the thesis is started by a presentation of the general method of modal analysis used in the investigation to be followed by steady-state performance studies on long-distance transmission lines. The analysis of transient studies of multiconductor lines then proceeds and the thesis is finally concluded.

CHAPTER TWO

PRESENTATION OF THE BASIC METHOD OF ANALYSIS

2.1 Introduction

The steady-state sinusoidal properties of a single conductor transmission line with an earth return path can be readily obtained from the solution of a single linear second order differential equation. For a multiconductor line, the solution of the resultant simultaneous dependent differential equations becomes more complex as the number of conductors in the system increase. WEDEPOHL[18] has provided a method whereby these complexities can be resolved and hence a solution obtained for the multiconductor line system of differential dependent equations. As the theory of modal analysis given in his paper has formed the basis of analysis in the present investigation for derivation of some of the properties of multiconductor transmisson lines, it is deemed necessary that detailed discussion of this theory now be provided.

From practical considerations the application of this new approach to the solution of transmission line problems requires a knowledge of the basic system parameters. These include the system impedances and system admittances which would be needed in deriving the system propagation characteristics. The formulation for these basic system parameters will be presented.

2.2 Multiconductor Line-Wave Equations

2.2.1 Derivation of Equations

The first order differential equations for voltage and current of a homogeneous multiconductor line derived for an elemental section of the line are given by:-

$$\frac{dV}{dx} = -ZI \qquad - (2.1)$$

$$\frac{dI}{dx} = -YV \qquad - (2.2)$$

V and I are column vectors the elements of which represent the voltages to ground on, and the currents flowing through the various conductors of the line.

Z and Y are the system impedance and system admittance matrixes. The diagonal elements of these matrixes stand for the self impedance or admittance terms of the conductors while the off-diagonal terms represent the mutual impedances or admittances between two pairs of conductors.

Differentiating (2.1) and substituting for $\frac{dI}{dx}$ from (2.2),

$$\frac{d^2V}{dx^2} = ZY.V \qquad - (2.3)$$

and similarly

$$\frac{d^2I}{dx^2} = YZ.I \qquad - (2.4)$$

Equations (2.3) and (2.4) are the generalized wave equations and define longitudinal electromagnetic propagation on a multiconductor line. For a two-wire line, which is an

equivalent of a single conductor and an earth return, the matrix terms in the wave-equation change to elements. The equations thereby reduce to a classical system of differential equations the solution of which yield the voltage and current at any point on the two-wire line. These are:-

$$v = C.\exp(-\gamma x) + D.\exp(\gamma x) \qquad - (2.5)$$

$$i = Y_0[C.\exp(-\gamma x) - D.\exp(\gamma x)] \qquad - (2.6)$$

where

$$\gamma = \sqrt{ZY} \quad ; \quad Y_0 = \sqrt{Y/Z}$$

C and D are arbitrary constants of integration to be determined from the system boundary conditions.

In their generalized form, however, the wave-equations of the multiconductor line are difficult to solve because of the presence of mutual terms in Z and Y which render the simultaneous differential equations dependent on each other. The difficulty can be overcome if these equations are transformed to a form where they become independent of each other and hence a solution becomes easy to obtain.

The elimination of the matrix off-diagonal elements in either equations (2.3) or (2.4) can be achieved by making use of matrix transformations in which the original equations are transformed into a new set of equations whose solution becomes straightforward.

Let

$$V = Qv \qquad - (2.7)$$

$$I = Si \qquad - (2.8)$$

$$P = ZY \qquad - (2.9)$$

where Q and S are square non-singular transformation matrixes of order "n×n"; n being the number of conductors considered in the system.

v and i are transformed voltage and current vectors of order "n×1".

Since for the kind of systems we will be dealing with both Z and Y are square symmetric matrixes, then

$$Z_t = Z \quad \text{and} \quad Y_t = Y$$

where Z_t and Y_t are the matrix transpose of Z and Y.

If P_t is the transpose of P, it therefore follows that

$$YZ = P_t$$

Equations (2.3) and (2.4) can now be written in terms of the new matrix products P, P_t.

$$\frac{d^2V}{dx^2} = PV \qquad - (2.10)$$

$$\frac{d^2I}{dx^2} = P_tI \qquad - (2.11)$$

Considering the voltage wave equation and substituting for V from (2.7), we get

$$\frac{d^2}{dx^2} Qv = PQv$$

i.e. $$Q\frac{dv^2}{dx^2} = PQv$$

multiplying both sides by Q^{-1}

$$\frac{d^2v}{dx^2} = Q^{-1}PQ.v \qquad - (2.12)$$

Similarly, substituting for I from (2.8) in equation (2.11) and rearranging, we get

$$\frac{d^2i}{dx^2} = S^{-1}P_tS.i \qquad - (2.13)$$

If in equation (2.12) the matrix Q is chosen in such a way that $Q^{-1}PQ$ becomes a diagonal matrix then the resultant set of independent equations can be solved in the ordinary manner for the transformed set of voltages v. The same argument is also valid for the current equation (2.13) when $S^{-1}P_tS$ is diagonalized.

The solution of the voltage equation will only be considered, the solution for the current will then follow from the first order differential equation given in (2.1).

2.2.2 Eigenvalues and Eigenvectors

It is required that:-

$$Q^{-1}PQ = \lambda \qquad - (2.14)$$

where λ is an unknown diagonal matrix of order "n×n" and Q is an unknown transformation matrix relating the phase voltages to a new set of voltages. P, however, is a known matrix.

Multiplying both sides of (2.14) by Q and rearranging

$$[P - \lambda U][Q] = [0] \qquad - (2.15)$$

where U is a "n×n" unit matrix and

[0] is an "n×1" zero vector.

Equation (2.15) represents a set of "n" homogeneous equations. These equations will have trivial solutions given by $Q \equiv 0$ unless the determinant of the system is zero. Therefore for a solution

$$\det[P - \lambda U] = 0 \qquad - (2.16)$$

Equation (2.16) is an algebraic equation of degree "n" in the diagonal elements of λ. This is known as the characteristic equation of the matrix P, and the elements of λ are known as the characteristic roots or eigenvalues of the matrix P. The solution of the characteristic equation of the matrix P therefore yields the unknown diagonal matrix λ.

In order to determine the matrix Q, this is split into column vectors Q_k each associated with an eigenvalue λ_{kk}.

Where $k = 1, 2, \text{---} n$

$$[P - \lambda_{kk} U]Q_k = [0] \qquad - (2.17)$$

Equation (2.17) can then be solved and the elements of Q_k determined. Q_k are known as the eigenvectors of the matrix P. It is important to note that equation (2.17) is a homogeneous set of equations and that one element of each vector Q_k need be specified while the other elements are determined in terms of this one. This specification is

generally arbitrary.

Starting with the relationship $S^{-1}P_tS$ it has been shown[18] that the eigenvalues of P_t are equal to the eigenvalues of P and that the eigenvectors Q and S are related to each other by a diagonal matrix D such that:-

$$S = (D.Q_t)^{-1} \qquad - (2.18)$$

Q_t is the transpose of Q.

Since the eigenvectors are arbitrarily specified these may be adjusted to satisfy the relationship

$$S = Q_t^{-1} \qquad - (2.19)$$

Equation (2.19) gives the relationship between the voltage and current eigenvector matrixes of the system and shows that generally the system voltages and currents transform differently in contrast to the held view that they transform according to the same matrix [14].

2.2.3 Solution of Wave-Equations

Having determined the eigenvalues and eigenvectors of the P matrix we now proceed to solve equation (2.12).

Rewriting equation (2.12) and substituting

$$\lambda = Q^{-1}PQ$$

$$\frac{d^2v}{dx^2} = \lambda v \qquad - (2.20)$$

Since λ is a diagonal matrix the solution of equation (2.20) reduces down to the solution of a set of simple wave-equations of the type illustrated in equation (2.5) for a

single conductor and an earth return.

Let $\gamma = \lambda^{1/2}$

Consider the k^{th} equation from (2.20)

$$\frac{d^2 v_k}{dx^2} = \gamma_k^2 v_k$$

its solution is given by

$$v_k = \exp(-\gamma_k x) v_{ik} + \exp(\gamma_k x) v_{rk}$$

where v_{ik} and v_{rk} are incident and reflected voltages for this wave; these are arbitrary constants of integration.

The complete matrix solution will then be

$$v = \exp(-\gamma x) v_i + \exp(\gamma x) v_r \qquad - (2.21)$$

Noting the transformation relationship given in equation (2.7), it will now be possible to obtain the solution of the actual phase voltages of the multiconductor line.

$$V = Q\{\exp(-\gamma x) v_i + \exp(\gamma x) v_r\}$$

but $v_i = Q^{-1} V_i$ and $v_r = Q^{-1} V_r$

$$\therefore \quad V = Q \exp(-\gamma x) Q^{-1} V_i + Q \exp(\gamma x) Q^{-1} V_r \qquad - (2.22)$$

If a matrix function ψ is defined such that

$$\psi = Q \gamma Q^{-1}$$

then using the properties of matrix functions[22,23],

equation (2.22) can be written as

$$V = \exp(-\psi x)V_i + \exp(\psi x)V_r \qquad - (2.23)$$

The current flowing in the conductors can be determined from equations (2.1) and (2.23).

From (2.1)

$$I = -Z^{-1}\frac{dV}{dx}$$

Substituting for $\frac{dV}{dx}$ from (2.23)

$$\therefore I = Z^{-1}\psi[\exp(-\psi x)V_i - \exp(\psi x)V_r] \qquad - (2.24)$$

The matrix equations (2.23) and (2.24) provide the complete solution for voltages and currents at any point distance x from the sending end of a multiconductor system. The voltage vectors V_i and V_r are the arbitrary constants of integration to be determined from the system boundary conditions.

It is clear that equations (2.23) and (2.24) resemble those obtained for the single conductor case. It will now be shown that the quantity $Z^{-1}\psi$ is in fact the multiconductor line characteristic admittance matrix.

The characteristic impedance of a transmission line is the relationship of voltage to current on an infinite line. For an infinite line there are no reflected waves. The voltage and current in this case are obtained from (2.23) and (2.24) by making the substitution $V_r = 0$

$$\therefore \quad V = \exp(-\psi x)V_i \qquad - (2.25)$$

$$I = Z^{-1}\psi \exp(-\psi x)V_i \qquad - (2.26)$$

or $V = \psi^{-1} Z.I$

∴ The quantity $\psi^{-1}Z$ is in fact the line characteristic impedance matrix "Z_0"

$$Z_0 = \psi^{-1}Z$$
$$= Q\gamma^{-1}Q^{-1}Z \qquad - (2.27)$$

The line characteristic admittance matrix "Y_0" is the inverse of Z_0

$$Y_0 = Z_0^{-1} \qquad - (2.28)$$

$$= Z^{-1}\psi$$
$$= Z^{-1}Q\gamma Q^{-1} \qquad - (2.29)$$

The interpretation[18] given to the solution of the wave equation of a multiconductor system is that propagation on the system takes place in the form of modes. The actual phase voltage or current may be considered as composed of components or modes each with its own propagation constant corresponding to an element of the diagonal matrix $\lambda^{1/2}$ whereas the distribution of voltage or current according to a certain mode is defined by a particular modal column of the voltage eigenvector matrix Q, or the current eigenvector matrix S where each column is associated with an eigenvalue λ_k.

There are generally as many modes of propagation as there are conductors in the system, earth wires included. For a three-phase system and ignoring the presence of the earth wires there would be three modes. The solution for the eigenvector matrix has revealed that the special type system representation by symmetrical components is well

taken care of by this in generalized theory.

2.3 Boundary Conditions

The arbitrary constants of integration can now be determined from a knowledge of the system boundary conditions. The equations can be expressed in the exponential form that has already been discussed and then extended to use the reflection factor concept[23]. They can also be written in the hyperbolic form which is a familiar form of the two-port equations of a two-wire line. The hyperbolic form of equations will be used throughout the present investigation. This form has been found useful since we will be dealing with problems of the kind where a point-to-point transmission line may be energised from both sending and receiving ends. In addition the line may have intermediate discontinuities which makes compounding of non-homogeneous sections necessary. In both these cases the hyperbolic form of equations is more suited for the type of studies involved and hence has been favoured. It is necessary, however, to arrange the hyperbolic expressions in a way which will render them stable for purposes of computation; this will be ensured if positive exponential functions are avoided.

The matrix hyperbolic equations defining propagation on a multiconductor line will now be derived.

Consider Fig. (2.1) in which a single line diagram of a homogeneous section of a multiconductor line has been shown. It will be assumed

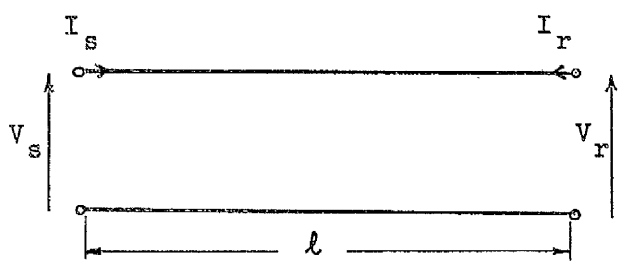

Fig.(2.1) SINGLE LINE DIAGRAM OF A MULTICONDUCTOR LINE

that the direction of current flow is positive when this enters the line at either sending or receiving ends. The following notation is used:-

v, v' = incident and reflected voltages at sending end

i, i' = incident and reflected currents at sending end

ℓ = section length

v, v', i, i' are all column vectors

we have,

$$V_s = v + v' \qquad - (2.30)$$

and $I_s = i - i'$

$$\therefore \quad Z_0 I_s = v - v' \qquad - (2.31)$$

$$V_r = \exp(-\psi\ell)v + \exp(\psi\ell)v' \qquad - (2.32)$$

$$Z_0 I_r = -\exp(-\psi\ell)v + \exp(\psi\ell)v' \qquad - (2.33)$$

Solving for v and v' from (2.30) and (2.31)

$$v = \frac{V_s + Z_0 I_s}{2} \qquad - (2.34)$$

$$v' = \frac{V_s - Z_0 I_s}{2} \qquad - (2.35)$$

Substituting (2.34) and (2.35) in (2.33)

$$V_r = \exp(-\psi\ell) \cdot \frac{V_s + Z_0 I_s}{2} + \exp(\psi\ell) \cdot \frac{V_s - Z_0 I_s}{2}$$

$$\therefore \quad V_r = \cosh\psi\ell \cdot V_s - \sinh\psi\ell \cdot Z_0 I_s \qquad - (2.36)$$

Also

$$Z_0 I_r = \{\exp(\psi\ell) - \exp(-\psi\ell)\} \cdot \frac{V_s}{2}$$

$$- \{\exp(\psi\ell) + \exp(-\psi\ell)\} \cdot \frac{Z_0 I_s}{2}$$

$$\therefore \quad Z_0 I_r = \sinh\psi\ell V_s - \cosh\psi\ell Z_0 I_s \qquad - (2.37)$$

From equation (2.37)

$$V_s = \coth\psi\ell Z_0 I_s + \operatorname{cosech}\psi\ell Z_0 I_r \qquad - (2.38)$$

Substituting equation (2.38) in equation (2.36)

$$V_r = \operatorname{cosech}\psi\ell Z_0 I_s + \coth\psi\ell Z_0 I_r \qquad - (2.39)$$

Equations (2.38) and (2.39) can be expressed in matrix form:-

$$\begin{bmatrix} V_s \\ V_r \end{bmatrix} = \begin{bmatrix} \coth\psi\ell . Z_0 & \overbrace{\operatorname{cosech}\psi\ell Z_0}^{Z_0 \operatorname{cosech}(\psi\ell)} \\ \operatorname{cosech}\psi\ell Z_0 & \coth\psi\ell Z_0 \end{bmatrix} \cdot \begin{bmatrix} I_s \\ I_r \end{bmatrix} \qquad - (2.40)$$

Equation (2.40) is the two-port impedance equation which relates the sending and receiving end voltages to their respective currents. The matrix function ψ is defined in terms of the diagonal matrix propagation constant "γ" and the line eigenvector matrix Q i.e. $\psi = Q\gamma Q^{-1}$.

For a particular mode k the propagation constant defines the attenuation constant and phase shift factor of that mode.

$$\text{i.e.} \qquad \gamma_k = \alpha_k + j\,\beta_k \qquad - (2.41)$$

The mode velocity is given by:-

$$c_k = \omega/\beta_k \qquad - (2.42)$$

ω being the angular frequency.

The two-port impedance equation given in (2.40) is suitable in mesh analysis. In nodalanalysis the two-port admittance equations in which the sending and receiving currents are expressed in terms of their corresponding voltages are very useful. The two-port admittance equations given in matrix form are:-

$$\begin{bmatrix} I_s \\ I_r \end{bmatrix} = \begin{bmatrix} Y_0 \coth\psi\ell & -Y_0 \operatorname{cosech}\psi\ell \\ -Y_0 \operatorname{cosech}\psi\ell & Y_0 \coth\psi\ell \end{bmatrix} \cdot \begin{bmatrix} V_s \\ V_r \end{bmatrix} \qquad - (2.43)$$

In the following analysis the elements of the connection matrix in equation (2.43) will be referred to as the section A,B constants. Written in terms of these constants equation (2.43) becomes

$$\begin{bmatrix} I_s \\ I_r \end{bmatrix} = \begin{bmatrix} A & B \\ B & A \end{bmatrix} \cdot \begin{bmatrix} V_s \\ V_r \end{bmatrix} \qquad - (2.44)$$

It is possible to incorporate the effect of terminating impedances and represent discontinuities in the two-port equation. More of this will be discussed with reference to particular cases of study.

2.4 Basic System Parameters

For the solution of the matrix two-port equation of a multiconductor line it is necessary to specify the line modal parameters. These parameters, as has already been seen, depend in the first place on the matrix product of the

system series impedance and shunt admittance matrixes. From this product the system eigenvalues λ and system distribution vectors Qk can be obtained and hence the various system constants including the matrix propagation constant and matrix surge impedance are determined. WEDEPOHL, SHORROCKS and GALLOWAY[24] have shown how the basic system parameters necessary in the derivation of multiconductor line properties can be obtained. A general discussion on the formation of the series impedance and shunt admittance matrixes will now be provided; formulae are given in Appendix (2).

2.4.1 Series Impedance Matrix

The system series impedance matrix is formed from the summation of three separate matrixes. These are:-

(i) a series impedance matrix which defines the self and mutual reactances due to the conductors spacings and their heights above ground[25]. Conductor bundling is taken care of by consideration of the geometric mean radius of the bundle in this matrix formation.

(ii) a series impedance matrix of self and mutual terms to account for the impedance of the earth return path. This has been obtained from Carson's infinite series and is arranged to deal with power frequency and high frequency problems in reference (24).

(iii) a series impedance matrix, of diagonal terms only, which takes into consideration the contribution due to the conductor's internal impedance. The internal resistance of the conductor is its a.c. resistance which at

power frequencies is obtained from its d.c. resistance. At high frequencies or when high permeability conductors are used, for example in the case of earth wires, the assumption of uniform current distribution on the conductor's cross-section which is valid at power frequencies, no longer holds. This is because at high frequencies skin effect becomes pronounced and the current is confined to the outer surface of the conductor. This problem has been recognised and a modification of the conductors a.c. resistance made[24].

The self reactance of the conductor, due to the conductor's internal flux is obtained for power frequency problems on the basis of geometric mean radius[25]. For high permeability steel cores and at high frequencies this reactance has also been modified[24].

2.4.2 Shunt Admittance Matrix

The shunt admittance matrix contains only susceptance terms due to the line geometry. The conductance of the air path and of insulator strings has been ignored. The inverse matrix consists of self and mutual logarithmic terms.

2.4.3 Elimination of Earth Wires

Both basic system matrixes contain terms relating to the system earth wires. The evaluation of the modal parameters will therefore not only define wave propagation properties of the phase conductors but will also give these properties for the earth wires. In the following steady-state and transient studies carried out for multiconductor lines, the propagation properties of the earth wires are not required and consequently these can be eliminated though their shielding

effect still retained. It will be assumed that the earth wire potential is zero along its entire length, an assumption which is not generally true[26] since the potential is only zero at the tower position. In Appendix (2) it is shown how the earth wires can be eliminated from the basic impedance and admittance matrixes on the assumption of zero earth wire potential.

2.4.4 Computation of System Parameters

The formation of series and shunt admittance matrixes has been obtained on the basis of the formulae presented in Appendix (2), from which the matrix product P = ZY may be formed. The system eigenvalues and eigenvectors are then calculated using a root-squaring method[24,27] and the system matrix propagation constant evaluated. The modes velocity and attenuation factor are then determined and the matrix surge impedances and surge admittance obtained after which the line A, B constants may be formed.

2.5 General Consideration

The modal method of analysis just described is applied in the following steady-state investigation on the properties of long-distance transmission lines. The transient performance of multiconductor lines presented later in the thesis has been obtained on the basis of this method in conjunction with the Fourier transform technique.

CHAPTER THREE

APPARENT IMPEDANCES SEEN BY DISTANCE RELAYS ON VERY LONG UNTRANSPOSED LINES

3.1 Introduction

The analysis of three-phase transmission lines under steady-state operating conditions yields the well known hyperbolic equations for voltages and currents in terms of the basic line constants, namely line characteristic impedance and line propagation constant. The equations are derived for one phase of a balanced three-phase system and are therefore assumed identical for the other two phases. The input impedance of such a balanced line if the line is short-circuited at the far end can be shown to be:-

$$Z_{in} = Z_c \tanh\gamma\ell$$

where $$Z_c = \sqrt{Z/Y} \quad \text{and} \quad \gamma = \alpha+j\beta = \sqrt{ZY}$$

Z and Y being the line series impedance and shunt admittance per unit length. If the line were lossless the input impedance becomes:-

$$Z_{in} = jZ_c\tan\beta\ell$$

In this case the input impedance is purely reactive. The variation of the input impedance of a short-circuited lossless line against the line electrical length is shown in Fig. (3.1.a). It is seen that the transmission line goes into a state of shunt resonance at a quarter wavelength or odd multiples of a quarter wavelength and into a state of series resonance at a half wavelength or multiples of a

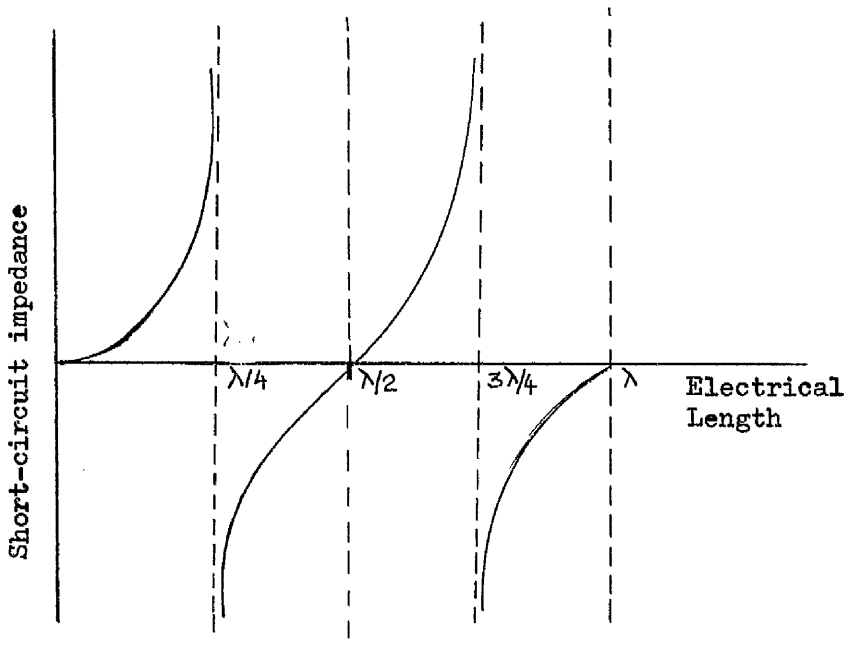

(a)

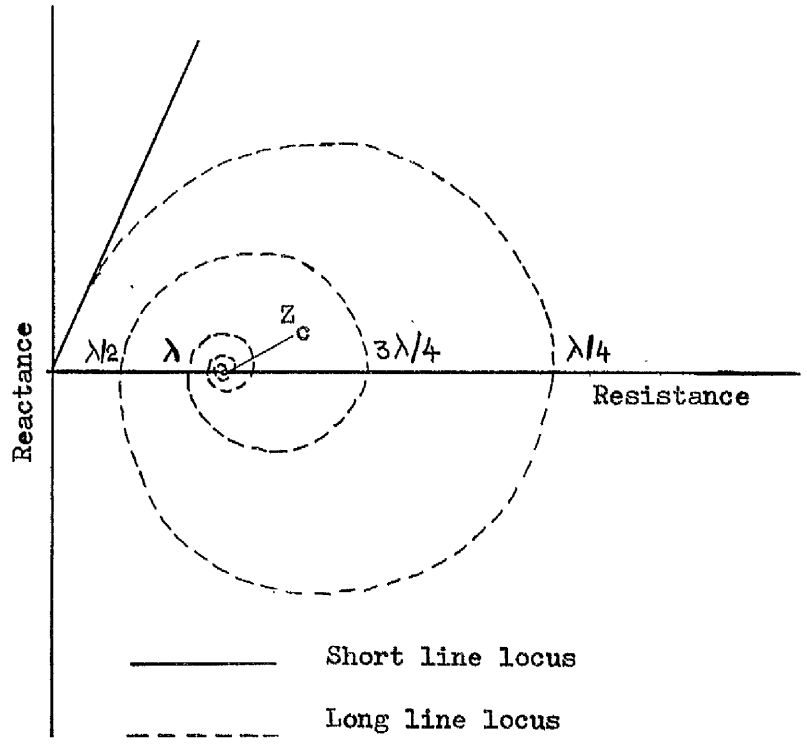

(b)

FIG. (3.1). SHORT-CIRCUIT IMPEDANCE LOCI OF LOSSLESS AND LOSSY LINES

half wavelength.

The short-circuit input impedance of a lossy line is a modification of the input impedance of a lossless line due to system losses. The variation of impedance with electrical length then takes the form shown in Fig. (3.1.b) in which the real and imaginary parts are plotted on the R-X plane. Shunt resonance occurs as in the lossless case at multiples of a quarter wavelength while series resonance at half wavelengths and in both cases the resonance impedance is purely resistive. When the line length increases indefinitely the short circuit impedance locus converges on the line characteristic impedance.

With the first resonance occurring at a quarter-wave point it is clear that a power frequency transmission line operating at or near this point is dangerously unstable. This makes the quarter-wave point therefore a limit for safe transmission. In terms of miles of line this point is 930 miles away from the input end for the case of a 50 Hz line.

Another property of the classical short-circuit impedance locus is that it is of a symmetrical nature and is confined entirely to the first and fourth quadrants of the R-X plane. For short lengths of line the input impedance is tangential to the impedance locus of long lines. This characteristic has been made use of in the design of distance relays.

Owing to the presence of different modes of propagation in the case of an untransposed multiconductor line it will be expected that the impedance loci of the individual phases

of such lines will be different from the conventional pattern described from classical line theory. These loci characteristics are extremely important since not only do they show the deviation from the conventional pattern only known till now but also highlight some of the complexities involved in the application of distance protection schemes to long-distance transmission lines.

In this chapter the method of analysis for evaluating impedance loci of multiconductor lines will be described followed by a discussion on some aspects of distance protection schemes in preparation for generalised numerical studies to be presented in the following chapter.

3.2 Method of analysis

3.2.1 Nodal Analysis Method

The method of analysis adopted throughout this investigation makes use of the two-port admittance equations of a multiconductor line in which the sending and receiving end currents are expressed as functions of sending and receiving end voltages. Thus:-

$$\begin{bmatrix} I_s \\ I_r \end{bmatrix} = \begin{bmatrix} Y_0 \coth \psi \ell & -Y_0 \operatorname{cosech} \psi \ell \\ -Y_0 \operatorname{cosech} \psi \ell & Y_0 \coth \psi \ell \end{bmatrix} \cdot \begin{bmatrix} V_s \\ V_r \end{bmatrix} \qquad - (3.1)$$

With the transmission line energised from either one or both ends, those ends are looked upon as active nodes through which currents I_s and I_r are injected. At a point of discontinuity where for example a fault has occurred an active node can also be created there with zero current being

injected through it. It is therefore possible to build up in a systematic manner and using nodal analysis method the matrix equations of the system.

In terms of nodal analysis[28] the interpretation of the connection matrix of equations (3.1) is as follows:-

Considering the node through which I_s is injected, this has a driving point admittance of $Y_0\coth\psi\ell$ and a transfer or mutual admittance of $-Y_0\operatorname{cosech}\psi\ell$ linking it to the node through which I_r is injected. Similarly for I_r, $Y_0\coth\psi\ell$ is the driving point admittance and $-Y_0\operatorname{cosech}\psi\ell$ its transfer admittance. Thus the distributed section of transmission line is effectively replaced by its driving-point and transfer admittances.

3.2.2 Fault Simulation

The fault occurring on a transmission line is represented by an "n×n" admittance matrix where n is the total number of phase conductors of the line. For double-circuit three phase lines this is a "6×6" matrix. For earth faults, only the matrix diagonal terms of the faulted conductors take the value of the reciprocal fault impedance to earth while all other terms are set to zero . For isolated faults the off-diagonal terms in the fault admittance matrix corresponding to the faulted conductors concerned take the values of the negated reciprocals of the fault impedance while their diagonal terms take reciprocal values; other terms in the matrix set also to zero values. Combined faults can similarly be represented.

The fault admittance matrix for a three-phase

double-circuit line with a line to ground fault on conductor "3" of the first circuit is given below where Z_f is the fault impedance

$[Y_f]$ =

	1	2	3	4	5	6
1	0	0	0	0	0	0
2	0	0	0	0	0	0
3	0	0	$1/Z_f$	0	0	0
4	0	0	0	0	0	0
5	0	0	0	0	0	0
6	0	0	0	0	0	0

The fault admittance matrix of an isolated line-to-line fault on conductors 4 and 5 of the second circuit is given below. It will be noted that the transfer admittance terms are entered as negative terms.

$[Y_f]$ =

	1	2	3	4	5	6
1	0	0	0	0	0	0
2	0	0	0	0	0	0
3	0	0	0	0	0	0
4	0	0	0	$1/Z_f$	$-1/Z_f$	0
5	0	0	0	$-1/Z_f$	$1/Z_f$	0
6	0	0	0	0	0	0

Whereas any type of fault occurring on any one circuit can be represented in a similar manner inter-circuit faults

can likewise be represented and their equivalent fault admittance matrix built up by filling in the appropriate off-diagonal terms in the above matrix.

3.2.3 Boundary Conditions

The transmission line is energised at either sending or both sending and receiving ends in these studies. The line is energised from a three-phase supply and as a result the energising voltage is treated as a column vector in the analysis, the elements of which are the line to ground voltages of the circuit under consideration with $0, -120°, 120°$ angle displacements.

$$V_s = \begin{bmatrix} V_{s1} \\ V_{s2} \\ V_{s3} \end{bmatrix} \text{ ; where } V_{s1} = V\underline{/0} \text{ ; } V_{s2} = V\underline{/-120°}; \quad V_{s3} = V\underline{/120°}$$

For a pure mode energisation V_{s1}, V_{s2} and V_{s3} correspond with the particular mode selected from the eigenvector matrix. Therefore at either one end of the line or the other the boundary conditions can be specified.

The source impedance of the system can be included in the analysis by a source impedance matrix. In a simple form of source representation the diagonal elements of this matrix are the values of the equivalent source impedance calculated from the system fault MVA and system voltage. This ignores mutual effects. In terms of nodal analysis the source admittance matrix will have all off-diagonal elements set to zero

$$[Y_s] = \begin{bmatrix} 1/Zs & 0 & 0 \\ 0 & 1/Zs & 0 \\ 0 & 0 & 1/Zs \end{bmatrix}$$

3.2.4 Mathematical Model for Fault Calculations

The mathematical models needed for the evaluation of apparent impedances seen on long lines will now be presented. In these models the source impedance has been ignored and the systems treated as if fed from infinite bus-system, since in the case of long lines neglecting source impedance will not have a considerable effect on the fault currents calculated.

3.2.4.1 Single-Ended System

The multi-conductor line is fed from one end only with the other end open-circuited.

(i) Variable line length with fault applied at its remote end

The system diagram is shown in Fig. (3.2a) while for the purpose of nodal analysis its equivalent is shown in Fig. (3.2b).

The homogeneous section between the sending end and fault points (SF) will be replaced by its driving point admittance matrix "A" and its transfer admittance matrix "B", where

$$A = Y_0 \coth\psi\ell$$

$$B = -Y_0 \operatorname{cosech}\psi\ell$$

At the fault point "F" a fault admittance matrix "Y_f" is

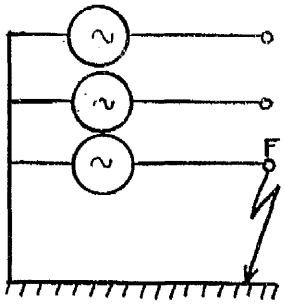

(a)

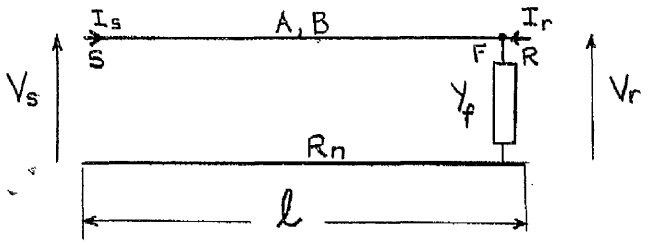

(b)

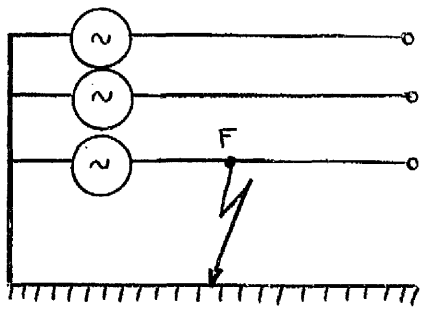

(c)

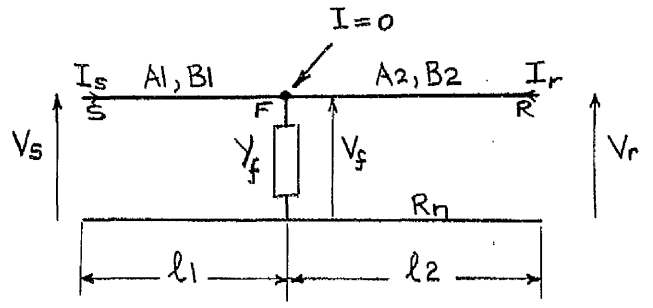

(d)

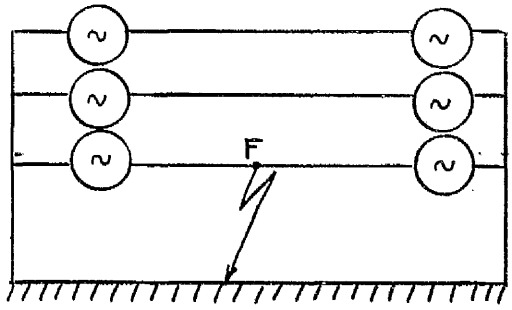

(e)

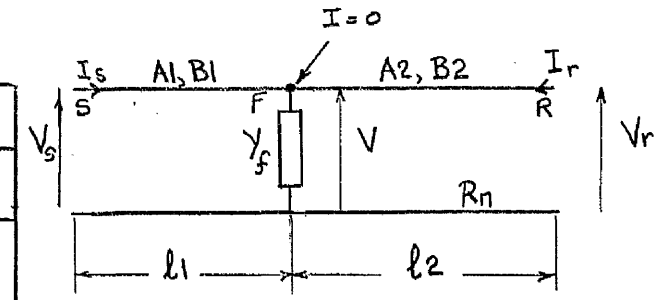

(f)

FIG. (3.2). SYSTEM CIRCUITS AND EQUIVALENT DIAGRAMS FOR APPARENT IMPEDANCE EVALUATION

connected to the reference node which is the neutral bus Rn. Assuming injection currents I_s and I_r at sending and receiving ends, the system equations will now be set up:-

$$\begin{bmatrix} I_s \\ I_r \end{bmatrix} = \begin{bmatrix} A & B \\ B & A+Y_f \end{bmatrix} \cdot \begin{bmatrix} V_s \\ V_r \end{bmatrix}$$

Since the receiving end has no source connected to it then the injected current there will be zero i.e. $I_r = 0$ and the above matrix equations reduce to

$$\begin{bmatrix} I_s \\ 0 \end{bmatrix} = \begin{bmatrix} A & B \\ B & A+Y_f \end{bmatrix} \cdot \begin{bmatrix} V_s \\ V_r \end{bmatrix}$$

solving for V_r from the bottom row

$$V_r = -(A+Y_f)^{-1} \cdot B \cdot V_s$$

and for I_s from the top row

$$I_s = [A - B(A+Y_f)^{-1} \cdot B] \cdot V_s \qquad - (3.2)$$

It is worthwhile noting that variation of the line section length will be represented in the A, B constants which makes equation (3.2) valid for faults at the end of different line lengths.

From a knowledge of the voltage column vector V_s, the current vector I_s appearing at the sending end of the line can therefore be evaluated for any type of fault for this case from equation (3.2).

The apparent impedance seen at the sending end on any

phase conductor is the ratio of voltage to current on that conductor.

Two types of apparent impedances can be found; those that would normally be seen by ground fault distance relays for earth faults and those that would normally be seen by phase fault relays due to faults involving more than one phase and ground or isolated from ground. These latter types of apparent impedances are obtained from the ratio of the difference between conductor to ground voltages to the difference between conductor currents. Thus the apparent impedance seen on phase "1" due to a line to ground fault on that phase is given by

$$Z_{s1} = V_{s1}/I_{s1}$$

and the apparent impedance seen between conductors 2 and 3 for a line-to-line fault at their end is given by:-

$$Z_{s23} = (V_{s2}-V_{s3})/(I_{s2}-I_{s3})$$

the particular elements of voltage and current are extracted from the column vectors V_s and I_s.

(ii) Fixed line length, variable fault point

With the fault varying position along the line the mathematical model can be built up in a similar manner to the previous case. Consider Figs. (3.2.c) and (3.2.d). Using the notation in the figure the system equations written in matrix form are:-

$$\begin{bmatrix} I_s \\ 0 \\ 0 \end{bmatrix} = \begin{bmatrix} A_1 & B_1 & 0 \\ B_1 & A_1+Y_f+A_2 & B_2 \\ 0 & B_2 & A_2 \end{bmatrix} \cdot \begin{bmatrix} V_s \\ V \\ V_r \end{bmatrix}$$

where

$$A_1 = Y_0 \coth \psi \ell_1 \; ; \; B_1 = -Y_0 \operatorname{cosech} \psi \ell_2$$

$$A_2 = Y_0 \coth \psi \ell_2 \; ; \; B_2 = -Y_0 \operatorname{cosech} \psi \ell_2$$

again since there is no generation at either F or R both I and I_r are zero.

Eliminating V and V_r and solving for I_s, we have:-

from third row

$$0 = B_2 V + A_2 V_r$$

$$\therefore \quad V_r = -A_2^{-1} B_2 V$$

from second row

$$0 = B_1 V_s + (A_1+Y_f+A_2)V - B_2 A_2^{-1} B_2 V$$

from which

$$V = -[A_1+Y_f+A_2-B_2 A_2^{-1} B_2]^{-1} B_1 V_s$$

and finally

$$I_s = \{A_1 - B_1[A_1+Y_f+A_2-B_2 A_2^{-1} B_2]^{-1} B_1\} V_s \qquad - (3.3)$$

Having determined the sending end currents for all various conductors it is possible to proceed in exactly the same way as outlined before to obtain the apparent impedances seen by the various relays. A movement of the fault position to any other

point on the line will only alter the values of the A, B constants in equation (3.3).

3.2.4.2 Double-Ended System

A transmission line energised at both ends with the fault occurring at some intermediate point will now be considered. The total system length is taken as fixed. Fig. (3.2.e) shows the system diagram with its equivalent given in Fig. (3.2.f).

The discontinuity at F divides the line into two sections with A, B constants dependent on the lengths of the individual sections. The system equations in this case are

$$\begin{bmatrix} I_s \\ 0 \\ I_r \end{bmatrix} = \begin{bmatrix} A_1 & B_1 & 0 \\ B_1 & A_1+Y_f+A_2 & B_2 \\ 0 & B_2 & A_2 \end{bmatrix} \cdot \begin{bmatrix} V_s \\ V \\ V_r \end{bmatrix}$$

From second row

$$0 = B_1V_s + (A_1+Y_f+A_2)V + B_2V_r$$

$$\therefore \quad V = -(A_1+Y_f+A_2)^{-1}(B_1V_s+B_2V_r)$$

$$I_s = [A_1-B_1(A_1+Y_f+A_2)^{-1}B_1]V_s - B_1(A_1+Y_f+A_2)^{-1}B_2V_r \quad - (3.4)$$

and $$I_r = [A_2-B_2(A_1+Y_f+A_2)^{-1}B_2]V_r - B_2(A_1+Y_f+A_2)^{-1}B_1 \cdot V_s \quad - (3.5)$$

Both sending and receiving end fault currents are therefore determined and hence the apparent impedance seen at those ends can be obtained.

3.3 Considerations on Application of Distance Protection to Long Multi-conductor Lines

3.3.1 General

The theory and practice of line distance protection have long been established [29,30]. The basic principle of this form of system protection depends on the comparison, at the relaying point, of the voltage and current so that on operation the relay passes proper signals to the circuit breaker which trips the line in the event of a fault occurring, normal system operation continuing otherwise. Impedance, therefore in this form of protection, is taken as a measurement of the distance to the fault point since the comparison of voltage and current yields this quantity.

The operating winding of the relay is energised via a current transformer from the system fault current while its restraint winding is energised via a voltage transformer from the system voltage. The two coils produce opposing torques and in the event of one torque exceeding the other the point of balance or "minimum setting" is disturbed and the relay thus operates. For faults or other system disturbances lying outside the zones it is protecting a distance relay must not operate; in other words it should have the ability to discriminate under various system operating conditions. Hence relays are designed to have this property of discrimination incorporated in them.

3.3.2 Characteristics of Distance Relays

The ratio between the voltage and current at a relaying terminal is termed the apparent impedance seen by the relay. In general this quantity has a real as well as

imaginary component and a relay is expected therefore to have characteristics which would enable it to respond to this type of quantity. The characteristic curve[31] of a relay defines the limits of operation of the relay. If the impedance seen by the relay falls inside the boundary of the characteristic curve then operation of the relay will occur but if the impedance falls outside then the relay will remain inoperative.

Plain impedance relays have circular characteristics with the origin of co-ordinates of the R-X plane as centre. Fig. (3.3.b) shows this characteristic. If the relay is located at the junction of two sections of a transmission line Fig. (3.3.a) then it is essential that the relay has discriminative properties to enable it to differentiate between faults on either section of the line and hence tripping of the faulty part only[32]. Such a characteristic is termed directional characteristic and the relay operates if the impedance seen at its terminals falls within the part bounded by the directional property and the continuous periphery. The relay is identified as impedance relay with directional characteristic and is shown in Fig. (3.3.c). Another variation of this relay is the off-set impedance relay, Fig. (3.3.d). Inherent directional properties are present in the mho relay[33] and no additional directional element is required for this type of relay as the circumference of its characteristic passes through the origin as shown in Fig. (3.3.e). The relay is therefore capable of identifying faults on the feeder OA.

Distance relays need not necessarily operate on the apparent

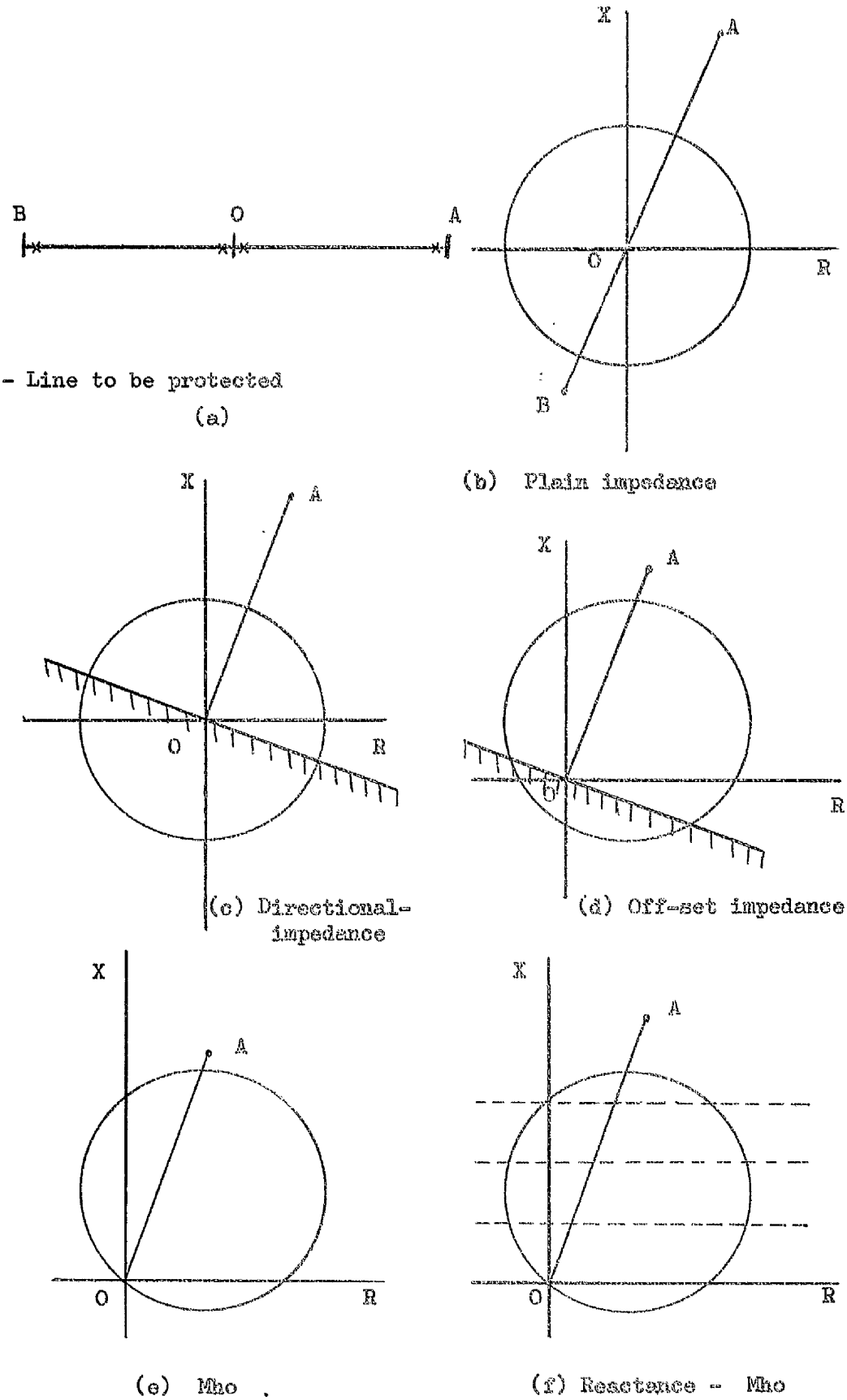

FIG. (3.3). PROTECTION RELAY CHARACTERISTICS

impedance of the fault path and it is possible to design these relays to operate on the reactance component of the fault impedance. This is advantageous since it eliminates possibilities of any variations introduced by the resistance of the arc[34] which almost invariably occurs in case of earth faults of high tension networks. Due to the presence of the arc resistance an impedance relay would interpret such types of fault as being a long distance from the relay location and hence will not operate. Reactance relays which can be made directional by incorporating in them the mho type characteristic can cope with such types of faults where their settings are not affected due to the presence of an arc resistance. Such relay characteristic is shown in Fig. (3.3.f).

3.3.3 Relaying Quantities and Principles of Sound-Phase and Residual Compensation

The indication of a fault through measurement of the impedance to the fault has already been established. When dealing with single phase systems the voltage to current ratio at the relay location gives this correct measure of distance to the fault but if an actual three phase system is considered then the ratio of voltage and current is no longer a direct indication of the impedance to the fault since the voltage drop between the relay and fault point contains terms resulting from mutual voltage drops of all phases. This will therefore give rise to errors in the measured impedance of a phase. With the introduction of principles of compensation[35] the apparent impedances would be obtained which give proper indications of distances to the fault. Under earth fault conditions the operating winding of a phase-to-

ground relay is energised with a signal which consists of the faulty phase current and a certain proportion of the healthy phases currents in which case the protection scheme is known as sound-phase or healthy-phase compensation scheme. This form of protection is valid for untransposed circuit lines. When the effect of non-transposition is ignored another scheme known as the zero-sequence compensation scheme is applied. Here the operating winding of a phase-to-ground relay is fed with a signal which contains the faulty phase current together with a proportion of the residual or zero-sequence current. In both these types of compensation the restraint winding of the relay is fed from line-to-ground voltage at the relay location. Appendix (3) shows how relaying quantities utilizing these schemes are derived for the case of solid faults. As shown in the appendix the apparent impedance seen by the relay when sound phase compensation is applied is the total earth-fault loop impedance whereas in the case of zero-sequence compensation the apparent impedance is the total positive sequence impedance up to the fault point. The apparent impedances seen by the phase relays for double-phase or three-phase faults are propotional to the positive sequence impedance as shown in part "B" of Appendix (3). The expressions are again derived for the case of solid faults assuming transposition as is the case in practice.

In practice errors arise in the application of these principles to the protection of high-voltage lines. Errors resulting from the variation of apparent impedance with change in source impedance were pointed out[36]. It was also shown that under earth fault conditions errors arose due to the

application of zero-sequence type of compensation to untransposed single circuit[37] and double circuit[38] lines. Distance relays equipment has also indicated errors due to the fact that complex proportions of sound-phase and residual currents have been represented as real proportions only.

3.3.4 Distance Protection Applied to Long Lines

The theory of distance protection schemes has been derived on the basis of short transmission lines. The validity of the theory for long lines has generally been accepted. The effect of the line capacitance current which is a significant factor in the case of long lines and which has so far been ignored has a substantial influence on the apparent impedance characteristic. It is the purpose of this investigation to explore the validity of existing distance protection schemes discussed earlier and highlight some of the protection problems involved in long multi-conductor lines under simple operating conditions. A single circuit point-to-point transmission line fed from an infinite bus system has been chosen for the analysis; this primitive scheme has been considered in order to avoid the masking effects that may arise from consideration of more complex power systems.

For the multi-conductor line the compensated apparent impedances seen by distance relays are obtained from the solutions to the fault currents in the mathematical models of section (3.2) and a knowledge of the system line to ground voltage by using the methods of Appendix (3).

CHAPTER FOUR

COMPUTATIONAL RESULTS OF IMPEDANCE LOCI AND APPARENT IMPEDANCES SEEN BY DISTANCE RELAYS ON VERY LONG LINES

4.1 Introduction

Detailed studies for uncompensated impedance loci seen by distance relays for very long multi-conductor horizontal and vertical lines will now be presented. The classical short-circuit impedance locus indicated earlier will be shown to be a special case only for the case of a balanced type of fault on the multiconductor line. For unbalanced or non-symmetrical faults the shape of the impedance locus is shown to be quite arbitrary. This is governed, however, by the phase on which the fault has been applied and also by the phasor voltage energising that phase. An extreme type of unbalance fault is shown to be very significant for very long lines not only from the shape of the impedance locus it produces but also from the view-point of the whole question of the safe theoretical limits of long distance transmission known up till now as the power frequency quarter wave-length lines. This length limit will now be shown to be an eighth of a wavelength.

In the design of distance protection schemes the line capacitance current has not been taken into consideration. This current is very significant in the case of long-distance lines. Results of studies relating to long line distance protection and presented here clearly show the complications involved with this form of protection and hence

point out to the need for a consideration of the philosophy of distance protection principles when applied to long multiconductor lines.

4.2 Description of Computer Program for Evaluation of Short-Circuit Impedance Loci

A flow diagram of the general computer program for the calculation of the short-circuit impedance loci for single-ended and double-ended systems is given in Fig. (4.1). The program can be divided into major sections, these will be described in turn.

(i) Transmission line input data

The line geometry is read in;this includes the total number of phase conductors and earth wires, their mean height above ground and their spacings apart. Phase bundles, if there are any, are specified. The earth resistivity, supply frequency, phase conductor and earth-wire relative permeability, inductance correction factor, strand diameters of conductors, number of outer strands and number of effective strands are also read in as part of the line input data for the program.

(ii) Calculation of line constants

The basic normalized system impedance and admittance matrixes are calculated as explained in section (2.4) from which the system eigenvectors and normalized eigenvalues are obtained with the actual eigenvalues being formed on multiplication by the normalization factor. The matrix propagation constant, matrix surge impedance and admittance are evaluated. The system modal velocities and

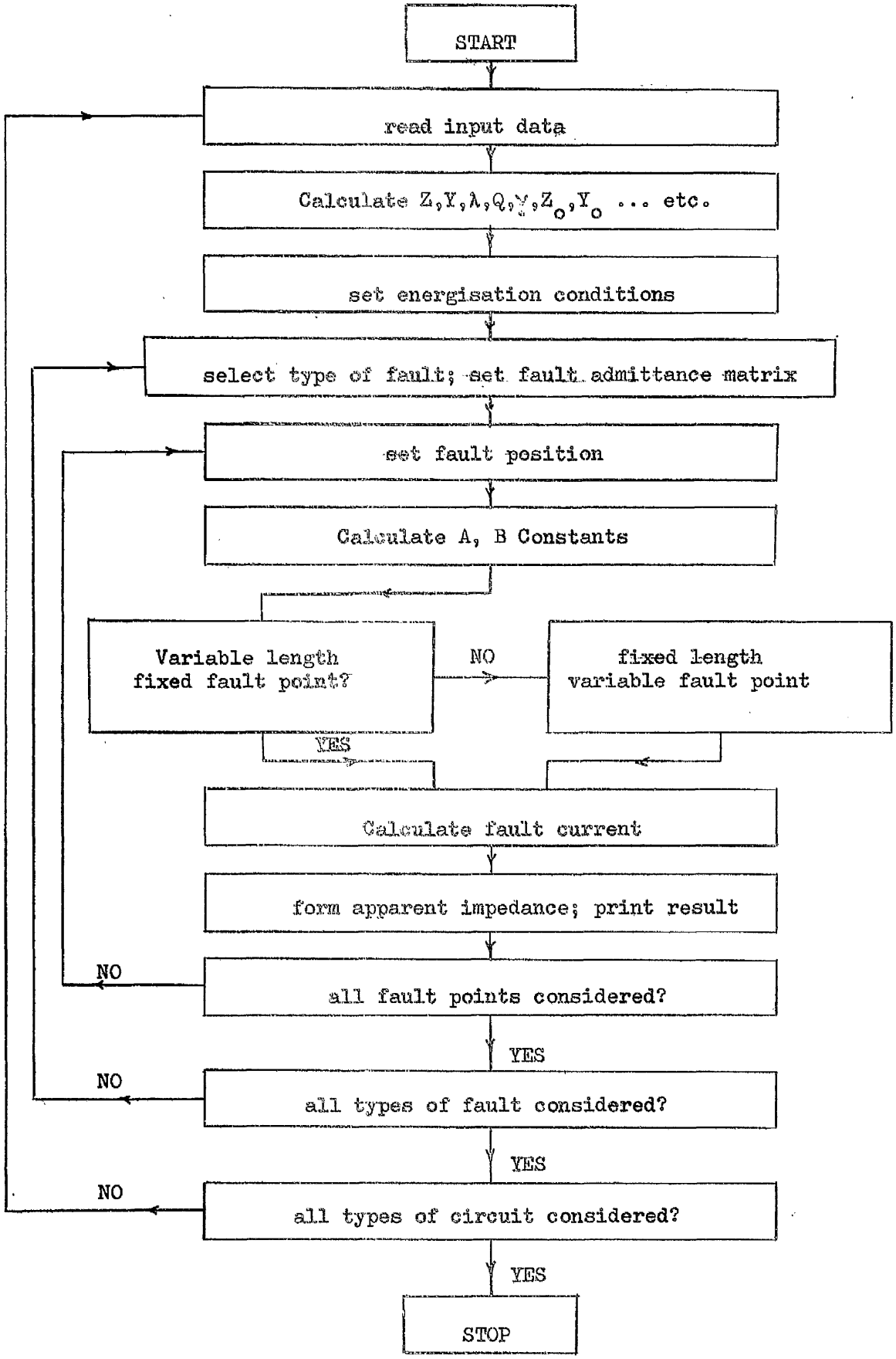

FIG. (4.1). FLOW DIAGRAM OF COMPUTER PROGRAM FOR DETERMINATION OF UNCOMPENSATED IMPEDANCE LOCI

attenuation constants are also determined. At this stage of the program some of the basic information about the line can be printed out if required.

(iii) Setting the line boundary conditions

In the studies considered the line may be energised at one end only, the sending end, with the receiving end open-circuited or at both sending and receiving ends. In either of these two cases the line energising conditions are specified in voltage magnitude and voltage phase angle. This can be a three-phase supply system or a supply system corresponding to the pure line modes i.e. a certain column of the eigenvector matrix.

(iv) Fault admittance matrix

The fault admittance matrix is formed by putting in the value of fault admittance in a location corresponding to the faulted phase(s) this depending on the type of fault.

(v) Calculation of impedance locus

Setting the line length as a cycle the line A, B constants are evaluated and the major part of the calculation to obtain the short-circuit currents at the sending end of the line is performed according to the mathematical models of Chapter "3" for either fixed length of line or variable line length. The final step in the calculation is the determination of the impedance seen at the input end of the short-circuited line and is obtained by dividing the line to ground voltage by the line current

for phase to ground loci or phase-to-phase volage by the difference of phase currents for line-to-line loci.

The results are printed out and the cycle of line length or fault point repeated.

4.3 Lines for Studies

Two types of circuit configurations have been studied. These are:-

i - Single circuit line of horizontal configuration

ii - Single circuit line of vertical configuration

A diagram giving the various distances between conductors and their mean height above ground is shown in Fig. (4.2).

i-Horizontal circuit line

This line has two earth conductor bundles with one conductor per bundle and three phase conductor bundles with two conductors per bundle separated by a distance of 15 inches. The phase conductors and earth wire specifications are:-

Phase conductors ... 2x54/7/0.139 in. aluminium/steel

Earth wires 7/0.144 in.

An earth resistivity of 600 Ω-meter is taken for the region that the line traverses.

The 50 Hz parameters calculated for this line are given in Table (4.1).

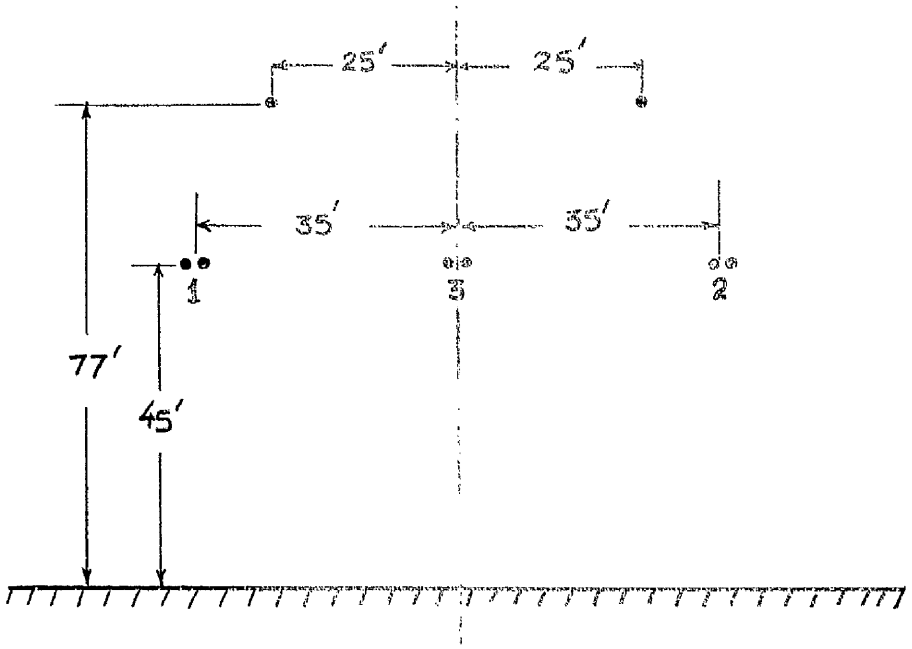

SINGLE CIRCUIT HORIZONTAL CONFIGURATION

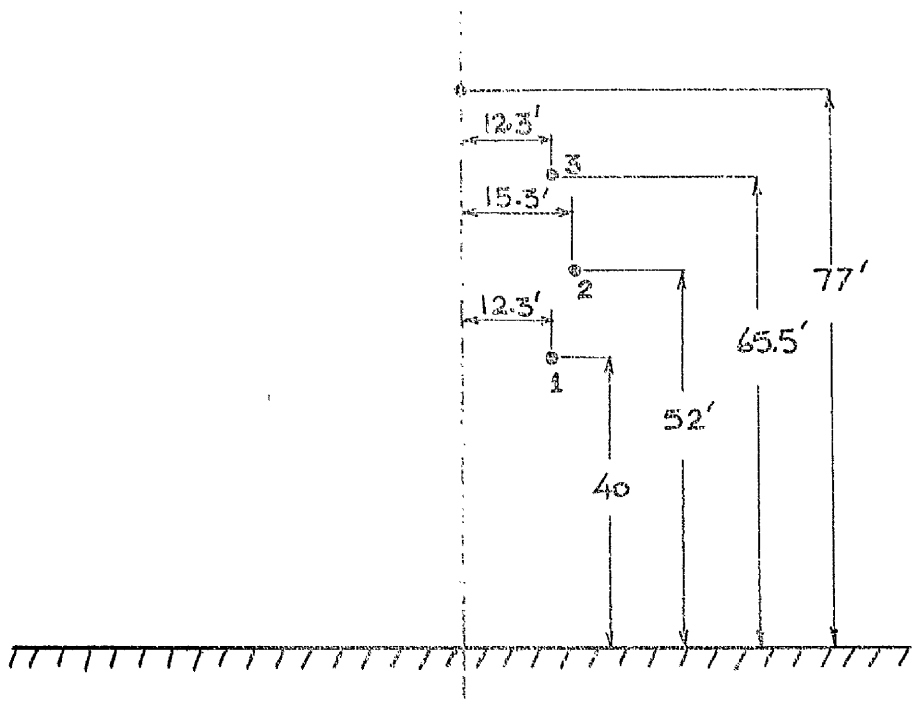

FIG.(4.2). SINGLE CIRCUIT VERTICAL CONFIGURATION

ii - Vertical-circuit line

The line has one earth wire and three-phase bundles with one conductor per bundle. The phase conductors and earth wire specifications are:-

Phase conductors ... 30/7/0.110 in.

Earth wires ... 7/0.110 in.

An earth resistivity of 300 Ω-meter has been taken for this line.

The 50 Hz. parameters calculated for this line are given in Table (4.2).

4.4 Results of Studies

The numbers marked on impedance loci diagrams refer to fault distances in miles from sending end.

4.4.1 Line Energised by Pure Modes

A horizontal line is energised by a pure mode corresponding to a particular column of eigenvector matrix given in Table (4.1) in order to determine the resonance points for the three modes of propagation. A three phase-to-ground fault is applied at the receiving end of the line and the input impedance locus obtained. This represents balanced conditions and it will be expected that the loci will have symmetrical patterns.

For mode "1" the impedance loci for the outer phase conductors are shown in Fig. (4.3.a), the outer conductors show identical classical loci. The centre phase is not involved in this mode. The first resonance point for this

TABLE (4.1). SINGLE CIRCUIT HORIZONTAL LINE 50 HZ CONSTANTS

Mode Number	Eigenvectors				Attenuation DB/KM	Velocity KM/SEC.
	Voltage		Current			
	modulus	angle deg.	modulus	angle deg.		
1	1.0000	0.000	1.0000	0.000	0.0004	289232
	1.0000	180.000	1.0000	180.000		
	0.0000	0.000	0.0000	-0.608		
2	0.9847	-0.314	1.0000	0.000	0.0012	175421
	0.9847	-0.314	1.0000	0.000		
	1.0000	-0.000	0.9283	0.478		
3	0.4642	-179.522	0.5078	-179.686	0.00046	295590
	0.4642	-179.522	0.5078	-179.686		
	1.0000	0.000	1.0000	0.000		

Note: The mode distribution vectors from top to bottom refer to the left outer (1), right outer(2) and centre (3) conductors respectively.

TABLE (4.2). SINGLE CIRCUIT VERTICAL LINE
50 HZ CONSTANTS

Mode Number	Eigenvectors				Attenu-ation DB/KM	Velocity KM/SEC
	Voltage		Current			
	modulus	angle deg.	modulus	angle deg.		
1	1.0000	0.000	1.0000	0.000	0.00204	228619
	0.9355	1.260	0.7836	3.334		
	0.8804	-4.472	0.8053	-7.332		
2	0.4591	-175.407	0.52906	-178.197	0.00210	287540
	1.0000	0.000	1.0000	0.000		
	0.4033	-171.112	0.4617	-174.975		
3	0.8192	176.011	0.8748	178.143	0.00187	288676
	0.06301	64.731	0.0432	93.577		
	1.0000	0.000	1.0000	0.000		

Note: The mode distribution vectors from top to bottom are for bottom, middle and top conductors respectively.

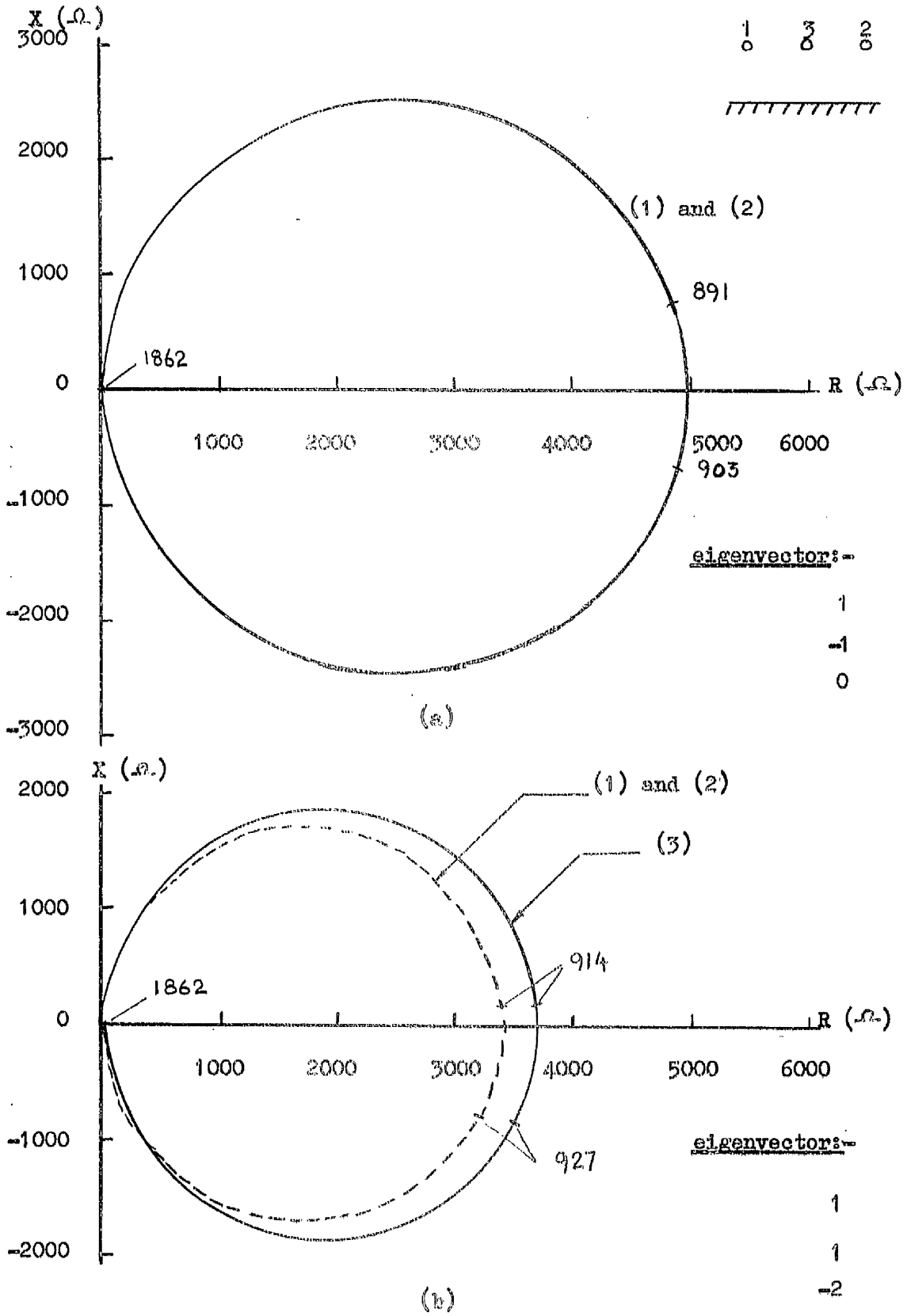

FIG.(4.3). PURE MODE ENERGISATION AND THREE PHASE-TO-GROUND FAULT

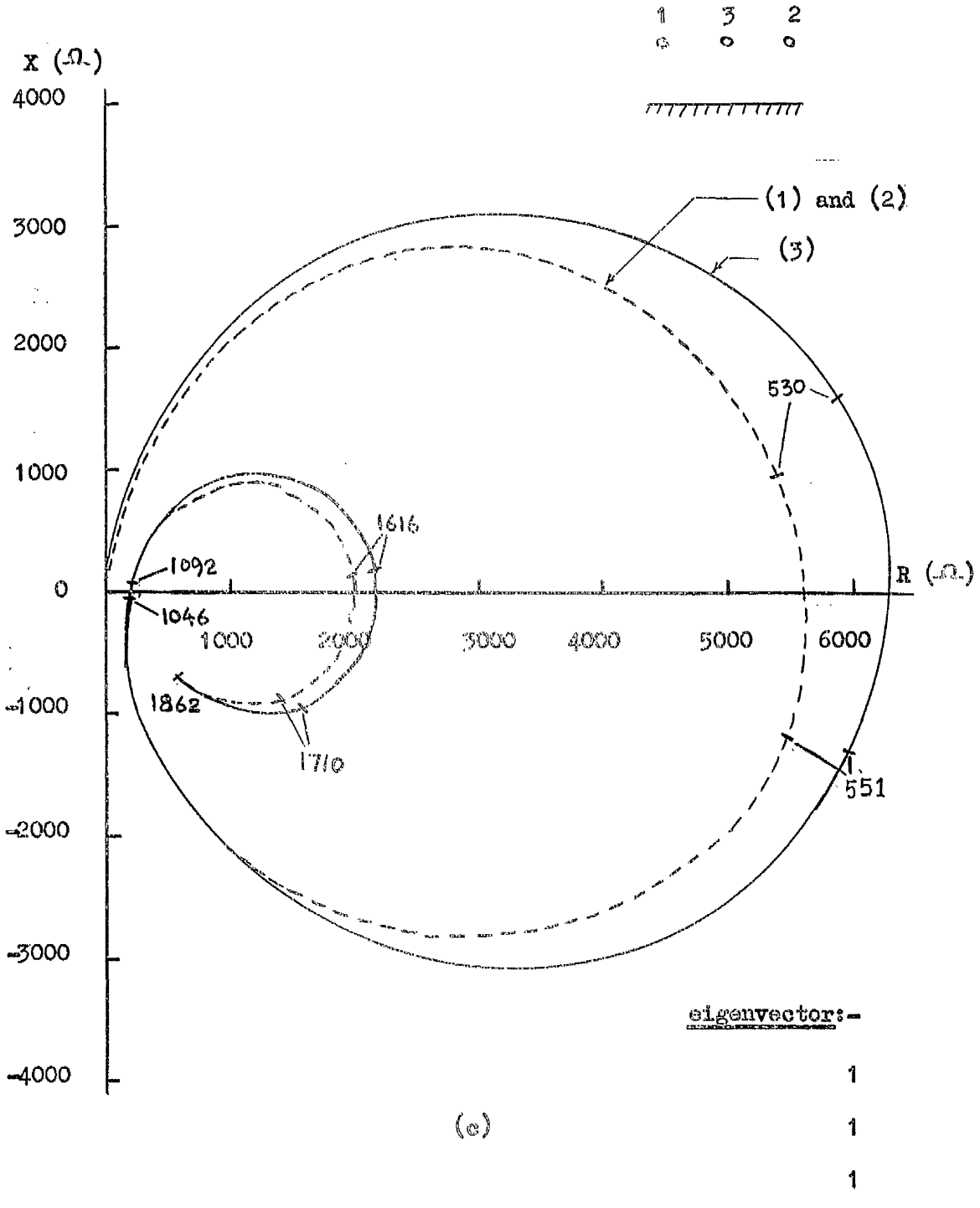

FIG.(4.3). PURE MODE ENERGISATION AND THREE PHASE-TO-GROUND FAULT.

mode is the quarter-wave point and the second resonance point occurs at approximately half-wave point; this is in keeping with the classical type locus predicted since in fact mode "1" corresponds to a positive sequence mode and hence the similarity between the two results.

When the line is energised by a set of voltages corresponding to a mode "3" distribution vector the loci characteristics for the three phases exhibit quarter-wave resonance as indicated by Fig. (4.3.b). Mode three is an aerial mode and can therefore be regarded as a positive sequence mode too. The slight deviation from the fault distance at which mode "1" resonates is due to the difference in the velocities of these two aerial modes.

When the mode of type zero sequence distribution energises the line the first resonance point occurs for all three phases in the neighbourhood of an eighth of a wavelength instead of a quarter wavelength as was the case of the previous two modes. This is shown in Fig. (4.3.c). Further increase in the line length shows that resonance occurs at multiples of an eighth wavelength. This important result shows that the presence of the earth mode in a three phase system is going to have pronounced effects on the shape of the short-circuit impedance loci.

4.4.2 Line Energised from Balanced Three-Phase System

4.4.2.1 Three Phase-to-Ground Faults

The effect of a balanced three phase-to-ground fault on the apparent impedance of a transmission line is shown in Fig. (4.4). The loci are given for the phase-to-

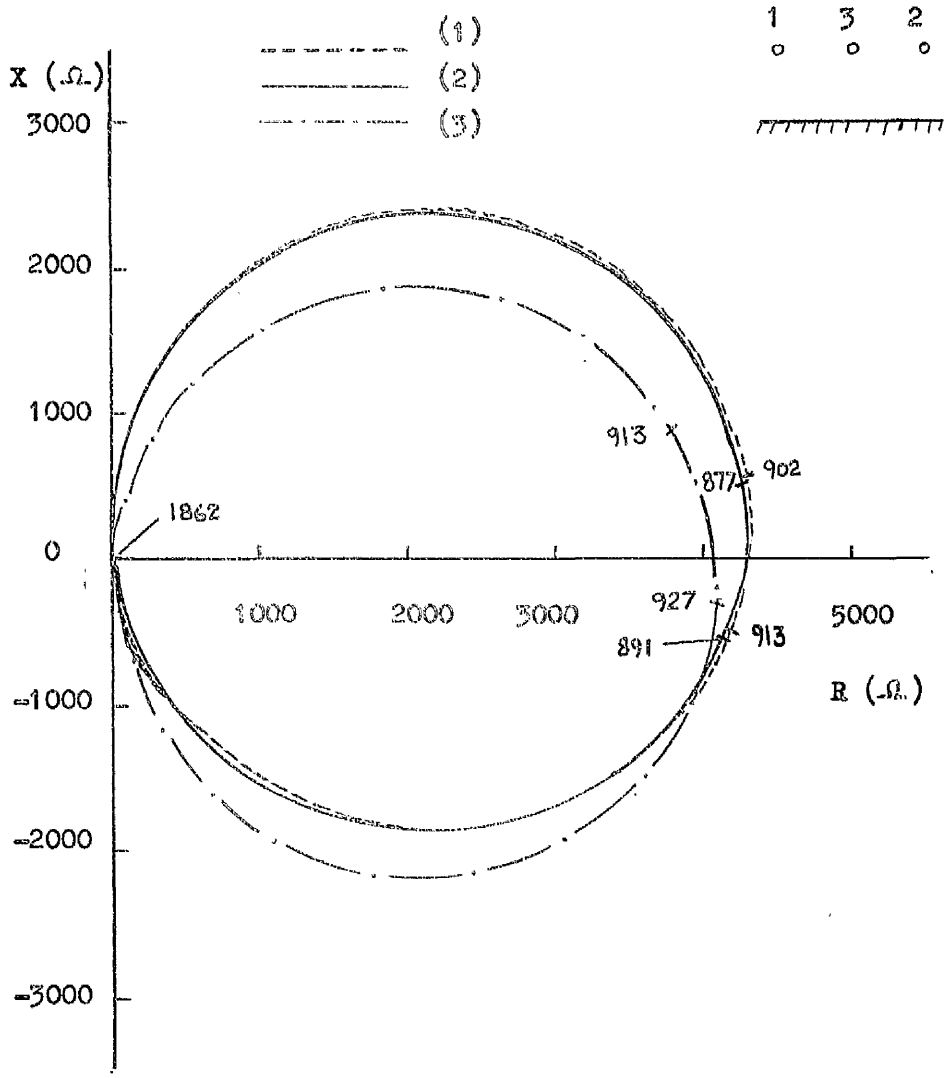

FIG.(4.4). UNCOMPENSATED IMPEDANCE LOCI FOR THREE-PHASE-TO-GROUND FAULT ON HORIZONTAL LINES

ground impedance seen on all three phases. The loci are symmetrical for this balanced system and resonance occurs at multiples of a quarter wavelength, in this way the result is a confirmation of the one obtained using the known hyperbolic equations of an equivalent single phase transmission line. This standard result has also been confirmed for the case of phase-to-phase apparent impedances seen on the input end of the faulted line of horizontal configuration for a balanced three-phase-to-ground fault.

4.4.2.2 Single Line-to-Ground Faults

A single line-to-ground fault is applied on each of the conductors of a flat line in turn and the resultant impedance loci obtained. Fig. (4.5.a) shows a spiral pattern of loci for the centre phase. This has the property that the line shows resonance conditions at intervals of an eighth wavelength and the impedance locus is nearly symmetrical about the resistance axis. When the fault is applied on the outer conductors of the circuit it can be seen from Fig. (4.5.b), which gives the loci for the outer phases, that the first resonance point still occurs about the eighth wavelength point but that the symmetry of the loci is lost thereafter in comparison with the centre phase locus and that in this case the apparent impedance has a negative resistance component. Clearly the impedance loci of all three phases show a considerable departure from the classical result of a balanced type fault.

The eighth wavelength resonance conditions are further

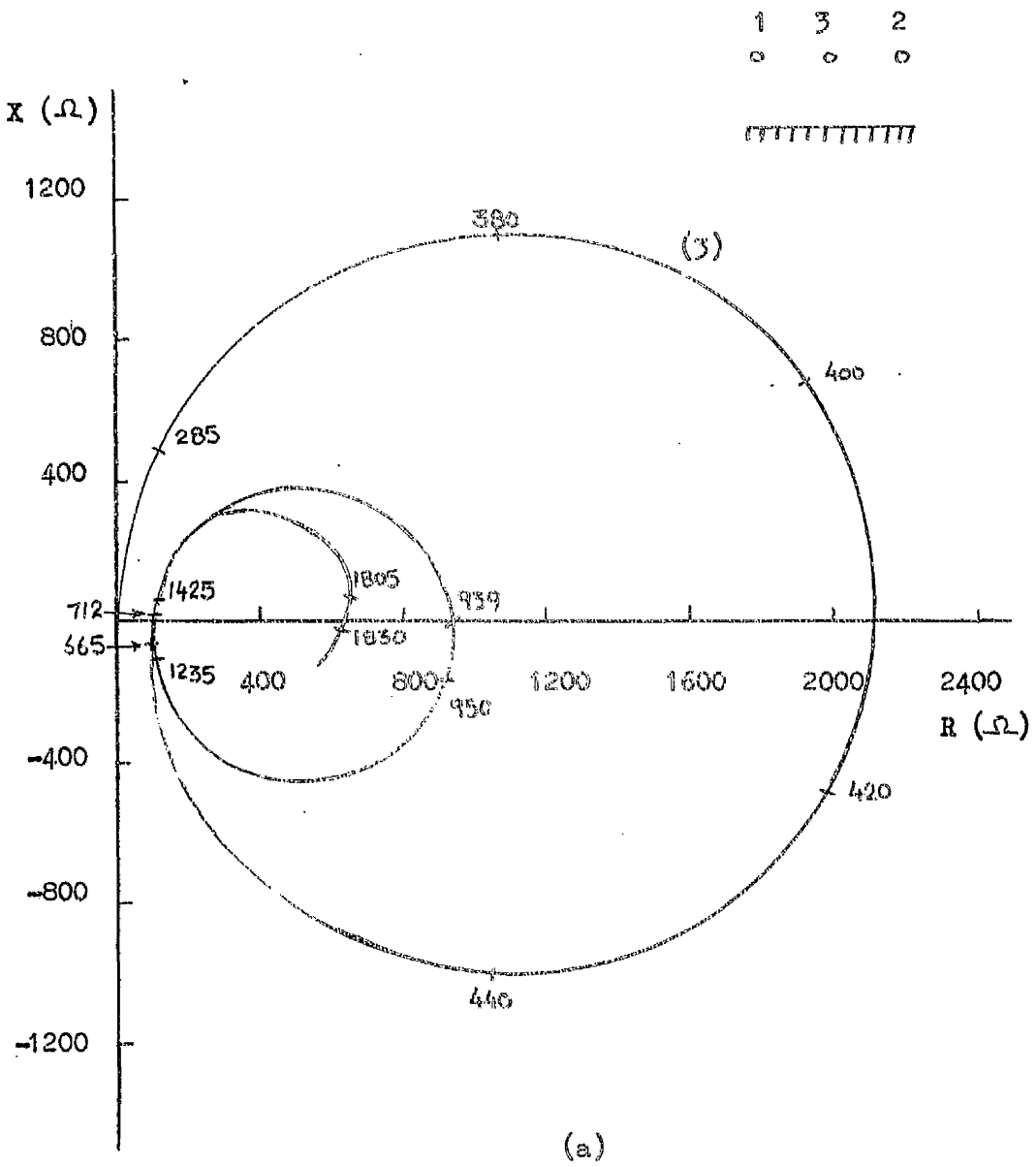

FIG.(4.5). UNCOMPENSATED IMPEDANCE LOCUS FOR SINGLE LINE-TO-EARTH FAULT ON HORIZONTAL LINES

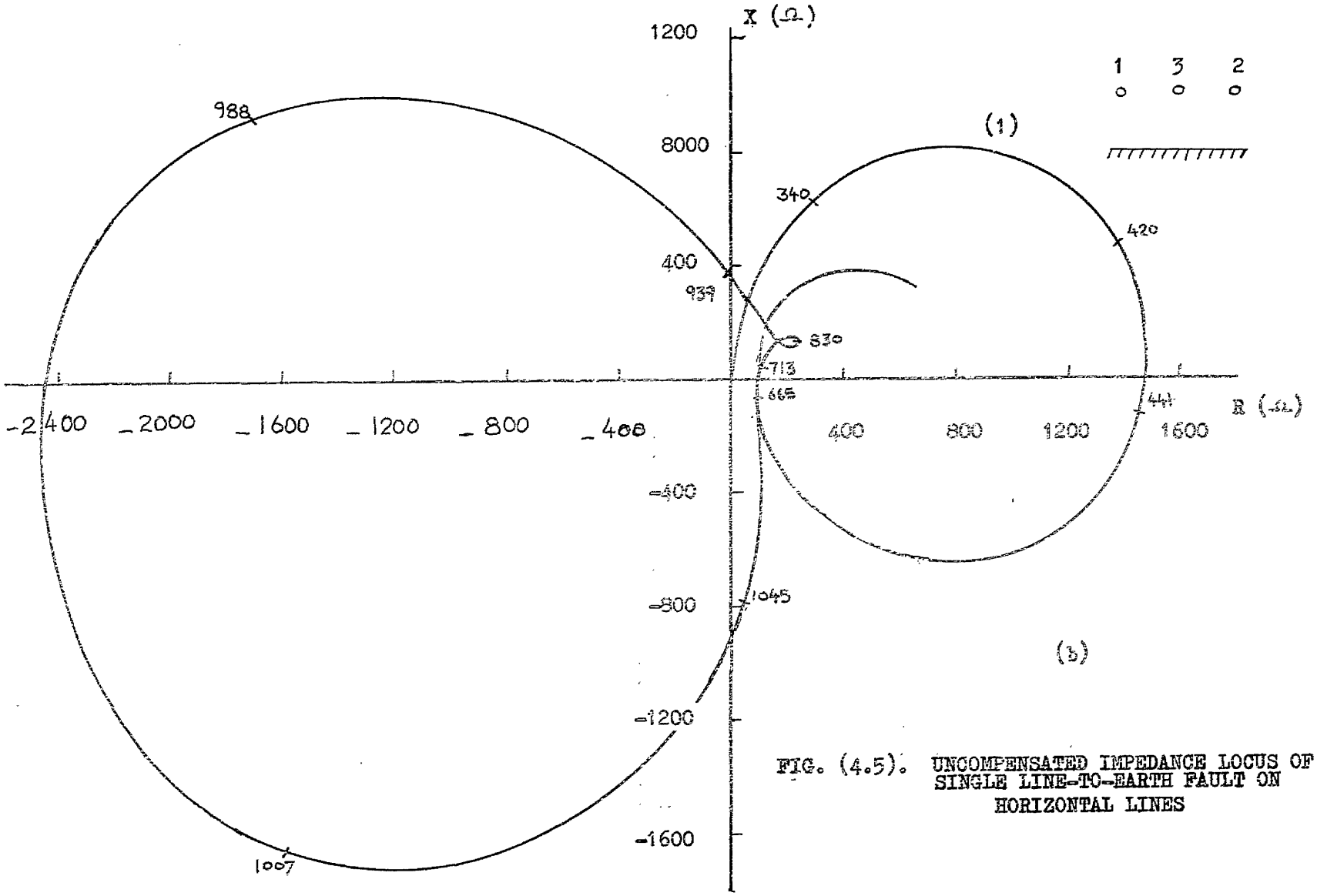

FIG. (4.5). UNCOMPENSATED IMPEDANCE LOCUS OF SINGLE LINE-TO-EARTH FAULT ON HORIZONTAL LINES

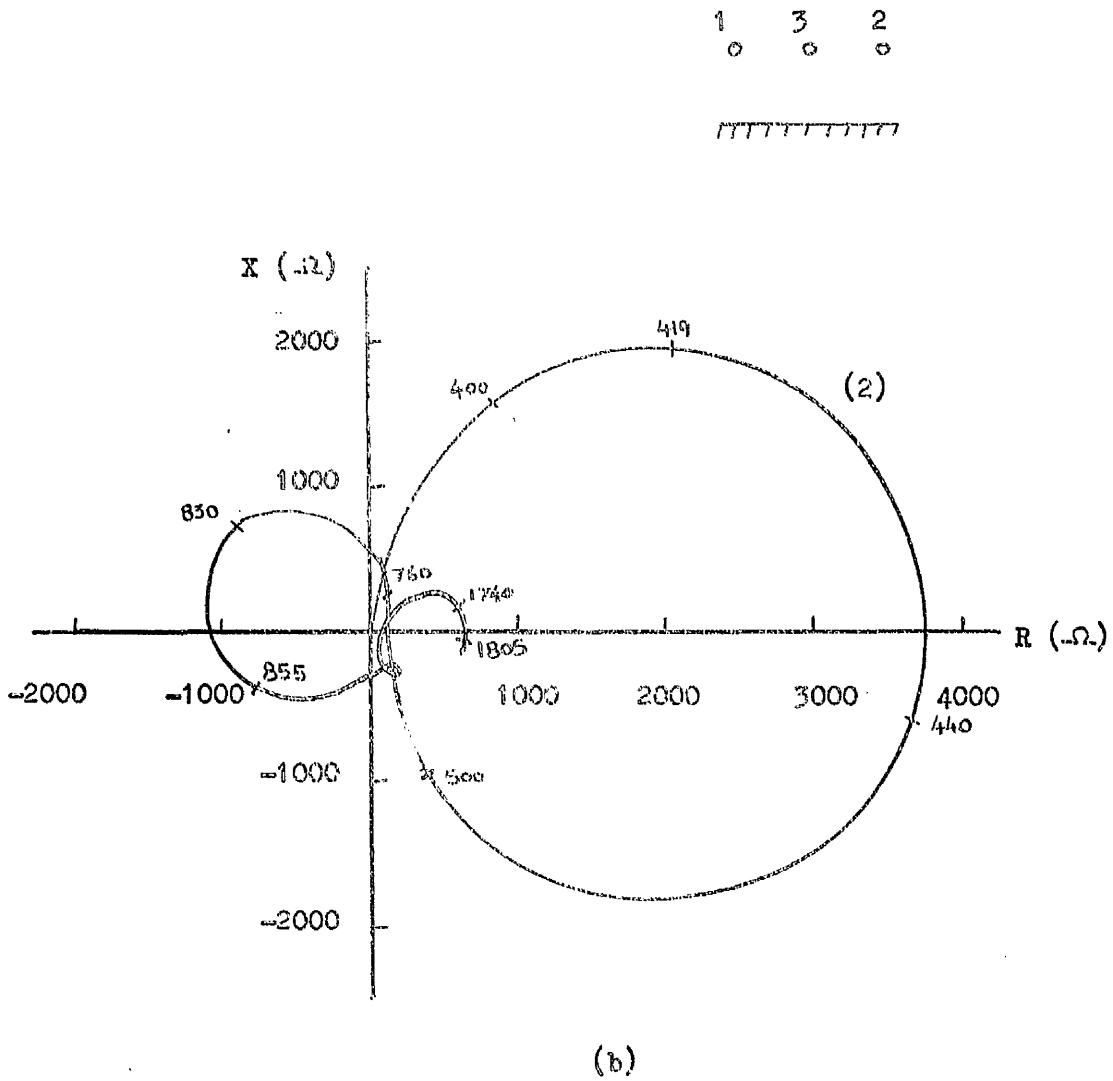

(b)

FIG. (4.5). UNCOMPENSATED IMPEDANCE LOCUS FOR SINGLE LINE-TO-EARTH FAULT ON HORIZONTAL LINES

confirmed for a fixed line length 450 miles long with the fault this time progressively changing position along the faulted conductor. The centre phase locus is also symmetrical for this case. The result is given in Fig . (4.6)

The apparent impedances seen due to single line to earth faults applied in turn to the phases of a vertical circuit line are shown in Fig. (4.7). The loci have similar characteristics to those of the flat line up to the eighth wavelength point but no symmetry is observed in their case. One common proeprty among the loci of the vertical circuit is that they are wholly contained within the first and fourth quadrants of the R-X plane. Again departure from the classical result is apparent.

4.4.2.3 Double line-to-Ground Faults

Three combinations of double-line-to-ground faults have been studied in order to draw out further comparisons between other types of unbalanced faults and balanced symmetrical faults. The fault involves two phases-to-ground at a time and the apparent impedances as seen by uncompensated ground relays have been determined. The results of studies are given for the horizontal line in Fig.(4.8) and Fig. (4.9). Fig. (4.8) shows the impedance locus of one of the two phases to which the fault has been applied while Fig. (4.9) shows the impedance locus of the other phase. For example, when a line-to-ground fault is applied on phases "1" and "2", the impedance locus for phase "1" is given in Fig. (4.8) and that of phase "2" in Fig. (4.9) and similarly for faults involving other phases as well. Normal phase rotation has been retained in the energisation voltages i.e. in the sequence a, b, c of a balanced three phase supply. It is clear that the input

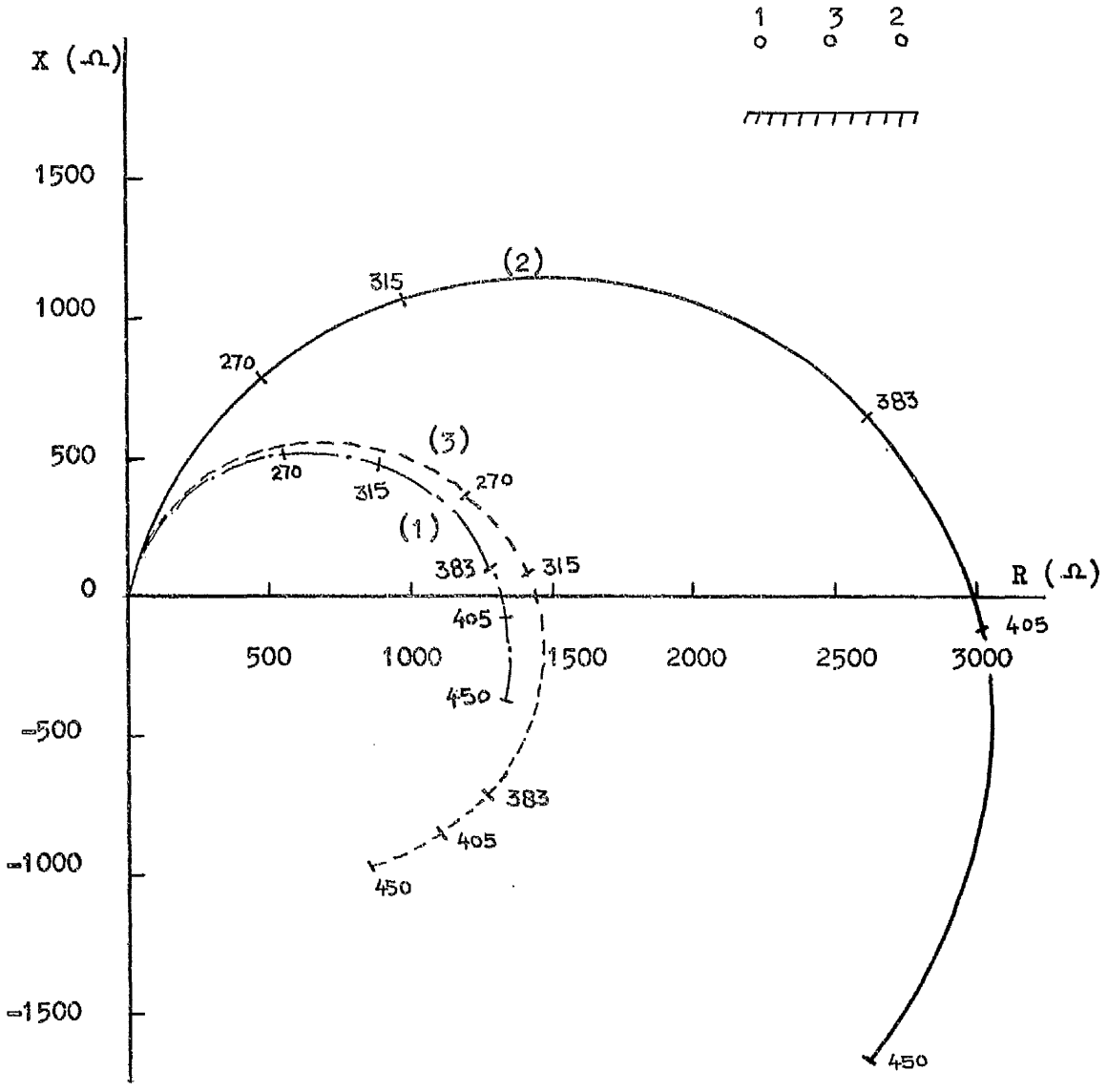

FIG. (4.6) UNCOMPENSATED IMPEDANCE LOCI OF SINGLE LINE-TO-EARTH FAULT ON 450-MILE HORIZONTAL LINE

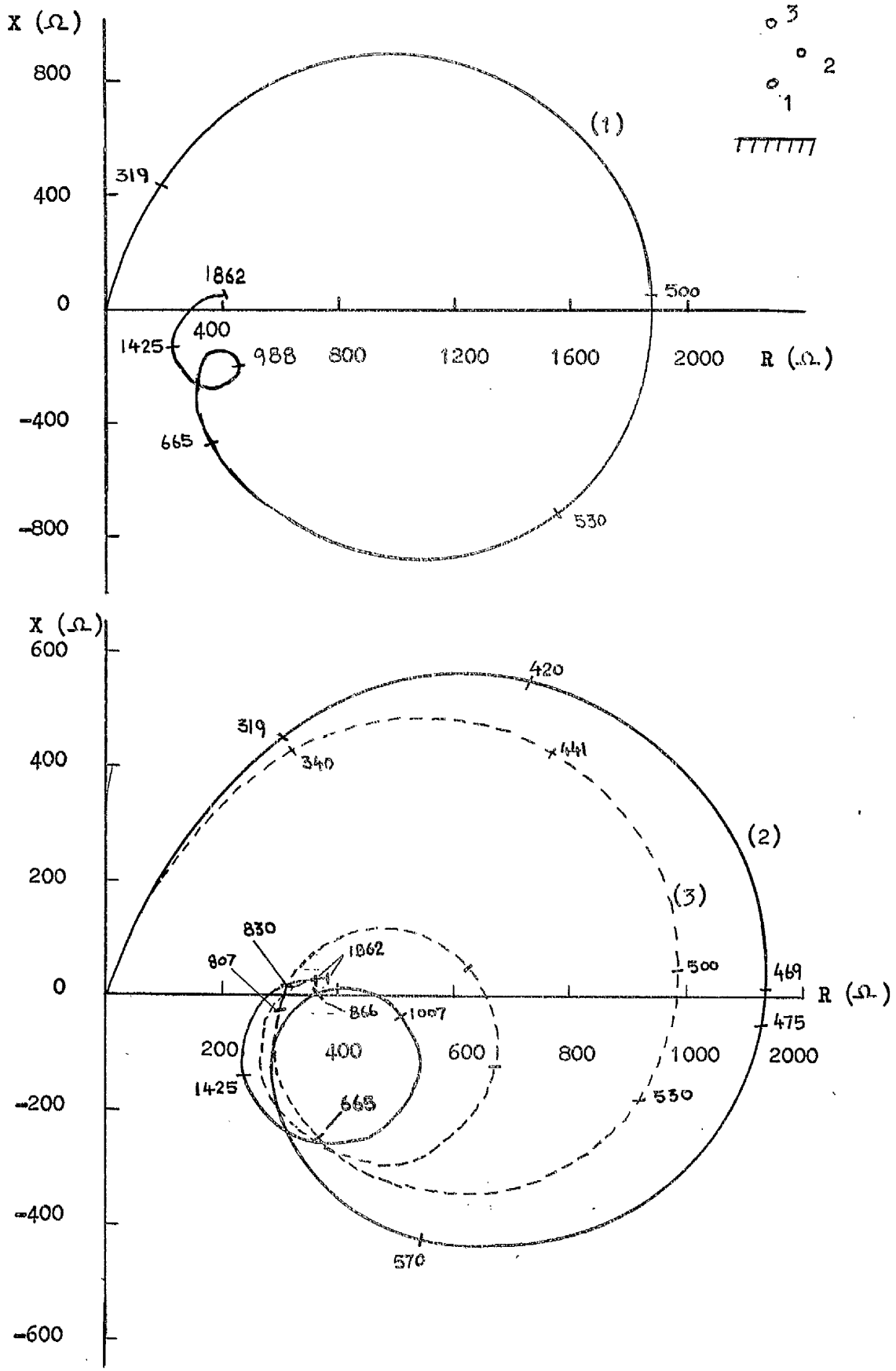

FIG. (4.7). UNCOMPENSATED IMPEDANCE LOCI FOR SINGLE LINE-TO-EARTH FAULT ON VERTICAL LINES

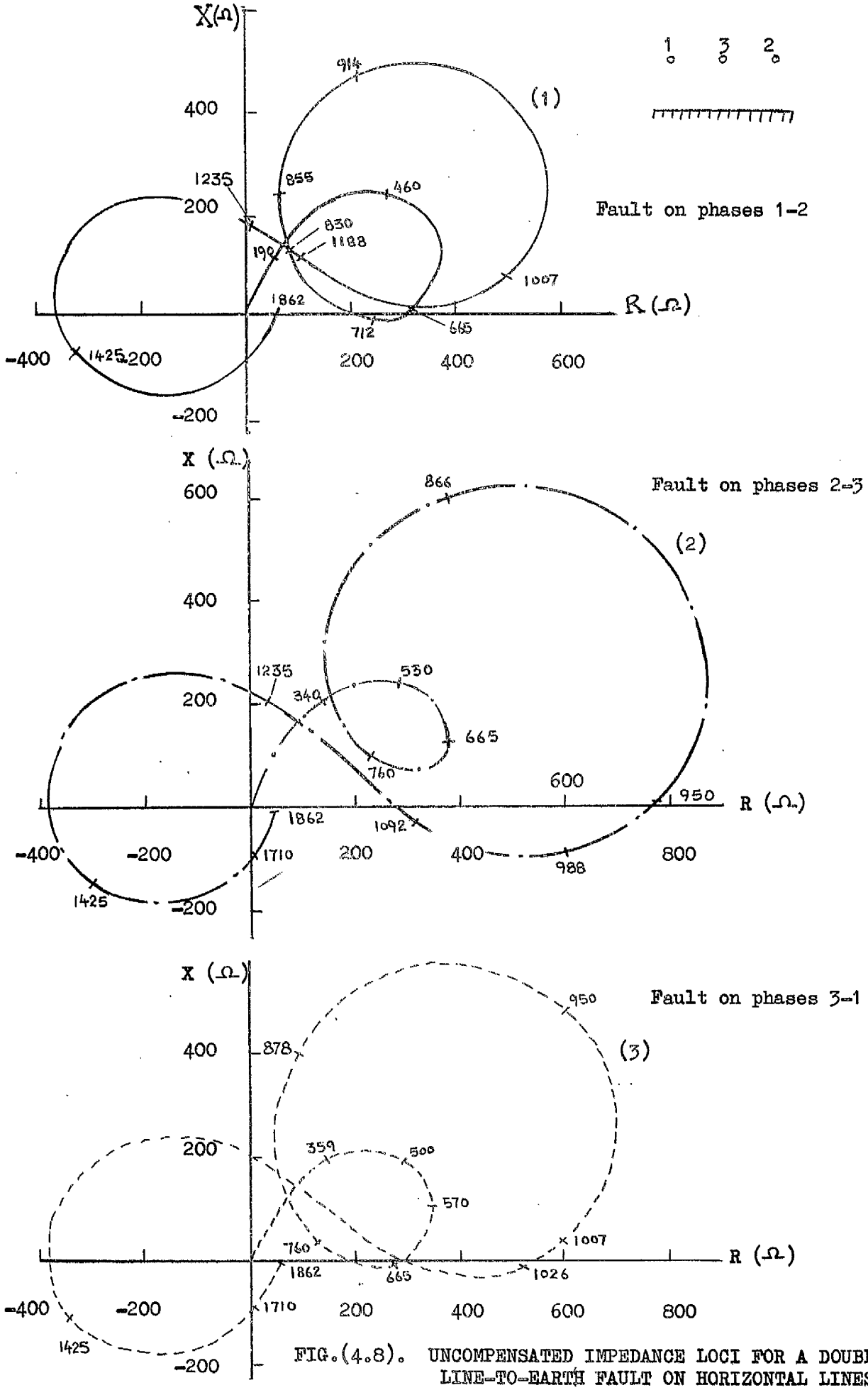

FIG.(4.8). UNCOMPENSATED IMPEDANCE LOCI FOR A DOUBLE LINE-TO-EARTH FAULT ON HORIZONTAL LINES

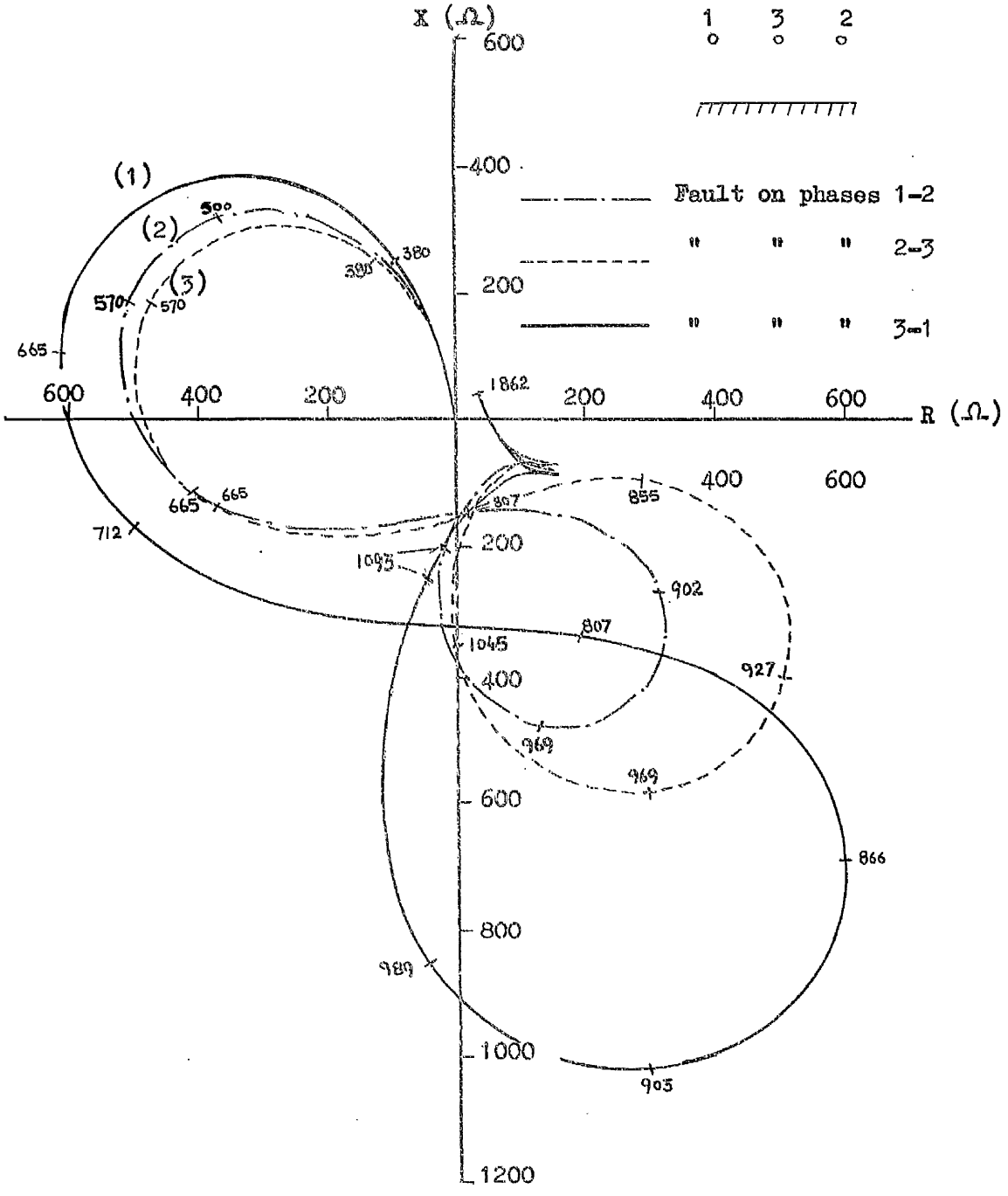

FIG.(4.9). UNCOMPENSATED IMPEDANCE LOCI FOR DOUBLE LINE-TO-EARTH FAULTS ON HORIZONTAL LINES

impedance of the leading phase of the two faulted conductors exhibited a tendency to resonate at the eighth wavelength point and later the quarter-wave point but thereafter has followed an arbitrary path which led into the second and third quadrants of the R-X plane following in this respect the trend of the single-line-to-ground phase impedance of the outer conductors of the same circuit. The lagging phase, however, has gone into "negative resonance" at the $\lambda/8$ point and this is confirmed for all such phases by Fig. (4.9). Though the apparent impedances for the leading phases bear a certain relationship to those predicted by conventional methods, their counterparts for the lagging faulted phase bear no relationship at all.

Similar types of results have been obtained for the vertical circuit line. The result is given in Fig.(4.10) for a double line-to-ground fault on the bottom and top conductors only as other phase combinations do not show marked differences in this general trend. The impedance locus of the leading phase for this line, in this case phase "3" is wholly contained within the first and fourth quadrants and hence shows similar characteristics to those of the phase impedance for a single line-to-ground fault on each of the conductors in turn.

4.4.2.4 Phase-to-Phase Faults

When isolated faults occur on long transmission lines then apparent impedances seen by relays which are fed by restraining signals proportional to the difference of line-to-ground voltages and operating signals

proportional to the difference of phasor currents are of interest. The ability of phase relays to discriminate against these types of faults depends mainly on whether the apparent impedance loci seen by the relay fall within the boundary of their characteristic. Before discussing the limitations involved studies for isolated phase impedance loci will be described for cases of isolated faults.

Results of loci characteristics for a phase-to-phase fault on bottom-middle, middle-top and top-bottom conductors of a vertical line are presented in Fig. (4.11). None of these phase loci resembles standard known results and the difference between the three loci particularly when they all appear as pure resistances is pronounced. An additional feature of these results is that the fault position at which resonance occurs varies from one set of phases to the other though there is a general tendency for conventional 50 Hz resonance to occur.

Results for two-phase isolated faults for horizontal lines are given in Fig. (4.12). With the fault occurring on the symmetrical outer conductors the result is typically conventional, the locus being symmetrical about the resistance axis and first resonance conditions being achieved at approximately a quarter wavelength. It has been confirmed that interchanging the phase rotation of the energising voltages from a forward sense, in which the normal sequence a, b, c corresponding with conductors 1, 2, 3 has been followed, to a reverse sense of a, c, b

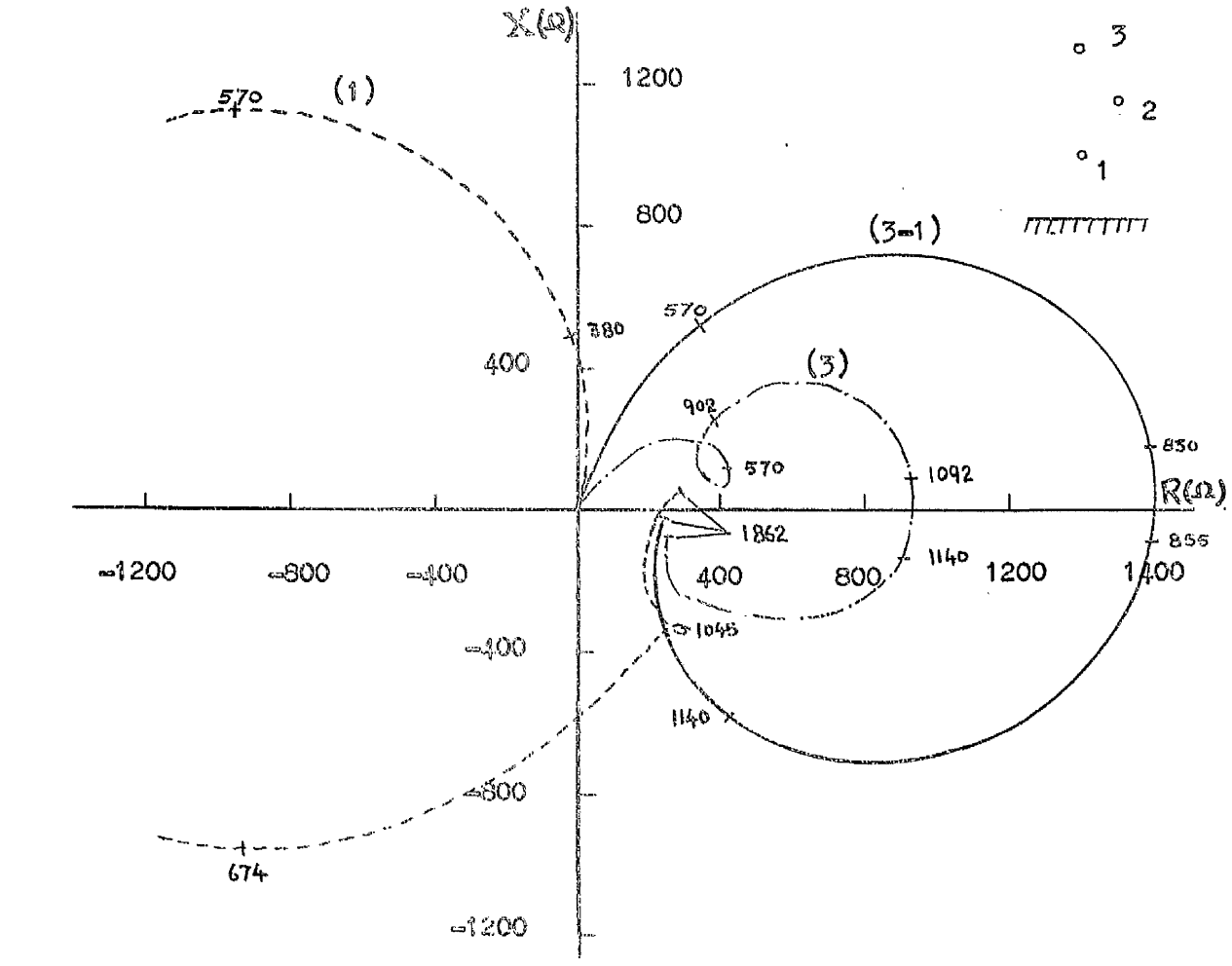

FIG. (4.10). UNCOMPENSATED IMPEDANCE LOCI FOR TWO LINE-TO-EARTH FAULT ON VERTICAL LINES

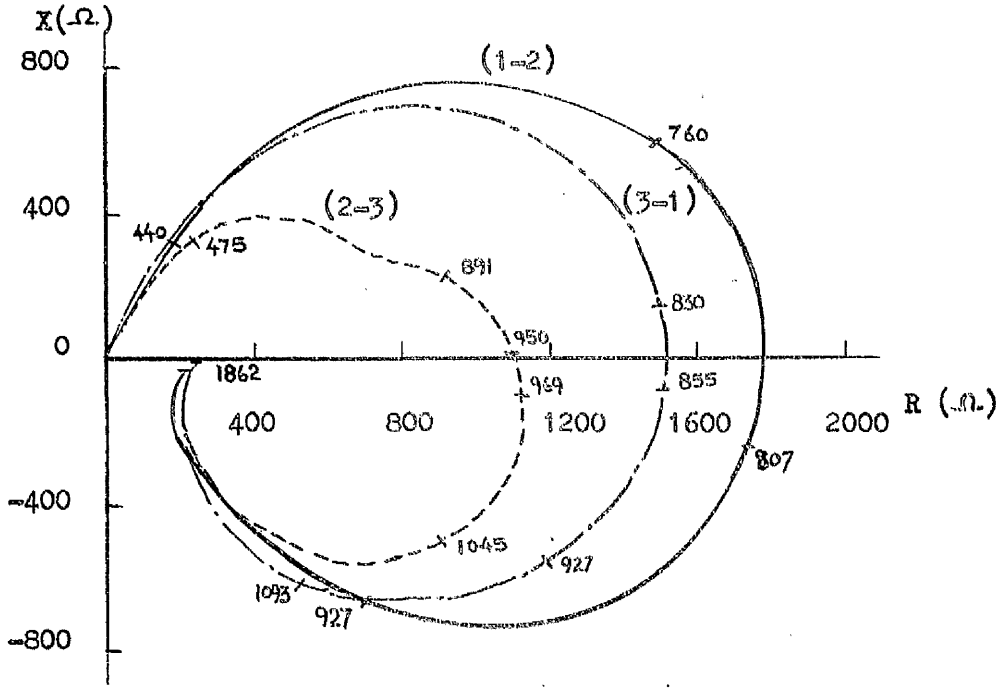

FIG. (4.11). UNCOMPENSATED IMPEDANCE LOCI FOR ISOLATED LINE-TO-LINE FAULTS ON VERTICAL LINES

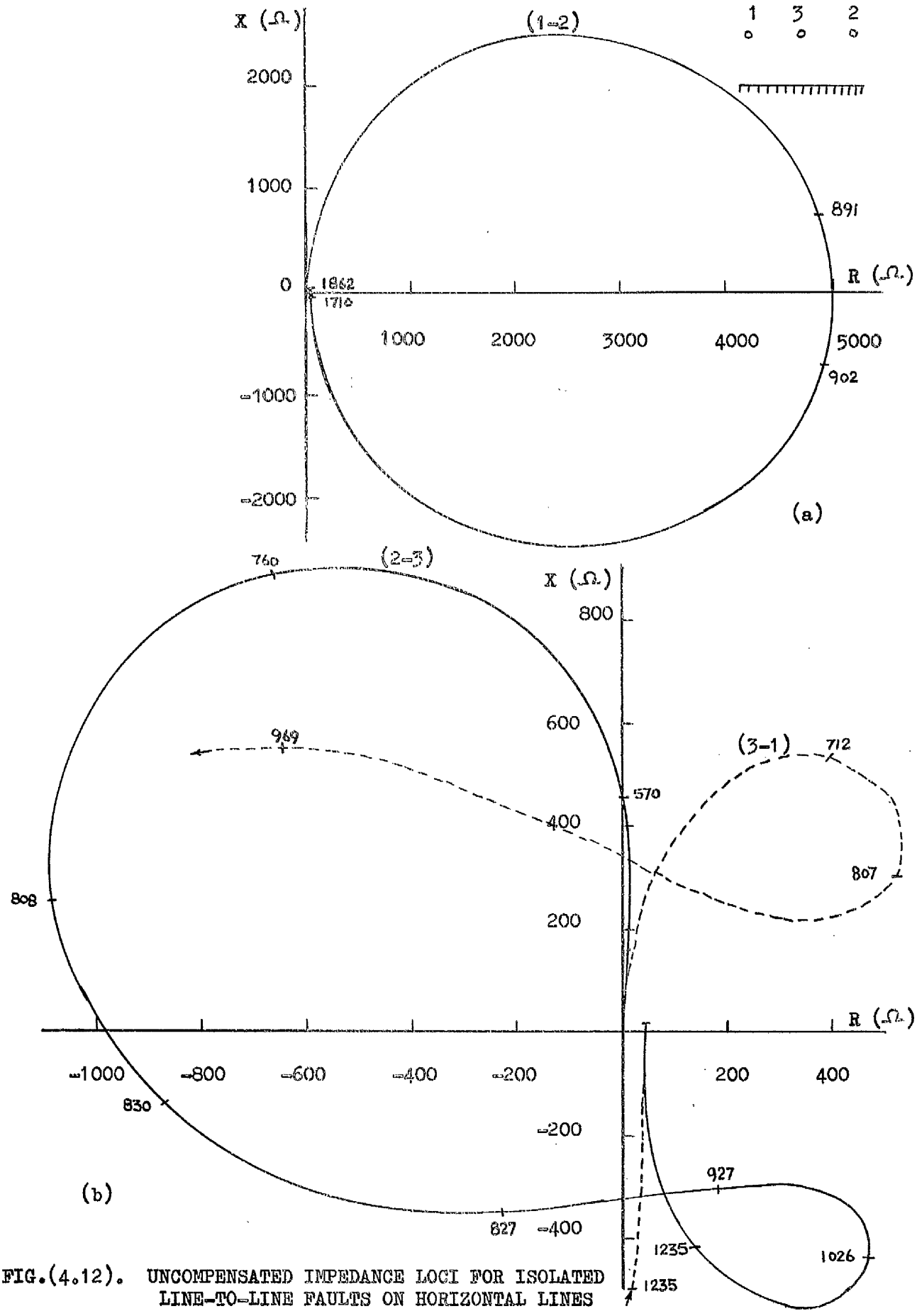

FIG.(4.12). UNCOMPENSATED IMPEDANCE LOCI FOR ISOLATED LINE-TO-LINE FAULTS ON HORIZONTAL LINES

for the same conductor arrangement does not alter in any manner the conditions shown in Fig. (4.12.a) for the symmetrical impedance locus.

Fig. (4.12.b) shows a set of conditions in which the fault has been applied between the centre and each of the outer conductors in turn. The departure of the characteristic from that of the classical case due to a fault on the outer conductors is clear and the appearance of negative resonance is indicated on the diagram. The impedance locus of phases "3-1" has been drawn for purposes of comparison on the same scale as that of phases "2-3". As the former occupies a bigger area of the second and third quadrants of the R-X plane it has therefore been confined to the limits indicated by the arrows. Phases "3-1" impedance locus intercepts the resistance axis at -1600 ohms for a fault distance of about 1111 miles from the sending end; it then curves round in a manner similar to that of phases "2-3" and passes through -800 -j1200 ohms at a fault distance of 1090 miles before it intercepts the reactance axis at -j580 ohms for a fault distance 1230 away from the source end. Phase rotation, however, for these unsymmetrical faults interchanges the loci so that the apparent impedance seen on phases "2-3" becomes that seen on phases "3-1" and vice-versa. The interpretation of this result will be discussed later.

4.5 Compensated Impedances Seen by Distance Relays for Faults on Very Long Lines

4.5.1 General

The apparent impedances discussed in the previous

section refer to uncompensated impedances seen on untransposed lines. The effect of the principles of compensation on the shape of these impedance loci will now be studied. The line considered in these studies is the horizontal line of section (4.3). The compensated impedance loci are presented for the case of a line fed from one end with the other end open-circuited and a line fed from both ends. Earth faults with sound phase and residual compensaton are considered. The line is energised from a balanced three-phase system and the effect of source impedance has been neglected. A description of a computer program for the evaluation of compensated apparent impedances will be given.

4.5.2 Computer Program for Evaluation of Apparent Impedances Seen by Distance Relays

The evaluation of apparent impedances seen by distance relays has been carried out using the short-circuit impedance loci digital computer program when the necessary modifications introduced by the theory of sound-phase and residual compensation derived on the basis of short lines have been used. The program is written out for all possible types of earth faults. It can handle cases where the line is fed from one end or from both ends. Fixed line lengths with faults varying progressively along their lengths or variable lengths with fixed faults at their receiving end terminals can be analysed.

A flow diagram of this program is shown in Fig. (4.13). The first stages of the program have already been described and reference is made to section (4.2) for

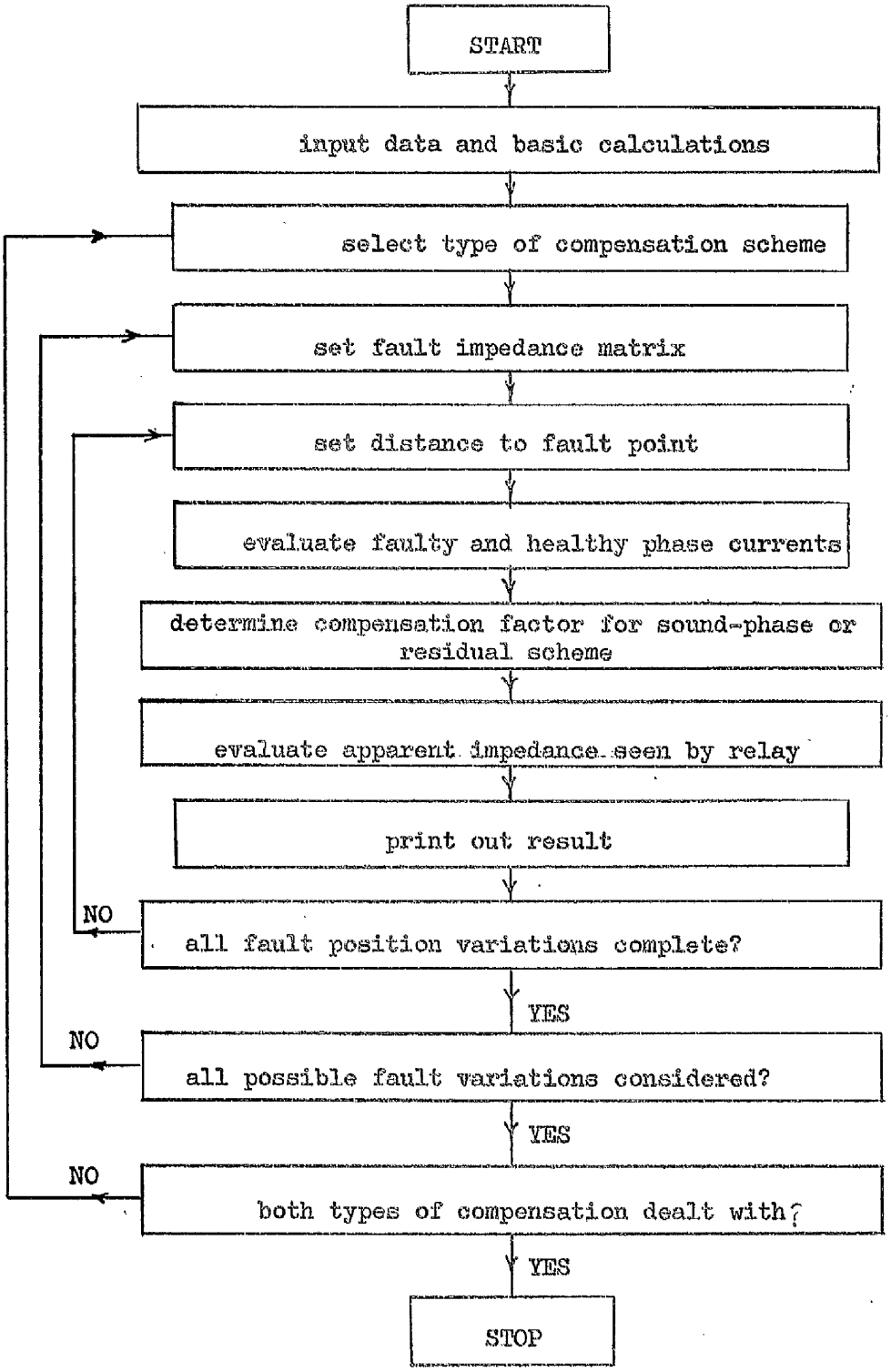

FIG. (4.13). FLOW DIAGRAM OF COMPUTER PROGRAM FOR DETERMINATION OF COMPENSATED APPARENT IMPEDANCES SEEN BY DISTANCE RELAYS

detailed discussion. It is important to include determination of the line positive and zero sequence impedances in the preliminary stages of the calculation since these will be needed in forming proportions of residual or sound-phase components needed in sound-phase and zero-sequence compensation.

The appropriate type of compensation scheme needed in the study is then selected, a switch facility is provided which enables this selection to be made. The choice of conductor or conductors to be faulted is followed by the setting of the fault admittance matrix. The distance to the fault is then cycled and this nominates the fault position on a line of fixed length or chooses a length of line with a fault applied at its receiving end terminals.

The process of computation for the apparent impedance seen by the relay starts by the evaluation of the faulty phase and healthy phase currents. The proportion of sound phase or residual currents is then obtained and the apparent impedance then determined. Results are then printed out.

The program then traverses a series of cycles to ensure that different fault locations, faults on all various conductors or combinations of conductors and different forms of relay compensation have been considered. The program then reaches its end.

4.5.3. Three-Phase-to-Earth Faults

4.5.3.1 200-mile line

The impedance loci of Fig. (4.14) show the apparent impedances seen by ground distance relays for the case of a 200-mile line with a three-phase-to-earth fault varying along its length. Fig. (4.14.a) gives the uncompensated impedances while Fig . (4.14.b) is indicating the zero-sequence compensated apparent impedances. From the results it has been found that the zero sequence compensation method is valid for the centre phase only with both real and imaginary components being equal to the positive sequence impedance of the section which is faulted. For the outer phases the reactive component of impedance agrees favourably well with the line positive sequence reactance but that its real component shows a big error in comparison with the line positive sequence resistance and negative resistance values as shown. The residual method of compensation is therefore valid only for the centre phase of this horizontal line.

4.5.3.2 450-mile line

The results are shown in diagrams (a), (b) and (c) of Fig. (4.15) for a transmission line 450 miles long for compensated and uncompensated impedance loci. The centre phase ground relay will respond correctly for this type of fault when residual method of compensation has been applied for faults distances covering 90% of the line but from there on the error is greater than 10%. In practice the result would be considered satisfactory for

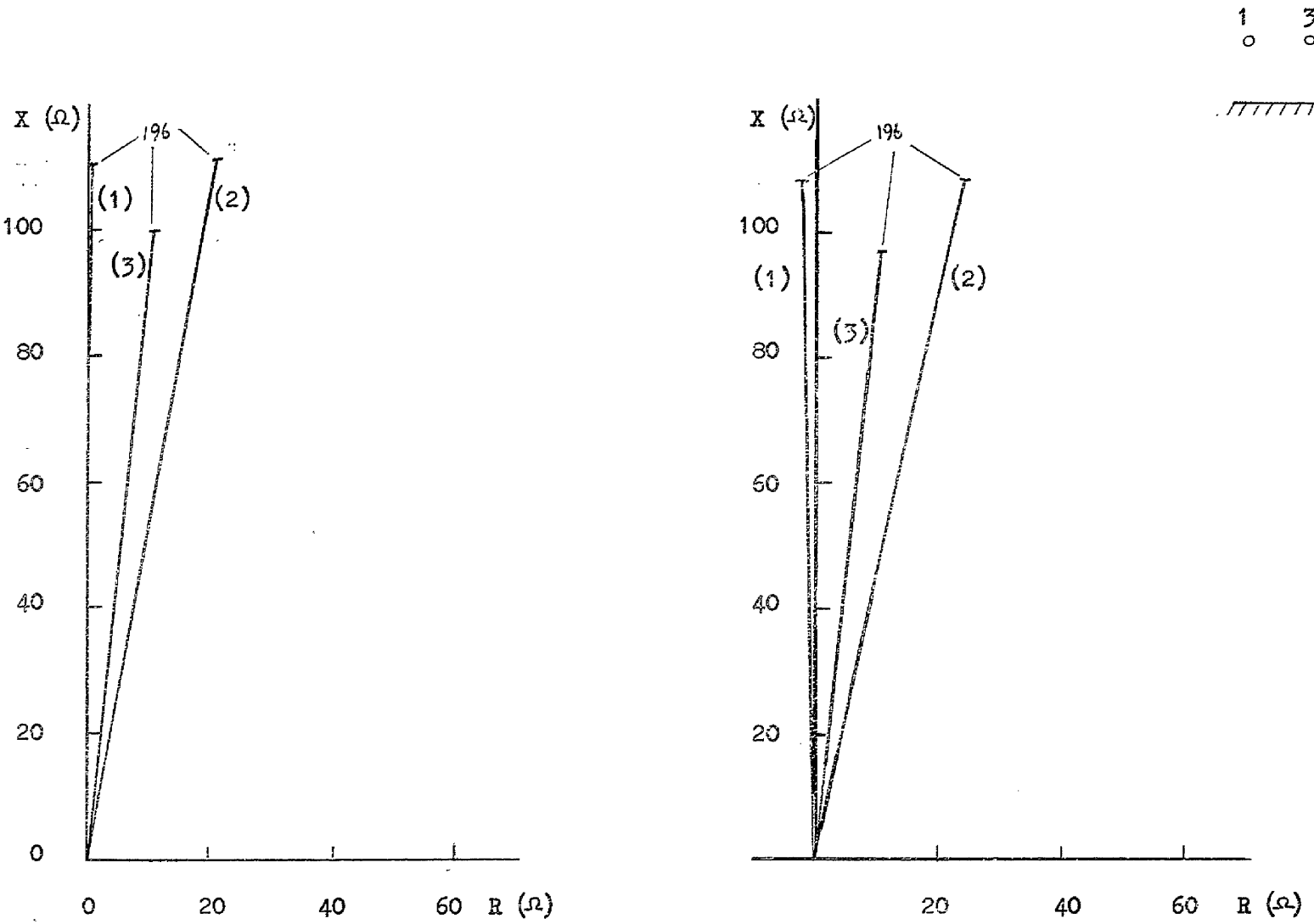

(a) Uncompensated impedance

(b) Zero-sequence compensated impedance

FIG. (4.14). COMPENSATED AND UNCOMPENSATED APPARENT IMPEDANCE LOCI FOR THREE PHASE-TO-EARTH FAULT ON 200-MILE LINE

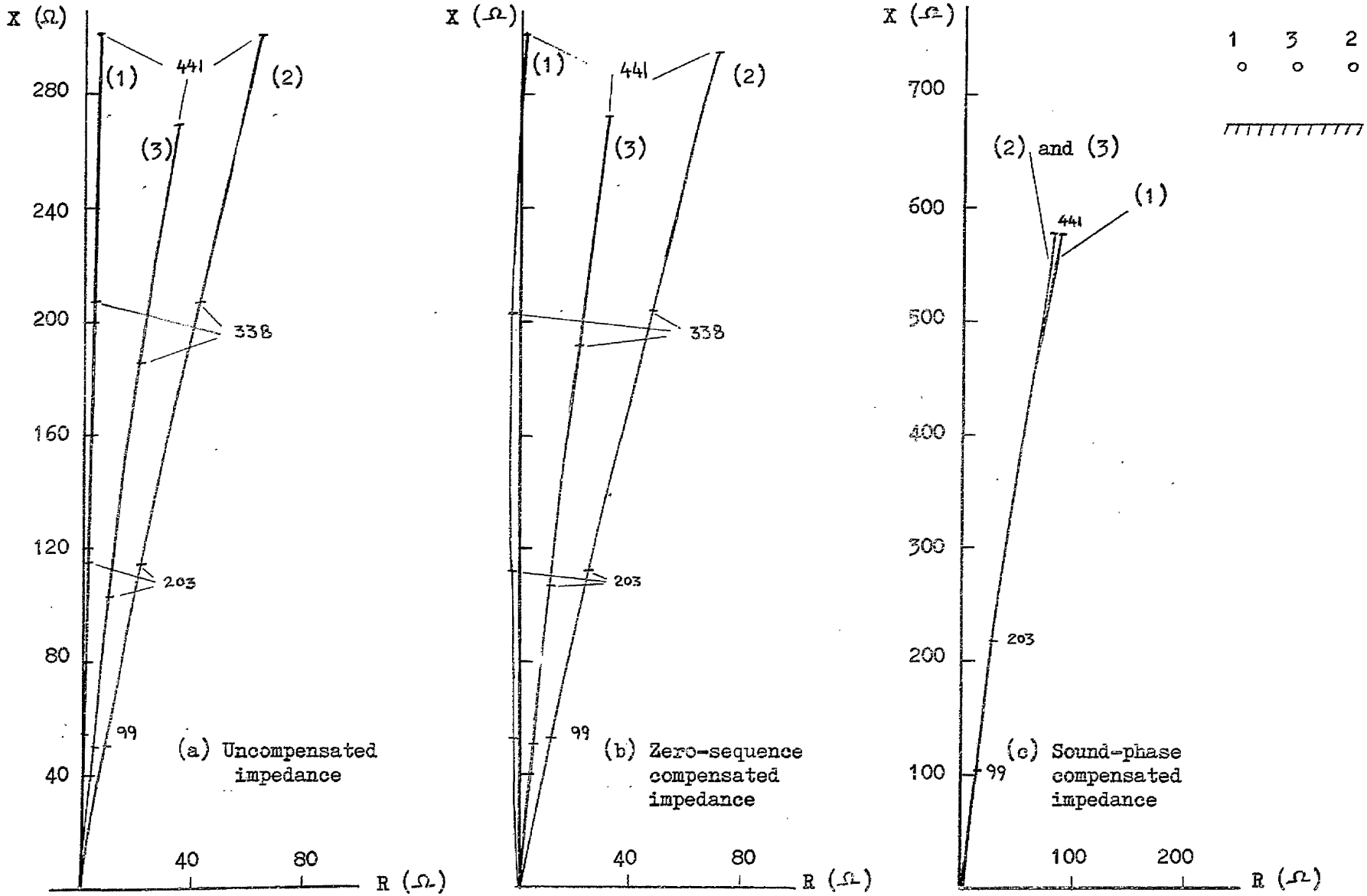

FIG. (4.15). COMPENSATED AND UNCOMPENSATED IMPEDANCE LOCI FOR THREE PHASE-TO-EARTH FAULT ON 450-MILE LINE

"zone one" relays [37,39]. When sound phase compensation has been applied, Fig. (4.15.c), the impedance characteristic coincides with their earth-loop impedance and for practical purposes the method is therefore workable for line lengths of the order considered for balanced 3-ϕ faults.

4.5.3.3 800-mile line

The deviation of the centre phase characteristic from positive sequence impedance when zero-sequence compensation has been applied has not been very pronounced for lines up to 450 miles long. The deviation becomes very noticeable as the line length increases further. A three phase-to-ground fault on an 800-mile line gives centre phase apparent impedances which are correct for fault distances lying within 38% of the line length only with maximum errors of about 4%. This method of compensation produces a pronounced deviation from the line positive sequence impedance for the apparent impedances of the outer phases. One phase resistive component takes negative values and the other phase resistive component takes large positive values which makes the overall apparent impedance in error compared with the line positive sequence impedance. The results are given in Figs. (4.16.a)and (4.16.b).

When sound phase compensation method has been applied it has been found that faults occurring within 25% of the line length show apparent impedances for all phases which have an error of 3.8% maximum from the earth-loop impedance. This error increases rapidly reaching a value of about 9% when the fault is 300 miles away from the source and 18%

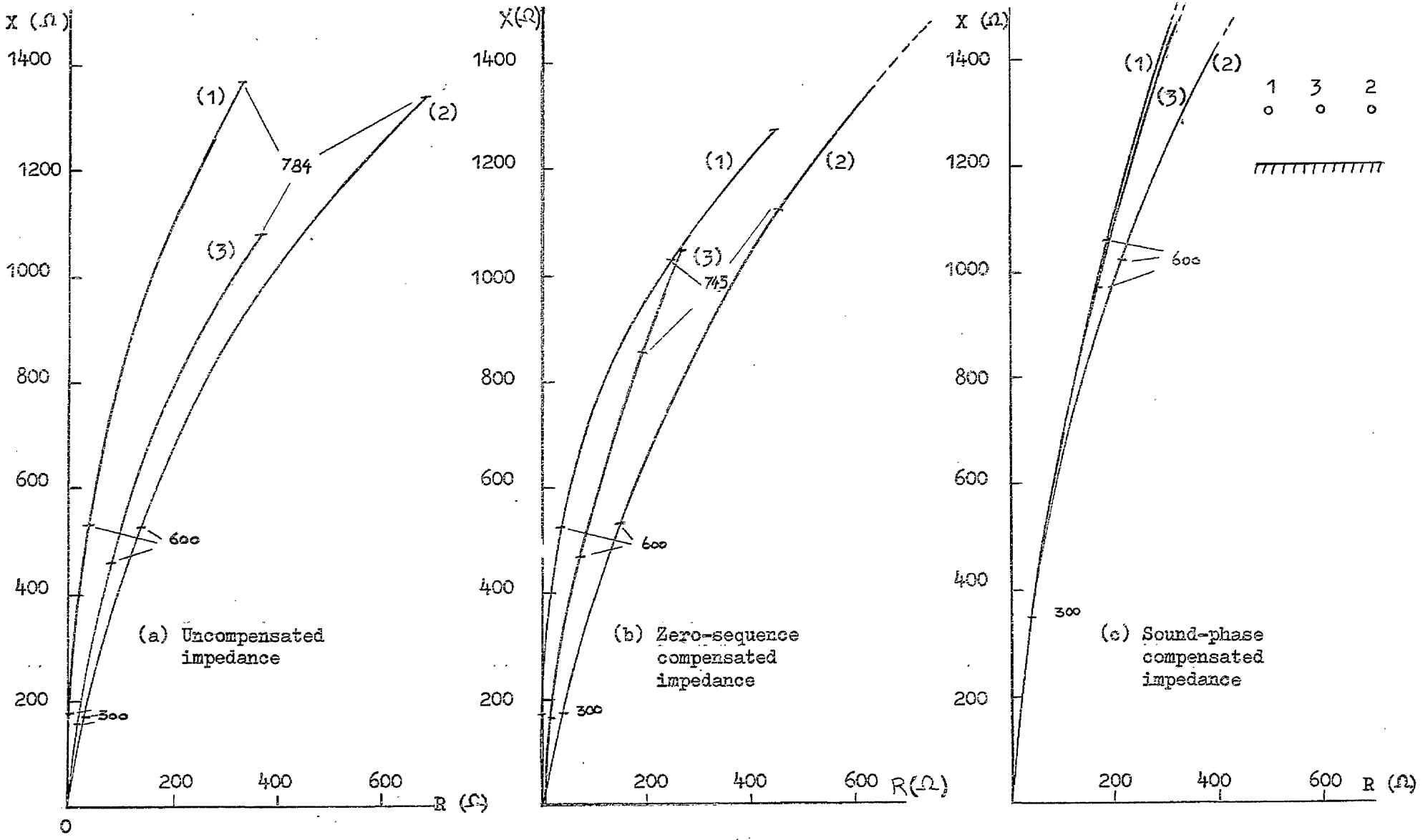

FIG. (4.16). COMPENSATED AND UNCOMPENSATED IMPEDANCE LOCI FOR THREE-PHASE-TO-EARTH FAULT ON 800-MILE LINE.

and 35% at 400 and 500 miles respectively with even greater percentage errors for greater fault distances. The loci characteristic is given in Fig. (4.16.c).

From these results it is clear that on the basis of accepted practices that neither method of compensation provides satisfactory operation of protection schemes under balanced faults for very long lines.

4.5.4 Single Line to Earth Faults

In the previous section a balanced type fault has been considered. Figs. (4.17), (4.18) and (4.19) show the compensated impedance loci for an unbalanced single line-to-earth fault. Uncompensated apparent impedance loci for the 450-mile line were given earlier in Fig. (4.6) . A feature of the 800-mile line is the pronounced asymmetry shown by the apparent impedances of the outer conductors when earth fault compensation has been applied. For this line both methods of compensation produce more regular patterns of loci from the completely distorted characteristic shown in Fig. (4.19.a) though in some cases these impedances fall in the second and third quadrants of the R-X plane.

4.5.6 Line-to-Line Fault

The cases of a 200- and an 800-mile lines have been considered for an isolated line-to-line fault and the apparent impedances seen by phase relays fed by signals proportional to the phasor difference of voltages and currents are given in Fig. (4.20). Whereas the 200-mile line can be easily protected in one stage by existing distance equipment for this type of fault, the 800-mile line

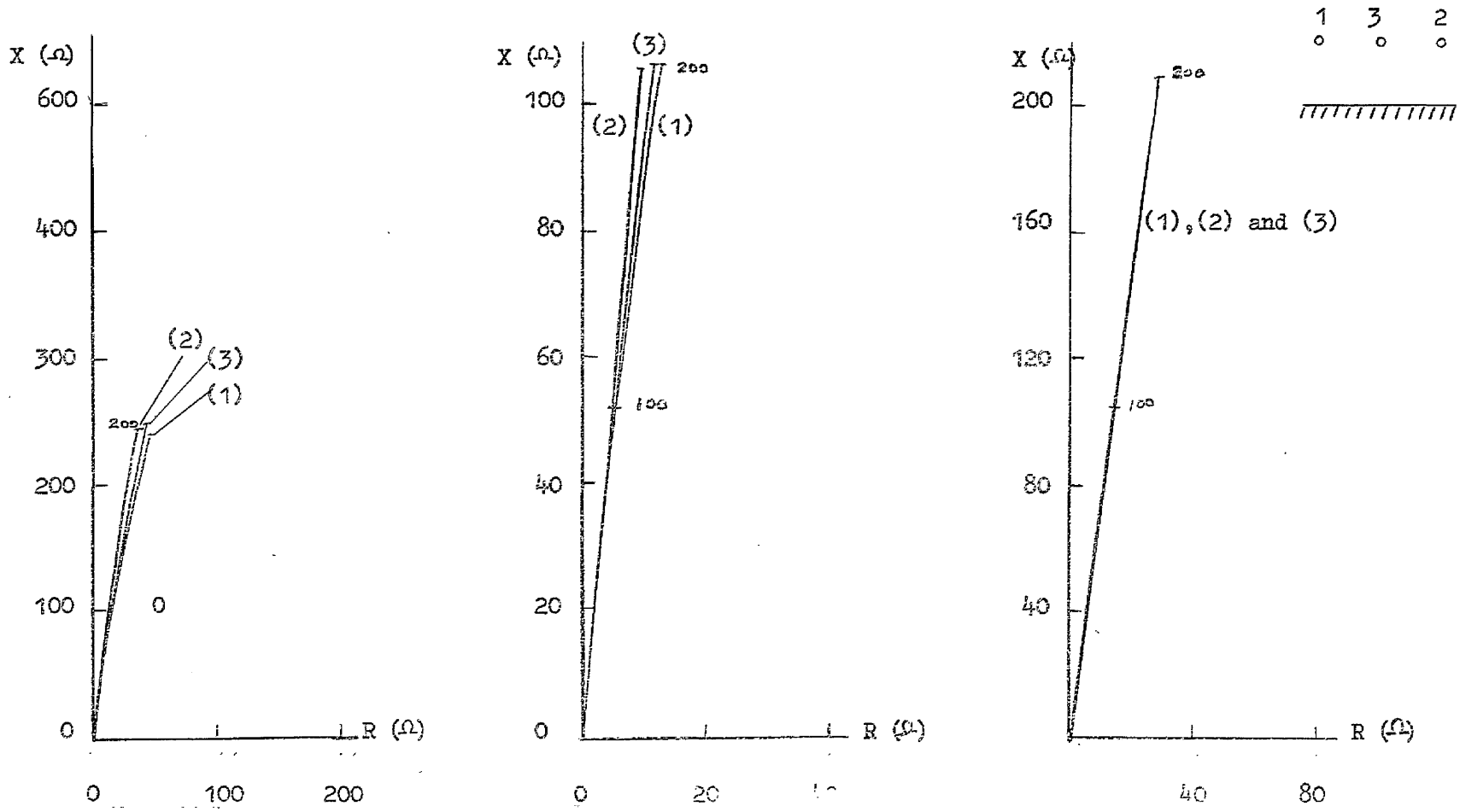

FIG. (4.17). COMPENSATED AND UNCOMPENSATED IMPEDANCE LOCI FOR SINGLE LINE-TO-EARTH FAULT ON 200-MILE LINE

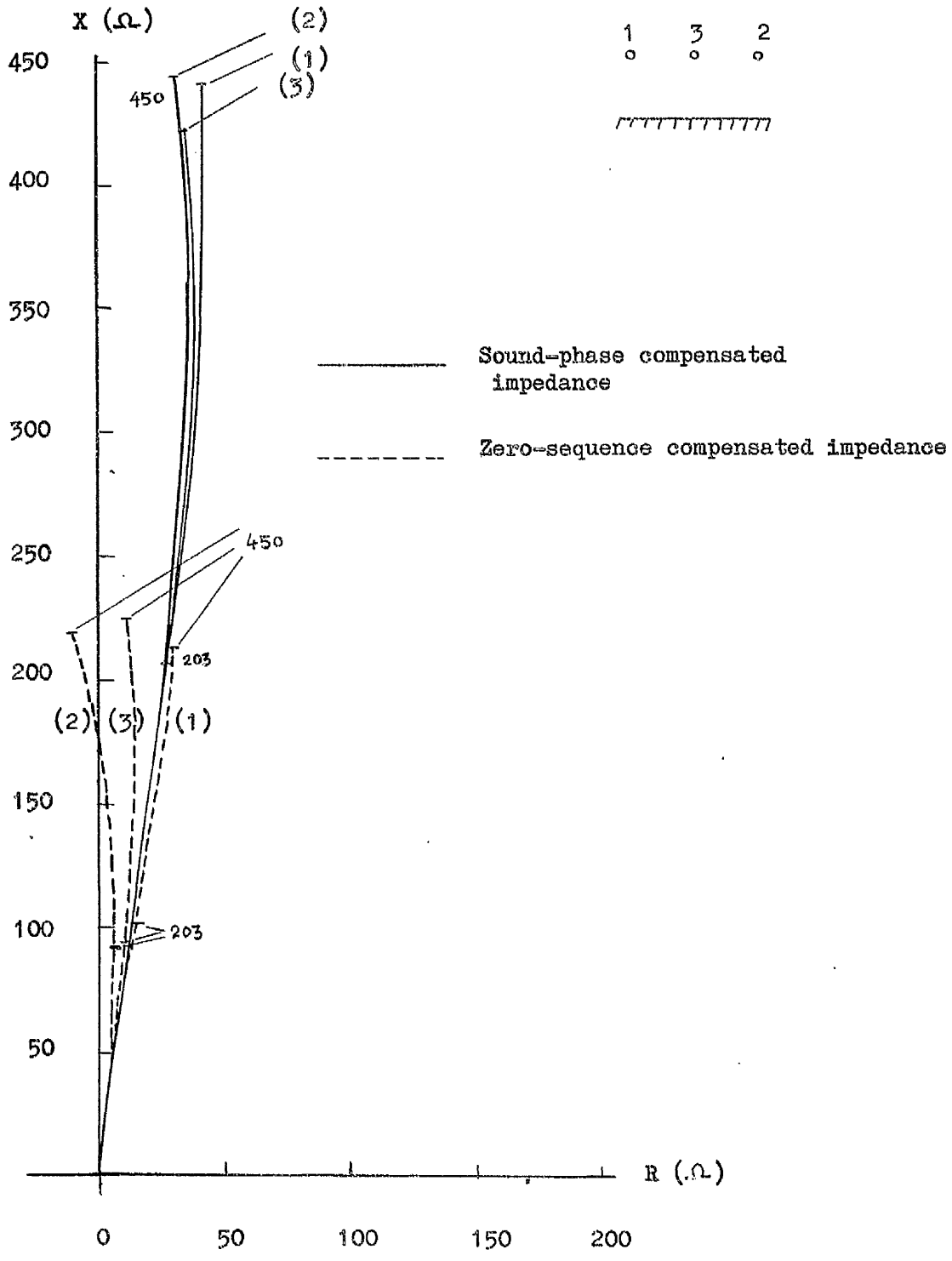

FIG. (4.18). COMPENSATED IMPEDANCE LOCI FOR SINGLE LINE-TO-EARTH FAULT ON 450-MILE LINE

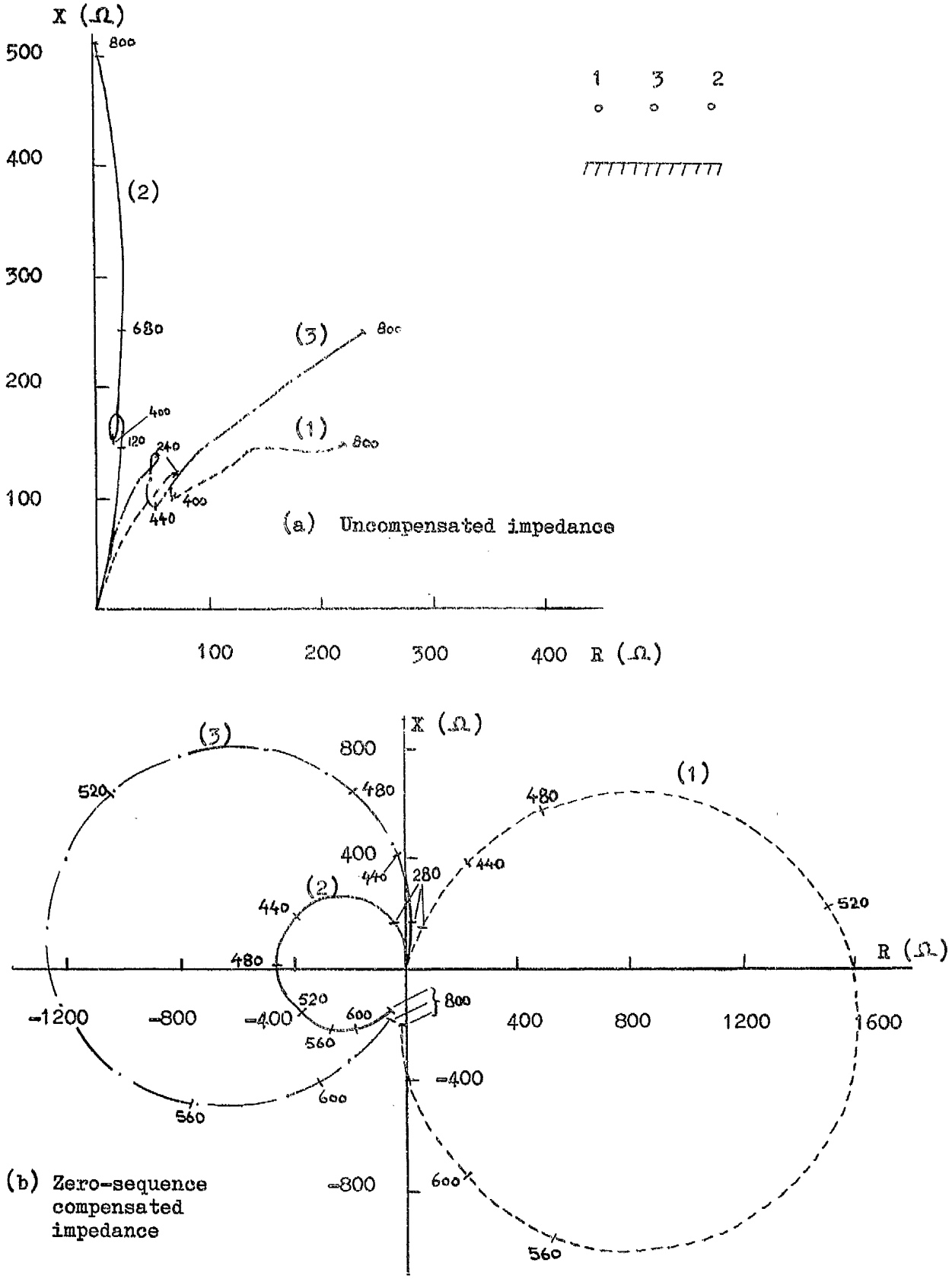

FIG. (4.19). COMPENSATED AND UNCOMPENSATED IMPEDANCE LOCI FOR SINGLE LINE-TO-EARTH FAULT ON 800-MILE LINE

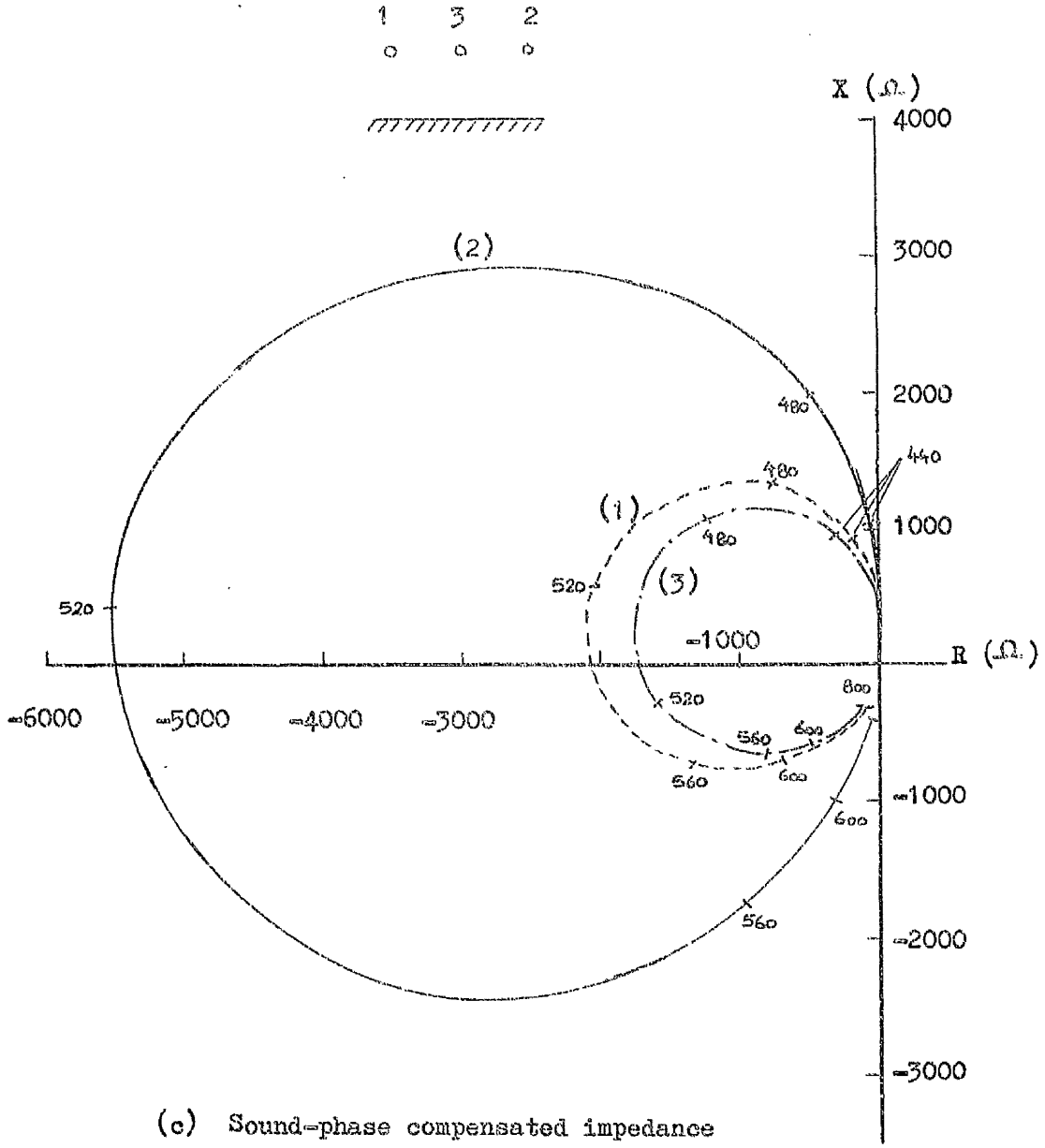

(c) Sound-phase compensated impedance

FIG. (4.19). COMPENSATED IMPEDANCE LOCI FOR SINGLE LINE-TO-EARTH FAULT ON 800-MILE LINE

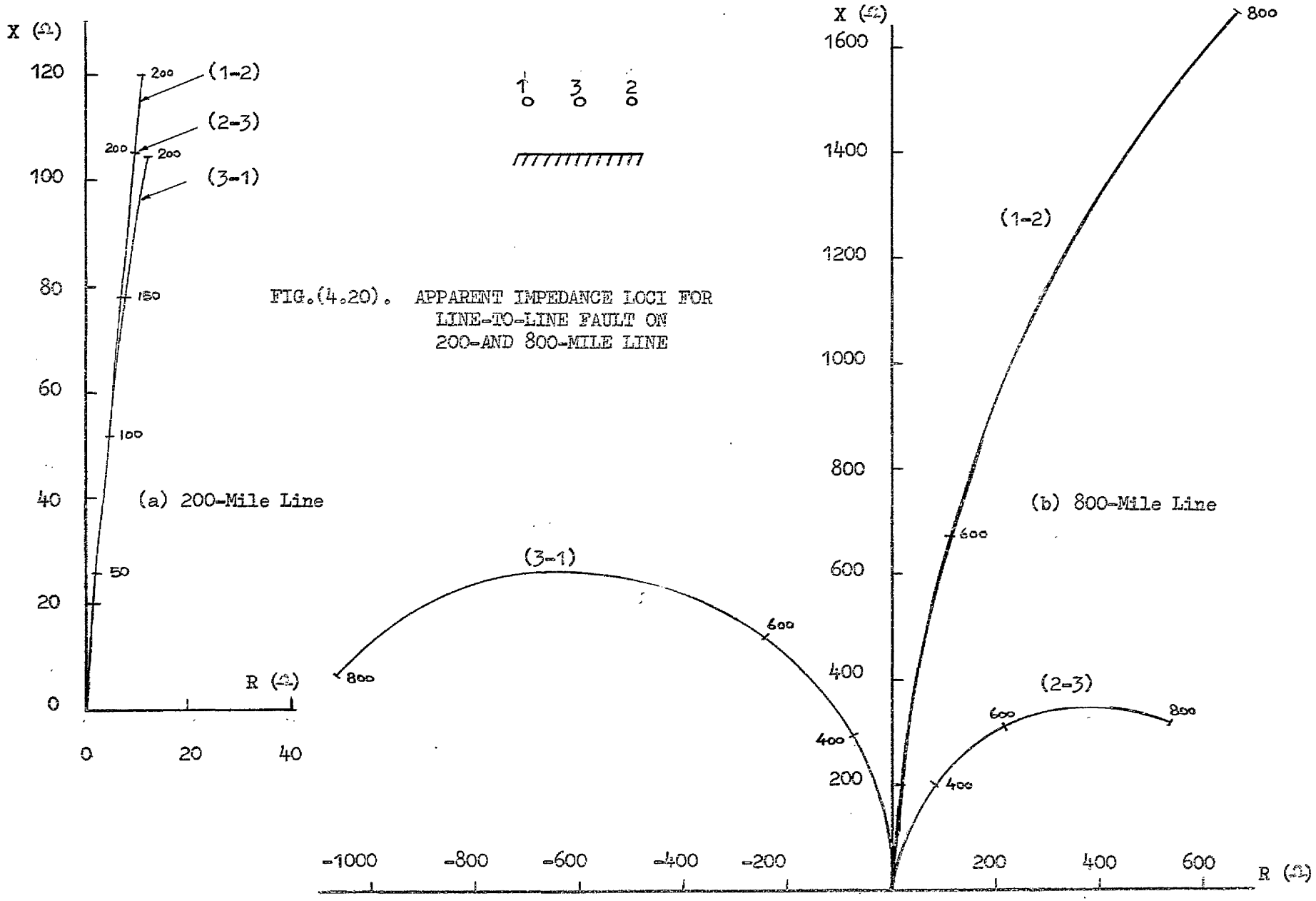

FIG.(4.20). APPARENT IMPEDANCE LOCI FOR LINE-TO-LINE FAULT ON 200- AND 800-MILE LINE

clearly presents complications as one phase locus - that of phases "2-3" - lies in the second quadrant and another locus - that of phases "1-3" - departs considerably from normal impedance-angle measurements of distance relays.

4.5.7 Distance Protection of Long Loaded Lines

An untransposed 800 miles long line is fed from both sending and receving ends from balanced three-phase systems with a load angle of 30°, this being a normal system operating angle for long lines. Single line-to-ground faults are applied on each phase in turn and the apparent impedance loci obtained after modification by principles of sound-phase and residual compensation It is evident from Fig. (4.21.a) that protection equipment utilizing residual methods of compensation would need special design considerations for detecting fault occurring at distances greater than 200 miles. The impedance seen is purely reactive for faults at 540, 340 and 460 miles on the first, second and thirdphases respectively. For greater fault distances a negative resistance component is indicated in the impedance loci of these phases.

Sound-phase compensation, however, extends the distance of possible fault detection to about 300 miles only, Fig. (4.21.b), but it is not until about 500 miles that the apparent impedance starts showing a negative resistance component. Special design considerations are also required.

For an isolated phase-to-phase fault at 300 miles from the sending end of the 800-mile line the theoretical

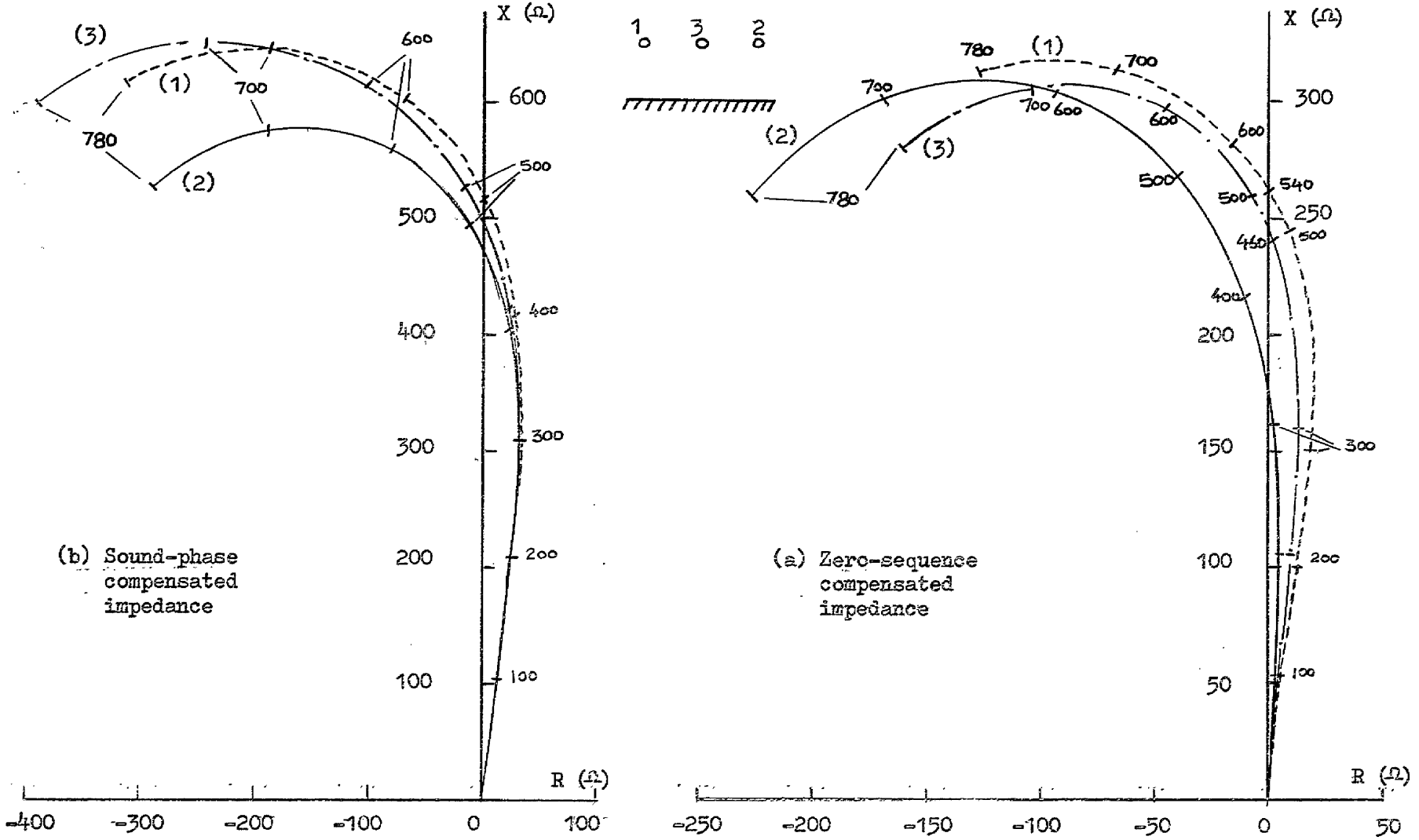

FIG. (4.21). COMPENSATED IMPEDANCE LOCI FOR SINGLE LINE-TO-EARTH FAULT ON 800-MILE LINE ENERGISED FROM BOTH ENDS

apparent impedances that would be seen at the relay locations are given below:-

$$\Delta Z_1 = 174 + j\ 14.2 \text{ ohms}$$
$$\Delta Z_2 = 152 + j\ 9.0 \quad "$$
$$\Delta Z_3 = 152 + j\ 9.0 \quad "$$

where ΔZ_1, ΔZ_2 and ΔZ_3 are apparent impedances seen by phase relays with a fault on phases "1-2", "2-3" and "3-1" respectively in accordance with part "B" of Appendix (3). The curves shown in Fig. (4.22) are a study of an isolated-type line-to-line fault applied to each phase pair of this line in turn. It is confirmed from a comparison with the theoretical figures just presented that for faults occurring at distances greater than 300 miles down the line that the errors between the theoretical and actual apparent impedances become intolerable and that distance protection for faults beyond this point need special consideration. A significant point to mention is that similar faults occurring on a line of comparable length but energised from one end only, a case which may arise in practice when the other end of the line has been tripped out, are capable of producing impedance loci which fall in the second quadrant of the R-X plane as shown in Fig. (4.20). In this respect a loaded line has at least some chances of being protected for faults occurring within specified zones of its length with present practice.

4.5.8 Effect of Fault Impedance

In order to illustrate the effect of fault impedance on the performance of distance protection on long

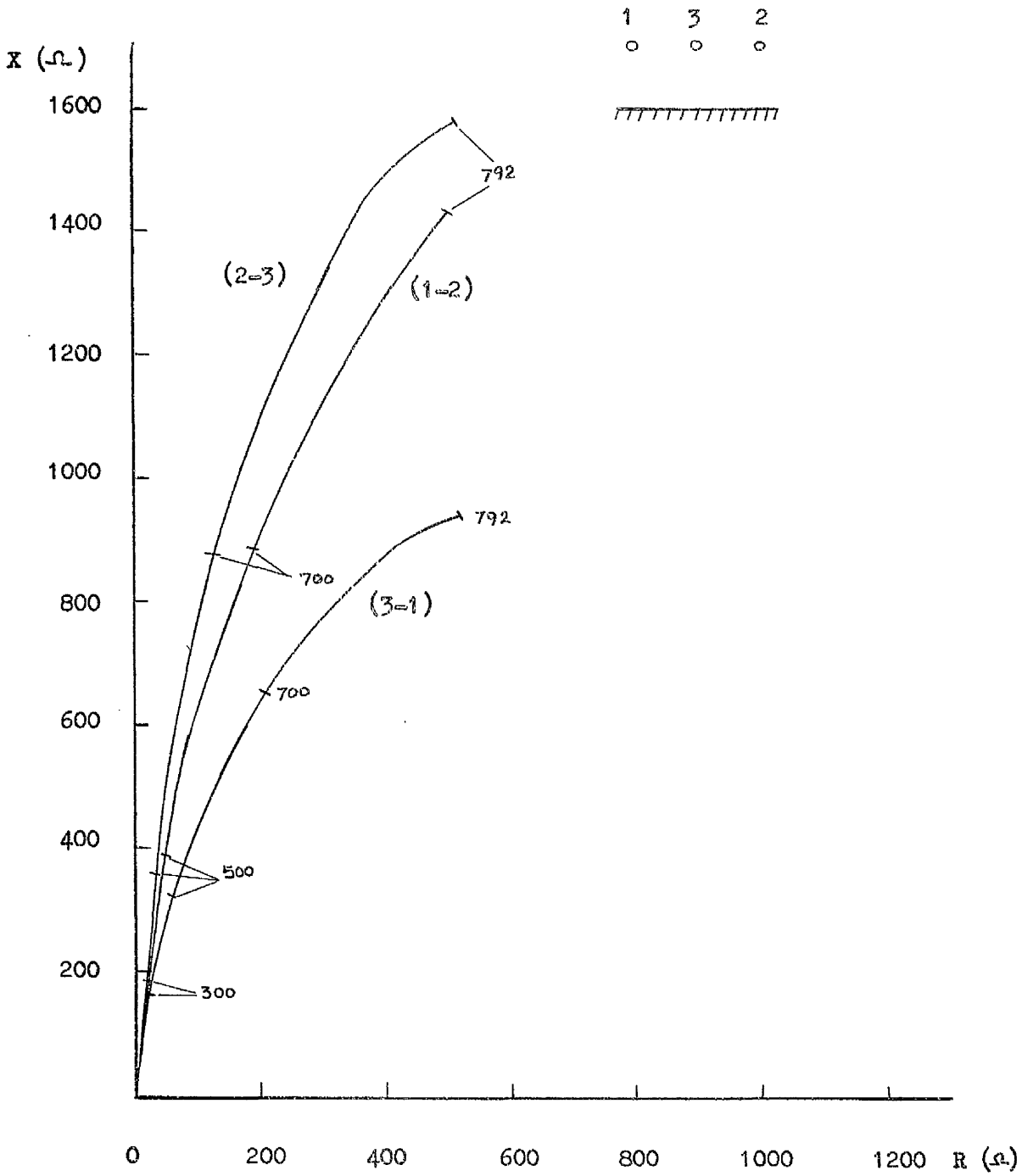

FIG. (4.22). APPARENT IMPEDANCE LOCI FOR ISOLATED LINE-TO-LINE FAULT ON 800-MILE LINE ENERGISED FROM BOTH ENDS

lines an 800-mile line has been considered; in one case fed from one end only and in the other fed from both ends with a transmission angle of 30°. The effect on sound-phase compensated impedance for a single line to ground fault applied on each of the three phases in turn is shown in Tables (4.3) and (4.4) for double-ended and single-ended systems respectively. The tables give comparative studies for solid faults and high impedance faults, the fault impedance being taken as purely resistive and of value 5 ohms. The earth-loop impedance of the conductors is also given for faults occurring at the specified distances shown.

For the double-ended system there is no marked difference in the magnitude of the apparent impedance for solid faults and faults through an impedance, but that the angle of impedance changes for the two cases for faults beyond 75% of the total transmission distance. Solid faults on single-ended systems produce greater apparent impedances than do faults through impedances for fault distances greater than 50% of the line length and the deviation between the two values of apparent impedances from thereon are very noticeable. For shorter distances resistance faults on such single-ended systems result in greater errors in the angle of apparent impedance as indicated by Table (4.4) where the error increases from 2.72, 5.75 and 11.25 per cent for decreasing fault distances from 200 miles.

4.6 Discussion and Interpretation of Results

The results presented in this investigation for an

TABLE (4.3). EFFECT OF FAULT IMPEDANCE ON APPARENT IMPEDANCE SEEN BY DISTANCE RELAYS FOR A DOUBLE-ENDED SYSTEM

Fault dist.	earth loop impedance ohms		apparent impedance due to solid fault (ohms)						apparent impedance due to fault through impedance (ohms)					
			phase (1)		phase (2)		phase (3)		phase (1)		phase (2)		phase (3)	
miles	mod.	angle	mod.	angle	mod.	angle	mod.	angle	mod.	angle	mod.	angle	mod.	angle
40	42.4	83.1	41.6	82.3	41.6	82.3	41.5	82.3	42.4	75.8	42.4	75.8	42.4	75.8
120	127.2	"	124.8	82.5	124.9	82.6	124.3	82.5	125.3	80.2	125.4	80.2	124.9	80.3
200	212	"	208.4	82.9	208.9	83.0	206.6	83.0	208.7	81.3	209.4	81.5	207.3	81.5
300	318	"	313.4	84.0	315.3	84.4	308.6	84.3	313.5	82.7	315.7	83.1	309.0	83.2
400	424	"	417.5	86.2	422.7	87.1	406.3	87.0	417.5	85.0	423.0	85.8	406.6	85.8
500	530	"	517.6	90.1	528.2	91.7	495.0	91.4	517.3	88.6	528.5	90.2	495.2	90.0
600	637	"	607.1	96.6	624.7	99.3	565.8	98.3	606.7	94.3	625.9	96.9	566.4	96.3
740	785	"	687.9	111.6	710.1	116.5	608.0	113.4	691.4	103.2	723.9	107.8	614.7	106.0
780	826	"	693.8	117.1	713.9	122.9	602.3	118.8	710.9	91.3	766.1	95.9	630.5	96.1

TABLE (4.4). EFFECT OF FAULT IMPEDANCE ON APPARENT IMPEDANCE SEEN BY DISTANCE RELAYS FOR A SINGLE-ENDED SYSTEM

fault dist.	earth loop impedance ohms		apparent impedance due to solid fault (ohms)						app. impedance due to fault through impedance (ohms)					
			phase (1)		phase (2)		phase (3)		phase (1)		phase (2)		phase (3)	
miles	mod.	angle	mod.	angle	mod.	angle	mod.	angle	mod.	angle	mod.	angle	mod.	angle
40	42.4	83.1	41.5	82.7	41.5	82.3	41.5	82.2	42.5	73.8	42.1	73.9	42.3	73.8
120	127.2	"	125.2	82.6	125.3	82.7	124.8	82.6	126.5	78.4	125	78.6	125.8	78.3
200	212	"	214.4	83.3	215.3	83.4	213.2	83.4	216.9	80	216	80	215.3	80
300	318	"	360	85.7	365	84.8	359.8	86	366	82.5	367.5	81.6	365.7	82.4
400	424	"	666.6	93.1	699.9	88.5	697.7	95.7	687	89	709.7	84	724	91.2
500	530	"	189 4	1382	3506	121	1789	164	2193	135	4192	107.6	2131	165
600	637	"	982.7	-132.5	1068	-107.5	704	-129	1002	-129	1075	104	716.1	-126
784	830	"	377	-111.6	378	-96.1	311	-110	378	-110	378	95.4	312.3	-110

untransposed multiconductor line have shown that the uncompensated short-circuit impedance loci of these lines are very different from those predicted by classical transmislsion line theory. An interpretation of the results may be made by considering that the current presented to the relay is made up of two components namely the falling fault current of the faulted conductors with increasing line length reaching a minimum value at the quarter-wave resonance point and the rising capacitance current of the floating conductors which increases with line length. This capacitance current is fed from the faulty conductors through the line mutual admittances. Since these two components have nearly opposite polarity it is evident that there must be a "false" resonance at a lower than normal frequency. This has been indicated for the case of unbalanced single line or double line to ground faults where interaction takes place between the capacity currents due to the floating conductors and the inductive currents due to the short circuited conductor resulting in an eighth wavelength resonance point.

This property of false resonance is not indicated in the case of a balanced three-phase-to-ground fault since the line capacitive admittances have been shorted out and hence the line shows conventional type loci for all three phases. In the case of an isolated fault on the outer phases of a horizontal line a similar type of result has been obtained. This is mainly due to the fact that the capacitance current components fed to the outer phases are

identical in view of the symmetry of the outer conductors of this line. In this case the phase impedance locus is formed from the difference of the line to ground voltages of those phases and the difference of phasor current; it is clearly seen as a result that the capacitance current cancels out and thus only a conventional type locus is obtained in this case. With the fault applied between a centre and an outer phase the phasor fault current difference will consist of a capacitive component as well as an inductive one since the two capacitance currents for this asymmetrical case are different. This leads to the peculiar patterns of loci shown for the centre and outer phases of a horizontal circuit line.

In the case of unbalanced faults the mutual current component to the unfaulted phases is the sum of all products of interphase voltages and corresponding mutual admittances. For a three-phase system since these voltages are displaced by 120 degrees from each other and 30/150 degrees to the phase-neutral voltage it is clear that the angle and modulus can be quite arbitrary and hence can give rise to apparent negative resistance. The converse argument applies in the case of phase-to-phase faults where the capacitance current component is a composite function of the phase-neutral voltages and hence negative resistance value shown in the loci.

In the case of the impedance loci obtained when the line has been energised from pure modes the loci patterns are conventional. The aerial modes give rise to differential

current modes which cancel out and hence do not affect the result. Since the aerial modes have phase velocities which are nearer to the velocity of light a quarter-wave resonance similar to the normal frequency quarter-wave resonance will be expected. This result has been confirmed. For the earth mode the velocity of propagation is much lower than in the case of the previous two modes, and as has been indicated by pure zero sequence mode energisation the line length for zero-sequence quarter-wave resonance is well below that of the positive-sequence mode resonance. The existence of an earth mode therefore in the case of line-to-ground faults will be expected to have a substantial influence on the shape of the impedance loci characteristic. In the case of isolated faults the earth mode content is much lower than in the case of earth faults owing to the fact that earth currents present are due to the line-to-ground capacitive current only and hence its influence will not be as pronounced as in the case of ground faults.

Whereas the interchange of the system phase-rotation interchanges the loci of a centre and an outer phase it has no effect on the loci of the outer phases of a flat line; this is because in the former case the contribution of the capacitance current has been interchanged while the phasor difference still exists but in the latter case the contribution is still zero since the two capacitance currents cancel out.

The general similarity of the results for the vertical and horizontal lines are seen, the minor differences in the

loci patterns are due to differences in the asymmetry of line conductors which is more pronounced in the case of a horizontal line. The phase velocities of the aerial and earth modes for the two types of line are also significantly different which accounts for the difference in the eighth wavelength resonance.

The results presented for the impedance characteristic of long-distance multiconductor lines for various types of fault clearly show the departure of this characteristic from the normal impedance angle measurement characteristic recognized in the theory of distance protection. The principles of compensation, in which the impedance seen by a distance relay is taken as a reliable indication of fault position, are derived on the basis of a short line where the line capacitance current is justifiably neglected. For long lines and unbalanced types of fault the uncompensated impedance loci characteristics presented have pointed out to the significance of the line capacitance current and hence the influence this may have on compensated impedance loci.

The negative apparent resistance component presented to certain distance relays for some isolated and earth faults on long untransposed lines call for a special consideration in the design characteristics of these relays which would enable them to cope with this negative quantity.

In practice it will be necessary to sectionalize the line and to carry out digital computer studies in order to evaluate apparent impedances to faults and hence determine relay settings.

4.7 Conclusions

1. This investigation has proved the limitations of classical transmission line theory in studying the short-circuit impedance loci properties of faulted power systems.

2. Predictions made earlier that resonance points of short-circuited lines occur at intervals of quarter wavelengths have been shown to be true only when balanced-type faults occur on these lines. In certain cases, and for unbalanced faults, resonance points occur at intervals of about one-eight wavelength.

3. In long distance a.c. transmission it will now be the eighth wavelength line rather than the quarter wavelength line which dictates the margin of safe transmission.

4. The investigation has pointed out the complications involved in the application of existing-type distance protective schemes to very long high-voltage lines. Owing to the influence of the line capacitance current the maximum length of line which can be reliably protected in one stage by distance protection is considerably less than previous predictions have implied. Attention is drawn to the need for a change in the philosophy of distance protection when applied to very long multiconductor lines. Here, digital calculations for the determination

of the line impedance characteristic become of extreme importance since the known concept of a vector of constant angle and modulus proportional to line length is no longer valid.

The digital studies presented will need confirmation by field tests.

CHAPTER FIVE

STEADY-STATE PERFORMANCE OF LONG UNTRANSPOSED LINES WITH REFERENCE TO REACTIVE COMPENSATION

5.1 Introduction

Unless special measures are taken, the amount of power which can be transmitted over a very long line is restricted, the main determining factor being the characteristic impedance. The almost universal adoption of bundled conductors [40,41] in these lines has been helpful in that the characteristic impedance has become smaller. Nevertheless, the problem is still acute and various power authorities [42,43,44] involved have had to take special measures to find a satisfactory solution.

From simple transmission theory the maximum power transfer is inversely proportional to the line inductive reactance. In long-distance transmission the line inductive reactance constitutes the greater part of the overall system reactance [10] with generators and transformers. In order to increase the transmission capacity it is therefore necessary that the line reactance be reduced. The use of bundled conductors is one way of reducing the line reactance and hence increasing the line capacity but since there are practical limitations on the number of sub-conductors to use in a phase bundle, the use of bundled conductors does not offer a complete solution. Other possible alternatives open for raising the system capacity is through the implementation of extremely high voltages or by the introduction of series capacitors to compensate for part of the line reactance [45].

The increase of transmission voltages is accompanied by considerable technical and economic problems in the design and operation of system apparatus. 400 KV voltage is now common practice in many developed countries though 750 is in use in Canada and 1000 KV is now being considered in certain places[2]. Such higher voltages will be of great help in increasing transmission capacities of long-distance lines in future but at present series compensation will still play a very important role in this direction.

A great deal of work [45,46,47,48] has been carried out on studies relating to series compensation as an effective means of raising the transmission capability of long-distance lines. Location of the series capacitors and selection of compensating station arrangements added to these the choice of optimum degrees of compensation to effect increases in power transfer over long distances have been discussed by several investigators in this field. Series capacitors have also been shown to have an influence on service frequency voltage rises resulting from Ferranti effect when the line is connected at one end only or internal voltage rises when the line is connected at two ends. Voltage profile requirements have henceforth dictated that series capacitors be installed at various locations throughout the length of the line to relieve the line and apparatus connected to it from possible damages due to insulation failure caused by these voltage rises. Since the capacitors are connected in series with the transmission line, under fault conditions the full line current will be flowing through them which would eventually give rise to serious over-voltages across the

capacitor terminals during fault conditions. These difficulties were realized and appropriate measures have been taken to safeguard series capacitor installations. Spark gaps are normally provided across the capacitor which will short out the element during faults and clear themselves as soon as the line current returns to normal. Failure of the spark gaps to operate would not only result in overvoltages across the capacitor terminals but would also affect the protection scheme of such lines as the impedances seen by the different line relays will be modified by the reactance of the series capacitor and this may result in incorrect tripping procedure for the various sections of the network [49].

Another major problem with long-distance transmission is the huge amount of capacitive power generated by the line. This power is capable of creating serious problems leading to instability of the generating plant and giving rise to greater voltage rises along the line length particularly under open-circuit receiving end conditions or low transmission conditions. To limit these voltage rises to within allowable limits of operation the line shunt capacitance has to be compensated. The connection of shunt reactors at the open end of the line will decrease the voltage rise there, whereas introduction of shunt reactors at intermediate points on the line would lead to a more even distribution of line voltage profiles and help in reducing the great reactive power demand on the system machines and hence improve on the otherwise poor power factors at either generation or load ends.

Like series compensation, shunt compensation has been widely accepted as an effective means of compensation in existing long-distance transmission projects[42,43,44]. The size and location of the compensating reactors is vital for achieving best results and a great deal of investigation is therefore essential to determine the best form of arrangement to be adopted for shunt compensation, the total degree of line capacitive power to be compensated and the voltage and size of the reactor to be used. Shunt reactors have the additional feature of discharging an energised line and hence reducing switching overvoltages.

From work carried out for the Swedish State Power Board[50] it has been pointed out that favourable system operating conditions are attained if the shunt reactors are directly connected to the line instead of through transformers. Another important consideration of shunt compensation is that intermediate shunt reactors tend to limit the active power transfer ability of the line and it is important that when considering shunt compensation to bear this in mind.

In the analysis of long-distance transmission design problems incorporating methods of series and shunt compensation previous investigations have used simple transmission line approach and relied on the single phase equivalent circuit for determination of long line properties. The tendency has been to ignore the non-transposed nature of these lines and hence their results of studies have obscured some system peculiarities. In the following sections of this investigation a better understanding of some of the

basic properties of long untransposed multiconductor lines will be made possible. Results of studies on series and shunt compensated lines are presented with reference to a 600-mile line with different possible series compensation arrangements and with combined series and shunt compensation to secure voltage stability and raise the line power-carrying capability. The limitation of phase unbalance on the maximum degree of series compensation thought to be 100% for a balanced line will be illustrated.

The difficulty arising from power unbalance of the separate phases in series compensated lines goes back to the general problem of unbalance in the basic untransposed circuit configurations. Apart from the cost involved in transposing overhead transmission lines the problem of transposition becomes more complex as higher voltages are being used and multiple conductor transposition becomes more of a problem. This means that circuits have to be used untransposed in order to avoid the mechanical difficulties that are involved. Untransposed lines fed from balanced generation and supplying balanced loads would still have certain degees of unbalance in them appearing in the form of negative and zero sequence currents. The flow of negative sequence currents increase stator losses and induce in the machines air gap a field rotating in the opposite direction generating currents of double frequency in their rotor which would contribute to increased losses in the machine[51]. Zero sequence currents are capable of affecting ground relays and thus producing false operation[52]. To overlook effects of unbalances in non-transposed circuit lines would mean to

ignore these serious problems. It has therefore been thought more useful to include a more accurate assessment for negative and zero sequence unbalances of untransposed circuit lines than has hitherto been given. The analysis is general and can be extended to cover series and shunt compensated lines as well. No attempt has been made in these preliminary studies to include studies on the methods of balancing the line.

5.2 Method of Analysis

5.2.1 Objectives

The general method of matrix analysis introduced in the previous chapters for investigating untransposed line behaviour under fault conditions will be also used in the present chapter for dealing with steady-state normal operating conditions. The two alternatives of solution discussed earlier, namely nodal analysis approach and reflection factor method are also relevant to the following sections though nodal analysis approach has been preferred as in general we will be dealing with a two-ended system for which this method is more favourable.

Before proceeding with the description of the mathematical models, a broad outline of the main objectives sought in this part of the investigation that will help provide a clear form of understanding for long line behaviour will now be laid down. This relates to:-

i. active and reactive power requirements of long lines under open circuit conditions

ii. receiving end voltages and Ferranti effect

iii. internal voltage rises under different operating conditions and variation of these with system length

iv. surge impedance loading criterion as an important factor for economic considerations

v. power capability of uncompensated lines and limitations set by system length on active power transfer. The problem of reactive power

vi. compensation of system shunt capacitance and system series inductance. Study of the effect of these on system internal 50 Hz over-voltages and overall power transfer conditions

vii. study of unbalances of untransposed circuit lines.

Assumptions will be made in the following analysis that the system boundary conditions are already known which is normally the case with long lines - these include a knowledge of transmission angle of the system and the voltage supply which would be taken as a three-phase balanced supply.

5.2.2 Analysis for Basic Studies

5.2.2.1 Voltage Profiles and Reactive Power Requirements of Long Lines

(a) Unloaded line

Consider the matrix two-port equations for the solution of the sending and receiving end currents

$$\begin{bmatrix} I_s \\ I_r \end{bmatrix} = \begin{bmatrix} A & B \\ B & A \end{bmatrix} \cdot \begin{bmatrix} V_s \\ V_r \end{bmatrix}$$

where

$$A = \coth\psi\ell\,;\quad B = -\operatorname{cosech}\psi\ell\,;\quad \psi = Q\lambda^{\frac{1}{2}}Q^{-1}$$

If the line is open-circuited at the receiving end then $I_r = 0$. From second and first rows

$$V_r = -A^{-1}B.V_s \qquad - (5.1)$$

$$I_s = [A - BA^{-1}B].V_s \qquad - (5.2)$$

Equations (5.1) and (5.2) then give the three-phase receiving end voltages and three-phase sending end currents. The three phasor power "S" at the sending end is obtained from the product of the voltage transpose and the current conjugate at the sending end

$$\therefore \quad S = V_{st} \cdot I_s^*$$

If equation (5.1) is reduced to a single phase equivalent system and assuming that the line is transposed the open-circuit receiving end voltage is given for a lossless line by:-

$$V_r = V_s/\cos\frac{2\pi}{\lambda}\ell$$

from which it is seen that $V_r \to \infty$ as $\ell \to \lambda/4$. In other words dangerous overvoltages arise at the open-circuited end of lines approaching a quarter wavelength. In a similar manner it can be shown that the magnitude of the sending end reactive power of such lossless lines can also be dangerously high. For systems with losses it is therefore possible to study their open circuit voltage

and reactive power requirements by equations (5.1) and (5.2).

(b) Loaded line

This is a variation of case (a) and deals with the case where the system is energised from both sending and receiving ends. In this case determination of voltage profiles along the length of line is necessary.

Consider Fig. (5.1) in which the multiconductor system is split into two sections at the intermediate point "i" as shown in Fig. (5.1.b). The line constants for the two separate sections are as shown.

It is now required to determine the intermediate voltage V_i on the line.

The two port current equation used for each individual section of the line shown in Fig. (5.1.b) will give

$$\begin{bmatrix} I_s \\ I_i \end{bmatrix} = \begin{bmatrix} A_1 & B_1 \\ B_1 & A_1 \end{bmatrix} \cdot \begin{bmatrix} V_s \\ V_i \end{bmatrix}$$

and

$$\begin{bmatrix} -I_i \\ I_r \end{bmatrix} = \begin{bmatrix} A_2 & B_2 \\ B_2 & A_2 \end{bmatrix} \cdot \begin{bmatrix} V_i \\ V_r \end{bmatrix}$$

On combining these matrix equations we get

$$\begin{bmatrix} I_s \\ 0 \\ I_r \end{bmatrix} = \begin{bmatrix} A_1 & B_1 & 0 \\ B_1 & A_1+A_2 & B_2 \\ 0 & B_2 & A_2 \end{bmatrix} \cdot \begin{bmatrix} V_s \\ V_i \\ V_r \end{bmatrix}$$

and solving for V_i

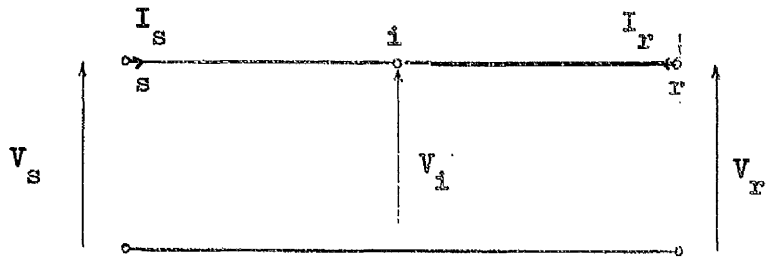

(a)

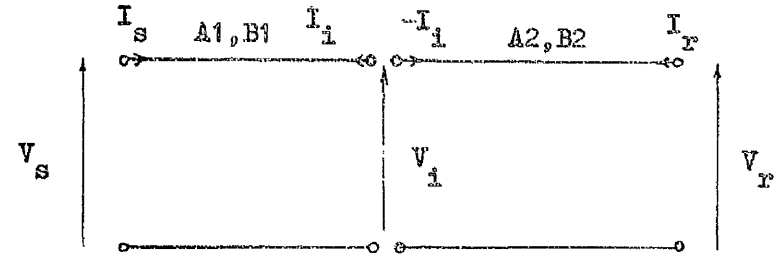

(b)

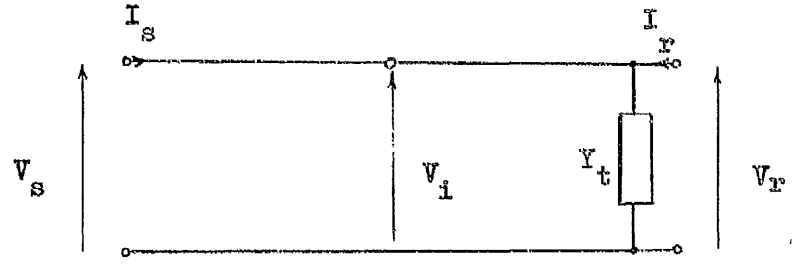

(c)

FIG. (5.1). SYSTEM DIAGRAMS FOR SOLUTION OF VOLTAGE PROFILES AND SURGE IMPEDANCE LOADING PROBLEMS

$$V_i = -(A_1+A_2)^{-1}(B_1V_s+B_2V_r) \qquad - (5.3)$$

and the input current at the sending end

$$I_s = \{A_1-B_1(A_1+A_2)^{-1}B_1\}V_s - \{B_1(A_1+A_2)^{-1}B_2\}V_r \qquad - (5.4)$$

It is also possible to write down the system equations given in the above matrix form directly by inspection if zero current is injected at node i and "A" and "B" constants are regarded as driving point and transfer admittances or self and mutual admittances of nodes s, i and r. By so doing it is possible to ignore the intermediate steps resulting from considerations of Fig. (5.1.b).

When the single phase equivalent case of a lossless transposed transmission line is considered, the reduction of equation (5.3) for the same voltage magnitude at sending and receiving end of line and zero transmission angle will yield infinite voltage at the mid-point of a quarter wavelength line. For other boundary conditions the voltage at the mid-point of the line is always higher than the voltage at either end.

The point on the line at which the internal voltage V_i is found is inherently included in the line section constants. This makes equation (5.3) general for the evaluation of the voltage at any point on the line and as such this equation forms the basis for the calculation of the voltage profiles of loaded transmission lines under different operating conditions.

The case of a general terminating impedance at either sending or receiving ends of the line is easy to consider. The intermediate voltages and sending end currents are given below for the case of a shunt load at the receiving end of the line shown in Fig. (5.1.c).

$$V_i = [A_1+A_2=B_2(Y_t+A_2)^{-1}B_2]^{-1}B_1.V_s \qquad - (5.5)$$

$$I_s = \{A_1=B_1[A_1+A_2=B_2(Y_t+A_2)^{-1}B_2]B_1\}V_s \qquad - (5.6)$$

The surge impedance loading properties of the line can be studied from (5.5) and (5.6) where the surge admittance matrix of the system replaces the general terminating admittance matrix Y_t in the above equations.

5.2.2.2 Power charts and Long Line Capabilities

Power charts and long lines carrying capacities can be derived from the equations established for the model of Fig. (5.1) since both active and reactive power at the sending and receiving ends are functions of the system currents which have been solved for in these equations. The variation of the transmission angle and the ratio of voltage magnitude at either end can easily be handled by the use of a digital computer. System length can also be freely varied. Representative studies have been carried out and will be presented.

5.2.3. Analysis For Series and Shunt Compensation Studies

5.2.3.1 General

The method of analysis outlined in the previous sections for obtaining some of the basic properties

of multiconductor lines will be extended here to cover more complex operating conditions. In long lines the need for series and shunt compensation has already been established. The introduction of compensating elements may take intermediate points on the line; the elements may also be located at the end points of the transmission line. System overvoltages to which the terminals of these compensating equipment are subjected are of major importance. In determining whether these system components have achieved their primary objective a knowledge about the line power carrying ability, line internal voltage profile is necessary for design considerations.

Owing to space limitations and multiplicity of compensating arrangements that are open for investigation it is not possible to give here detailed analysis for every case studied. The generality of the method will therefore be illustrated by typical system arrangements for series, shunt and series-shunt compensation.

In multi-conductor analysis the series compensating station at a particular location is represented by an impedance matrix the diagonal elements of which are the individual capacitor reactances introduced along the phase conductor to compensate for part of the phase inductive reactance. The series capacitive reactance matrix for a three-phase single-circuit line will be of the following form:-

X_{c11}	0	0
0	X_{c22}	0
0	0	X_{c33}

The capacitive reactances X_{c11}, X_{c22} and X_{c33} are formed from the line positive sequence inductive reactance thus making the assumption that the circuit is ideally transposed and we therefore deal with a balanced capacitive reactance matrix whose diagonal elements are X_{c1}.

Simiarly, and in shunt compensation the shunt admittance matrix of the compensating reactors formed from the line positive sequence admittance matrix takes the following form:-

Y_{s11}	0	0
0	Y_{s22}	0
0	0	Y_{s33}

the diagonal elements being equal on the assumption that the circuit is transposed.

Since nodal analysis method has been adopted the equivalent admittance matrix of the series capacitors will be dealt with.

5.2.3.2 Series and Shunt Compensation for Untransposed Lines

i. Compensation lumped at one point only

The system diagram is shown in Fig. (5.2.a) and the model for analysis given in Fig. (5.2.b). Assuming that V_1 and V_2 are the intermediate voltages at the capacitor terminals the relationship between the high-side sending and receiving end voltages and the unknown quantities I_s, I_r, V_1 and V_2 can be expressed in the following matrix form:-

$$\begin{bmatrix} I_s \\ 0 \\ 0 \\ I_r \end{bmatrix} = \begin{bmatrix} A_1 & B_1 & 0 & 0 \\ B_1 & A_1+Y_c & -Y_c & 0 \\ 0 & -Y_c & Y_c+A_2 & B_2 \\ 0 & 0 & B_2 & A_2 \end{bmatrix} \cdot \begin{bmatrix} V_s \\ V_1 \\ V_2 \\ V_r \end{bmatrix}$$

Through a process of elimination the solution for the intermediate voltages and the sending and receiving end currents are obtained.

$$V_1 = -\{A_1+Y_c-Y_c(Y_c+A_2)^{-1}Y_c\}^{-1}B_1V_s - \{A_1+Y_c-Y_c(Y_c+A_2)^{-1}Y_c\}^{-1}Y_c \times (Y_c+A_2)^{-1}B_2.V_r \quad - (5.7)$$

$$V_2 = (Y_c+A_2)^{-1}.Y_cV_1-(Y_c+A_2)^{-1}B_2.V_r \quad - (5.8)$$

$$I_s = A_1V_s + B_1V_1 \quad - (5.9)$$

$$I_r = B_2V_2 + A\ V_r \quad - (5.10)$$

Equations (5.7) to (5.10) then give the complete solution.

ii. Compensation divided between two capacitor stations symmetrically located about the centre of the line

With reference to Figs. (5.2.c) and (5.2.d) the system equations are written out in the following matrix form,

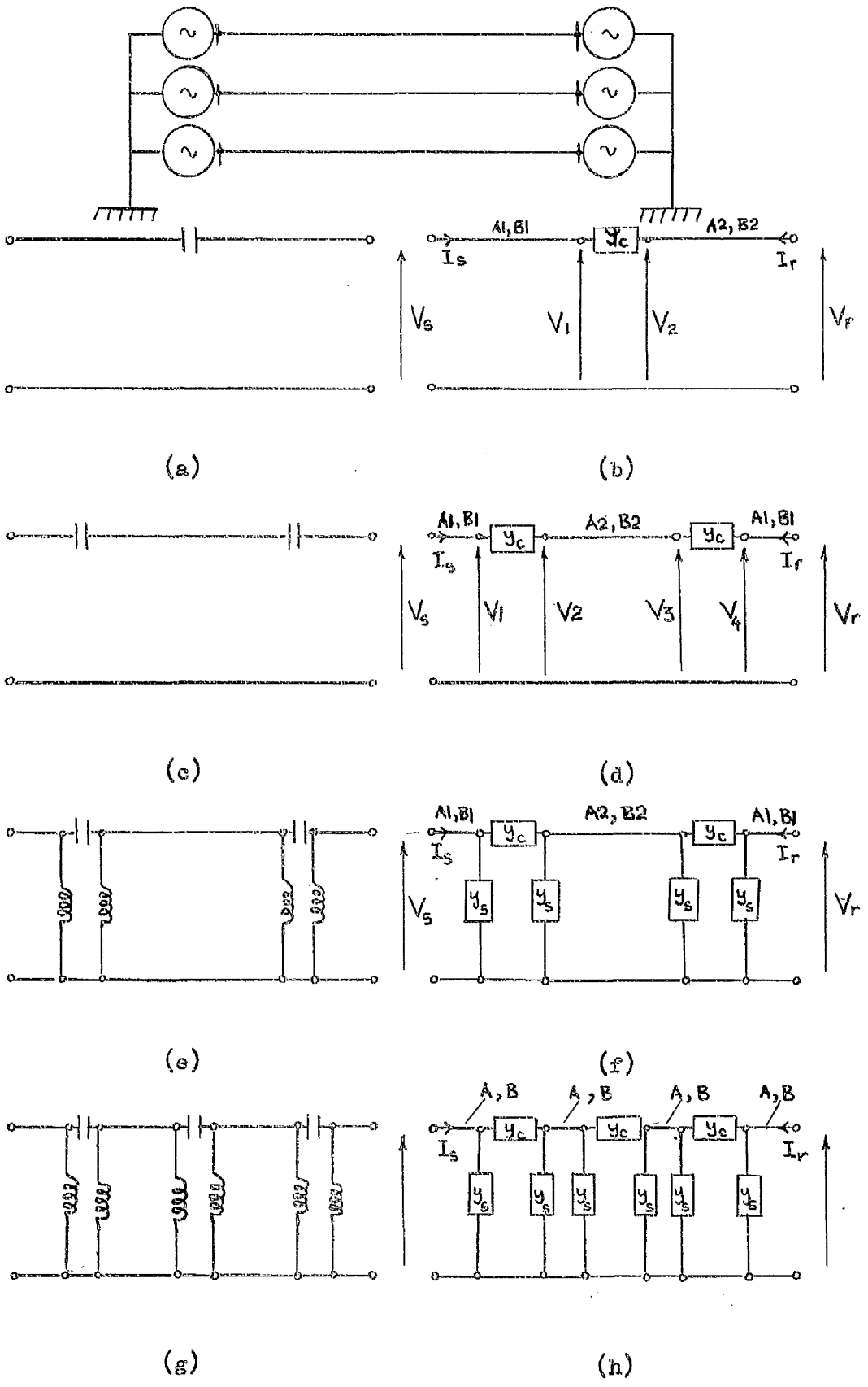

FIG. (5.2). SERIES AND SHUNT COMPENSATION ARRANGEMENT

noting that the first and third sections of the transmission line are of equal length and hence of identical propagation constants.

$$\begin{bmatrix} I_s \\ 0 \\ 0 \\ 0 \\ 0 \\ I_r \end{bmatrix} = \begin{bmatrix} A_1 & B_1 & 0 & 0 & 0 & 0 \\ B_1 & A_1+Y_c & -Y_c & 0 & 0 & 0 \\ 0 & -Y_c & Y_c+A_2 & B_2 & 0 & 0 \\ 0 & 0 & B_2 & Y_c+A_2 & -Y_c & 0 \\ 0 & 0 & 0 & -Y_c & Y_c+A_1 & B_1 \\ 0 & 0 & 0 & 0 & B_1 & A_1 \end{bmatrix} \cdot \begin{bmatrix} V_s \\ V_1 \\ V_2 \\ V_3 \\ V_4 \\ V_r \end{bmatrix}$$

The solution of the above equations will give expressions for the different unknowns.

iii. <u>Two or three series/shunt compensating stations</u>

As a means of reducing overvoltages resulting at the capacitor terminals shunt reactors are connected there. The case shown in Figs. (5.2.e) and (5.2.f) will be analysed. It is assumed that the compensating stations are located symmetrically about the centre of the line and that the overall series and shunt compensation is equally shared among the individual elements. The resultant system matrix will then be:-

$$\begin{bmatrix} I_s \\ 0 \\ 0 \\ 0 \\ 0 \\ I_r \end{bmatrix} = \begin{bmatrix} A_1 & B_1 & 0 & 0 & 0 & 0 \\ B_1 & S & -Y_c & 0 & 0 & 0 \\ 0 & -Y_s & T & B_2 & 0 & 0 \\ 0 & 0 & B_2 & T & -Y_c & 0 \\ 0 & 0 & 0 & -Y_c & S & B_1 \\ 0 & 0 & 0 & 0 & B_1 & A_1 \end{bmatrix} \cdot \begin{bmatrix} V_s \\ V_1 \\ V_2 \\ V_3 \\ V_4 \\ V_r \end{bmatrix}$$

where $S = A_1 + Y_s + Y_c$

and $T = Y_c + Y_s + A_2$

The method can similarly be extended for the analysis of a case where compensation is shared among three series/shunt stations as shown in Figs. (5.2.g) and (5.2.h).

Though only symmetrical compensating arrangements have been considered which are symmetrically located about the centre line of the transmission system there is no reason why this method of analysis can not be extended to cover other forms as well. Symmetrical arrangements have been chosen here as these help establish fundamental principles on the theory of compensation applied to long untransposed lines. Individual particular cases can be tackled in similar ways.

5.2.3.3 Compensation for Transposed Line

If the multiconductor line is assumed to be transposed then under balanced operating conditions we will be dealing with one form of propagation, namely positive sequence propagation. In this case the matrix constants reduce to single elements i.e. those of positive sequence network and all the general equations derived so far for the compensated untransposed line would be relevant for the equivalent single phase case with positive sequence propagation constants being substituted in place of the matrix propagation constants.

5.2.4 Source Effects

In the above analysis source effects have not been

taken into consideration. The system source can be represented in the mathematical model by assuming a source admittance matrix at sending and receiving end. This source admittance matrix is the inverse of the source impedance matrix calculated from the system short circuit MVA and system voltage. In long line steady-state studies source side representation is not very important and can be ignored.

5.3 Digital Computer Studies

5.3.1 General Considerations

The digital computer studies on some aspects of long multiconductor lines will now be discussed. Results shown are relevant to the horizontal line described in section (4.3) and nominal voltages of 330 KV and 400 KV have been selected for the purpose of studies. A point-to-point transmission system has been considered energised from three-phase balanced system at either sending or sending and receiving ends. The effect of source impedance has been ignored. A general purpose program has been developed for the numerical evaluation of the steady-state performance properties of long-distance lines. This program will now be discussed.

5.3.2 Description of Computer Program

The flow diagram for the computer program is given in Fig. (5.3). The initial stages of the program are similar to those described in the previous chapter for the impedance loci and distance protection problems. In brief, the program starts by reading in the conductors'

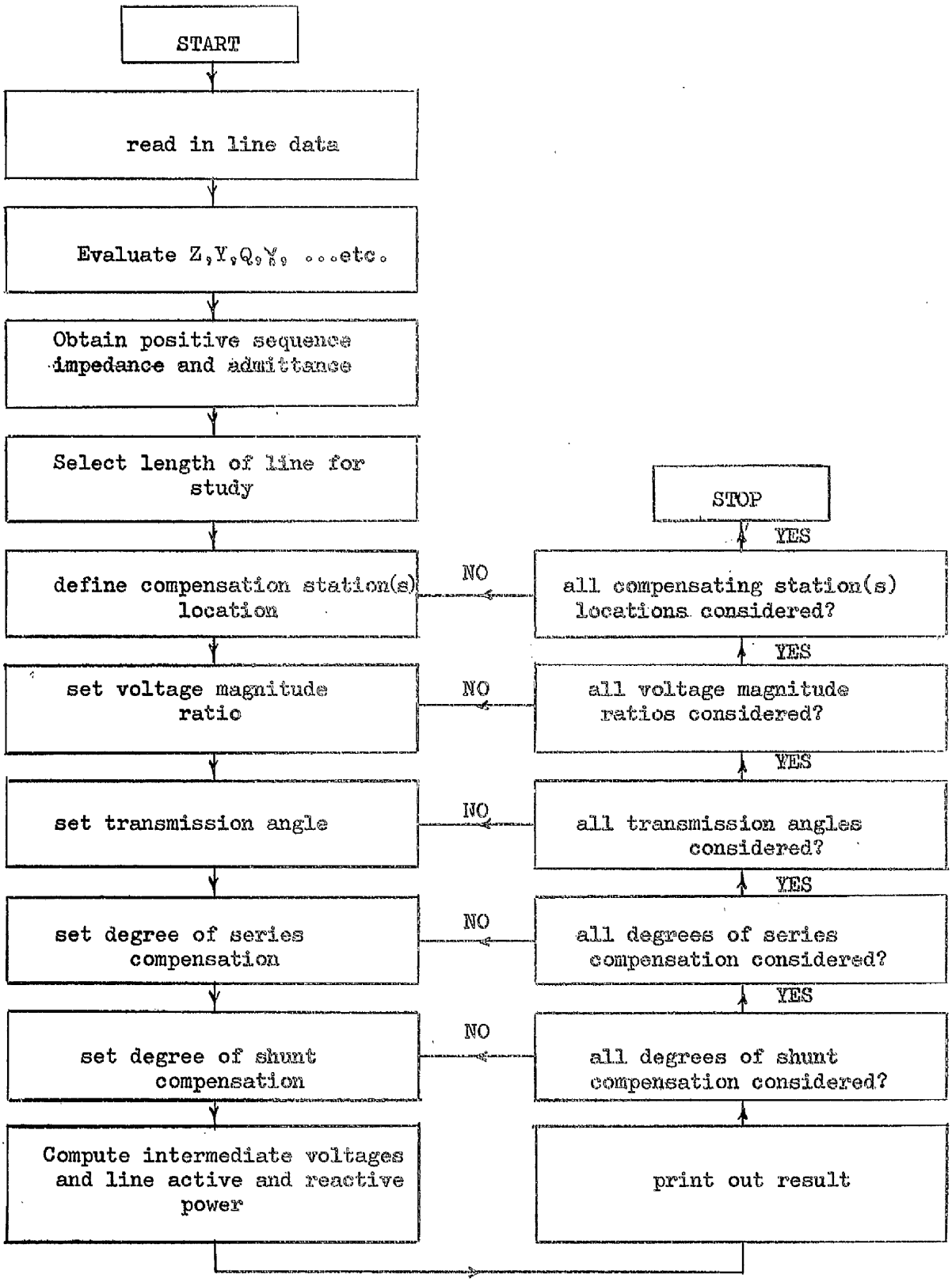

FIG. (5.3). FLOW DIAGRAM OF DIGITAL COMPUTER PROGRAM FOR REACTIVE COMPENSATION STUDIES OF LONG MULTICONDUCTOR LINES

spacings and mean heights above ground together with various other line parameters needed in the calculation of the basic impedance and admittance matrixes of the system. Eigenvalues and eigenvectors are then obtained. The line positive sequence impedance and positive sequence admittance are evaluated.

The next section of the program deals with selecting the line length and location of compensating stations needed in the study. Then follows the setting of the high-side terminal conditions, normally these are balanced three-phase voltages. The voltage magnitude between sending and receiving ends together with the transmission angle are set and the line A, B constants or the individual sections of line constants are determined. The selection of the degree of series and shunt compensation follows after which the value of the necessary series capacitor and shunt reactor for introduction at the compensating station(s) location is determined.

The program then proceeds with the evaluation of the line power transfer ability and reactive power imposed on the terminations, currents, power factors --- etc. Intermediate voltages at the capacitor and reactor terminals are also determined and the various results printed out. The program goes through a number of set cycles and terminates at their end when it has dealt with the full line studies.

5.4 Basic Long Line Properties

The variation of the open-circuit voltage and reactive

power imposed on the source of an open-circuited line are shown in Fig. (5.4). As the line length approaches a quarter wavelength the open-circuit voltages on the different phases rise sharply and approach extremely high values. Owing to the system finite losses these voltages do not become infinite as predicted earlier for the simple case of a lossless line. There is also a significant unbalance in the magnitude of the overvoltage experienced by the three phase conductors; both the circuit inductive and capacitive unbalance are responsible for these.

In Fig. (5.4.b) the overall sending active and reactive powers versus system length are shown for an open-circuited line at the receiving end. Losses become prohibitive as the line length approaches a quarter wavelength and line charging requirements become so great that they inevitably lead to machines instability.

Figs. (5.5.a) and (5.5.b) give the intermediate voltages that would appear on the centre phase of the line for different line lengths and different operating conditions. In this case the line is fed at both sending and receiving ends. The sending end voltage is fixed and the receiving end voltage magnitude and phase are varied in different degrees. It is clear from the diagram that line lengths in the region of 1000 - 1500 miles experience voltages at their intermediate points far in excess of their normal operating conditions. The voltage profile characteristic of a typical 400 KV line 600 miles long are shown in Fig. (5.5.c).

The importance of natural power or surge impedance

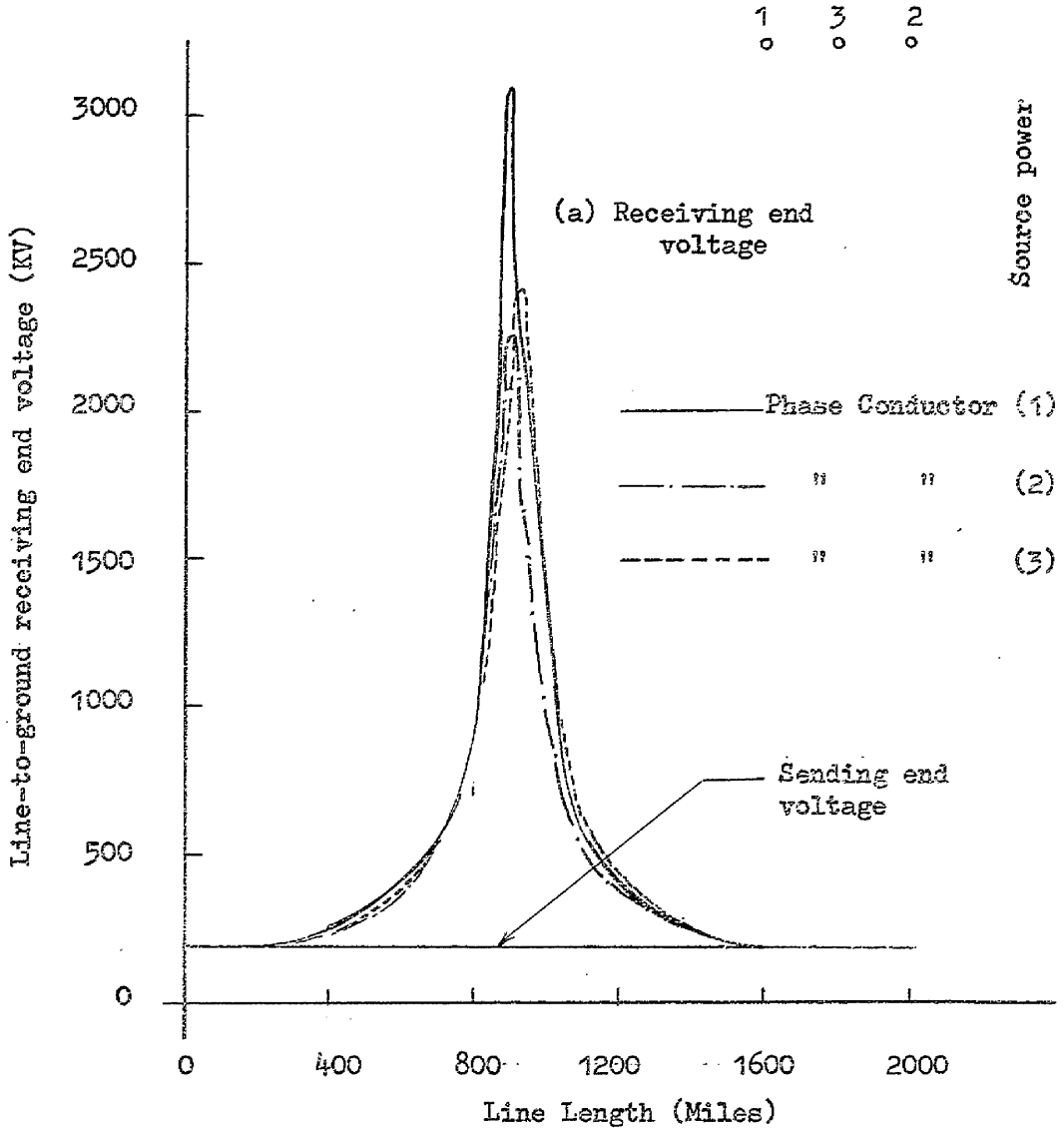

FIG. (5.4). RECEIVING END VOLTAGE AND SOURCE POWER OF OPEN-CIRCUITED LONG LINES

FIG.(5.4a)

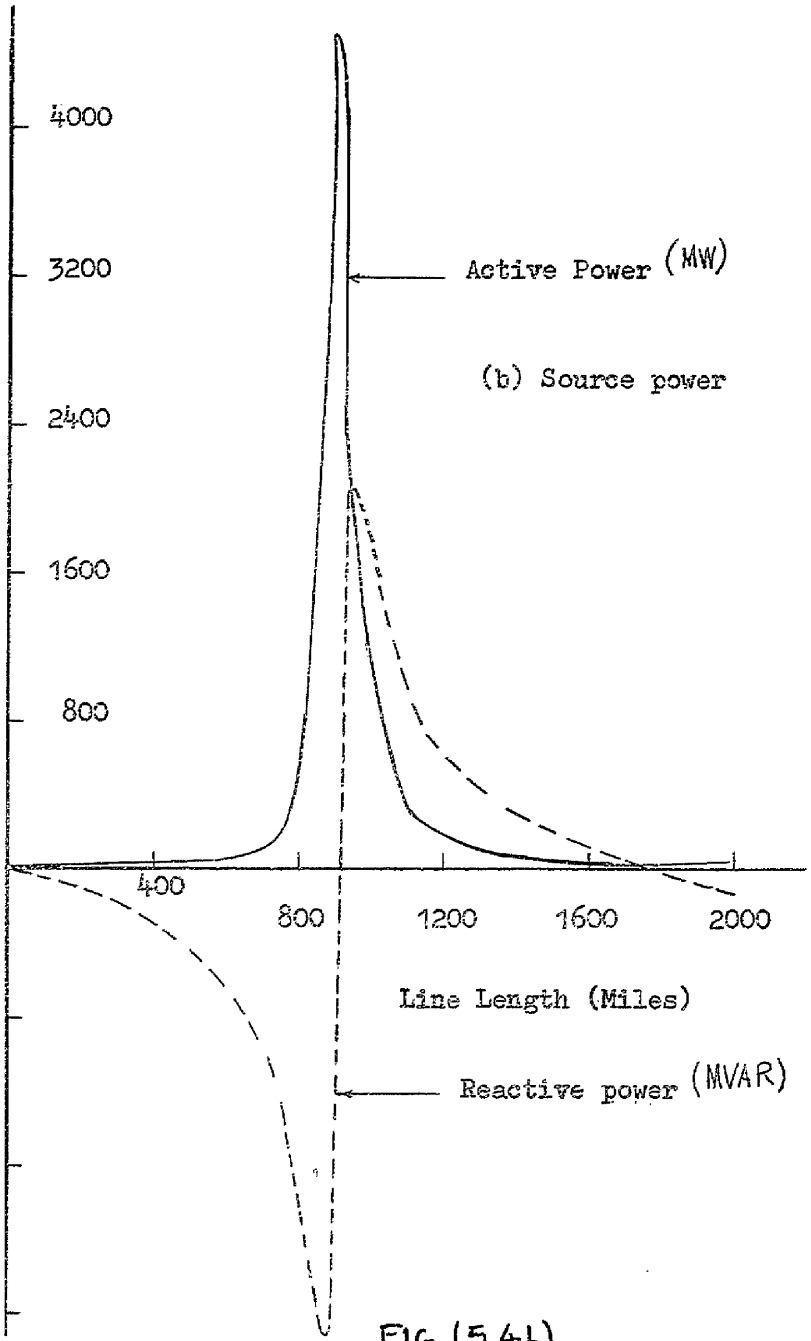

FIG.(5.4b)

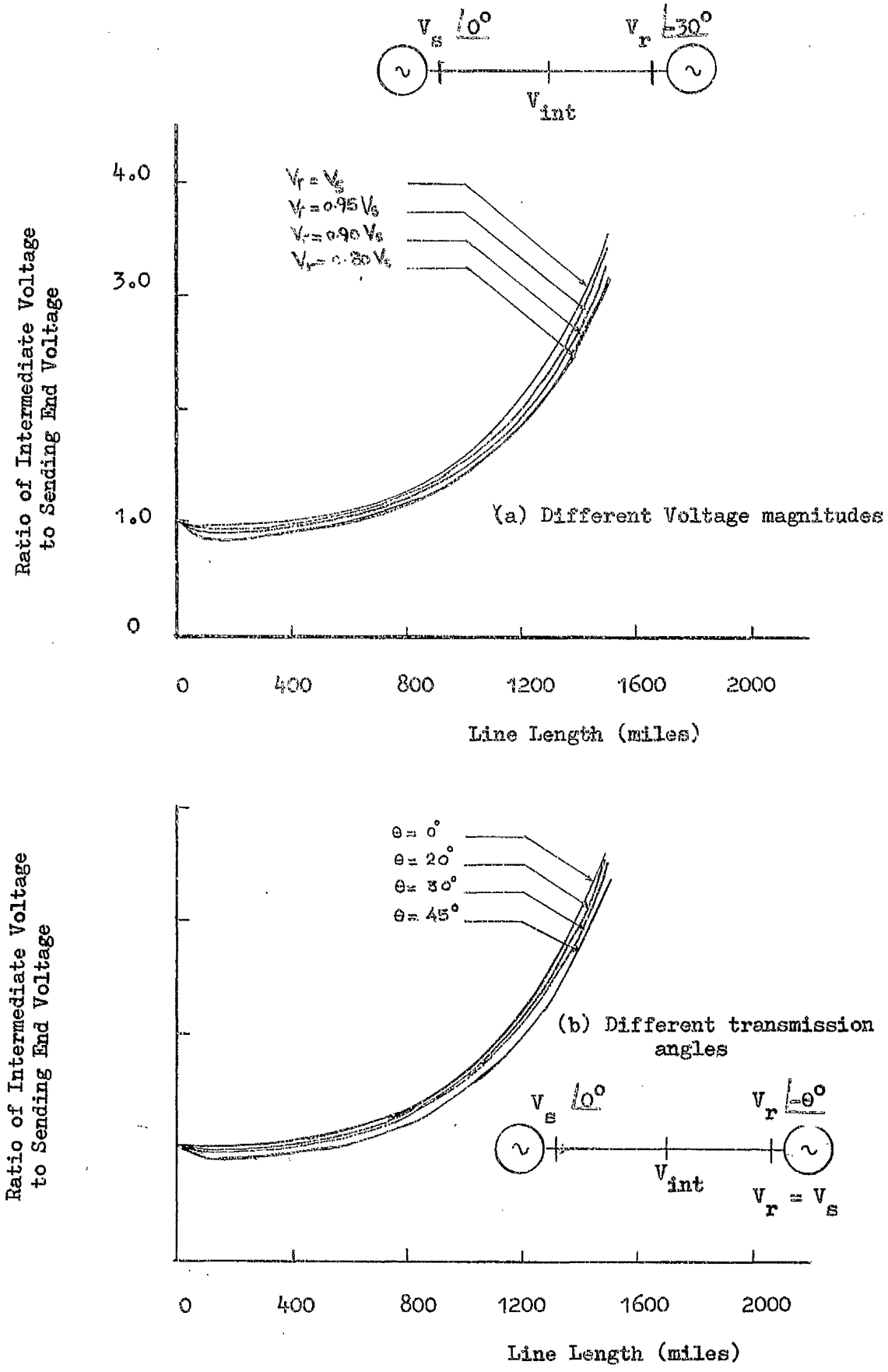

FIG. (5.5). VARIATION OF INTERMEDIATE VOLTAGE WITH LINE LENGTH

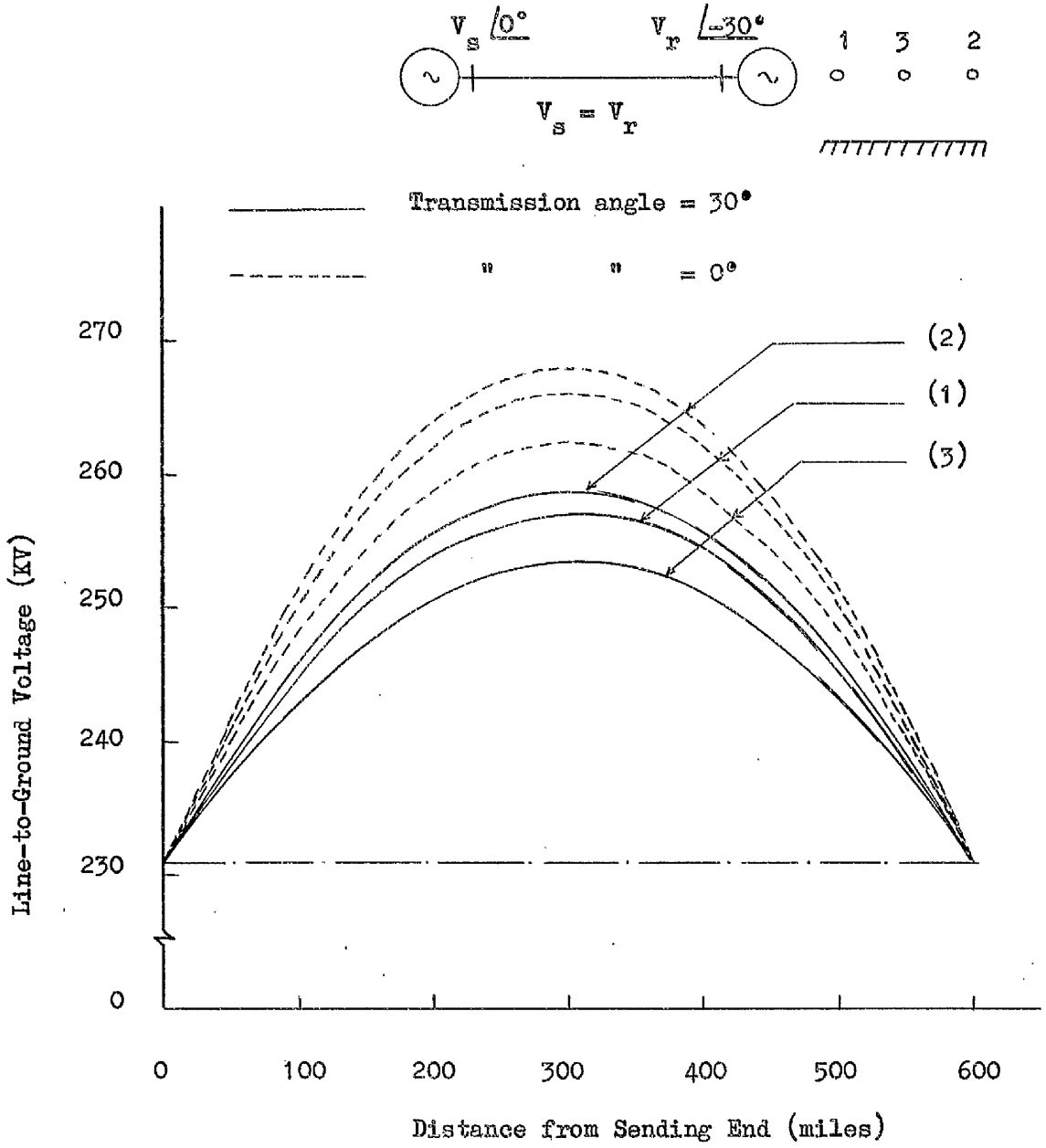

FIG. (5.5.C). VOLTAGE PROFILE OF 400 KV, 600-MILE LINE

loading of a transmission line has long been recognized as a measure of economic transmission over long distances[53]. The definition of surge impedance loading or SIL, as it is referred to, is the amount of power transferred over a transmission line when this is terminated by its characteristic impedance. Under surge impedance loading conditions the line internal reactive power requirements are completely balanced and as a result it is not necessary to supply reactive power from any external sources. Owing to the absence of line reactive current the total current flowing along the line is a minimum and consequently the line I.R losses are minimum for this loading condition.

In Fig. (5.6) the load carrying ability of different lengths of 330 KV line under various operating conditions are shown. The lines have a common surge impedance loading of 350 MW which is marked on the diagrams. It is evident from these diagrams that for normal long line operating conditions, i.e. a transmission angle of 30° and a voltage magnitude ratio not far off from unity, that power transfer close to the line surge impedance loading can only be carried out for distances in the region of 300 miles. Beyond this distance the power tapers off reaching very low values for transmission distances of 800 miles.

Additional problems of long-distance high voltage lines operating at loads other than their natural power are connected with capacitive generation. Comparative studies carried out for lines of 100, 300, 600 and 800 miles are given in the sending and receiving end power charts

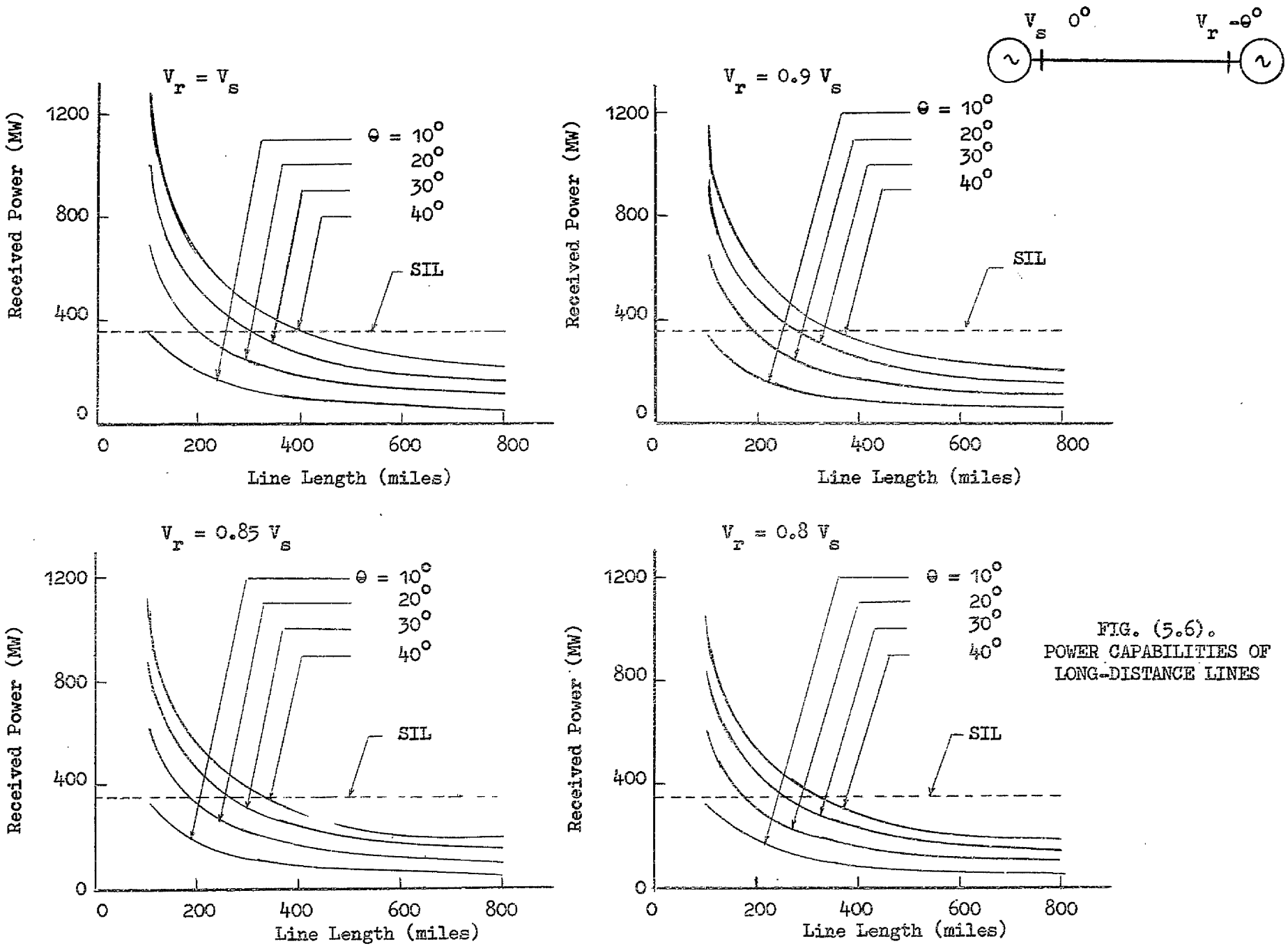

FIG. (5.6).
POWER CAPABILITIES OF
LONG-DISTANCE LINES

of Figs. (5.7) to (5.10). These figures cleary indicate that the longer lines absorb greater leading MVARs at both load and generation points which are capable of causing unstable behaviour of the machines at those ends unless some form of compensation has been provided from external means.

So far, some of the basic problems encountered in the steady-state performance of long lines have been raised. To overcome the considerable voltage rises which will endanger both line and electrical equipment caused by the line capacitive power, it is necessary to neutralize this capacitive power by the installation of shunt reactors along the line. The size and location of these reactors will be the subject of discussion. With the increase in system length the system inductance as has already been demonstrated, impairs the transfer of economic blocks of power over longer distances. Series capacitors introduced along the line provide a means of neutralizing desired proportions of the line inductance and hence contributing to the solution of this problem. Proposition regarding arrangement of series capacitors for long lines will be given. The maximum permissible limits of series compensation dictated by the untransposed nature of these lines will also be pointed out.

5.5 Effects of Series Compensation

Fig. (5.11.a) shows the results of studies carried out on a 400 KV, 600-mile line with a load angle of 30°. The sending and receiving end voltages are maintained equal. The figure shows the power transfer for different degrees of compensation of one series capacitor introduced at sending end, receiving end and intervals of 150 miles from sending

FIG. (5.7). POWER CHART FOR 330 KV 100-MILE LINE

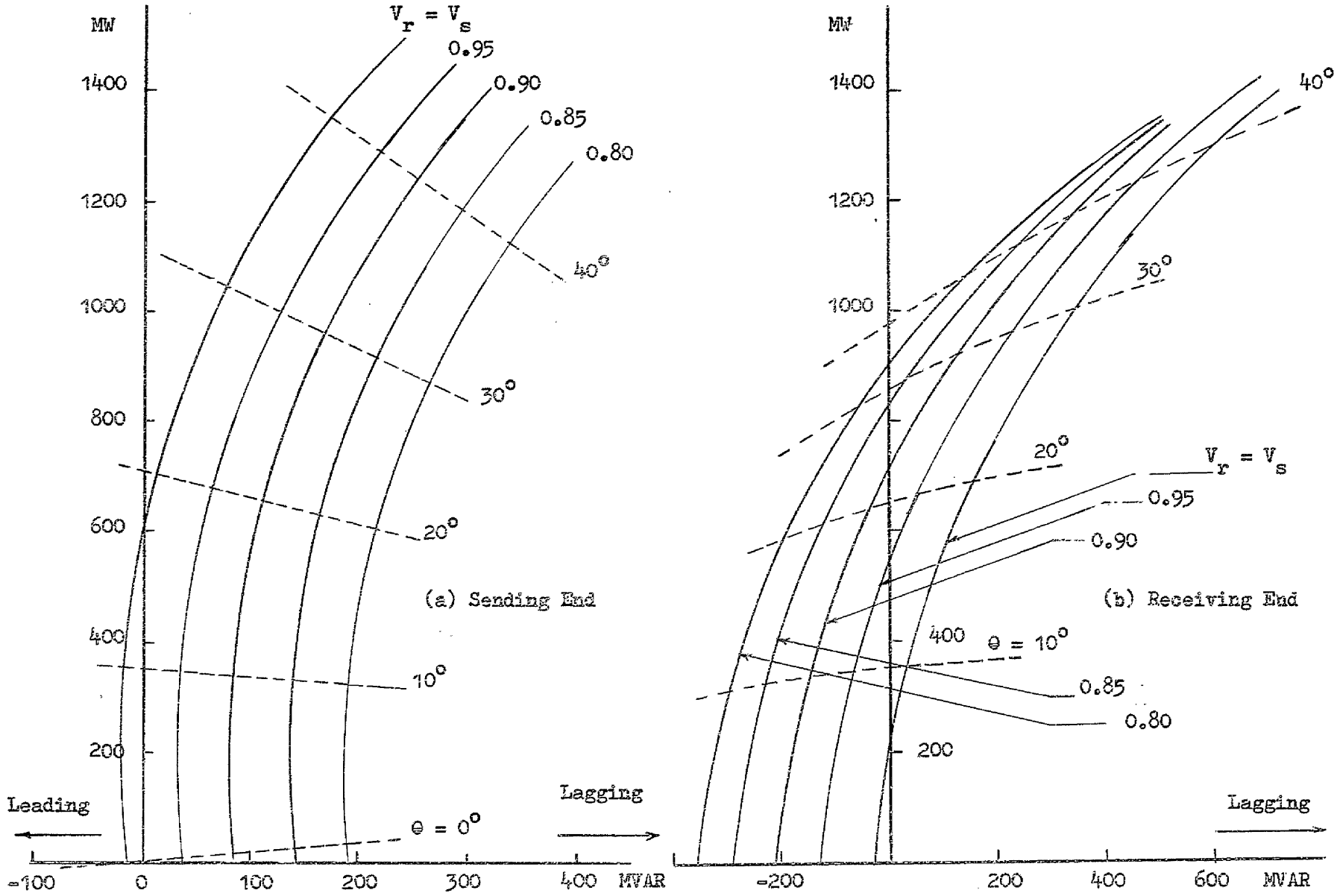

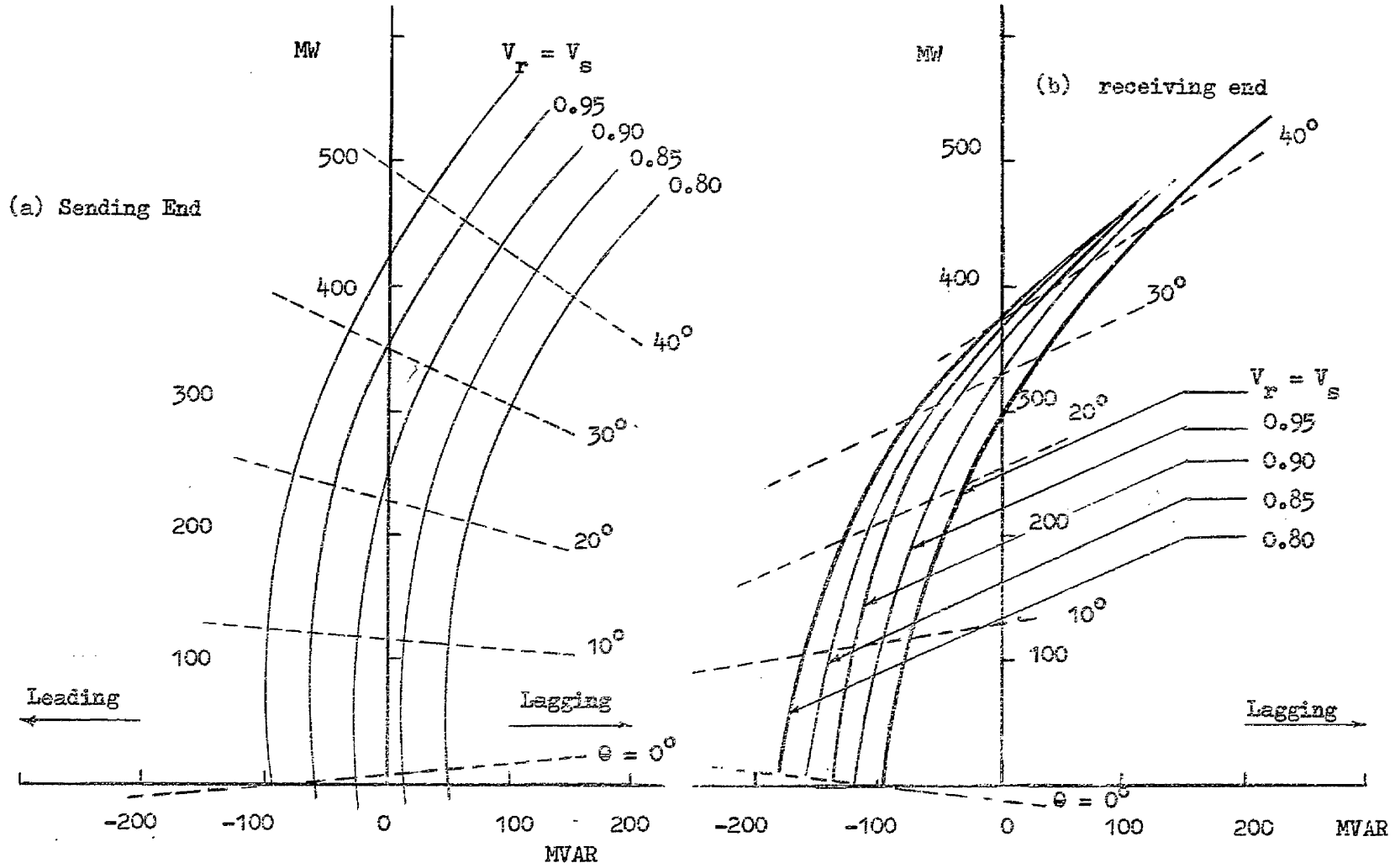

FIG. (5.8). POWER CHART FOR 330 KV, 300-MILE LINE

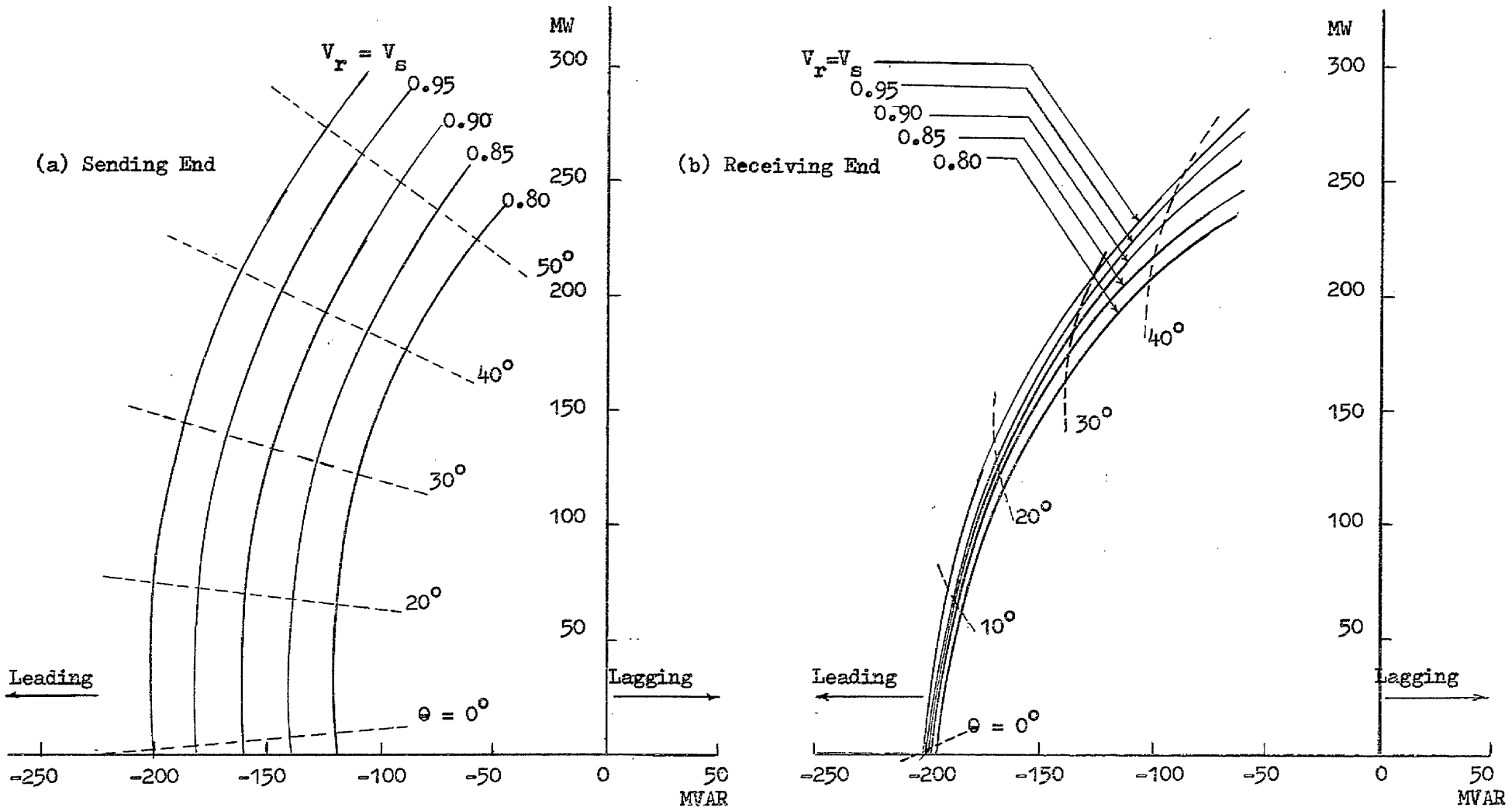

FIG. (5.9). POWER CHART FOR 330 KV, 600-MILE LINE

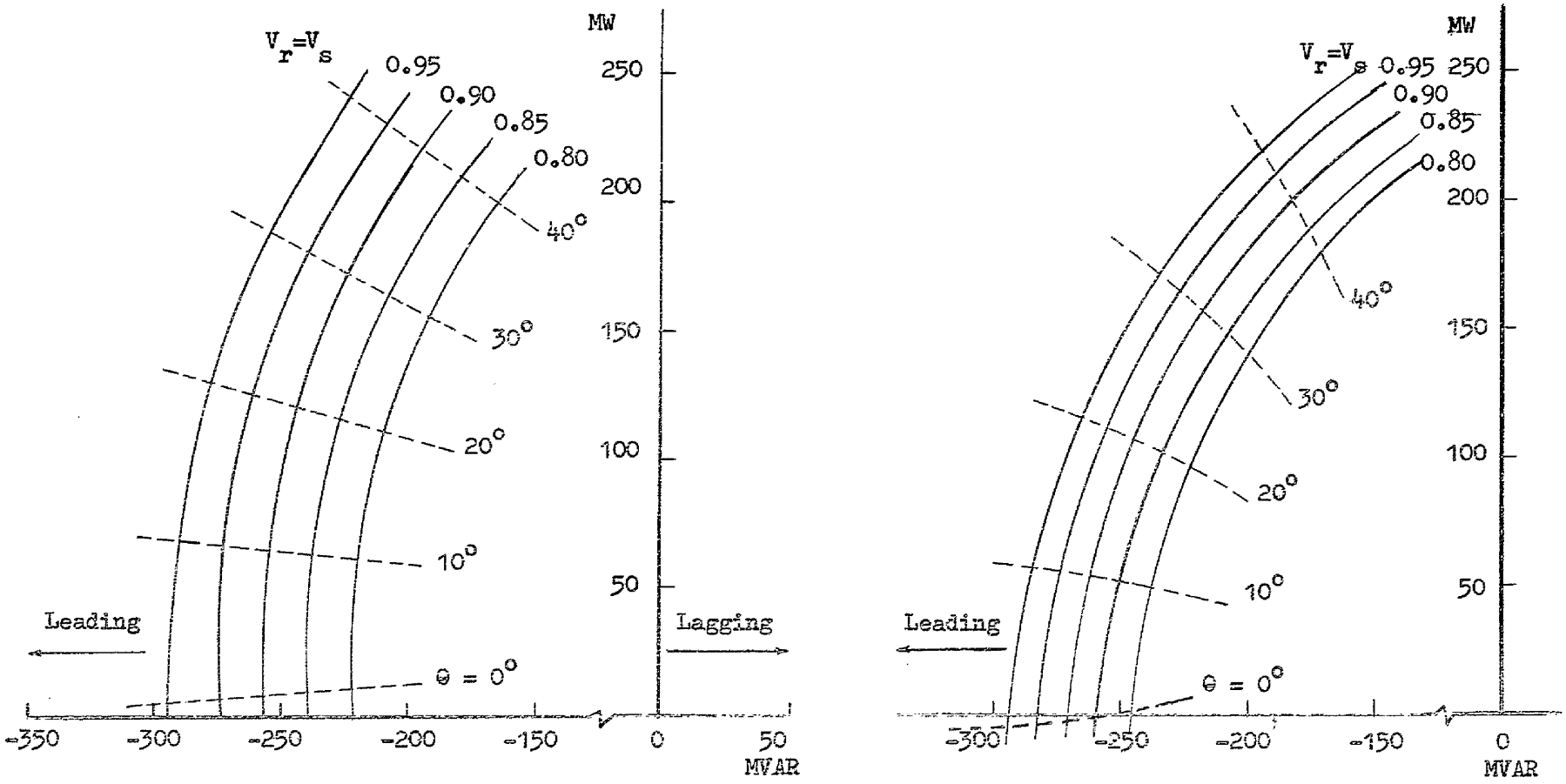

FIG. (5.10). POWER CHART FOR 330 KV, 800-MILE LINE

end in turn. The line has surge impedance loading of 538 MW. The diagram reveals that for maximum power transfer conditions the best location of the capacitor would be in the mid-point of the line and that the capacitor placed at the sending end of the line is an ineffective way of increasing the line transfer ability. Fig. (5.11.b) shows the variation of received power with capacitor location for three chosen degrees of compensation.

From equivalent single phase considerations it will be reasonable to expect an increase in the transferred power with increase in the degree of series compensation up to a maximum limit of 100%. With untransposed lines equal compensation on all phases need not necessarily mean that the power transfer ability of the individual phases is the same, in actual fact this is not so. Figs. (5.12) and (5.13) show both sending and receiving end power of individual phases of an untransposed line. The dotted curve is obtained on the assumption that the line is transposed, in which case the power carried by either of the three phases is one third of the total power; this has been confirmed from single phase equivalent studies. From these figures it is clearly evident that there is a considerable degree of unbalance in the separate phases' power carrying capability for the same degree of compensation. This is reasonable since the series capacitor introduced along the three phases has been based on the assumption that the lines were transposed. With this manner of compensation the maximum limit on the degree of compensation is well below 100% as confirmed here.

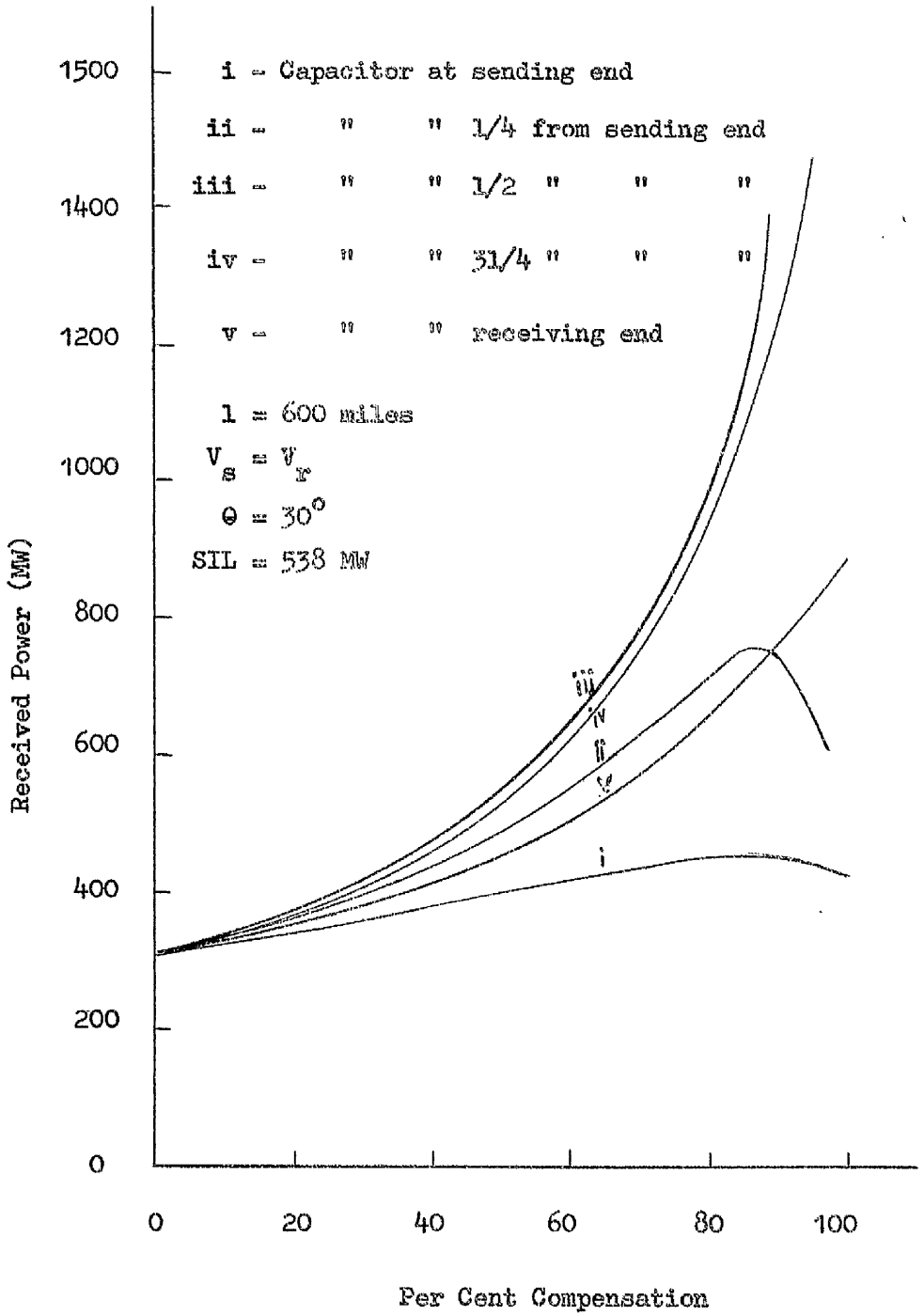

FIG. (5.11a). POWER TRANSFER VERSUS DEGREE OF SERIES COMPENSATION FOR 400 KV SYSTEM

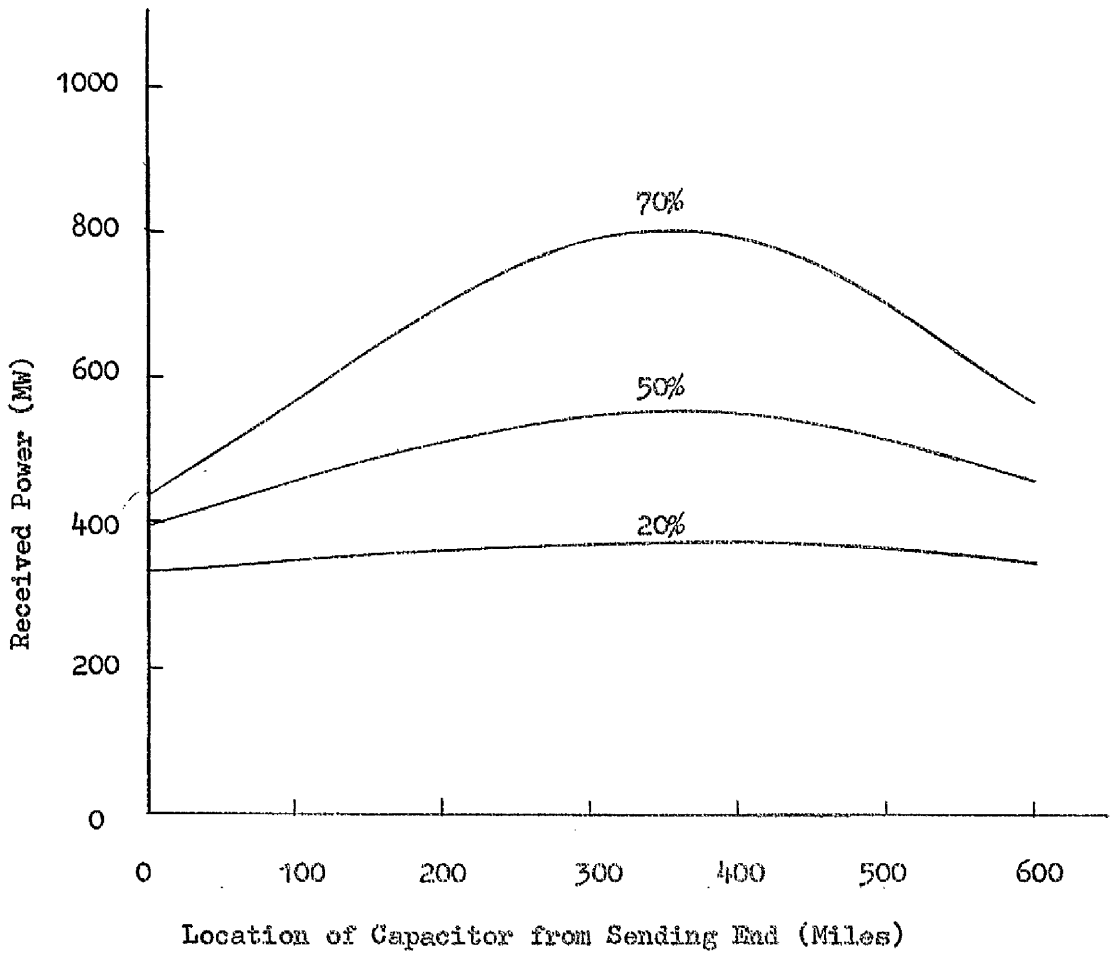

FIG. (5.11b). VARIATION OF RECEIVED POWER WITH CAPACITOR LOCATION FOR DIFFERENT DEGREES OF SERIES COMPENSATION

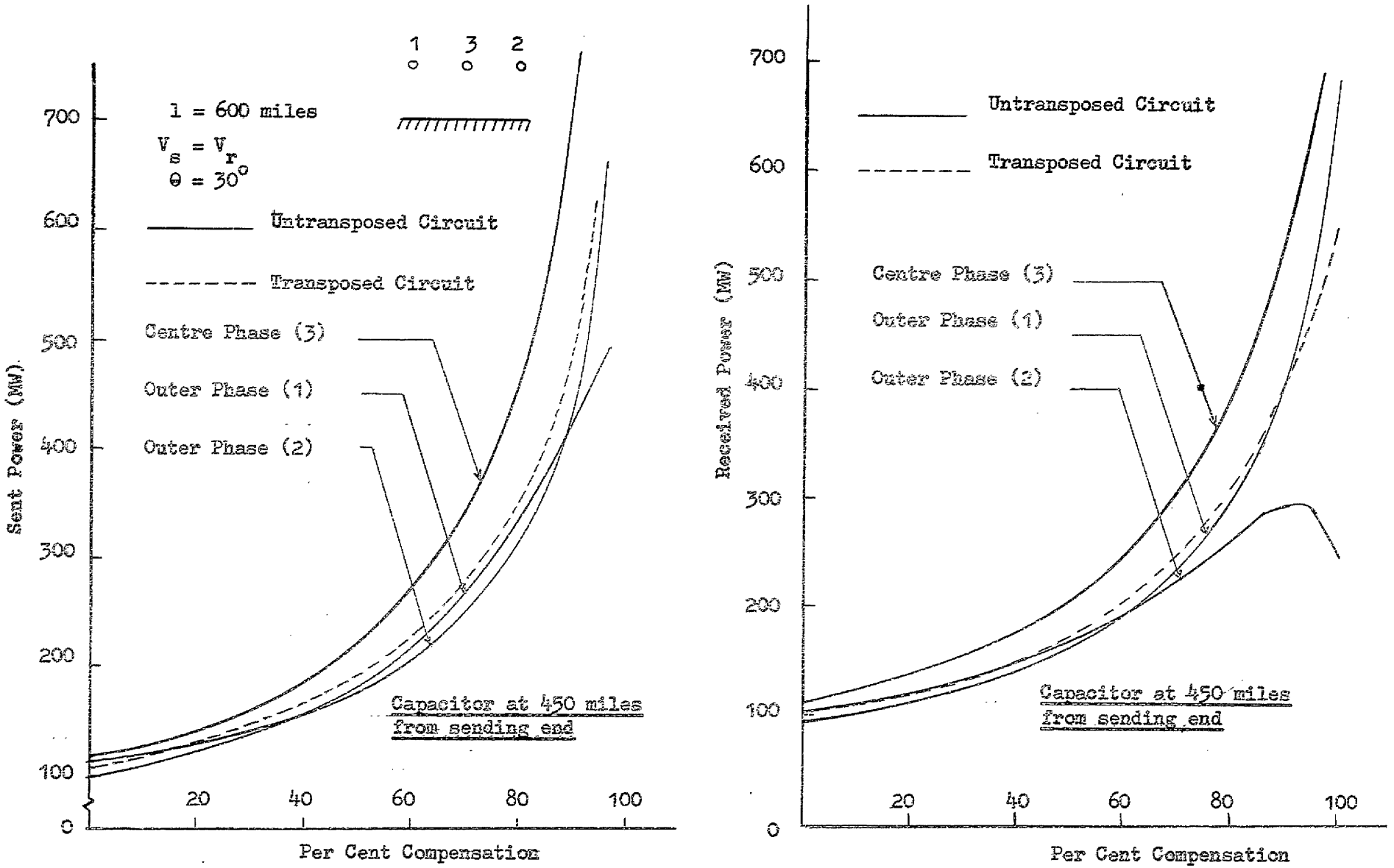

FIG. (5.12). INDIVIDUAL PHASE POWER VERSUS DEGREE OF SERIES COMPENSATION FOR 400 KV TRANSPOSED AND UNTRANSPOSED CIRCUITS

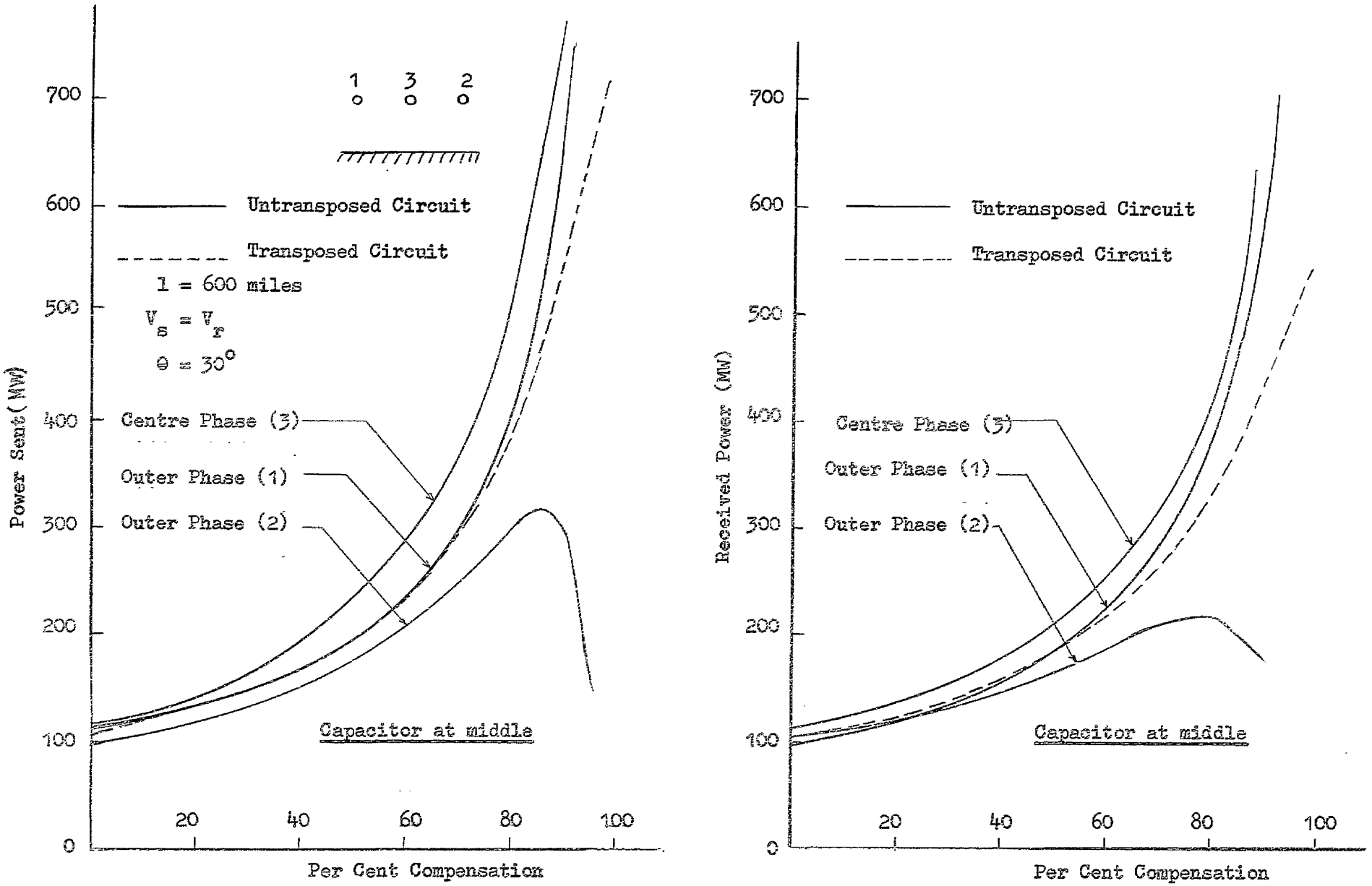

FIG. (5.13). INDIVIDUAL PHASE POWER VERSUS DEGREE OF SERIES COMPENSATION FOR 400 KV TRANSPOSED AND UNTRANSPOSED CIRCUITS

As far as overall maximum power transfer is concerned there are no advantages to be gained from breaking down the series capacitor into smaller units and distributing these along the line length as shown in Fig. (5.14) where two and three series compensating stations have been considered. The results presented for the two series capacitor case deal with a situation in which these are symmetrically spaced about the centre of the line and their distances varied in steps of 50 miles from 100 miles off the line centre. With the three capacitor stations the line is divided into four equal sections and the three capacitors introduced at the junction of two such sections.

From an overvoltage point of view there are, however, merits to be gained from breaking down the series capacitor. In Fig. (5.15) the line voltage profiles are shown for three degrees of series compensation: 20, 50 and 70 per cent for the case where the compensation is lumped at one station placed in the middle of a 600-mile line and the case where this is divided equally between two stations placed at 1/3 and 2/3 the distance from the sending end. The voltage profiles are formed from a knowledge of the capacitor terminal voltages and assuming these to vary linearly; the intermediate voltages will lie beneath the straight line section of the profiles and therefore there are no advantages to be gained from computation of intermediate points. In this manner a saving in computation time is achieved.

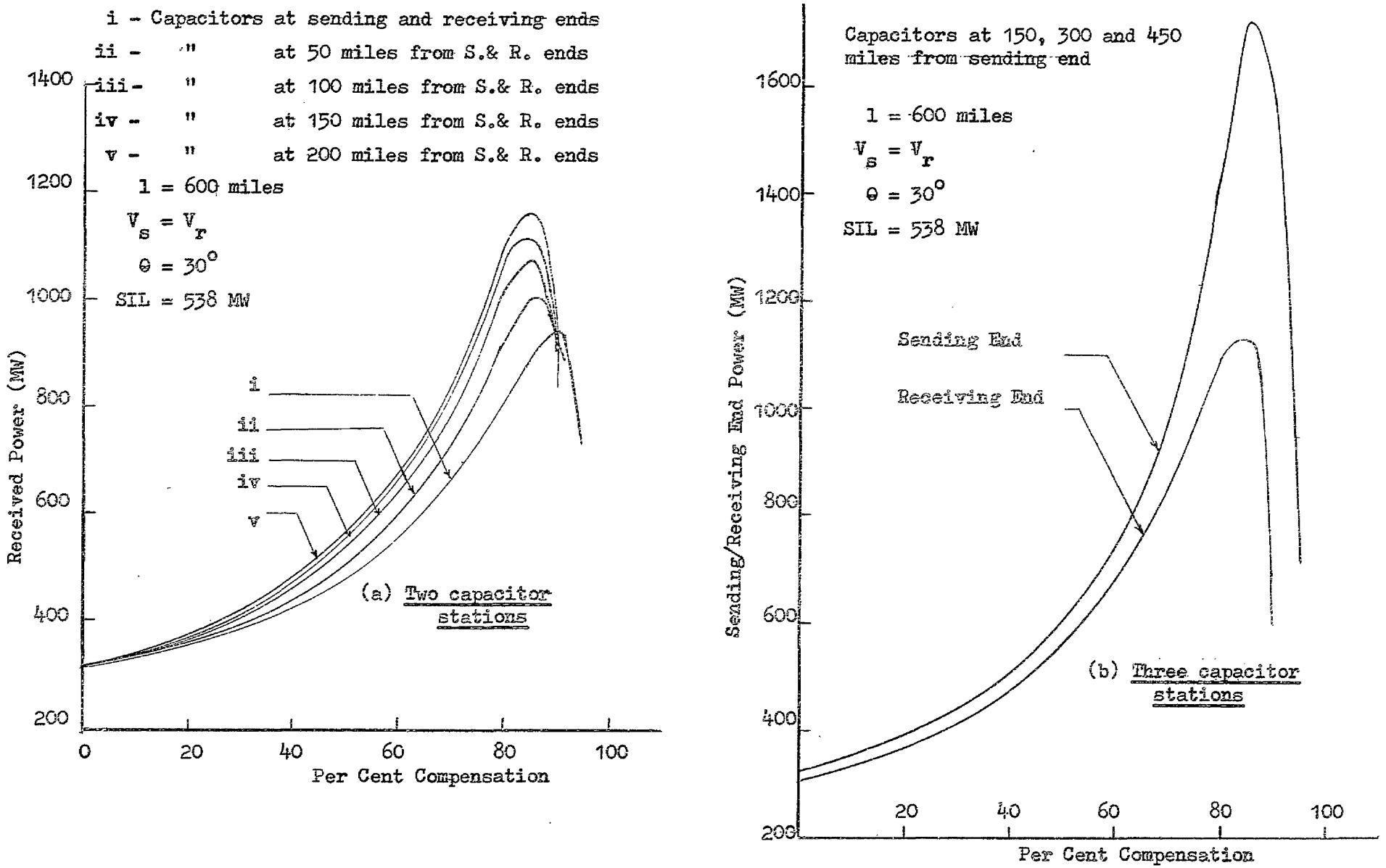

FIG. (5.14). POWER TRANSFER FOR TWO AND THREE CAPACITOR STATIONS ON 400 KV, 600-MILE LINE

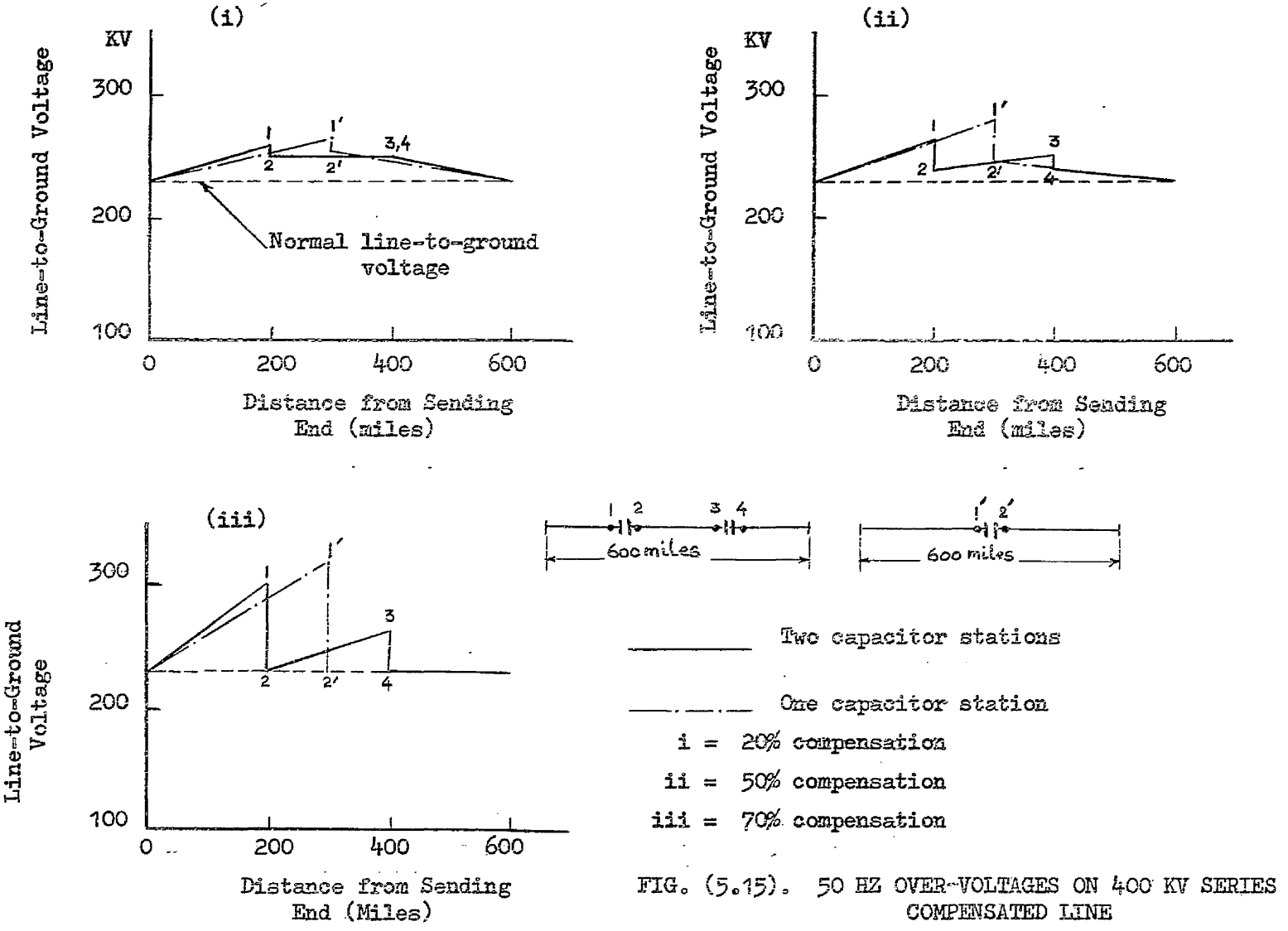

FIG. (5.15). 50 HZ OVER-VOLTAGES ON 400 KV SERIES COMPENSATED LINE

The profiles show the considerable improvement in the state of internal overvoltages when two compensating stations are employed. The normal line-to-ground voltage is included in these diagrams. It is seen, however, that for medium and heavy load conditions overvoltages exceeding the limits of normal service conditions appear on the capacitor terminals. For example overvoltages of the order of 140% and 130% appear on the terminals of the single capacitor scheme and one of the capacitors of the two capacitor schemes which render both schemes unsuitable for the case of 70% series compensation. It is possible to break the capacitor into further smaller units and thereby obtain workable conditions for up to 50% compensation as shown in Fig.(5.16) for the case where three such stations have been used. There are still intolerable voltage rises for still higher degrees of series compensation.

Though it is technically possible, as has been shown, to reduce internal voltage rises by purely distributed series capacitors placed in many locations along the line, economically this is not sound policy as with the increase in the number of compensating stations their fixed and running costs also increase.

The problem of capacitive generation has up to now not been completely solved since the line shunt capacitance has not been fully compensated by the introduction of series capacitors. The long line large capacitive generation calls for the installation of shunt reactors. If these reactors are connected at the series capacitor terminals they can also be useful in reducing down the overvoltages appearing

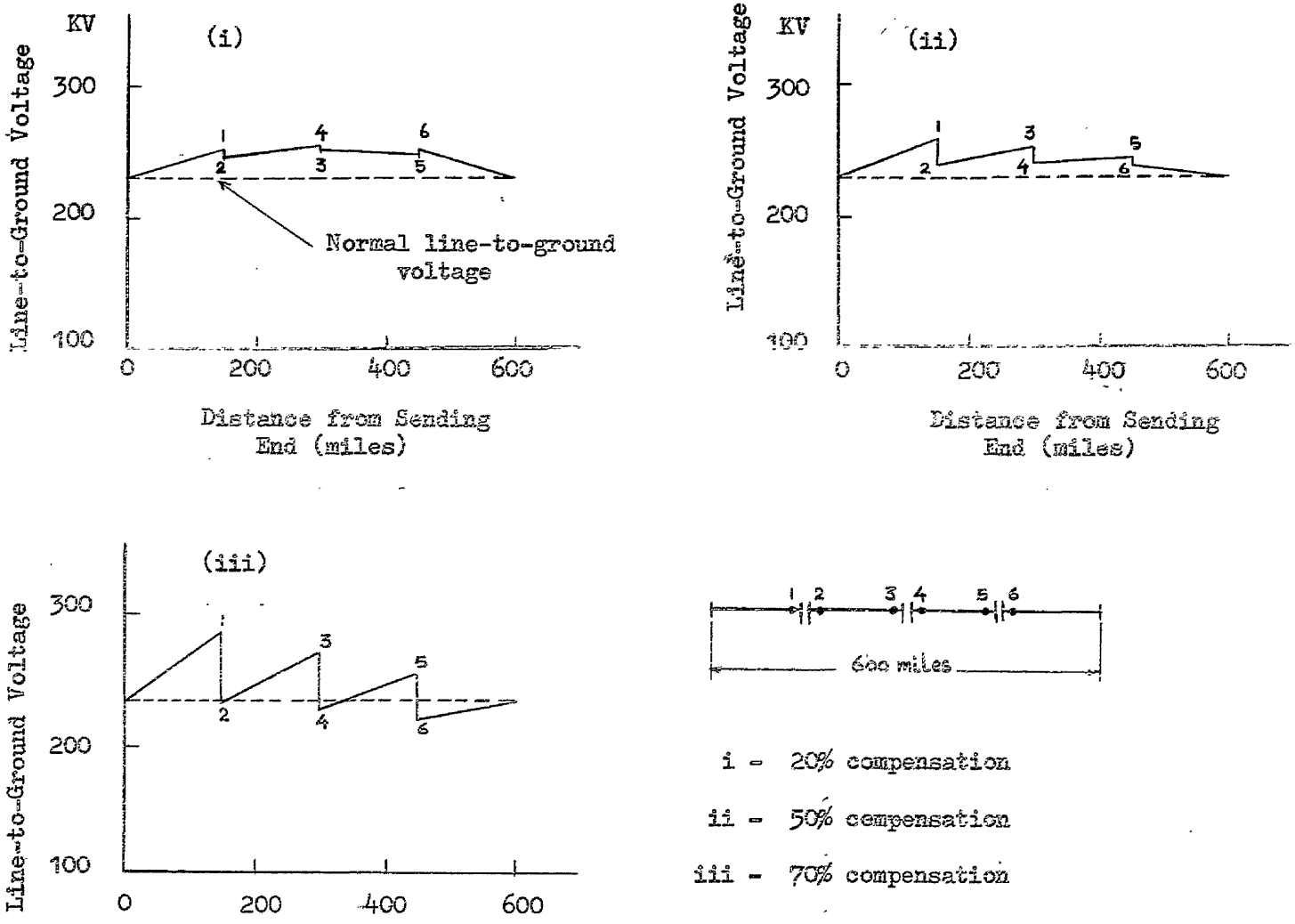

FIG. (5.16). 50 HZ OVER-VOLTAGES ON 400 KV SERIES COMPENSATED LINE

at their terminals.

5.6 Effect of Series and Shunt Compensation

Two possible compensating stations arrangements have been considered. In one case the reactors are placed at the generation and load points and in the other the reactors are placed at the series capacitor terminals. It has been found that the latter arrangement yielded better results from an overvoltage and reactive powerpoint of view and for this reason this arrangement is adopted in the following study.

Series and shunt compensation have been applied for three power transfer conditions on a 600-mile line

i - power transfer below surge impedance loading
ii - power transfer at surge impedance loading
iii-power transfer above surge impedance loading

The total degree of shunt compensation is the fraction of total line positive sequence admittance from which the equivalent compensating reactor has been obtained. Results will be given for both sending and receiving end active and reactive powers and also for voltage magnitudes at the terminals of the compensating stations and appearing on all phases. The capacitive reactance per station and the value of the shunt reactor and its power will also be included. For purposes of comparison the uncompensated line power and voltages are given.

5.6.1 Two capacitor/reactor stations

The results for this case are given in Table (5) , The

study reveals that when the level of power transferred over the line is below or at surge impedance loading the internal voltage rise can be brought to within practical tolerance limits by the introduction of two series/shunt compensating stations. For higher loads there are significant voltage rises especially on the sending end side of the compensating station which renders this arrangement unsuitable.

5.6.2. Three capacitor/reactor stations

With three compensating series/shunt stations evenly distributed over a 600-mile line the results of study given in Table (5) show that in general satisfactory operating conditions as regards voltage rises are attained for the three types of loads mentioned above. It may be necessary to install some form of compensation at the receiving end of the line to improve the load power factor for the case of higher loads. For practical purposes this type of compensating stations arrangement is then quite satisfactory.

5.7 Non-transposed Lines Unbalance Studies

5.7.1 General

The method used for the estimation of unbalances resulting from untransposed lines is to compare the line negative sequence and zero sequence currents with the line positive sequence current. LAWRENCE and POVEJSIL[52] estimated unbalances due to capacitive currents alone and combined them with unbalances due to inductive or load currents to obtain an overall picture of the total degree of unbalance. In developing their mathematical models for the electromagnetic and electrostatic unbalance, the authors made the assumption

TABLE (5-1). EFFECT OF SERIES AND SHUNT COMPENSATION ON POWER TRANSFER AND INTERNAL VOLTAGES OF 400 KV, 600-MILE LINE

i - Power transfer SIL = 538 MW

No. of Comp. Stations	Power transfer (MVA)					
	Below SIL		At SIL		Above SIL	
	send.end	receiv. end	send.end	receiv. end	send.end	receiv. end
0	320-j242	305-j203	-	-	-	-
2	354-j89	336-j25	585-j133	537+j39	983-j225	844+j250
3	340-j23	323+j41	580-j121	533+j50	982-j205	839+j324

ii - Capacitor reactance and reactor power

Loading	Two stations		Three stations	
	Cap.reactance	reactor MVAR	Cap.reactance	reactor MVAR
Below SIL	30.93	89.3	20.62	134
At SIL	77.32	62	51.55	67
Above SIL	108.25	29.8	72.17	67

SIL .... Surge Impedance Loading

TABLE (5) CONT'D. INTERNAL VOLTAGES.

1. Without Compensation

Phase	Voltage (KV) at Compensating Station location	
	1st Station	2nd Station
1	254.00	254.47
2	255.72	255.89
3	250.92	251.14

2. Two Compensating Stations

i - below SIL

Phase	1st Station		2nd Station	
	send. end terminal	receiv. end terminal	send. end terminal	receiv. end terminal
1	230.62	230.70	231.12	231.20
2	233.93	231.04	232.72	229.83
3	231.14	229.25	230.47	228.83

ii - at SIL

Phase	1st Station		2nd Station	
	send. end terminal	receiv. end terminal	send. end terminal	receiv. end terminal
1	237.74	235.87	235.69	239.17
2	251.32	230.62	242.39	227.17
3	246.24	229.88	238.47	226.37

iii - above SIL

Phase	1st Station		2nd Station	
	send. end terminal	receiv. end terminal	send. end terminal	receiv. end terminal
1	255.32	243.10	243.12	255.99
2	292.20	221.05	261.49	209.76
3	297.52	224.38	261.71	223.44

TABLE (5.) CONT'D. INTERNAL VOLTAGES

3. Three Compensating Stations

i - below SIL

Phase	Voltage (KV), at Compensating Station Location					
	1st Station		2nd Station		3rd Station	
	send. trm.	receiv. trm.	send. trm.	receiv. trm.	send. trm.	receiv. trm.
1	224.55	225.79	223.93	224.00	226.23	225.24
2	227.27	226.43	225.81	223.95	226.94	223.97
3	225.48	225.29	224.03	222.87	225.86	223.74

ii - at SIL

Phase	1st Station		2nd Station		3rd Station	
	send. trm.	receiv. trm.	send. trm.	receiv. trm.	send. trm.	receiv. trm.
1	234.52	233.45	234.69	235.25	233.55	236.02
2	245.39	231.27	242.05	229.98	237.14	227.06
3	240.47	229.61	237.16	228.47	233.99	227.49

iii - above SIL

Phase	1st Station		2nd Station		3rd Station	
	send. trm.	receiv. trm	send. trm.	receiv. trm.	send. trm.	receiv. trm.
1	238.46	234.18	236.81	237.06	234.31	239.47
2	270.10	223.04	257.45	214.11	244.34	204.21
3	271.91	223.08	257.11	216.20	243.49	210.28

that the charging current was supplied from one end of the line. Since this is not necessarily the case estimations of unbalances made were therefore not truly representative of untransposed lines unbalances. It has already been seen in the present investigation that the total transmission currents have been precisely calculated and no such assumption has been made for a two-ended system for separate calculation of inductive and capacitive unbalance. More accurate estimations of overall unbalances can therefore be obtained from the digital computer program at either load or generation end.

Using the method of symmetrical components[54] the line positive, negative and zero sequence currents are obtained; positive sequence current representing generation or load current of a transposed line. The degree of unbalance expressed as a percentage is then obtained. In these preliminary calculations line series and shunt compensation have been ignored and the results are therefore valid for uncompensated circuit lines only.

5.7.2 Horizontal and Vertical Line Unbalances

Unbalance estimations have been carried out for single circuit lines of horizontal and vertical configuration with earth wires. Description of both circuits is given in section (4.3). The degrees of unbalances have been calculated for different transmission angles and different ratios of voltage magnitude between sending and receiving end voltages. The effect of line length on unbalance has also been studied. Figs. (5.17) and (5.18) are a summary

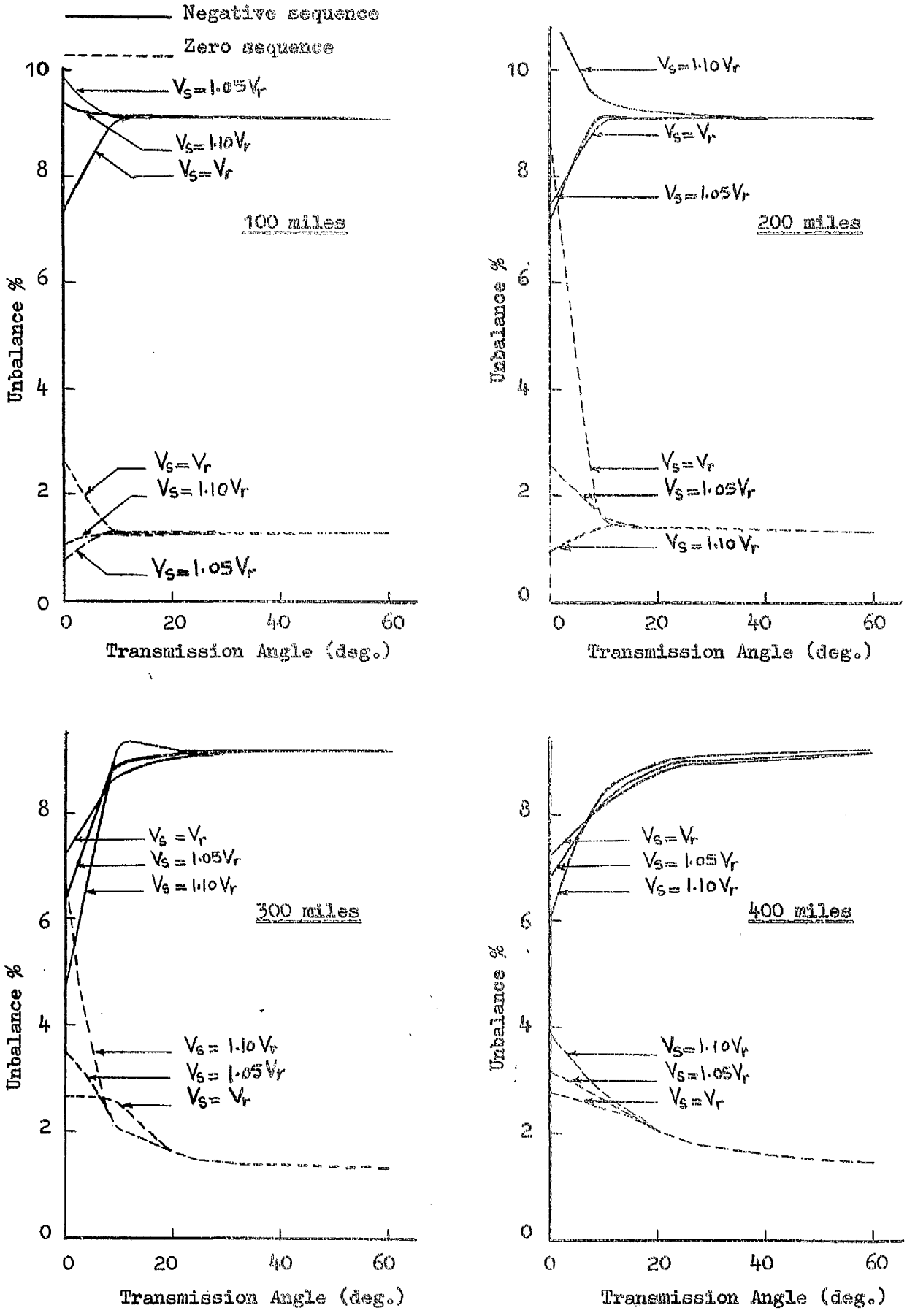

FIG. (5.17a). SENDING END UNBALANCE FOR HORIZONTAL LINES

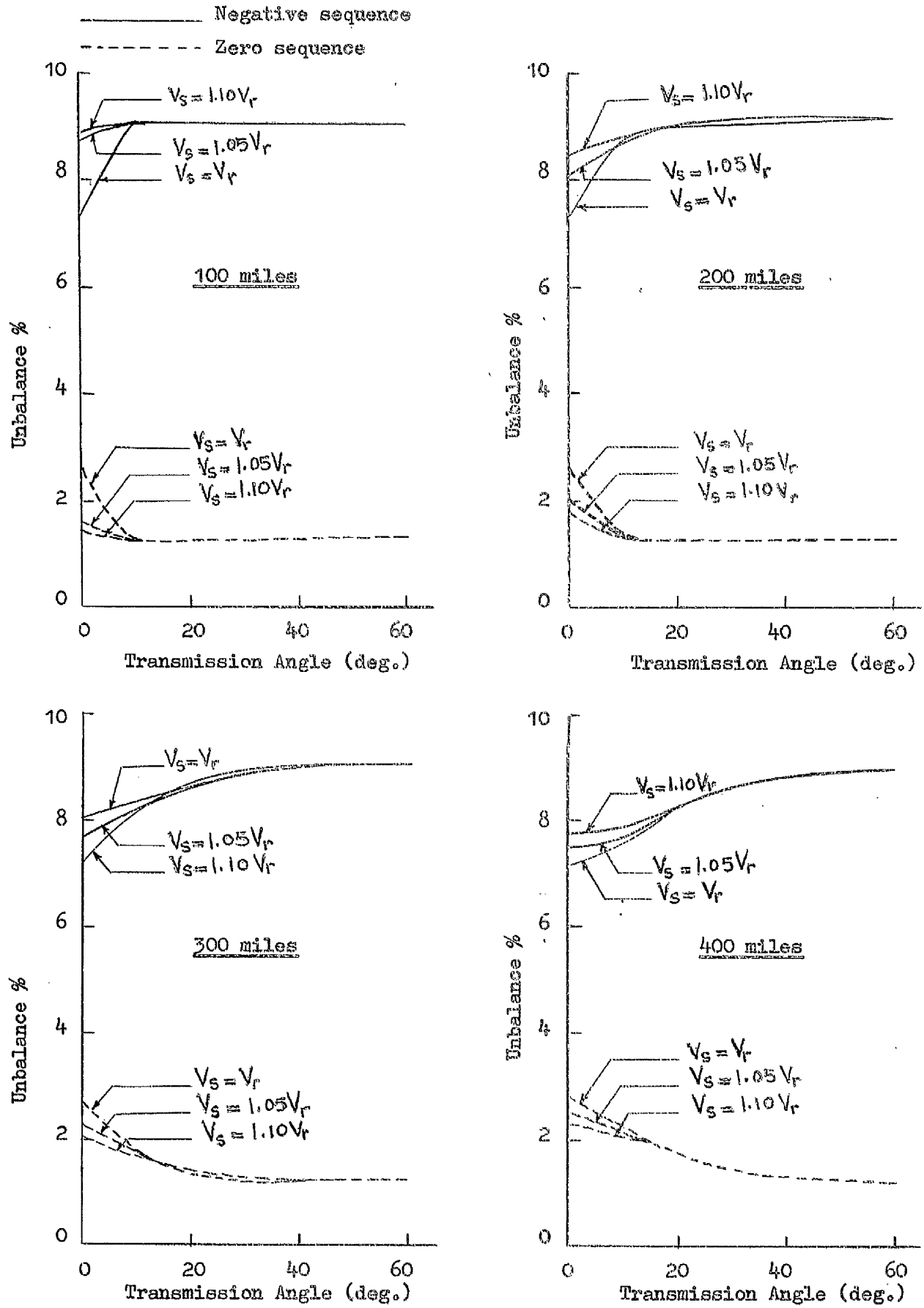

FIG. (5.17b). RECEIVING END UNBALANCED FOR HORIZONTAL LINES

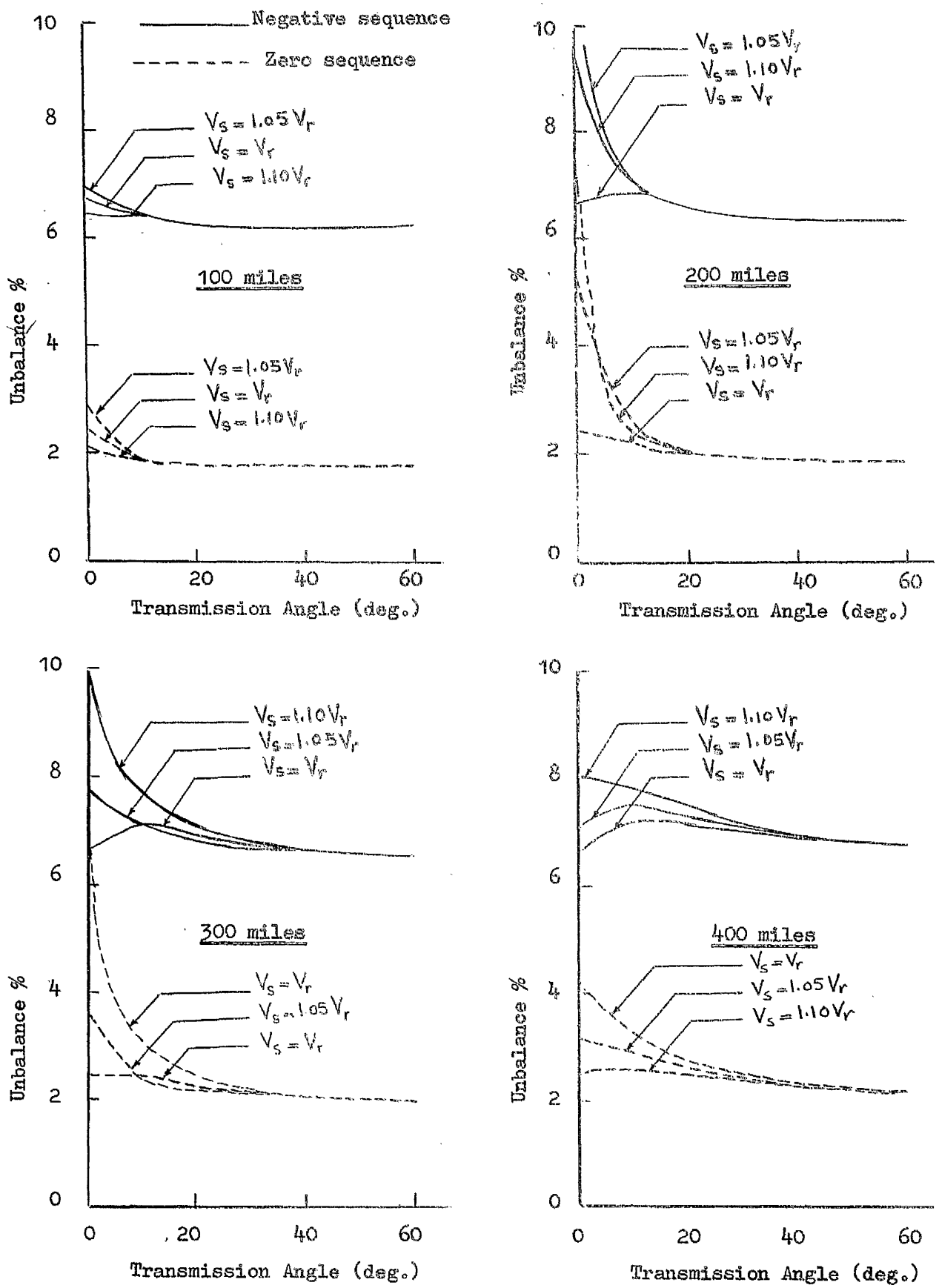

FIG. (5.18a). SENDING END UNBALANCE FOR VERTICAL LINES

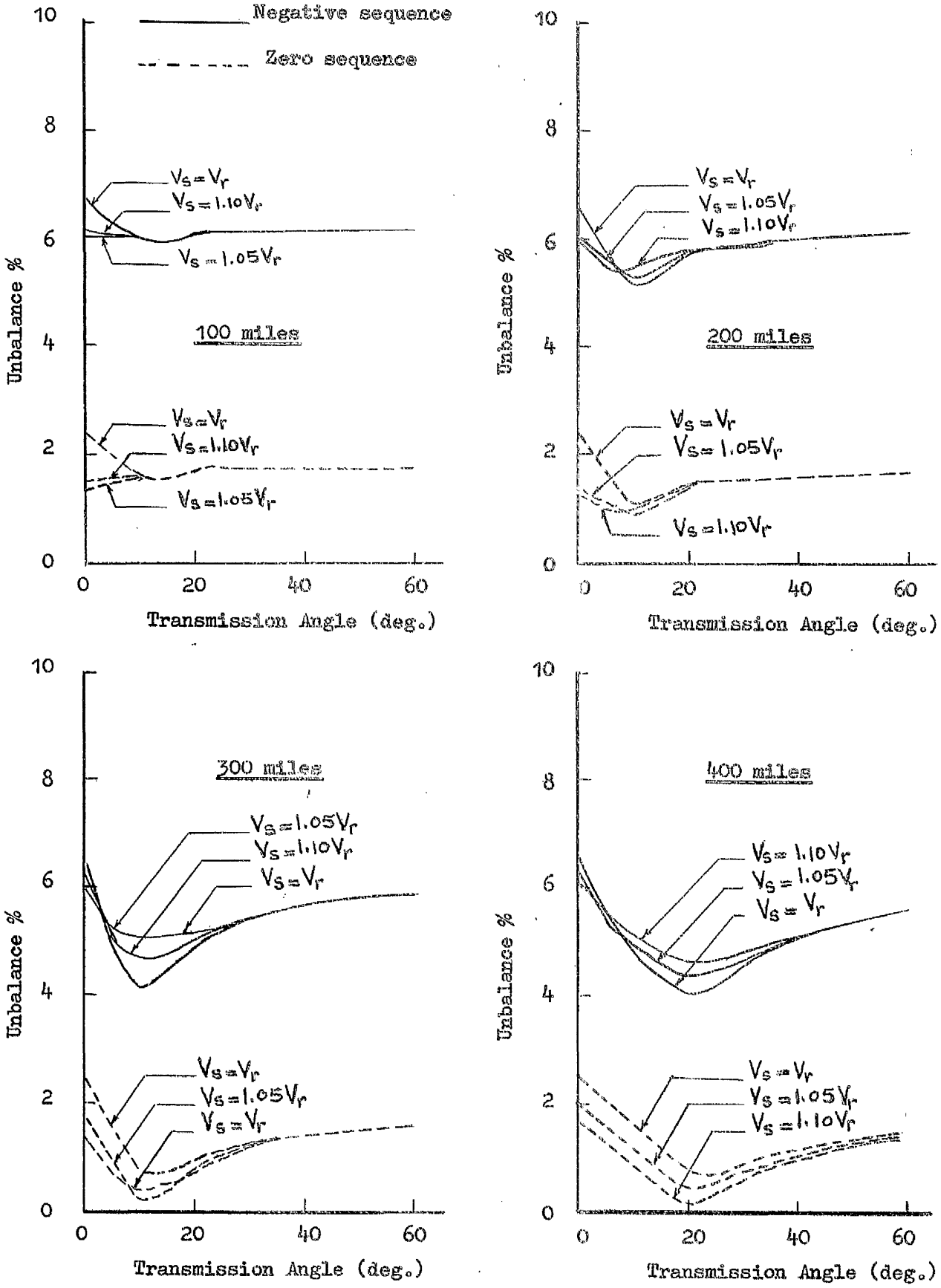

FIG. (5.18b). RECEIVING END UNBALANCE FOR VERTICAL LINES

of the results of studies. The following conclusions are drawn:-

i. that for low transmission angles there are wider variations in unbalance factors for different sending/receiving end voltage ratios for all line lengths and for both types of circuit arrangements. This is brought about mainly due to the effect of capacitive unbalance since for low transmission angles the line charging current is more dominant than the load current and as the charging current depends on the voltage magnitude at both ends, changes in these magnitudes will be expected to have an influence on the capacitive current unbalance. As the transmission angle increases, the load current becomes more dominant and both negative and zero sequence unbalance are then due to electromagnetic effects and hence little changes are noticeable for different voltage ratios.

ii. that negative sequence unbalance factors are higher for a horizontal line than for a vertical line particularly for higher operating transmission angles. This conforms with the fact that there is less dissymmetry in the case of a vertical line.

iii. that percentage unbalances resulting from negative and zero sequence currents have comparable values at both sending and receiving ends of a horizontal line irrespective of the transmission length for operating angles in excess of 10°.

5.8 Conclusions

(1) Some fundamental long line properties have been shown to agree in principle with predictions of classical transmission line theory.

(2) Series compensation studies show that the introduction of series capacitors along a transmission line is an effective method of increasing the power capability of the line. The maximum degree of series compensation possible for the case of an untransposed line is governed by the power carrying capacity of the individual phases which need not necessarily be the same for all phases. In this respect a transposed line behaves differently since the total power is shared equally among all phases of a three-phase system and as a result 100% degree of series compensation is possible on all phases.

(3) It is advantageous to break the series capacitor into smaller units and spread these on the line as such arrangement is useful in obtaining smooth voltage profiles. Since the cost of compensation will increase the total cost of the transmission system it is necessary from an economic point of view to keep down to a minimum the total number of compensating stations. From the studies carried out it appears that one compensating station every 200 miles is a satisfactory arrangement for long distance-lines.

(4) A reduction in reactive powers imposed on the source can be successfully brought about by the installation of shunt reactors for the absorption of the transmission line capacitive power. The installation of the shunt reactors

at the terminals of the series capacitors is an additional aid for more uniform voltage profiles and ensures that the voltage appearing at the terminals of the series capacitors are within allowable design limits.

(5) Preliminary investigations of uncompensated line unbalances show that the magnitudes of negative sequence unbalances are pronounced. This indicates the importance attached to studies of this nature as regards methods of balancing compensated long-distance lines. The introduction of unbalanced capacitive and inductive compensating elements on different phases of an untransposed line may provide a possible means for off-setting these unbalances. If achieved then it would be possible to do without the costly procedure of transposing high voltage lines.

(6) Though applied for point-to-point transmission the method of analysis presented here is general and is capable of extension for more complex power system arrangements.

CHAPTER SIX

GENERAL SURVEY OF SOLUTION OF TRANSMISSION LINE SWITCHING TRANSIENTS

6.1 Introduction

Extra high voltage transmission lines are susceptible to internal as well as external disturbances which cause dangerous phases of operation indicated as severe overvoltages in excess of the normal operating conditions of the line. Among the internal causes of voltage failures are:-

i. system resonance
ii. switching operations
iii. insulation failure due to earthing of line. Whereas voltage failures due to external causes are mainly brought about by lightning surges.

With the continuous increase in system operating voltages, switching surges which are proportional to operating voltage increase in importance relative to lightning surges, which are sensibly independent of system conditions. Consequently in very high voltage lines the impulse levels are more and more dependent on switching overvoltages and not on natural phenomena. It is this fact which has stimulated so much interest in the analysis of switching phenomena in relation to insulation coordination in the last decade. A knowledge of the magnitude, wave-shape and duration of switching surges that may be applied to power apparatus is extremely important for the correct

establishment of their insulation strength. In network planning it has therefore become vitally necessary that both a quantitative as well as qualitative knowledge of switching surges caused as a result of system energisation or system de-energisation be readily available for the determination of safe margins of operation[55]. Three types of approach for assessing transient overvoltages are already known. These are

1. System models (experimental)
2. Theoretical studies (analysis)
3. Field tests.

A brief description of each of the three methods will now be dealt with for purposes of bringing out the various merits and demerits of each of these methods.

6.2 Methods of Assessing Transmission Line Transient Performance

6.2.1 Transient Analysers

The high cost involved and limitations regarding coninuity of the power supply have rendered the precise field test methods impractical in determining transient overvoltages resulting from switching operations. The complexity of the problem and the absence of the proper analytical tools in the past made the solution to the transients problem on power system networks almost impossible. Efforts were therefore directed earlier on towards the miniature systems-approach[56]. The calculating board or network analyser played an important role in the transient analysis and performance of power systems carried out on single phase or three phase

basis[57]. Network analyser methods were then applied whereby a circuit model of the actual system under investigation was set up on these machines. Lumped-parameter circuit elements and distributed parameter networks, specified by their nominal-T or -π equivalent, can be represented on these machines and circuit-breaker operations are simulated with switches for opening or closing the circuit. Owing to the speed with which the transient dies away the problem of obtaining the transient response is facilitated by the use of a cathode ray oscilloscope with possible adaptations for oscillographic records.

Dependent on the accuracy of system representation in particular distributed-constant elements such as transmission lines and cables the transient network analyser provides a convenient means of obtaining accurate information about the system under transient conditions. In a recent paper Uram and Feero[58] compared results of transient overvoltages due to line energisation obtained from a digital computer study based on a sophisticated mathematical approach with results arrived at from a transient analogue analyser. Close agreement between the two methods of approach have been confirmed and have thus revealed the usefulness of these machines. From a teaching point of view transient analysers can be very useful too due to possible "feel" for the transient performance of power system networks.

6.2.2 Field Tests

The limitation of transient analysers in representing distributed parameter networks and in failing to handle effects of certain system characteristics such as corona, drew

the attention of investigators[59,60,61] to the need for more accurate studies regarding magnitude, wave shape and duration of switching surges to enable proper and adequate measures to be taken against these types of disturbances. The exact behaviour of a transmission line subjected to switching conditions is accurately known if the actual line is subjected to field tests. Field measurements then faithfully reproduce true system performance within the limits imposed by the measurement system itself. A variety of effects such as prevailing climatic conditions which are not possible to simulate on analogue machines are better represented in field measurements approach.

For purposes of recording transient overvoltages due to switching surges cathode ray oscilloscopes and high frequency-response measuring techniques are employed. These instruments can be located at various points on the network wherever the system response is desired. McELROY and SMITH[62] have carried out extensive site test programs of energisation and re-energisation on 345 KV transmission lines and have thus demonstrated the effectiveness of the method of field measurements in obtaining a great deal of useful information for a variety of system conditions.

When precise measurements and recordings are carried out on an actual transmission system subjected to switching conditions the results obtained can serve as a means of checking corresponding information obtained from an analytical approach by, for example, a digital computer and hence any disparities immediately revealed. The theoretical

assumptions, therefore, on which the numerical calculations have been based can then be revised and wherever possible amended. Field tests are also a good means for providing accurate data for theoretical studies.

Although site tests are ideal in obtaining a comprehensive information about the system transient behaviour they are an extremely costly process. A transmission project is not always available for site tests to be carried out as this would entail power cuts and hence several inconveniences; on the other hand during preliminary stages of design no such project would exist in any case. Though a wide range of investigations revealing the effects of various factors on system performance such as system parameters, circuit configurations, source representations --- etc. can be handled directly in the field, the diversity of these factors and the several possible combinations they produce tend to limit the versatility of the method of field measurements. In this respect transient analysers and digital computers are more favourable.

6.2.3 Analytical Methods of Study

The basic problem encountered in the evaluation of transmission line transients is the solution of the system partial differential equations. If boundary conditions are ignored then the system equations reduce to the equations of an initial value problem the solution of which can be obtained by classical methods of approach. Reference is made here to the "p" operator method treated extensively in many text-books where the algebraic equations of the system

are formed then solved and the time solutions obtained from standard inversion tables. The simplifications made for the reduction of the transient problem to an initial value problem make the conclusions drawn from this type of approach to be rather limited since only simple quantitative analyses can be carried out.

For exact solutions the partial differential equations of the transmission system must be considered in their entirety. This makes a purely analytical solution difficult to obtain and it becomes necessary that numerical solutions should be attempted. Numerical solutions necessitate the use of an automatic means of computation. With systematic formulation of system equations a digital computer is a great help in obtaining such numerical solutions. Several methods that make use of digital computers in the solution of transmission line transients have been suggested. It has been thought that it will be relevant to the present work that a brief comparison be given here of the outline of these methods before detailed discussion is presented for the method used in this investigation.

6.2.3.1 Lattice Diagram Solution

The calculation of transmission line transient voltages resulting from switching operations can be obtained by treating the resulting surges as travelling waves, travelling along the line, and then applying Bewley's lattice diagram technique to the determination of the effect of these surges at any point along the line [63]. The lattice is a time-space graph which defines the response of the system

resulting from the arrival, reflection and transmission of a travelling wave at a particular junction. Single phase or three phase networks can be treated by this method provided that reflection and refraction coefficients at the junction are known together with the surge impedance of the line.

The lattice diagram method has formed the basis of many transmission line transient calculations. BARTHOLD and CARTER[64] put a slightly different interpretation on the method based on the fact that on the arrival at a junction the original wave generated at the junction ~~two~~ waves travelling in both directions from the discontinuity whereas itself passes unaltered past the discontinuity. They developed a digital computer program for single-phase equivalent systems based on a travel time matrix for a multi-bus sytem with the off-diagonal terms in the matrix representing the transit time between two buses and the diagonal elements representing the travel time of a bus to itself being set to zero. A reflection factor matrix was also used, this specified the reflection coefficient at any bus. Complex terminal impedances were represented in their program by open-circuited or short-circuited stub transmission lines for what was effectively capacitive or inductive terminations. These stub lines were so chosen that their travel times were short compared with the basic time interval selected for the study. Successive displaced positive and negative step functions could be added in their method to simulate the effect of injecting into the switch point inputs other than step functions. Their method is thus based on certain approximations. McELROY and PORTER[65]

indicated the way in which the above method could be extended to cover transient calculations for three phase as well as single phase equivalent systems taking into consideration the effects of ground wave on the transient performance of these networks which were completely ignored in BARTHOLD and CARTER's program. They proposed a method whereby an electric network could be decomposed into finite and semi-infinite lines with propagation from one bus to the other defined in terms of transfer coefficients. Lumped parameters were again represented by distributed parameter networks and certain non-linear principles such as lightning arrester operation were tackled.

Both methods cited in references (64) and (65) above have not taken into consideration the time variation of the system parameters. This makes their calculations valid only for one frequency - that at which the parameters were calculated. This assumption sets a limitation on their methods of approach and makes them fall short of a true representation of a system transient response which in practice is subjected to a wide range of frequency variations under transient disturbances.

The evaluation of transmission line transients for single-phase and three-phase networks resulting from switching operations taking into effect earth propagation characteristics was dealt with by BICKFORD and DOEPEL.[66] The calculations obtained from a digital computer program were based on the Bewley lattice diagram method with the

usual manner for the representation of transmission lines and cable systems and the treatment of lumped inductive and capacitive elements by transmission line stubs. The authors work referred to the solution of transmission line transients problems by the Fourier transform theorem to obtain the response in the frequency domain and the application of the inverse transform to arrive at the response in the time domain. In their view the authors believed that this latter approach was unsuitable for handling non-linear problems and that the costs of computation incurred from its application were so high that rendered its use uneconomic, from this angle they favoured the facilities provided by the lattice diagram method. The authors, however, found it necessary to apply the Fourier transform method to obtain the step response of the system and then used the lattice-diagram technique to obtain the overall response and thereby made sure that the frequency variation of the system parameters was taken care of. For economies in computation the authors represented part of the power system by what they called step response generators situated at the switching station bus-bar - this is a form of source-side network simulation. A comparative study presented between two cases, one in which the whole system was being considered and the other in which part of the system was represented by a step response generator indicated good agreement. That was a reasonable justification for the replacement of those parts of the network that were of no immediate consequence to the main transients investigation.

An important point tackled by the authors in their

lattice-diagram program was the problem of non-simultaneous closure of a circuit breaker poles not considered in any of the previous methods discussed. Though this is a non-linear problem in nature the lattice-diagram method does provide a solution since the change of conditions at the breaker poles on the instant of switching is simulated by a change of terminal impedance matrixes i.e. reflection factor coefficients. From an insulation co-ordination point of view for the power system the authors quoted a figure of 2.5 p.u. as acceptable for transient overvoltages and suggested that for practical purposes overvoltages exceeding this figure should be reduced to safeguard against possible system failure. They demonstrated that resistance switching provided an effective means of reducing transient overvoltages and also application of shunt reactor compensation especially for the case of long distance lines.

A common feature to all investigations carried out on the evaluation of transient response of transmission systems is the limitation of these methods on the representation of lumped parameter system components by distributed parameter networks i.e. transmission line stubs. The travel time for these stubs was assumed to be small compared with the time step duration chosen for the transient study. In other words, if it has been found necessary to carry out a detailed study of the front characteristics of a switching surge which demanded a finer interval of time then this will not be possible as the transmission line stub would depart from the lumped parameter value it is representing. The method also fails to offer accurate representation to

such system components as generator transformers.

6.2.3.2 Laplace Transform Method

The general partial differential equations of a transmission line can be solved analytically for the ideal case of an infinite lossless line by the application of Laplace transform theorems[67]. Propagation along the line for such systems is defined in terms of a single velocity, that of free space and one coefficient of attenuation without any distortion effects being considered in this case. The solution takes the form of converting the partial differential equations into ordinary differential equations, solving these by standard methods and then inverting to obtain time solutions. For lossy systems numerical solutions become a necessity for these partial differential equations.

URAM and MILLER[68] presented a method for dealing with the transient performance of practical transmission lines. They showed the way in which the general simultaneous partial differential equations of multiconductor transmission lines would be reduced to ordinary differential equations by the Laplace transform method. In their paper the authors introduced matrix methods for the transformation of the second-order interdependent differential equations into a set of independent differential equations. The solution in the 'Laplace domain' is thereby obtained on application of classical methods and the time response due to the appropriate disturbances is derived by inverse Laplace transformation.

On the assumption that the line was transposed two modes

of propagation were only considered by this method, an aerial mode and an earth mode. This assumption puts a restriction on their method of analysis and makes the studies presented in the paper by URAM and FEERO[58] and based on this method of a rather limited nature since they represent only a particular case of the general multiconductor line problem as dealt with by WEDEPOHL.[18]

URAM and FEERO developed a digital computer program for the study of switching transients on terminated and unterminated transposed transmission lines under different operating conditions, this program being based on a Laplace transform mathematical model of the companion paper by URAM and MILLER. Agreement between the digital calculations obtained and oscillographic records derived from an analogue computer study was found to be reasonable, this led the authors to draw the conclusions that the mathematical approach was therefore sound for the analyses of such types of study. The agreement between the analogue and digital result is no indication, in actual fact, on the accuracy of the method proposed by URAM and MILLER since the system parameters used for both digital and analogue machine calculations ignored the frequency dependence of these parameters. The system constants were represented at only one frequency. This is a major drawback, therefore, on the use of the Laplace transform method in obtaining the transient response of transmission systems. The method has nevertheless an advantage over the lattice diagram technique in that lumped capacitive and inductive elements are represented as they are and that there is no need

for stub-line representation.

6.2.3.3 Modal Theory and Fourier Transform Method

The analysis of the steady-state performance of a poly-phase multiconductor line has already been discussed in earlier sections of this investigation. This involved calculation of the system constant at only one frequency, namely the power frequency of the supply. Under transient conditions, since these networks are subjected to disturbances varying over a wide range of frequencies it would be essential to take into consideration the frequency dependence of the network parameters and hence its propagation constants for an accurate assessment of transient response. The development of the theory of modal propagation on transmission systems has opened a new scope for the solution of the transient problem on multiconductor lines. The theory reduces the complexity of the transient problem and turns it into a steady-state calculation over the frequency range of interest. The elimination of the time variable in the system partial differential equations is made possible on application of the Fourier transform theorem. The theorem states that

$$f(\omega) = \int_{-\infty}^{+\infty} f(t)\, \exp(-j\omega t)dt \qquad - (6.1)$$

and its inverse

$$f(t) = (1/2\pi) \int_{-\infty}^{+\infty} f(\omega).\exp(j\omega t)d\omega \qquad - (6.2)$$

(6.1) and (6.2) are known as the Fourier transform pair

and deal with evaluation of the time function f(t) or system transient response from a knowledge of its frequency response f(ω) or the response of the system in the frequency domain.

Determination of the system response in the frequency domain due to a certain input time function derived by its Fourier transform as in (6.1) can be numerically calculated, frequency by frequency, in an exact manner to the steady-state calculations using the theory of modal propagation. The system transient or time response is then obtained by using the inversion integral given in (6.2) above.

In contrast to the form of the Laplace transform method described in section 6.2.3.2 the time dependence of the system parameters is taken care of by this method as has just been pointed out. The representation of lumped and distributed elements by their algebraic expressions frees the modal-Fourier method from any limitation on the duration of the time interval dictated by transmission stub representation. Precise wavefront studies are thus made possible. Other system components such as transformers can be well represented from considerations of their steady-state equivalent form of representation.

In view of the fact that in general, f(ω) is a non-analytic function the numerical evaluation of the inversion integral becomes a necessity. Certain problems arise from attempts of numerical evaluation of the integral given in equation (6.2). These problems will be subject to detailed discussion in the following chpater and means

of overcoming difficulties pointed out.

The power of the modal-Fourier transform method lies in its ability to handle linear as well as non-linear problems. Until very recently the analyses of non-linear transmission problems such as sequential pole closure, sequential pole tripping, lightning arrester operation and resistance switching have been thought to be a closed research field as far as this method is concerned. In the present work such beliefs will be shown to be unrealistic.

6.3 General Considerations

The evaluation of transmission line transients by analogue methods has long been established; results obtained from transient analysers or analogue computers being restricted by the accuracy of representation of distributed parameter networks by lumped-circuit elements. Analytical solutions are not easy to obtain owing to the complexity of the problem. Mathematical methods have been developed which make use of a digital machine for automatic computation of system responses - among these are the lattice diagram, Laplace transform methods. The limitation of these methods is that they fail to consider the time dependence of the system parameters. The lattice diagram method has its field of application in linear and non-linear problems.

The modal theory of propagation with the Fourier transform technique offers a very elegant approach to the solution of transient problems in multiconductor transmission lines. Linear as well as non-linear problems

can be handled with ease as will be shown in further sections. Analytical discussion to such problems will be made and numerical calculations presented. There are, however, important fundamental aspects attached to this method to be used in the present investigation; these will be discussed first before any numerical calculations are made.

CHAPTER SEVEN

APPLICATION OF THE THEORY OF MODAL PROPAGATION AND FOURIER TRANSFORM TECHNIQUE FOR THE ANALYSIS OF MULTICONDUCTOR LINE TRANSIENTS

7.1 Introduction

The analysis of multiconductor transmission lines under steady-state conditions has been covered using the concept of natural modes. Since under steady-state conditions the interest in the system behaviour is centred around one frequency, namely the frequency of the supply, calculation of the line propagation properties is done for this particular frequency. The same method of approach would be applied to the analysis of the transient response of transmission lines but use is made here of the Fourier transform pair. The numerical evaluation of the inversion integral for the determination of the time response presents certain problems some of which are concerned with the stability of the integral in the regions of discontinuities of the frequency response and others are related to economies and efficiencies in computation. The general aim here being that as much reduction as possible being carried out on computation of the system response in the frequency domain. Calculation of the system eigenvalues and system eigenvectors necessary for the determination of the frequency response takes quite a considerable amount of computation time in the digital computer program. The theory behind and possible means of achieving reduction in frequency response computation time will be discussed in detail here.

7.2 The Modified Fourier Inversion Integral

The Fourier pair given by equations (6.1) and (6.2) will be given here as more reference will be made for these in the present chapter. Equation (7.1) defines the Fourier integral and (7.2) its inverse.

$$f(\omega) = \int_{-\infty}^{+\infty} f(t).\exp(-j\omega t)\, dt \qquad - (7.1)$$

$$f(t) = \frac{1}{2\pi}\int_{-\infty}^{+\infty} f(\omega).\exp(j\omega t)\, d\omega \qquad - (7.2)$$

For the evaluation of both formulae the integration is carried out between $-\infty$ and $+\infty$. Analytic functions involved in the above integrals may be evaluated by the ordinary or contour methods of integration and since energising functions of transmission lines fall within this class there appears to be no difficulty with such types of function. If either $f(t)$ or $f(\omega)$ are known only numerically, and this is normally the case for the open-circuited or short-circuited transmission line in the time and frequency domains, then analytic evaluation of these integrals is not possible. MULLINEUX and others[19,20] have indicated that two major problems arise when the inversion integral (7.2) is being evaluated numerically. One of these is related to the behaviour of the function round a discontinuity when Gibbs oscillations occur on the function and the other resulting from the fact that the poles of $f(\omega)$ lie close to the path of integration and hence give rise to instabilities in the function $f(t)$. Having discussed these problems in detail the authors have

produced a modification on the inversion integral whereby the resulting difficulties mentioned are overcome. Owing to the importance of the modified Fourier transform method in the present analysis it is thought reasonable to discuss the details of this method particularly since further basic considerations regarding the numerical evaluation of the inversion integral will be introduced.

7.3 Physical Interpretation of the Fourier Transform Method

In evaluating the inversion integral given in (7.2) numerically it becomes necessary to choose a finite step length "ω_0" and discrete values $f(n\omega_0)$ of the frequency function $f(\omega)$ where n refers to a particular frequency harmonic. The integral then changes into a summation form that can be determined if use were made of a digital computer to reduce the amount of labour involved in evaluating the sum of this series. The integral thus changes into a summation form:

$$f(t) = (1/2\pi) \sum_{-\infty}^{+\infty} f(n\omega_0) \cdot \exp(jn\omega_0 t) \cdot \omega_0$$

if $\omega_0 = (2\pi/T)$

then

$$f(t) = (2/T) \sum_{=\infty}^{+\infty} f(n\omega_0) \cdot \exp(j\frac{2\pi}{T} \cdot nt) \qquad - (7.3)$$

where

$$f(n\omega_0) = \int_{-\pi/\omega_0}^{\pi/\omega_0} f(t) \cdot \exp(-jn\omega_0 t) dt$$

The function f(t) given by (7.3) is the definition of the complex form of the Fourier series with a repetition period T. Therefore the Fourier inverse integral changes to a repetitive Fourier series whose fundamental frequency is $\omega_0/2\pi$. At best, therefore, the function is well represented in the range $0 \leq t \leq T/2$ where T/2 is known as the observation period in transient analysis. Equation (7.3) represents an array of harmonically related sinewaves and the total response of the system is obtained by summing up the responses due to each individual wave.

In systems in which the transient time constants are long compared with the observation time, the series representation, equation (7.3) becomes divergent. Physically this means that a system which is subject to a repetitive stimulus does not behave in the same way as one subjected to a single stimulus of the same form because the cumulative effect of successive stimuli completely distorts the result.

In order to overcome this difficulty it is important that the observation time between such successive stimuli be chosen large enough and by so doing it will then be possible to avoid errors building up in the response pattern since the system will come to rest. This manner of solution to the problem is not economic since it does not lead to efficiency in computation. Longer times are usually associated with a larger number of harmonics for accurate representation of the system transient response and this should be avoided.

For practical purposes equation (7.3) is evaluated between trunction frequency limits -W and +W and the series then becomes:-

$$f(t) = \sum_{-W}^{+W} f(n\omega_0).\exp(j\frac{2\pi}{T}.nt) \qquad - (7.3)$$

which also means that the inversion integral of eqn. (7.2) is evaluated over these limits of integration.

7.4 Gibbs Oscillations and the Sigma Factor

The trunction of the infinite inversion integral to the limit W which is necessary in practice causes a form of instability at points of discontinuity of the function $f(\omega)$ known as Gibbs oscillations which appear on $f(t)$. In order to smooth out these oscillations Lanczos[69] suggested that the mean value of the function be obtained over a complete period of the oscillation. By so doing a weighting factor known as the sigma factor has been introduced which modifies the value of the function $f(\omega)$ in such a way that negligible Gibbs oscillations appear on its inverse that give rise to a poor form of representation for $f(t)$. The value of the sigma factor derivable from this concept is now given. Consider the inverse integral between the truncation limits $\pm W$:—

$$f(t) = (1/2\pi) \int_{-W}^{+W} f(\omega).\exp(j\omega t)\, d\omega$$

if $f'(\tau)$ is the local average of $f(t)$ between the limits $\tau \pm \pi/W$ then :-

$$f'(\tau) = (W/2\pi) \int_{\tau-\pi/W}^{\tau+\pi/W} (1/2\pi) \int_{-W}^{+W} f(\omega)\exp(j\omega t)d\omega\, dt$$

where τ is the periodic time of the high frequency oscillations $\tau = {}^{2\pi}/W$.

Changing the order of integration

$$f'(\tau) = ({}^{1}/2\pi) \int_{-W}^{+W} d\omega . f(\omega) . ({}^{W}/2\pi) \int_{\tau-{}^{\pi}/W}^{\tau+\pi/W} \exp(j\omega t)dt$$

$$= ({}^{1}/2\pi) \int_{-W}^{+W} f(\omega) . \frac{\sin({}^{\omega\pi}/W)}{({}^{\omega\pi}/W)} . \exp(j\omega\tau)\ d\omega$$

Let

$$f'(\omega) = f(\omega) . \frac{\sin({}^{\omega\pi}/W)}{({}^{\omega\pi}/W)}$$

$\therefore$

$$f'(\tau) = ({}^{1}/2\pi) \int_{-W}^{+W} f'(\omega) \exp(j\omega\tau)d\omega \qquad - (7.4)$$

Equation (7.4) is the inverse integral of the new function $f'(\omega)$ which is related to the old function $f(\omega)$ by the standard sigma factor "σ" where

$$\sigma = \frac{\sin({}^{\omega\pi}/W)}{({}^{\omega\pi}/W)} \qquad - (7.5)$$

For the n^{th} harmonic the standard sigma factor is

$$\sigma_n = \frac{\sin({}^{n\pi}/N)}{({}^{n\pi}/N)}$$

where N is the ratio between the truncation frequency W and the fundamental frequency ω_0.

The result of the smoothing operation carried out on the function f(t) by the application of a sigma factor is a reduction by a factor of 2, in the slope of the function at the discontinuity. The function takes some time to reach its maximum value, this time known as the rise time. If T is the periodic time of the Fourier series and T_0 is the observation time needed in the transient response calculations then $T_0 = T/2$ and the fundamental frequency ω_0 is $2\pi/T$. The rise time due to the sigma factor is limited to π/W. This makes the ratio of the observation time to the rise time equal to N, the total number of harmonics chosen in the calculation. The implications of this will be discussed later.

The occurrence of rise times tend to limit greater precisions which may be required in wave-front studies. MULLINEUX, SYLVIA DAY and REED[20] have shown that a modified form of the sigma factor produces improvement on rise time. The modified sigma factor has been derived from considerations on an average over an arbitrary range of time.

7.5 The Modified Fourier Transform

In their paper MULLINEUX, SYLVIA DAY and REED[19] have indicated a method whereby the problems connected with the Fourier series explained in section (7.2) can be avoided.

Going back to the Fourier integral, the authors have pointed out that when the singularities of the frequency function $f(\omega)$ lie close to the path of integration then this has given rise to instabilities in f(t) corresponding to these singularities. As an alternative

the authors introduced the Modified Fourier transform in which the path of integration has been shifted in the negative imaginary direction by a constant "a". This is justified because in a real physical system all singularities lie on or above the real frequency axis.

$$f(t) = (1/2\pi) \int_{-\infty-ja}^{+\infty-ja} f(\omega)\exp(j\omega t)\, d\omega$$

Substituting $\omega-ja$ for the variable ω, changing the limits of integration accordingly

$$f(t) = (1/2\pi) \int_{-\infty}^{+\infty} f(\omega-ja).\exp[j(\omega-ja)t]\, d\omega$$

$$= \frac{\exp(at)}{2\pi} \int_{-\infty}^{+\infty} f(\omega-ja)\, \exp(j\omega t) d\omega \qquad - (7.6)$$

Equation (7.6) gives the modified Fourier transform.

WEDEPOHL[70] gave a physical interpretation of the modified Fourier transform. In his explanation equation (7.6) without the exponential term exp(at) represented a Fourier inverse integral of the original function modified by an exponentially decaying factor, exp(-at). This was true since if the Fourier transform of f(t) was f(ω) then the Fourier transform of f(t).exp(-at) would be f(ω-ja). The system response obtained in this way, according to his interpretation, thus corresponded with the response of a system which had been subjected to a series of repetitive decaying stimuli and that by the suitable choice of the constant "a" the system could be brought to rest

after application of a stimulus before the next discontinuity occurred. In this way possible interference between the successive stimuli could be avoided as was explained earlier in the Fourier series representation. This avoided therefore, the necessity of introducing a long observation time between the successive signals and hence the time of computation brought about by the choice of a larger number of harmonics. This artificial form of attenuation could then be corrected for by multiplication of the computed response by the positive exponential term exp(at) and the actual system response thus obtained.

To within engineering accuracy it will be sufficient to regard that the system has attained a state of rest when the system response computed from the modified Fourier transform has settled down to approximately 1.0 per cent of its initial value at the end of the observation time of the transient T_0. This then gives

$$\exp(aT_0) = 0.01$$

$$\text{or} \qquad aT_0 = 4.6 \qquad - (7.7)$$

"To" being related to the periodic time T of the Fourier series by $T_0 = T/2$.

7.6 Practical Considerations

Since equation (7.6) is a combination of even and odd harmonics it can be further reduced when the imaginary terms are ignored since these add up to zero over the limits of integration. We need therefore evaluate only the real part of the integral.

i.e. $f(t) = \text{Re}\ \frac{\exp(at)}{\pi} \int_0^{+\infty} f(\omega - ja).\exp(j\omega t)\ d\omega$ - (7.9)

where Re denotes "real part".

Since this is an even function twice the value of the integral has been taken from $0 \rightarrow \infty$.

On truncating the range of integration and introducing the standard sigma factor for the reduction of Gibbs oscillations we will have

$$f(t) = \frac{\exp(at)}{\pi} \sum_0^W \text{Re}\ \{f(\omega - ja)\ .\ \frac{\sin(\frac{\omega\pi}{W})}{(\frac{\omega\pi}{W})} \exp(j\omega t).\Delta\omega\}$$

$$= \frac{\exp(at)}{\pi}\ \text{Re} \sum_0^W f(\omega - ja).\frac{\sin(\frac{\omega\pi}{W})}{(\frac{\omega\pi}{W})} \exp(j\omega t).\Delta\omega \quad - (7.10)$$

Numerical calculations were carried out using equation (7.10) for the synthesis of a step function in order to determine the optimum number of harmonics needed for the convergence of this series and to assign an empirical relationship between the shift constant and the fundamental frequency ω_0 based on considerations of equation (7.7).

The function $f(\omega)$ was divided into rectangular strips and a step length of "$2\omega_0$" was used. Satisfactory convergence was attained when fifty odd harmonics or a total number of a hundred harmonics were taken with a shift constant equal to the frequency step length i.e. of twice the value of the fundamental frequency. It was noticed that the step function representation was satisfactory up to about 85% of the observation time and that for the latter 15% the function

became unstable and that oscillations appeared about the value of the step. In an attempt to improve the situation by increasing the number of harmonics it was found that no significant improvement had been achieved by a total number of harmonics greater than a hundred. Fifty odd harmonics and an "a" factor of twice the value of fundamental frequency were therefore considered as optimum.

Studies of multiconductor transmission line transients discussed in later sections of this thesis made use of the modified Fourier transform method in their method of analysis. The need, however, of a more efficient computational method to cut down on the computing time required for the determination of the line constants has been recognised and thoughts along this direction have been forming. The theoretical limitations imposed on the observation time to half the periodic time of the fundamental frequency (Fourier series representation) and practical conditions which showed that even this limit could not be achieved properly coupled with a necessarily more thorough understanding of the Fourier inversion integral have also been contributing factors for the need of a more fundamental method that can cope with these various aspects. In the following sections the theoretical basis of such a method will be brought out.

7.7 Analytical Formulation of the Fourier Inversion Integral

7.7.1 General

In an earlier section the representation of the Fourier inversion integral took the form of a Fourier series. This immediately put a limit on the observation

time and it has been pointed out that at best f(t) could be represented to half the periodic time of the Fourier series fundamental frequency. In order to extend this limit of observation, analytical formulation of f(t) has been thought to be essential. The theoretical aspects will now be presented and further illustrated with an example.

7.7.2 Theoretical Basis of Method

Consider the Fourier inversion integral between truncation limits $\pm W$

$$f(t) = (1/2\pi) \int_{-W}^{+W} f(\omega).\exp(j\omega t).d\omega$$

If $f(\omega)$ defined within the range $-W \leq \omega \leq W$ is represented within this range as a Fourier series then f(t) can be evaluated from this analytical definition of $f(\omega)$ and f(t) will no longer be a repetitive function represented by a Fourier series. This is the basis of the method described here.

$$\text{Let } f(\omega) = (\pi/W) \sum_{-\infty}^{+\infty} C_n \exp(-jn\omega\pi/W) \qquad - (7.11)$$

The coefficients C_r of this series are given by

$$C_r = (1/2\pi) \int_{-W}^{+W} f(\omega) \exp(jr\omega\pi/W)d\omega \qquad - (7.12)$$

The ratio π/W still defines the rise time "t_0" and on substituting "t_0" the above expressions become

$$f(\omega) = t_0 \sum_{-\infty}^{+\infty} C_n \exp(-jn\omega t_0) \qquad - (7.13)$$

$$C_r = (1/2\pi) \int_{-\pi/t_0}^{\pi/t_0} f(\omega).\exp(j\omega t_0).d\omega \qquad - (7.14)$$

and the Fourier inversion integral is

$$f(t) = (1/2\pi) \int_{-\pi/t_0}^{\pi/t_0} f(\omega).\exp(j\omega t)\ d\omega$$

f(t) obtained from this new definition of f(ω) will be

$$f(t) = (1/2\pi) \int_{-\pi/t_0}^{\pi/t_0} t_0 \sum_{-\infty}^{+\infty} C_n \exp(-jn\omega t_0) \exp(j\omega t).d\omega$$

Rearranging

$$f(t) = \sum_{-\infty}^{+\infty} t_0 C_n .(1/2\pi) \int_{-\pi/t_0}^{\pi/t_0} \exp\{j\omega(t-nt_0)\}d\omega$$

$$= \sum_{-\infty}^{+\infty} C_n \cdot \frac{\sin \pi(t/t_0-n)}{\pi(t/t_0-n)} \qquad - (7.15)$$

$$\frac{\sin \pi(t/t_0-n)}{\pi(t/t_0-n)} = \begin{cases} 0 \text{ for } t = rt_0 \text{ and } r \neq n \\ 1 \text{ for } t = rt_0 \text{ and } r = n \end{cases} \qquad - (7.16)$$

where r and n are integers.

(7.15) is therefore a statement of the fact that the values of the function f(t) calculated at discrete points rt_0 are identical with the Fourier series coefficients given in (7.14).

i.e. $f(rt_0) = C_r$

The identity between $f(rt_0)$ and C_r can further be seen if "rt_0" is substituted in the inversion integral

formula. Equation (7.15) also shows that f(t) is no longer represented by a Fourier series and henceforth that the observation time limit encountered in the Fourier series representation is not valid for this new approach. In theory there should be no limit to the time of observation. Practical restrictions on the infinite limits of observation predicted here will be discussed later.

If instead of the exponential form of the inversion integral the sine and cosine forms due to SOLODOVNIKOV and others[71] are used together with a sine or cosine series representation for f(ω) then similar expressions will be obtained to the one shown in equation (7.15) derived from the complex form of the inversion integral and a complex form of representation for f(ω). The two results are given below and the derivations shown in Appendix(7).

Using a sine transform

$$f(t) = \sum_{-\infty}^{+\infty} b_n \frac{\sin \pi(t/t_0 - n)}{\pi(t/t_0 - n)} \qquad - (7.16)$$

and using a cosine transform

$$f(t) = \sum_{-\infty}^{+\infty} a_n \frac{\sin \pi(t/t_0 - n)}{\pi(t/t_0 - n)} \qquad - (7.17)$$

Either of the three forms of the inversion integral can be used to obtain the system response. In practice the exponential and cosine forms of the inverse transform would involve a knowledge of the d.c. response of the system and since this presents difficulties the sine integral transform is preferred.

The variation of the time functions at points of a time interval "t_0" other than its mean value is not known. This is a result of the application of finite truncation frequency and therefore if the definition of the time response is required at intermediate points of a specified time interval then this can only be achieved by shortening the duration of such interval. This will be done at the expense of increasing the truncation frequency "W".

Numerical evaluation of $f(rt_0)$, assuming use of the sine transform equation, will then take the form of approximating the curve of the imaginary part of $f(\omega)$ i.e. $I(\omega)$ to a polynomial of degree "n" and then evaluating the integral analytically. In practice where there are no regions of too rapid variation a parabolic form of approximation would be sufficient to define the curve of $I(\omega)$.

7.7.3 Shift Constant

By the choice of a shift constant "a" the values of the function $f(t)$ at intervals "t_0" are modified by $\exp(-at)$. Since these values correspond with the Fourier coefficients of $f(\omega)$ as explained before then accurate values of $f(rt_0)$ can only be obtained if the coefficients of $f(\omega)$ have errors in them which are greater than or equal to the known errors in the representation of $f(\omega)$. This provides a sound basis for the choice of the shift constant "a" and is a merit of this method.

7.7.4 Application

An example for the synthesis of a modified step function will now be considered using this method. The step function transform is $1/(a + j\omega)$ and its imaginary component is $-\omega/(a^2+\omega^2)$.

An examination of the first derivative of this imaginary component reveals a maxima at $\omega = a$ and of the second derivative a point of inflection at $\omega = \sqrt{3}.a$ after which the function falls gradually to zero at the truncation point, W. The function is characterised by a rapid change in the region $0<\omega<2a$. The representation of $f(\omega)$ should then take into consideration the shape of the "ω" curve. A poor representation of $I(\omega)$ in this low frequency end of the curve will reflect on the longer time representation of $f(t)$. The high frequency end of the curve is responsible for short time definition of $f(t)$ and a good definition there would require an accurate representation at the high frequency end of the "ω" curve.

Divide $f(\omega)\sigma(\omega)$ into N strips each of width ω_0 and let $f(\omega)\sigma(\omega)$ be represented as a Taylor's series within such a strip. Expand $f(\omega)$ about the point "$n\omega_0$" where n is an integer and ω_0 is the chosen step length, then

$$f(\omega)\sigma(\omega) = f_n + f'(\omega-n\omega_0) + \frac{f''}{2!}(\omega-n\omega_0)^2 + \cdots$$

where the first and second derivatives are given by

$$f' = (f_{n+1} - f_{n-1})/2\omega_0$$

$$f'' = (f_{n+1} - 2f_n + f_{n-1})/\omega_0^2$$

where f_{n-1}, f_n and f_{n+1} are the values of $f(\omega)$ at $(n-1)\omega_0$, $n\omega_0$ and $(n+1)\omega_0$.

The complete expression for $f(\omega)$ is therefore

$$f(\omega) = f_n + [(f_{n+1} - f_{n-1})/2\omega_0].(\omega - n\omega_0) + [(f_{n+1} - 2f_n + f_{n-1})/2\omega_0^2].(\omega - n\omega_0)^2$$

But $f(t)$, using Solodovnikov formula is given by

$$f(t) = -(2/\pi) \int_0^W f(\omega).\sin \omega t \, d\omega$$

$$\therefore f(rt_0) = \sum_{n=1}^{N-1} -(2/\pi) \int_{(n-1)\omega_0}^{(n+1)\omega_0} \{f_n + [(f_{n+1}-f_{n-1})/2\omega_0].(\omega - n\omega_0) + [(f_{n+1}-2f_n+f_{n-1})/2\omega_0^2]. (\omega - n\omega_0)^2\}.\sin\omega rt_0 \, d\omega$$

$n = 1,3,5,\ldots,N-1$

Changing the limits of integration

$$f(rt_0) = -(2/\pi) \sum_{n=1}^{N} \int_{-\omega_0}^{+\omega_0} \{f_n + [(f_{n+1}-f_{n-1})/2\omega_0].\omega + [(f_{n+1}-2f_n+f_{n-1})].\omega^2\} \times \sin [(\omega + n\omega_0)rt_0).d\omega \qquad - (7.18)$$

On evaluating the integral (7.18), the following result is obtained

$$f(rt_0) = -(4/\pi rt_0) \sum_{n=1}^{N} (I_1 + I_2 + I_3) \qquad - (7.19)$$

where

$$I_1 = f_n \sin(n\omega_0 rt_0).\sin\omega_0 rt_0$$

$$I_2 = [(f_{n+1}-f_{n-1})/2]\cos(n\omega_0 rt_0).[\cos(\omega_0 rt_0) - (1/\omega_0 rt_0))\sin\omega_0 rt_0]$$

$$I_3 = [(f_{n+1}-2f_n+f_{n-1})/2]\ \sin(n\omega_0 rt_0).[(1-2/(\omega_0 rt_0)^2)\sin\omega_0 rt_0 + (2/\omega_0 rt_0).\cos\omega_0 rt_0]$$

Equation (7.19) then yields an expression from which the value of the time function at the specified time points rt_0 can be determined numerically.

In the example considered the curve of the imaginary part of $f(\omega)$ is divided into 100 steps each of width ω_0. As pointed out a non-linear step could be taken when using this method for better definition of regions of rapid change in the value of the frequency function. For a step function this region is $0 < \omega < 2\omega_0$. As an illustration to the method three cases will be considered.

i. The step function is synthesised using the Fourier series method of representation and the sine transform $f(\omega)$ is divided into 100 linear steps of width ω_0 and an "a" shift factor of twice step length.

ii. Using this new method of approach an "a" factor of twice W/50 with total number of harmonics still 100.

iii. Using this new method and a non-linear step length. Six additional strips are considered at the front end

of the "ω" curve each of width $\omega_0/4$. This is the region where $I(\omega)$ varies rapidly. The total number of steps used is then 106. The value of the shift constant in this case is W/200.

The results are given in Fig. (7.1).

This shows immediately the following points:-

(1) The step function immediately acquires its terminal value of unity at the first step t_0. Since the function is not known to better than the average value over this interval, this defines the rise time as t_0.

(2) The increase of "6" harmonics (6% in computation), the observation time is extended four times for the same rise time. In order to achieve this same result with a linear step length, 400 harmonics would have been needed. The improvement in computational efficiency by the use of a non-linear step length is self-evident.

The illustration indicates scope for further work. In practice the regions of rapid change of $f(\omega)$ are not necessarily known in advance and the full advantage of a non-linear step length can only be exploited by some dynamic programming technique in which the step length is automatically adjusted on the basis of tests on the behaviour of $f(\omega)$ on previously calculated points. A detailed investigation of this point is outside the scope of this thesis, but is nevertheless so important that it

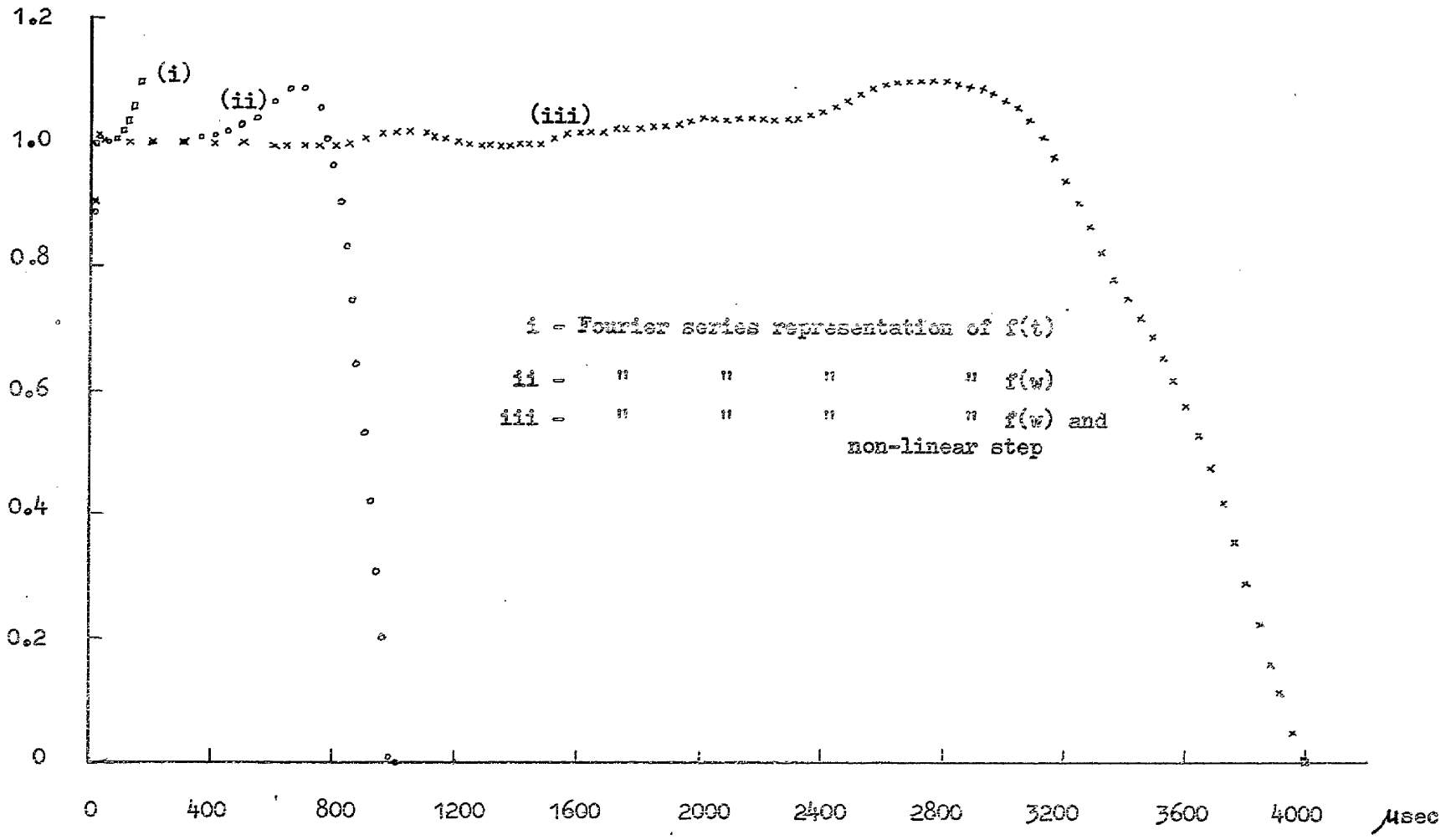

FIG. (7.1). SYNTHESIS OF STEP FUNCTION USING SOLODOVNIKOV SINE INTEGRAL

is worth noting.

7.8 Procedure for Numerical Evaluation of Transient Response

The formulation of the system equations for handling the solution of transient response will now be discussed. Two types of problems generally arise. First the determination of the system response when the form of the disturbance applied to the system is known analytically and its Fourier transform is thus readily obtained and that the boundary conditions are linear i.e. there is no change in the system impedance matrix with respect to time. Typical cases of these linear problems are the cases of simultaneous energisation of all phases of a transmission line and the case of the first phase being energised only. Second there is the determination of system response when non-linear problems are involved. Sequential pole closure and sequential pole tripping are a class of these problems. The procedure described here will apply to the general manner of solution of both types of problem though more elaboration on the handling of non-linear problems will be given in the following chapter since a special technique will then be developed which copes with the formulation of Fourier transforms of non-analytic disturbances encountered in non-linearities.

The system response is given by

$$f(t) = (1/2\pi).\exp(at).\mathrm{Re}\int_0^\infty f(\omega-ja).\exp(j\omega t)d\omega$$

where

$$f(\omega-ja) = Z(\omega-ja).I(\omega-ja)$$

$Z(\omega-ja)$ is the system transfer impedance matrix and $I(\omega-ja)$ is the transform of the input current matrix applied to the network; both Z and I being evaluated at a complex harmonic frequency $(\omega-ja)$. When dealing with linear problems analytical transforms are usually known since in practice step, ramp and sinusoidal input functions are considered in the process of circuit energisation or circuit interruption. The transfer impedance of the system which is frequency dependent can be calculated in the same manner as for the steady state at the particular transient frequency from a knowledge of the circuit constants obtained at that frequency. The method of modal analysis described earlier is used to obtain this transfer impedance matrix.

For purposes of computation the integral above is truncated and the sigma factor applied in the usual manner to avoid instability resulting from Gibbs oscillations. If 2N is the total number of harmonics chosen then for purposes of evaluating the frequency response $f(\omega-ja)$, only odd harmonics need be considered with a step length equal to twice the fundamental frequency ω_0.

$$\therefore \quad f(t) = (\omega_0/\pi).\exp(at)\ \mathrm{Re} \sum_{n=1}^{N-1} Z(\omega-ja).I(\omega-ja).\sigma.\exp(j\omega t)$$

where

$$\omega = (2n-1)\omega_0$$

$$\sigma = \frac{\sin\{(2n-1)\pi/2N-1\}}{\{(2n-1)\pi/2N-1\}}$$

The fundamental frequency ω_0 is related to the observation

time by

$$\omega_0 = \pi/\text{observation time}$$

The analysis dealt with is valid for the calculation of switching transients so far, has assumed a knowledge of analytical transforms for the input current matrix when all breaker poles close simultaneously. Pre-striking conditions in practice, before metallic contact of the circuit-breaker poles is complete, render simultaneous pole closure for all phases not possible [66,72]. As a result a time delay occurs and the poles close sequentially. The analysis of sequential pole closure and sequential pole opening of a circuit breaker and other non-linear problems, for instance, resistance switching and lightning arrester operation necessitate careful consideration. The input current matrix $I(\omega-ja)$ and the system transfer impedance matrix $Z(\omega-ja)$ will both change with time. Once this has been realized the procedure outlined, then exactly follows for this class of problems.

The behaviour of the system under first pole closure conditions is of interest since this case constitutes unbalanced energisation of the line and it is important to realize the effects of the severity of this extreme unbalance condition. The solution to this case presents no problem since the state of the first pole only to close can be simulated on the injection current transform matrix with the element corresponding to the phase energised set to the transform of the energising function. The current transform of other unenergised phases is set to zero.

CHAPTER EIGHT

ANALYTICAL METHOD FOR OBTAINING TRANSIENT RESPONSE OF SYSTEMS WITH NON-ANALYTIC FORCING FUNCTIONS

8.1 Introduction

It is essential in studies of a precise nature for the realization of the performance of a transmission line under energisation or de-energisation conditions to pay attention to the fact that sequential pole closure and sequential pole tripping take place in practice and the effect that such action may have on the system transient response. During the instant of time following first pole closure of a circuit breaker the unenergised phases have induced in them voltages which vary in a random manner and as such have no analytical transforms but as soon as the poles corresponding to these phases close they impose on the system forcing functions whose transforms are generally known analytically. The historical state of these poles is rather essential in the evaluation of the overall system response and as such a method has been designed to define these states analytically.

8.2 Physical Illustration

Consider a three-phase line energised from an infinite bus source. A few milliseconds after the first breaker pole closes, the second pole follows and later on in time the third pole closes. During the interval of time between the first and second pole closure a certain amount

of energy transfer takes place between the energised conductor of the system and the other two floating conductors. The coupled conductorsthus acquire voltages above ground which varies in a random manner with the progress of time before any other action takes place in the state of the circuit energised while switching surges travel up and down the line. When the second pole of the breaker closes the line side voltage of the corresponding phase conductor suddenly jumps up to the instantaneous value of the supply wave and stays there for the whole of the observation period of interest. Meanwhile the third conductor still open acquires a new voltage whichisinduced from both energised conductors until the third pole angle has reached such a value that the third pole comes into operation. As soon as this happens the voltage on the third phase then corresponds with the voltage of the supply.

If the problem were to be solved physically in order to determine the response of the line due to sequential pole closure then the following procedure would be adopted:-

i. With the second and third phases left open-circuited a time-varying generator is connected up to the first phase at the instant of switch closure. This generator would have a voltage $\hat{V}\cos(2\pi f_s t + \phi_1)$ up to the end of the observation time.

ii. At the instant of second pole closure two such generators would be required, one to represent the supply voltage $\hat{V}\cos(2\pi f_s t + \phi_2)$ and a dummy generator to simulate the exact conditions on the input end of the second phase prior to the second pole closure. The two generators which would

be connected up in series with no power transfer between them would remain there till the end of the observation period.

iii. The closure of the last breaker pole on to the third phase can be realized also from the connection of two generators, one of voltage $\hat{V}\cos(2\pi f_s t + \phi_3)$ and the other in series with it representing the random conditions of the input end of the third phase prior to the moment of its energisation. Again for this state to be represented precisely there should be no energy transfer between these two generators.

For a summary of the physical procedure just outlined reference is made to Fig. (8.1).

A similar form of physical argument can be carried out for problems of sequential pole tripping encountered in fault current interruption.

8.3 Digital Simulation of Non-Simultaneous Switching Operations

The difficulty in analysing sequential pole closure and sequential pole tripping using a digital computer lies in the irregular nature of the responses simulated by the dummy voltage or current generators. This seems to place a restriction on the use of the Fourier transform methods otherwise proved to be successful when dealing with functions whose analytical transforms happen to be known. If some means is therefore available for determining the Fourier transforms of the random voltage or current waveforms appearing at the input end of the line then the concept introduced in the physical illustration can be employed to obtain a numerical

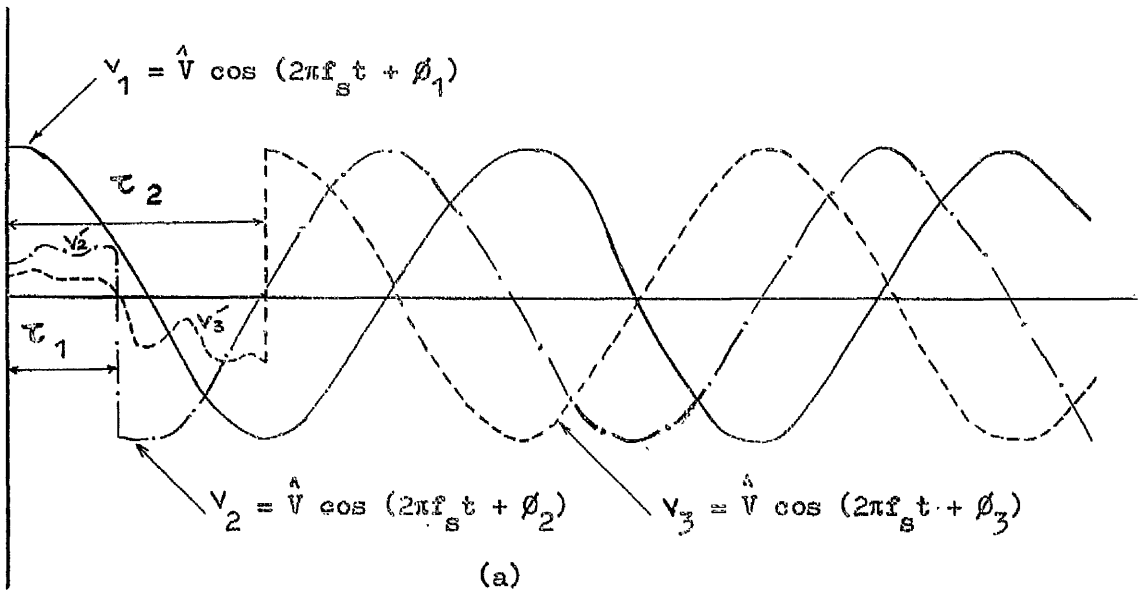

τ_1 and τ_2 are times of second and third poles closure

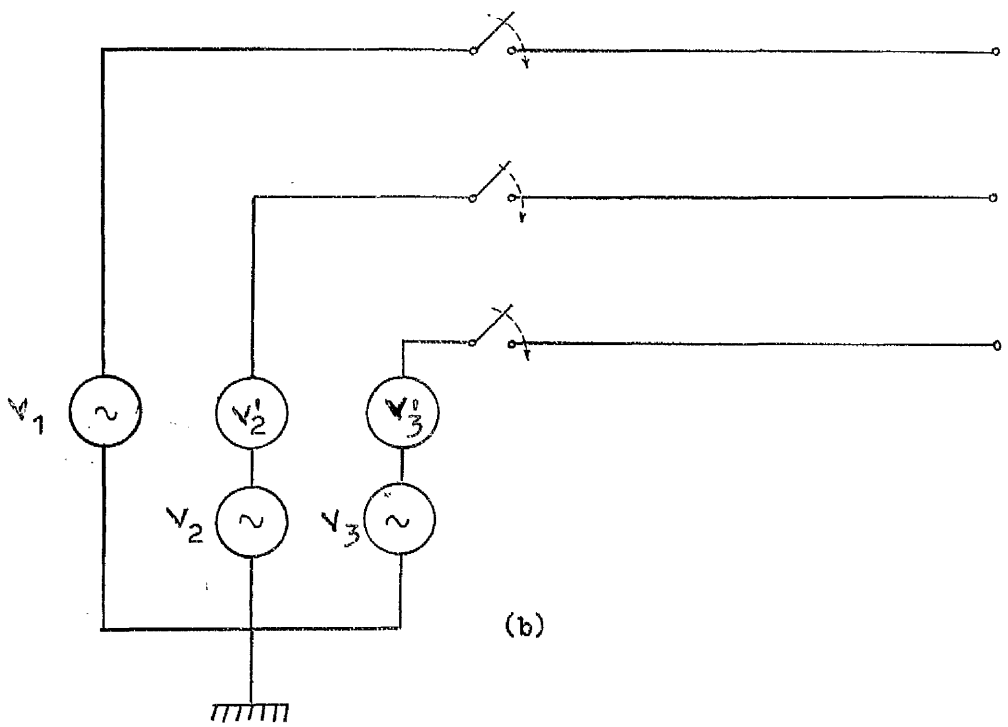

FIG. (8.1). PHYSICAL REPRESENTATION OF SEQUENTIAL POLE CLOSURE PROBLEM

solution on the digital computer and henceforth give the Fourier transform method more versatility.

As indicated earlier the condition of the first pole to close is easily dealt with since the transform of the energising function at time zero is readily known. With reference to Fig. (8.1) the second and third pole closure conditions can simiarly be dealt with if the appropriate transforms energising the second and third phases are known. For the second phase the energising function consists of a delayed analytic function v_2 whose transform is known (in this case delayed cosine wave) together with an arbitrary time function v_2^0 in the interval of time $0 - \tau_1$. Similarly also for phase three where the analytic energising component is the delayed voltage wave v_3 and the arbitrary component in the interval of time $0 - \tau_2$ is v_3^0. The problem therefore reduces down to finding the Fourier transform of the arbitrary functions v_2^0 and v_3^0 and then using the principle of superposition to evaluate the response of the system as in the usual manner. Similarly, other non-linear problems in transient response calculations with randomly varying exciting functions can be represented by approximate analytic Fourier transform. Owing to its importance in handling general non-linear problems in transient response calculations, a method will now be described for obtaining Fourier transforms of arbitrary-varying time functions.

8.4 Fourier Transform of Numeric Functions

8.4.1 Criticism of Classical Approach

Consider the Fourier transform

$$f(\omega) = \int_{-\infty}^{+\infty} f(t).\exp(-j\omega t)\ dt$$

With the kind of systems we will be dealing with f(t) is defined only from time $t \geq 0$. We will therefore have

$$f(\omega) = \int_{0}^{\infty} f(t).\exp(-j\omega t)\ dt$$

and since we are only concerned with an upper limit of $t = \tau$

$$f(\omega) = \int_{0}^{\tau} f(t).\exp(-j\omega t)\ dt$$

If f(t) is known only numerically at discrete intervals of time rt_0, where r is an integer r = 0,1,2,3,--- etc. then following the classical methods of numerical integration the tendency for the evaluation of the Fourier coefficients $f(\omega)$ would be to choose a suitable step length t_0 and use either the rectangular strip rule or better still Simpson's rule to evaluate the integral from

$$f\{(2n-1)\omega_0\} = \sum_{r=0}^{N_{t-1}} f(rt_0).\exp[-j(2n-1)\omega_0.rt_0].t_0 \Bigg|_{n=1}^{N_f} \qquad - (8.1)$$

where $f[(2n-1)\omega_0]$ .. are the Fourier coefficients required.

N_t ... is the total number of time intervals chosen of width "to" which divide f(t)

N_f ... is the total number of odd harmonics

$\omega_0 = \pi/T_0$

$t_0 = T_0/N_t$

where T_0 is the observation period.

Since we are interested in the modified Fourier coefficients of $f(rt_0)$ the corresponding terms of thismust be multiplied by $\exp(-art_0)$ where "a" is the shift factor.

The method just described therefore hinges on evaluating the area under the f(t) curve by dividing it into strips. This approach used in the calculation of the Fourier coefficients of f(t) by equation (8.1) makes the basic assumption that ωt_0 is constant over the range $t \rightarrow t+t_0$.

The validity of this assumption will now be examined carefully.

Consider the n^{th} strip of f(t) shown in Fig. (8.2) and let us proceed with the above assumption in order to obtain the area under the strip by the ordinary method of integration i.e. assuming that ωt_0 is constant over this range.

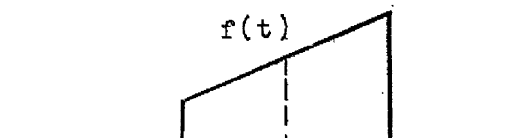

Fig. (8.2)

f(t) is taken as the mean value between two successive ordinates

$$f(t) = (f_{n-1} + f_n)/2$$

Now

$$f(\omega) = \int_{(n-1)t_0}^{nt_0} \{(f_{n-1}+f_n)/2\} \exp(-j\omega t)dt$$

$$= \int_{(n-1)t_0}^{nt_0} [(f_{n-1}+f_n)/2].\exp[-j\omega\{(n-1)t_0+t_0/2\}].dt$$

i.e. $f(\omega) = [(f_{n-1}+f_n)/2].\exp[-j\omega(n-\frac{1}{2})t_0] \times t_0$

This represents therefore the area under the strip $f(t).\exp(-j\omega t)$.

In order to see to what extent we are justified in making the assumption that ωt_0 is constant over the integration range considered let us now evaluate the function by a Taylor's series expansion and assume as a first approximation linear variation between $(n-1)t_0$ and nt_0.

Expand $f(t)$ about the point $(n-\frac{1}{2})t_0$, assuming $f(t)$ constant

$$f(t) \approx [(f_{n-1} + f_n)/2][1 - j\omega[t - (n-\tfrac{1}{2})t_0]] \times \exp[-j\omega(n-\tfrac{1}{2})t_0]$$

The term $\exp(-j\omega t)$ has now become $[1 - j\omega[t - (n-\frac{1}{2})t_0]].\exp[-j\omega(n-\frac{1}{2})t_0]$ and for practial purposes the new expression will be constant if $(\omega t_0/2) < 1/10$. For large values of ω it is evident that this condition will not be satisfied. In general therefore there is no guarantee that this condition will be satisfied every time the synthesis of an arbitrary time function is sought and therefore the assumption on which the classical method of evaluating the Fourier coefficients is based restricts the use of this method to particular cases only in which the condition $(\omega t_0/2) < 1/10$.

8.4.2 Piecewise Synthesis Approach

8.4.2.1 Theory

If the function f(t) known at discrete intervals t_0 is divided into N strips and if the strip width is small enough the variation of the function between two successive times can be approximated to a straight line. An analytical expression for the transform of the strip can then be found. On using the superposition theorem the transform of the individual strips is added up to give the resultant transform of f(t). Although linearization over the time interval "t_0" will be considered here, account of too rapid variation in the value of the function f(t) can be better dealt with if the function is approximated to a series of parabolas over the interval selected.

Let f(t) be divided as shown in Fig. (8.3.a) and linearized over the strip width. Consider a typical strip. If f_{n-1} and f_n are the values of the function at "$(n-1)t_0$" and "nt_0" then the Fourier transform of the function bounded by $(n-1)t_0 \rightarrow f_{n-1} \rightarrow f_n \rightarrow nt_0$ can be found if the function is decomposed into a series of standard functions whose transforms are already known. The step function and the ramp function are chosen as basic components. The step function transform is $P/j\omega$ and the ramp function transform is $Q/(j\omega)^2$ where P and Q are the magnitude of the step and the slope of the ramp function respectively.

The series of reductions carried out on the n^{th} strip are shown in Fig. (8.3). The transform of the strip is finally represented by the transform of two ramp functions,

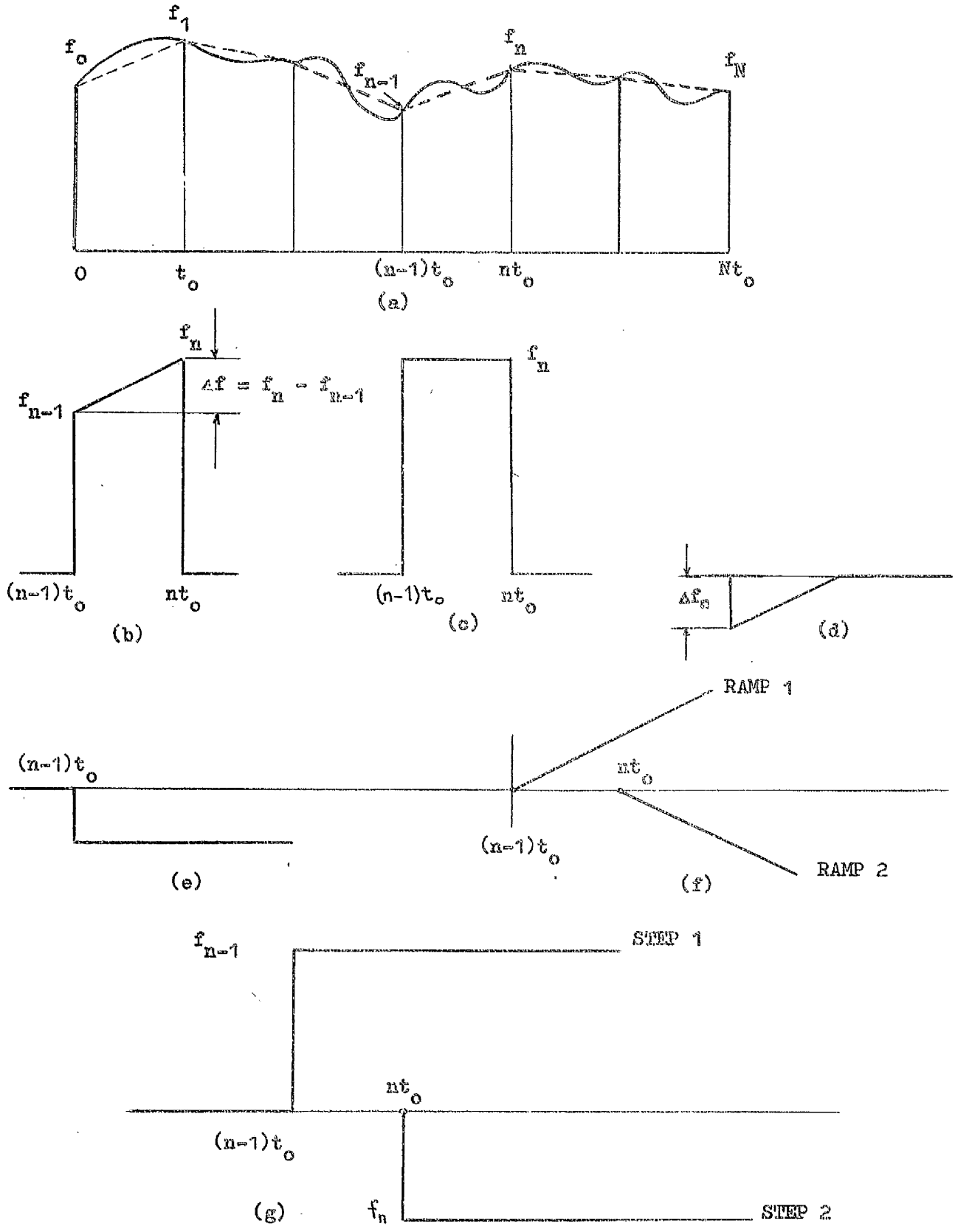

FIG. (8.3). PIECEWISE SYNTHESIS TRANSFORM DIAGRAMS

Fig. (8.3f) and two step functions, Fig. (8.3.g). The magntiudes of the steps are f_{n-1} and f_n whereas the slope of the positive ramp is $\Delta f/t_0$ and the negative ramp is $-\Delta f/t_0$.

The Fourier transform of STEP 1 and STEP 2 is given by

$$[f_{n-1}/j\omega][\exp(-j(n-1)\omega t_0)] - [f_n/j\omega].[\exp(-jn\omega t_0)]$$

The exponential terms are shift operators which account for the time delay of these functions.

If the transform contribution from all strips of f(t) is added up then the transform due to all such steps will be found. It will be noticed that intermediate terms cancel out since they appear twice in the summation once with a negative sign due to a former strip and once with a positive sign due to a latter strip. Finally the transform due to the step functions is:-

$$f_s(\omega) = (1/j\omega)\{f_0 - f_N[\exp(-jN\omega t_0)]\} \qquad - (8.2)$$

The Fourier transform of RAMP 1 and RAMP 2 with positive and negative slopes of magnitude $(f_n - f_{n-1})/t_0$ is

$$[\Delta f_n/(-\omega^2 t_0)].[\exp[-j(n-1)\omega t_0] - \exp(-jn\omega t_0)]$$

Summing up the contribution due to all such ramps we get:-

$$f_r(\omega) = -(1/\omega^2 t_0) \sum_{n=1}^{N} \Delta f_n\{\exp[-j(n-1)\omega t_0 - \exp(-jn\omega t_0) \qquad - (8.3)$$

where

$$\Delta f_n = f_n - f_{n-1}$$

Equations (8.2) and (8.3) can now be combined to yield the complete transform of f(t) but a further reduction of equation (8.3) is beneficial for economies in computation.

If equation (8.3) is expanded and like terms collected together the result will be

$$f_r(\omega) = -(1/\omega_0^2 t)\cdot\left[f_1 - f_0 - \{f_N - f_{N-1}\}\{\exp(-jN\omega t_0) + \sum_{n=1}^{N-1}\{f_{n+1} - 2f_n + f_{n-1}\} \times \exp\{(-jn\omega t_0)\}\right] \quad - (8.4)$$

The complete transform is

$$f(\omega) = f_s(\omega) + f_r(\omega)$$

$$\therefore f(\omega) = (1/j\omega)\cdot\left[f_0\{1 - (1/j\omega t_0)\} + f_1/j\omega t_0 + [(f_{N-1}/j\omega t_0) - f_N\{1+(1/j\omega t_0)\}].[\exp(-jN\omega t_0)] + (1/j\omega t_0)\sum_{n=1}^{N-1}[f_{n+1} - 2f_n + f_{n-1}][\exp(-jn\omega t_0)]\right] \quad - (8.5)$$

Errors resulting from assuming that the function starts and finishes at zero are insignificant. By assuming that the function starts and finishes at zero possible step discontinuities at the start and finish of f(t) are avoided. Therefore putting $f_0 = 0$ and $f_N = 0$ a more practical formula of the Fourier transform of f(t) is thus obtained

$$f(\omega) = -(1/\omega^2 t_0)\cdot\left[\begin{array}{l} f_1 + f_{N-1}\{\exp(-jN\omega t_0) \\ + \sum_{n=1}^{N-1} \{f_{n+1} - 2f_n + f_{n-1}\}\{\exp(-jn\omega t_0)\end{array}\right] \quad - (8.6)$$

8.4.2.2 Fourier Coefficients Using the Concept of Complex Frequency

The transform of the time response f(t) defined at discrete time intervals has been found on the assumption that the integration process is carried out on the real axis. Problems that arise due to this have been discussed and the use of the modified Fourier transform to overcome these difficulties has been pointed out. The use of the modified transform results in the definition of a new function f'(t) whose transform is f(ω-ja) where "a" is the shift constant. This new function is related to f(t) by

$$f'(t) = \exp(-at).f(t) \quad - (8.7)$$

It has been shown accordingly that the inversion of the modified Fourier transform should be modified by the exponential factor exp(at) in order to obtain the desired time response.

It would appear from this argument and equation (8.7) that the ordinates of f(t) in equation (8.6) have to be modified by $\exp(-ant_0)$ in order to relate the Fourier coefficients thus calculated to the complex transform f(ω-ja). It will now be shown that this will only be valid for high frequencies.

(i) Consider a rectangular pulse Fig. (8.4.a), of width t_0 and amplitude f_1.

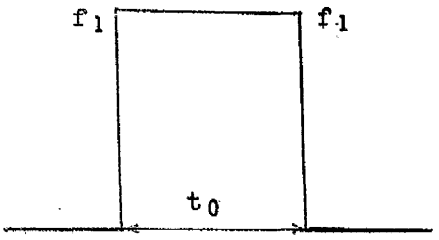

(a)

The Fourier transform is given by

$$f(\omega) = f_1/j\omega - (f_1/j\omega)\exp(-j\omega t_0)$$

Substituting $(\omega - ja)$ for ω the transform becomes:-

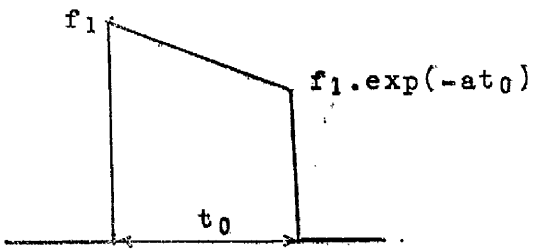

(b)

Fig. (8.4)

$$f(\omega-ja) = \{f_1/(a+j\omega)\}\{1 - \exp(-at_0).\exp(-j\omega t_0)\} \quad - (8.8)$$

Equation (8.8) is a true definition of the modified Fourier transform of the rectangular pulse.

(ii) Let the amplitude of the rectangular pulse be modified by $\exp(-at_0)$ first and its corresponding transform then found; this is the sum of the transform of two steps and two ramps. See Fig. (8.4.b).

<u>For steps</u>

$$f_{s(\omega - ja)} = (f_1/j\omega) - \{f_1.\exp(-at_0)/j\omega\}.\exp(-j\omega t_0)$$

<u>For ramps</u>

$$f_{r(\omega - ja)} = \{[f_1 - f_1.\exp(at_0)]/(-\omega^2 t_0)\} \times \{[f_1 - f_1.\exp(at_0)]/(-\omega^2 t_0)\}$$

The complete transform is

$$f'(\omega-ja) = [f_1/j\omega][1-\exp(-at_0).\exp(-j\omega t_0)]$$

$$- [f_1\{1-\exp(-at_0)\}/(-\omega^2 t_0)][1-\exp(-j\omega t_0)]$$

- (8.9)

It is evident that equation (8.9) approaches equation (8.8) in the limit of large values of ω only.

In order, therefore, to obtain the modified Fourier transform using the piecewise synthesis approach the complex frequency $(\omega-ja)$ is substituted in equation (8.6) in place of the real frequency ω. The resultant coefficients will then be:-

$$f(\omega-ja) = - \frac{1}{(\omega-ja)^2 t_0} \left[\begin{array}{l} f_1 + f_{N-1}\{\exp[-jN(\omega-ja)t_0]\} \\ + \sum_{n=1}^{N-1} \{f_{n+1}-2f_n+f_{n-1}\}\{\exp[-jn(\omega-ja)\}t_0]\} \end{array} \right]$$

- (8.10)

Equation (8.10) then gives the transform of $f(t).\exp(-at)$ over the frequency range.

8.4.2.3 Examples on Synthesis Method

To illustrate the validity of the synthesis method given by equation (8.10) an example will now be considered. A time function f(t) is known at discrete time intervals over a period of 3.3 msec, the time step is 75 μsec. The function is synthetised from its Fourier coefficients obtained from

(i) Ordinary numerical integration using

rectangular strips rule and Simpsons rule

(ii) Synthesis method of Equation (8.10).

The result is shown in Fig. (8.5). In the case of Simpson's rule and this new method the computation is carried beyond the observation time of 3.3 msec. It has been confirmed that the values of the function obtained beyond 3.3 msec are zeros.

It is seen from the figure that whereas both methods of the ordinary numerical integration have failed to represent the chosen function within the time period selected, the new method has produced a result which is in very good agreement with the theoretical function considered. The discrepancy at time zero is due to the fact that equation (8.10) does assume that the function starts at zero where the chosen function here does not. The synthetised function also shows a certain rise time; this is the rise time already encountered in the inversion process of the modified Fourier transform. It has also been confirmed that, by choosing an observation period of 6.6 msec, the synthetised function is well represented up to about 85 to 90% of this observation period after which the zero values of f(t) show errors in them. This again is in agreement with results obtained earlier from the modified Fourier transform technique.

It is concluded that this new method is satisfactory in deriving the modified Fourier transforms of functions whose values are only known numerically. The transform takes the

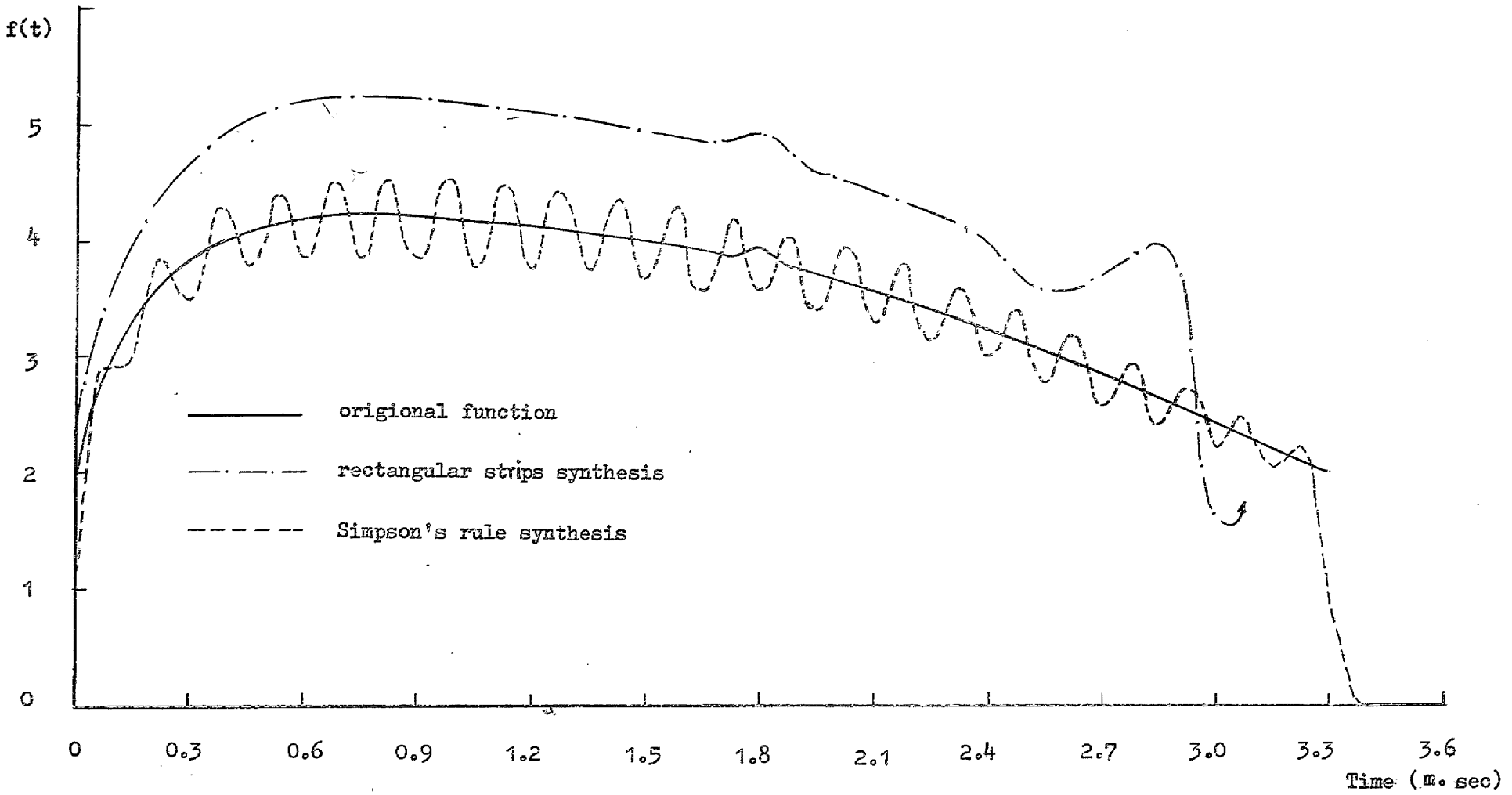

FIG. (8.5a). SYNTHESIS OF FUNCTION USING ORDINARY METHODS OF INTEGRATION

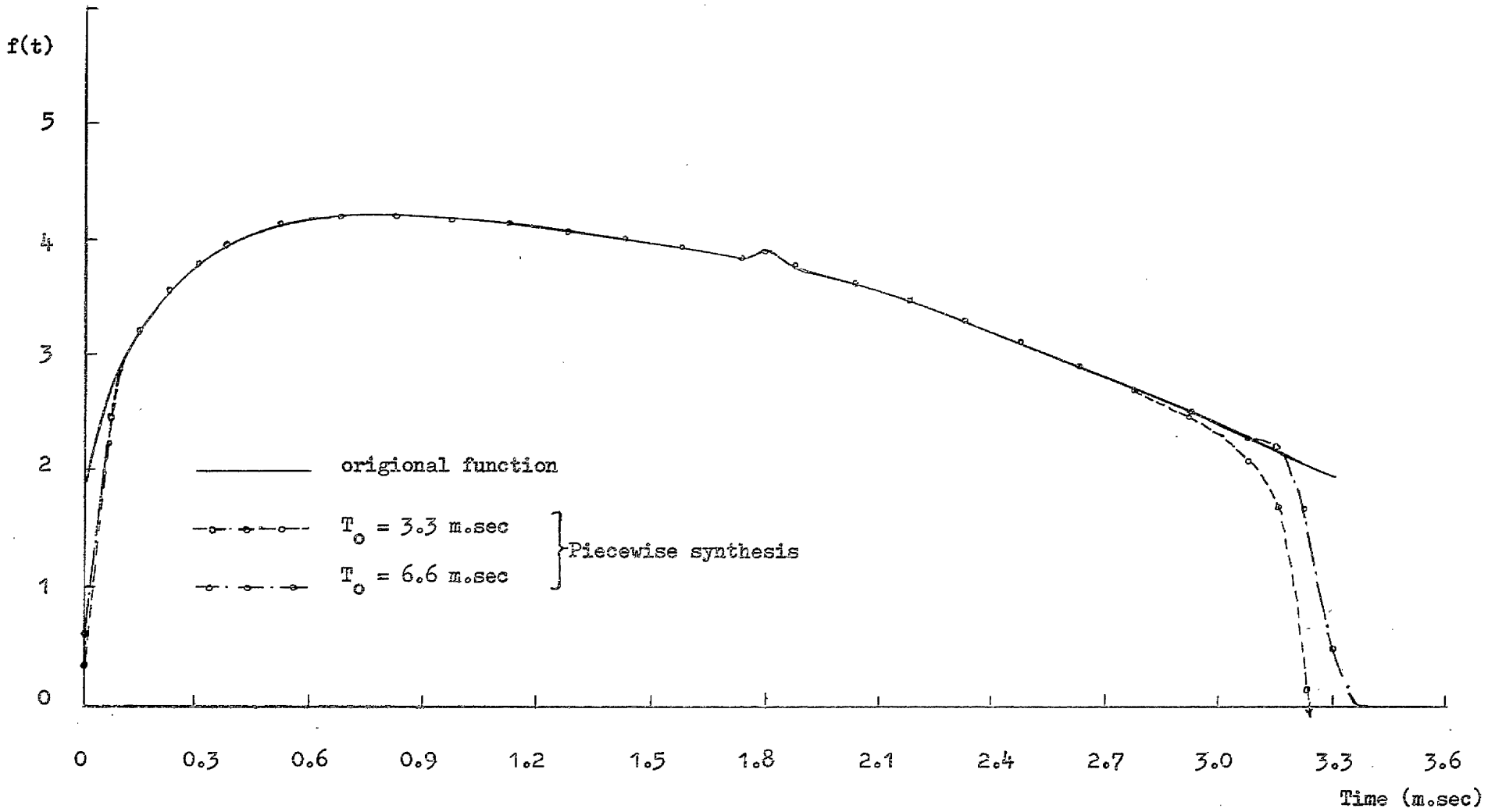

FIG. (8.5b). SYNTHESIS OF FUNCTION USING PIECEWISE SYNTHESIS APPROACH

form of complex coefficients evaluated over a certain frequency spectrum. As such, the transient response due to any arbitrary-varying forcing functions will be readily known since now "equivalent" analytical transforms are found for these.

8.4.3 Applications of Synthesis Method

The method of piecewise synthesis is most useful in the analysis of switching surges in multiconductor lines resulting from sequential line energisation or de-energisation. In the light of previous discussion on this problem the system boundary conditions, on sequential energisation, between the instants of closure of the first and second poles, second and third would be mathematically realizable since the transform of the induced voltages at the input end of these phases can be correctly determined using this method. These transforms add vectorially to the already known analytic transforms of the appropriate phase of the system supply. The digital analysis of sequential pole closure will be dealt with in greater detail in further sections.

The study of recovery voltage transients due to clearing of faults on transmission lines requires a knowledge of the Fourier transform of the current wave-form to be interrupted. A precise definition of the leading front is of vital importance in determining the rate of rise of the restriking voltage transients. The method of piecewise synthesis provides a very useful means of obtaining to greater degrees of accuracies the transform of interrupted currents

and hence in the solution of the restriking transients problem. More about how to tackle this problem with results of numerical studies will be considered later.

In general the method opens a new scope for the analysis of a wide range of non-linear transmission problems through the modal propagation - Fourier transform technique.

CHAPTER NINE

COMPUTATIONAL RESULTS OF TRANSIENT VOLTAGES ON MULTICONDUCTOR LINES

9.1 Introduction

In the previous chapters analytical methods have been discussed for the evaluation of multiconductor line transients using modal propagation and Fourier transform techniques. Ideas have also been put forward regarding special problems of sequential pole energisation of transmission lines and handling of general non-linear problems. It is the purpose of this chapter to present numerical solutions on the propagation of switching surges on multiconductor lines in order to illustrate the validity and power of these analytical methods and to explain some fundamental aspects relating to these surges. Detailed analysis of transient overvoltages resulting from first pole closure are dealt with and some of the longer line problems under energisation conditions are presented. In the earlier part of this work the effectiveness of series and shunt compensation on the steady state performance of long-distance lines has been described. In this chapter line compensation will be studied as a means of reducing the level of severe transient overvoltage on long lines. Compensating elements are treated as lumped parameter elements.

The practical sequential energisation problem of multiconductor lines is presented with a numerical example for a short line and a check for the method of analysis has been provided. The close agreement between the two

sets of results shown is a further proof of the validity of the theoretical approach proposed. The transient response of a short line subjected to simultaneous pole energisation is included in this study.

The generality of the piecewise synthesis approach to the solution of non-linear problems is evinced by applications on circuit-breaker restriking voltage calculations. It is shown in this chapter how these problems can be analysed, and a numerical illustration is provided.

The analysis and results presented here have been carried out without recourse to source representation, the complexities involved may mask some fundamental points sought here and for this reason considerations of source representation have been deferred at present but will be discussed in the following chapter.

Digital computer programs used in the numerical calculations are outlined whenever these are thought to be significant.

9.2 Mathematical Models

In the derivation of the following model it is assumed that a transmission line is energised from an infinite bus and that the effect of generator transformer, bus-bar capacitance and capacitance of potential transformer has been ignored. Two cases will be dealt with in one of which the simultaneous closure of all phases will be considered and in the other, the more practical case of sequential closure

will be analysed. A general terminating impedance matrix $[Z_t]$ is connected to the receiving end of the line.

Consider Fig. (9.1.a) in which a three-phase line is energised from a three phase system. By a Thévenin-Norton conversion theorem , Fig. (9.1.b), it is possible to reduce the boundary conditions at the energised end from a voltage form into a current form. The reason for this is that when dealing with sequential pole closure the voltages on the floating conductors owing to first pole closure are not known. The problem becomes solvable, however, if use is made of the fact that the currents of those conductors are zero. The system diagram shown in Fig. (9.1.a) now takes the form shown in Fig. (9.1.c) and the terminating impedances at the receiving end of the line are changed into their admittance form to facilitate use of nodal-admittance two-port equations used earlier in the steady-state calculations.

In deriving the transient response of a transmission line the observation points of interest are normally the sending end, receiving end and perhaps some intermediate point. In the following derivation equations are derived for the transient response at an arbitrary point distance x from the sending end.

An equivalent single-phase diagram of the line is shown in Fig. (9.2). If the line is energised from the sending end, then receiving, the receiving end injected currents are zero. The line constants to the left hand side of P are A_1, B_1 and to the right hand side are A_2, B_2 where

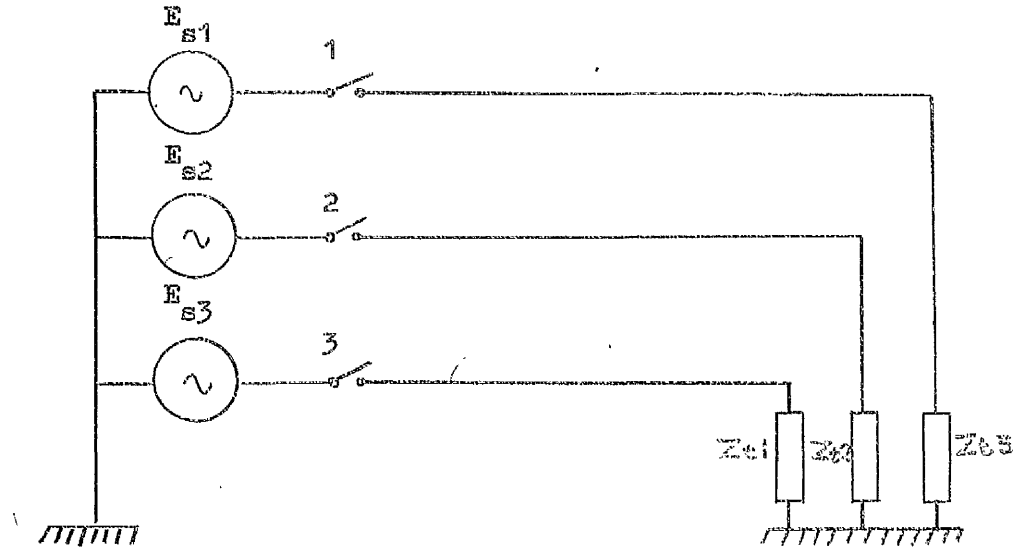

(a)

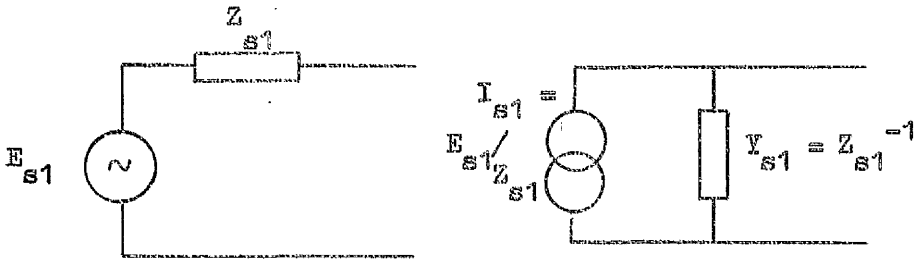

Thevenin's Equivalent Norton's Equivalent

(b)

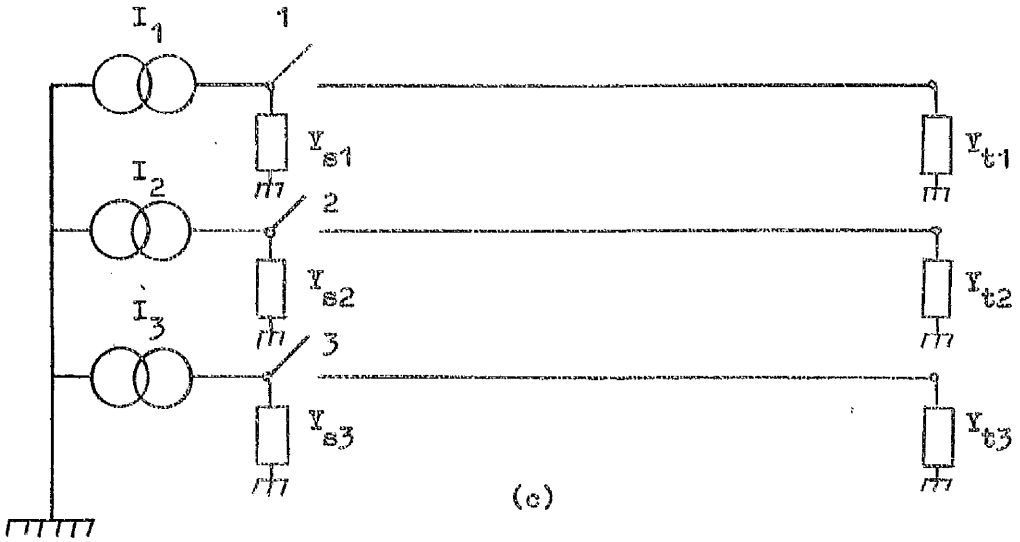

(c)

FIG. (9.1). SYSTEM DIAGRAM AND THEVENIN'S AND NORTON'S EQUIVALENTS

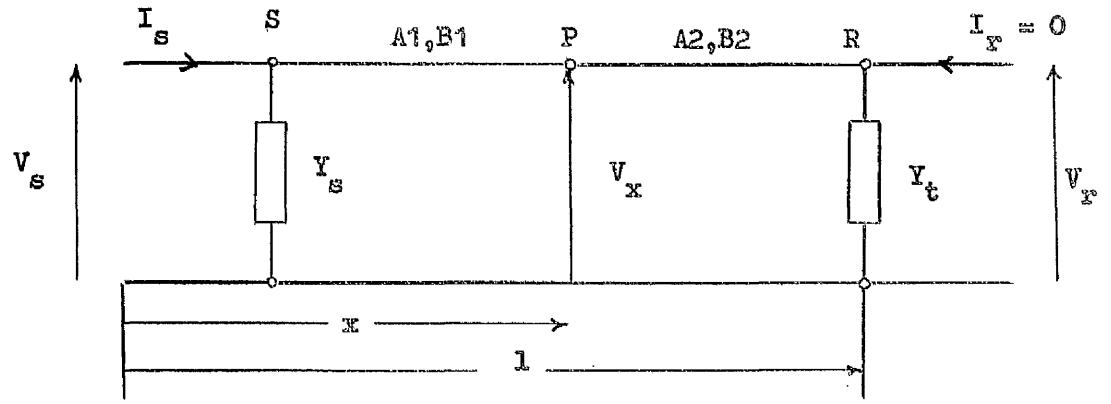

(a)

$\bar{I}_{s1}$	Y_{s1}	0	0
$\bar{I}_{s2}$	0	Y_{s2}	0
$\bar{I}_{s3}$	0	0	Y_{s3}

Y_{t1}	0	0
0	Y_{t2}	0
0	0	Y_{t3}

(b)

$\bar{I}_{s1}$	Y_{s1}	0	0
0	0	0	0
0	0	0	0

Y_{t1}	0	0
0	Y_{t2}	0
0	0	Y_{t3}

(c)

FIG. (9.2). SINGLE PHASE EQUIVALENT CIRCUIT AND SYSTEM MATRIXES

using the usual notation

$$A_1 = Y_0 \coth \psi x \quad ; \quad B_1 = -Y_0 \operatorname{cosech} \psi x$$

$$A_2 = Y_0 \coth \psi(\ell - x) \quad ; \quad B_2 = -Y_0 \operatorname{cosech} \psi(\ell - x)$$

Using nodal analysis, the system equations written in matrix form are

$$\begin{bmatrix} \bar{I}_s \\ 0 \\ 0 \end{bmatrix} = \begin{bmatrix} A_1+Y_s & B_1 & 0 \\ B_1 & A_1+A_2 & B_2 \\ 0 & B_2 & A_2+Y_t \end{bmatrix} \cdot \begin{bmatrix} \bar{V}_s \\ \bar{V}_x \\ \bar{V}_r \end{bmatrix}$$

Solving for $\bar{V}_r$ from the bottom row

$$\bar{V}_r = -(A_2+Y_t)^{-1} . B_2 . \bar{V}_x \qquad - (9.1)$$

and for $\bar{V}_x$ from second row

$$\bar{V}_x = -[A_1+A_2-B_2(A_2+Y_t)^{-1}B_2]^{-1} . B_1 \bar{V}_s \qquad - (9.2)$$

and for $\bar{V}_s$ in terms of the line constants and the known injected currents $[\bar{I}_s]$

$$\bar{V}_s = [A_1+Y_s-B_1[A_1+A_2-B_2(A_2+Y_t)^{-1}B_2]^{-1}B_1]^{-1} . \bar{I}_s \qquad - (9.3)$$

On substituting (9.3) in (9.2) the voltage $\bar{V}_x$ at any point on the line can therefore be determined where $\bar{V}_x$ is given by

$$\bar{V}_x = [A_1+A_2- B_2(A_2+Y_t)^{-1}B_2]^{-1}B_1 \times$$

$$[A_1+Y_s- B_1[A_1+A_2-B_2(A_2+Y_t)^{-1}B_2]^{-1}B_1]^{-1} . \bar{I}_s \qquad - (9.4)$$

From a practical point of view it is sufficient to know the transient response at the sending end, receiving end and mid-point of the line. Since most of the computation time goes for the evaluation of the line constants it is advisable to use equations (9.1) to (9.3) for economies in computation. These offer the necessary solution and are more favourable to use than equation (9.4) since the line constants have to be calculated only once for the three observation points. It is worthwhile noting that the coefficient of equation (9.4) is the system transfer function $Z(\omega)$ and that both $\bar{V}_x$ and $\bar{I}_s$ are the Fourier transforms of the corresponding time variables. Since $\bar{I}_s$ is known analytically or can be found numerically and $Z(\omega)$ is readily known the line frequency response $\bar{V}_x$ is obtainable. In order to evaluate the time response the inverse transform of $\bar{V}_x$ is found using the methods described in Chapter(7)

9.3 Boundary Conditions

The mathematical model is suitable for the calculation of transient voltages resulting from simultaneous or sequential pole closure with changes only in the line boundary conditions.

9.3.1 Simultaneous Pole Closure

When the breaker poles close simultaneously the elements of the current vector are the Fourier transforms of the three sine waves coming from the three-phase supply given by:-

$$\begin{aligned} v_1 &= \hat{V} \cos(\omega_s t + \phi_1) \\ v_2 &= \hat{V} \cos(\omega_s t + \phi_2) \\ v_3 &= \hat{V} \cos(\omega_s t + \phi_3) \end{aligned} \qquad - (9.5)$$

where ϕ_1, ϕ_2 and ϕ_3 are the general angles of the pole closure. The Fourier transforms of the expression given by (9.5) can be found by splitting these into sine and cosine transforms as illustrated in Appendix (9.3). Having defined the voltage transforms, the injected current transforms can be determined from the Thevenin-Norton representation and this involves multiplication by the source admittance. Since we are dealing with an infinite-bus sytem the diagonal elements of the source impedance matrix are of the order of $^1/_{10}$ ohms which simulate this condition well enough. This means that the elements of the source admittance matrix given in Fig. (9.2.b) will each have the value of 10 mhos. For practical purposes 10 mhos is considered sufficiently low but could be made much lower if felt necessary.

9.3.2 First Pole Closure

To simulate conditions relating to first pole closure the second and third elements of the current vector transform are set to zero and the diagonal elements in the admittance matrix corresponding to the second and third phase are also set to zero. These conditions are shown in Fig. (9.2.c). If the second and third phases are closed first then the injected currents for these phases and the equivalent admittance only of those phases are considered, while other elements in the matrixes similarly set to zero values.

9.3.3 General Sequential Pole Closure

The boundary conditions for closure of the first breaker pole are dealt with as explained above. There

then follows the second pole in which case the current and the admittance matrixes are modified. Using superposition, the current transform $\bar{I}'_{s2}$ is a combination of two transforms: an analytical transform defining the energising function and a synthesis transform obtained from the response of the second phase at the input end of the line during the period following the first pole closure and finishing just before the second pole closure. This transform component is obtained as explained in section (8.4.2). The admittance element Y_{s2} set to zero during the interval of time prior to second pole closure takes a value of 10 mhos as soon as the pole closes. In a similar manner as soon as the third pole closes Y_{s3} changes from zero to 10 mhos and $\bar{I}_{s3}$ to the sum of analytical and synthesis transforms; the synthesis transform representing the third phase response before third pole closure and the analytical transform that of the energising function.

It is important to note that since there is a general delay time τ from time zero, the time of closure of the first breaker pole, that the appropriate delay operator $\exp(-j\omega\tau)$ be applied to the analytical transforms $\bar{I}_{s2}$ and $\bar{I}_{s3}$ i.e.

$$\bar{I}_{s2} \text{ becomes } \bar{I}_{s2}.\exp(-j\omega\tau_2)$$

and

$$\bar{I}_{s3} \text{ becomes } \bar{I}_{s3}.\exp(-j\omega\tau_3)$$

in which case τ_2 and τ_3 are the corresponding times of these poles closure.

The sequence of pole closure explained above is 1,2,3,

though this is no restriction on the method since in a similar manner any sequential form of closure is possible. When all three breaker poles close the input current and admittance matrixes take the same form of simultaneous pole closure conditions shown in Fig. (9.2.b) with perhaps different values for the elements of $\bar{I}_s$.

As with the previous cases a general terminating admittance Y_t has been considered though in the present investigation transient voltages due to open-circuited lines at the receiving end have been studied. This case is thought to represent the severest system condition, in which case the elements of the matrix Y_t are all zeros.

9.4 Description of Digital Computer Programs

Two general programs to handle balanced or unbalanced line energisation and sequential energisation will be described. Transient voltages resulting from the effect of the first pole closure only can be studied from the balanced energisation program by setting the input currents of the unenergised conductors to zero values and modifying the input admittance matrixes there. A common feature of both programs is that they are general to any circuit configuration, and can be applied to single-circuit or double circuit lines fed from a source of infinite capacity. Observation time is included as a cycle to enable detailed or global studies to be undertaken on the transient. Effect of line length is also included since it has been the intention of carrying out some transient investigations on long lines.

9.4.1 Simultaneous Energisation Program

The input data to this program, the flow diagram of which is shown in Fig. (9.3) include reading in the line geometry, phase and earth wire specifications, earth resistivity and system frequency etc. The line length is then introduced as a cycle and so is the observation time to enable different line lengths and shorter or longer observation periods of study to be dealt with. The phase to be energised is then specified. Some basic calculations are then made to evaluate the fundamental frequency "ω_0" and the axis shift constant "a".

The total optimum number of harmonics chosen for the study is 100 but the system frequency response is evaluated at odd harmonics only. The frequency cycle is therefore set and the harmonic of interest selected, this is a complex quantity. The evaluation of the line constants for this case follows exactly their evaluations in the steady state calculations program where these are found for the real system power frequency. These parameters are the basic impedance and admittance matrixes, eigenvalues, eigenvectors, surge impedance and surge admittance matrixes. A facility is included in the program to print out the modal quantities of the circuit if these are needed. The determination of the line constants is followed by the evaluation of various transfer functions needed in the calculation of the system response in the frequency domain; at this stage the transform of the energising currents are set up together with the network input source admittance to simulate pole closure.

The frequency response of the system for the particular

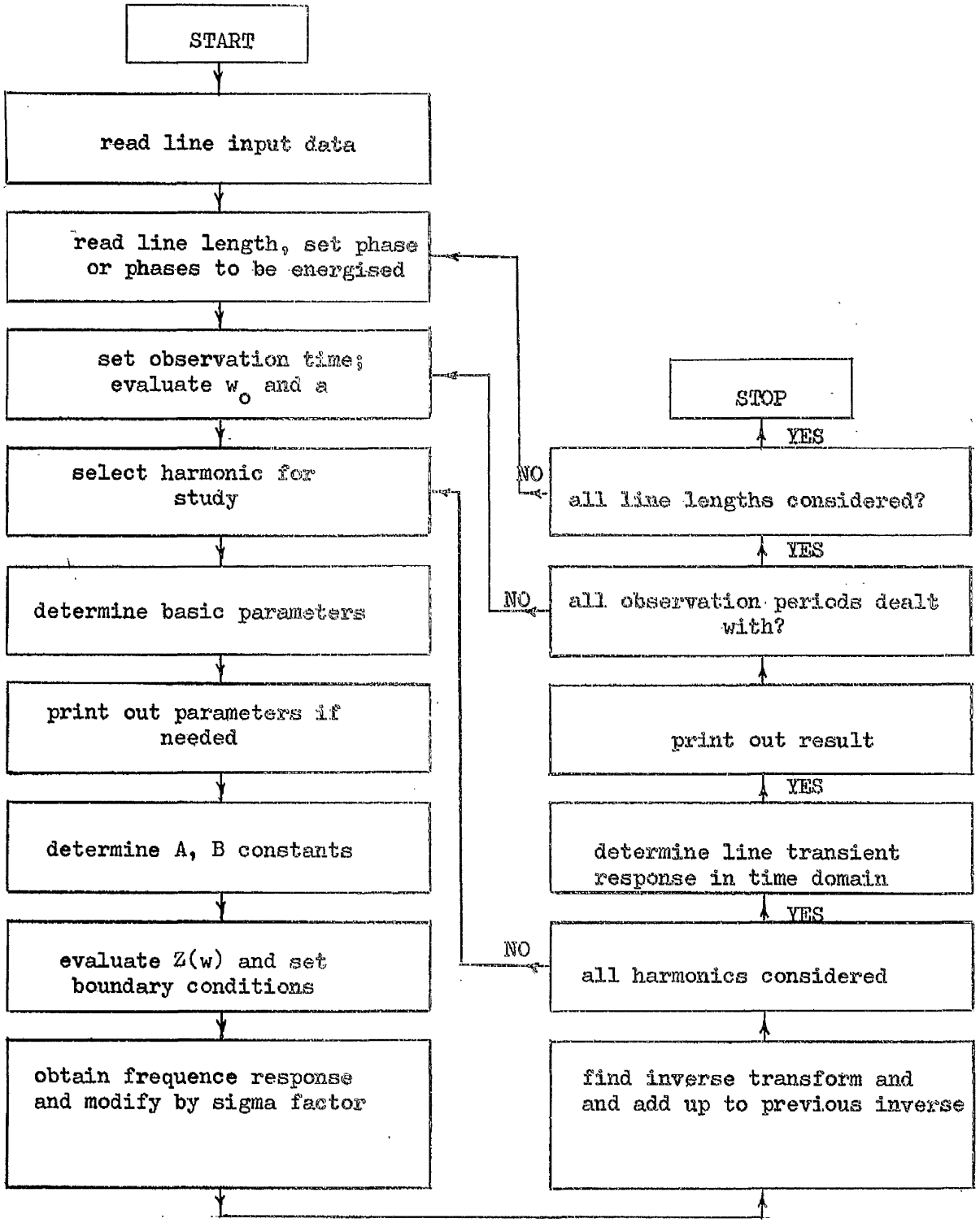

FIG. (9.3). FLOW DIAGRAM OF DIGITAL COMPUTER PROGRAM FOR SIMULTANEOUS POLE CLOSURE PROBLEM

harmonic is then obtained and then modified by the standard sigma factor before the inverse transform is found and added up to the previous value. The frequency cycle is repeated in order to determine the response due to all harmonics chosen. At the end of this cycle the time response is evaluated and the result is printed out.

The program tests that different observation periods, different line lengths and all circuit configurations have been dealt with before it reaches its end.

9.4 2. Sequential Energisation Program

This program uses basically the same steps to calculate the line frequency response as the simultaneous energisation program. Other major differences occur in the setting up of system boundary conditions. For this reason the details written out in the program will not be repeated here. It will be understood that these are inherently included in this program.

Consider the flow diagram shown in Fig. (9.4) . After the input data has been read in and some of the basic calculations made a condition is set signifying first pole closure, then the setting up of the frequency cycle followed by steps leading to the formation to the A, B line constants. The energising conditions for the case of the first pole to close are set up and the time response obtained by going through the intermediate stages of the program of Fig. (9.3) up to the instant in time of the second breaker pole closure. The Fourier synthesis routine is then entered and there the Fourier coefficients of the induced

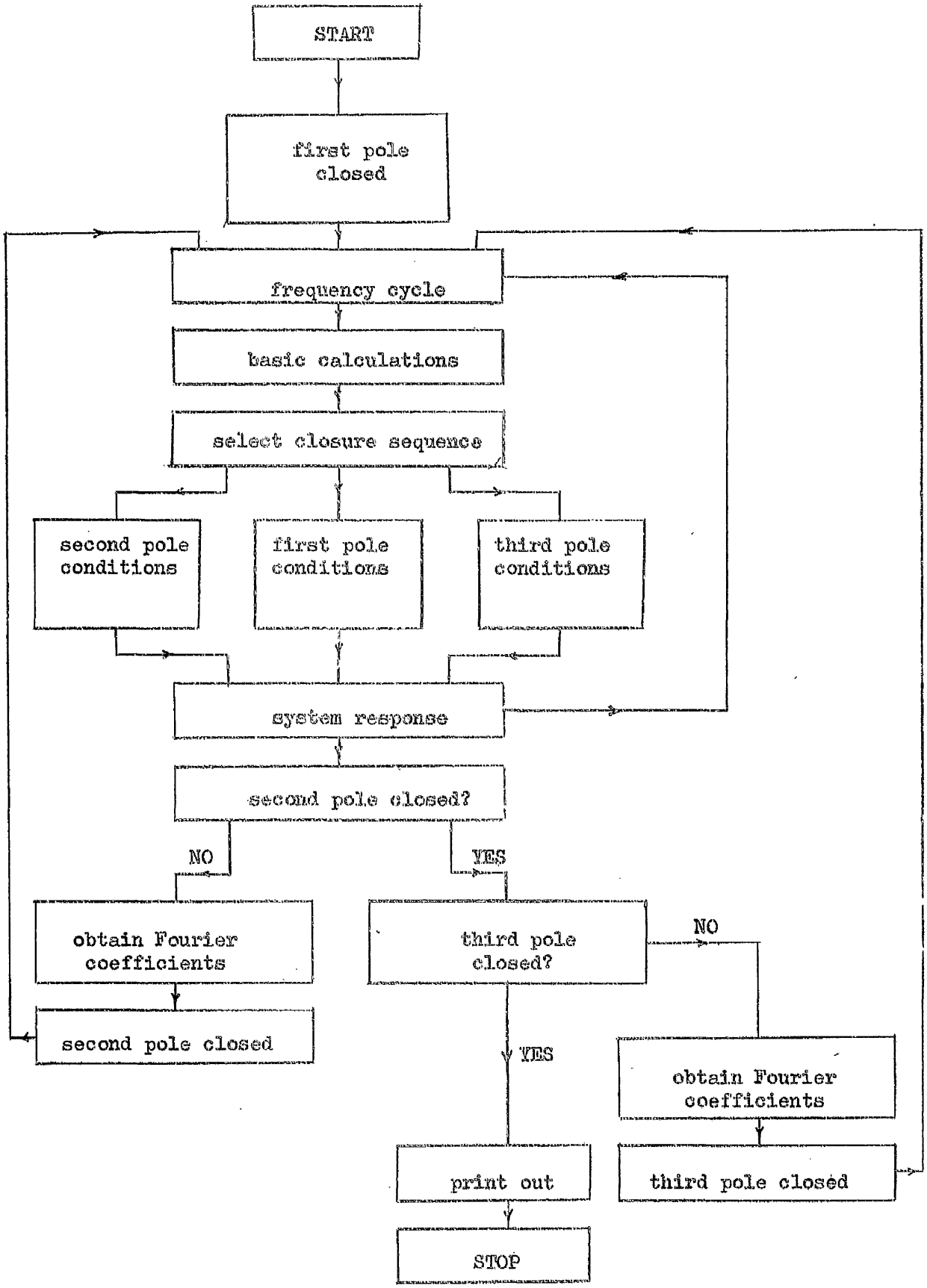

FIG. (9.4). FLOW DIAGRAM OF DIGITAL COMPUTER PROGRAM FOR SEQUENTIAL POLE CLOSURE PROBLEM

voltage, or its current equivalent, on the second phase are found for the odd harmonics used; these terms adding up to the analytical transform of the energisation voltage i.e. current equivalent on the second phase. A condition indicating second pole closure is signified and this moves control to the frequency cycle where the calculation is started with the boundary conditions now including second phase energisation as well (remembering to introduce the delay operator in the analytical contribution of the energising voltage). The response is finally obtained up to the moment when the third breaker pole is about to close. At this moment the Fourier synthesis sub-routine is entered and the Fourier coefficients then obtained for the induced voltage on the third phase from the time of first pole closure. The procedure is repeated in a similar manner to second phase energisation and the final stages of system response following all poles closure is determined. When this condition has been reached the time response is printed out. Other steps are similar to those of program shown in Fig. (9.3).

An additional step has been introduced in this program though not included in the flow diagram. This serves as a useful means of checking the method of analysis presented in sequential pole closure. When all breaker poles have closed the line response in the time domain is obtained right from time zero. This result should be identical to the one obtained without making this additional step.

9.5 Line Data

A single circuit quad conductor 400 KV line is chosen for transient studies. Fig. (9.5) shows a diagram of circuit arrangement. The data for this line are

Phase Conductors:-

4×54/7/0.125 in. S.C.A. per phase with 1 ft. bundle spacing.

Earth Wires:-

1×54/7/0.125 in. S.C.A.

Earth Resistivity:-

30 Ω-meters.

The 50 Hz parameters for this line are given in Table (9.1) and parameters calculated at a complex frequency of 350-j100 Hz. in Table (9.2).

9.6 Studies Relating to First Pole Closure of 120-Mile Line

The interaction among various forms of propagation taking place when the three phases of a line are energised either simultaneously or sequentially present certain difficulties against carrying out some fundamental investigation relating to the propagation of switching surges on multiconductor lines particularly since three forms of propagation are involved for the three-phase line. Transient overvoltages resulting from first pole closure of a circuit breaker are therefore of extreme importance since they serve as guide lines for the resultant overall system transients occurring when all phases have been closed. Since the whole system is floating prior to first phase energisation then it will be

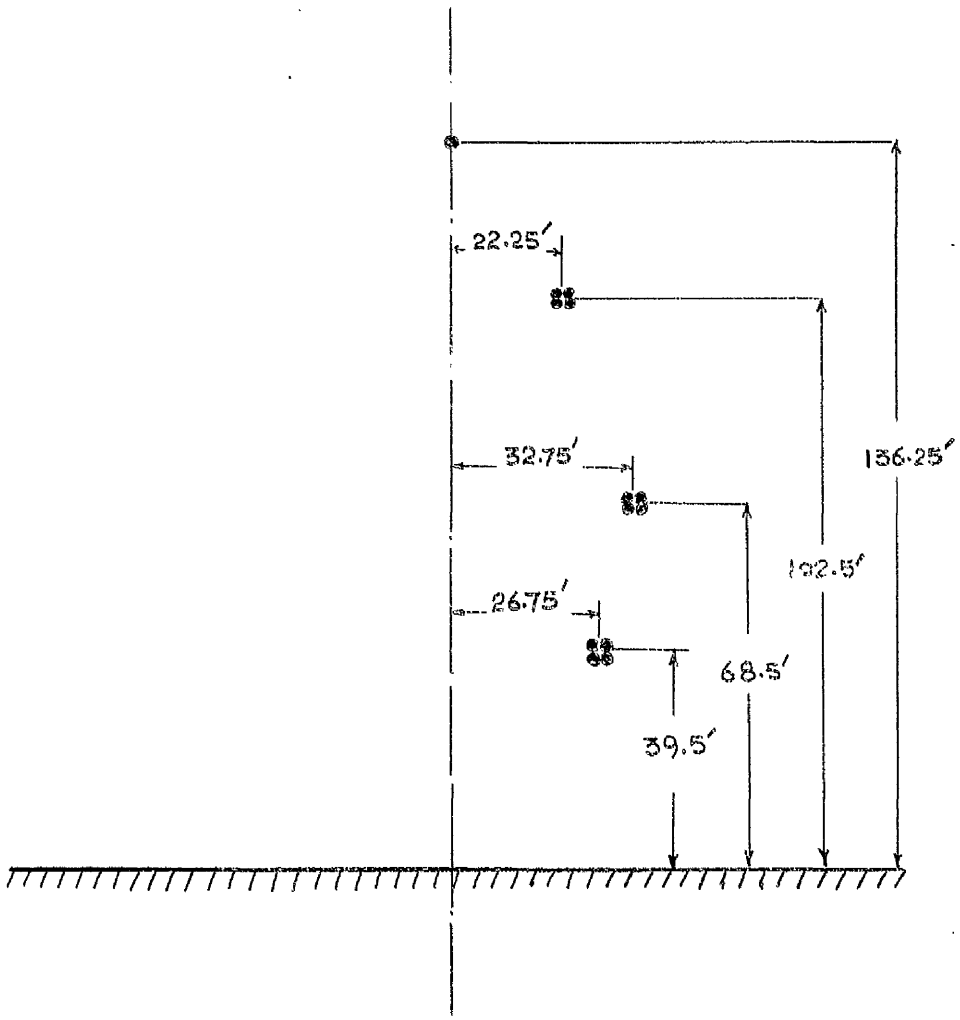

FIG. (9.5). 400 KV QUAD CONDUCTOR LINE

TABLE (9.1). 50 HZ PARAMETERS OF QUAD CONDUCTOR VERTICAL LINE

Z_o (ohms)

Bottom Conductor : 364.36 -2.97°

Middle " : 126.37 -4.79° 376.67 -2.92°

Top " : 84.60 -6.79° 119.90 -4.88° 372.19 -2.95°

Y_o (millimhos)

Bottom Conductor : 3.162 2.37°

Middle " : 0.928 -178.65° 3.229 2.30°

Top " : 0.420 177.9° 0.830 -178.90° 3.048 2.35°

Mode Number	Eigenvector				Attenuation DB/KM	Velocity KM/SEC
	Voltage		Current			
	Modulus	Angle deg.	Modulus	Angle deg.		
1	1.0000	0.000	1.0000	0.000	0.00079	227704
	0.8612	-0.657	0.6110	-0.534		
	0.7134	-3.139	0.5031	-5.231		
2	0.3542	-163.31	0.4533	-166.73	0.00034	297453
	1.0000	0.000	1.0000	0.000		
	0.5801	163.73	0.6099	167.96		
3	0.6874	168.89	0.9294	167.48	0.00031	296122
	0.3173	-25.99	0.2947	-39.14		
	1.0000	0.000	1.0000	0.000		

TABLE (9.2). 350 HZ PARAMETERS OF QUAD CONDUCTOR VERTICAL LINE

Z_o (ohms)

Bottom Conductor : 351.25 -1.69°

Middle " : 114.19 -4.29° 365.03 -1.44°

Top " : 73.59 -5.88° 109.51 -3.72° 362.85 -1.19°

Y_o (millimhos)

Bottom Conductor : 3.214 0.94°

Middle " : 0.890 178.60° 3.257 0.61°

Top " : 0.383 176.37° 0.803 179.02° 3.074 0.58°

Mode Number	Eigenvectors				Attenuation DB/KM	Velocity KM/SEC
	Voltage		Current			
	Modulus	Angle deg.	Modulus	Angle deg.		
1	1.0000	0.000	1.0000	0.000	0.02612	244293
	0.8383	-1.157	0.5874	-1.676		
	0.6734	-2.544	0.4579	-4.157		
2	0.7631	176.10	1.0000	0.000	0.01875	296587
	0.5197	-1.841	0.4754	179.96		
	1.0000	0.000	0.8935	-176.66		
3	0.2292	-175.01	0.3237	-176.66	0.01867	297731
	1.0000	0.000	1.0000	0.000		
	0.7879	178.25	0.7667	178.57		

expected that severe transient overvoltages will occur. These considerations, it has been thought, form reasonable justification for carrying out system transient studies under first phase energisation and hence not only establish the validity of the method of analysis presented but also deduce some basic properties on the transient behaviour of a multi-conductor transmission line.

Studies have been carried out on the vertical circuit described for a line length of 120 miles. If the effect of different modal velocities is ignored then it takes an electromagnetic disturbance approximately 5 μsec to traverse one mile of line, assuming propagation at the velocity of light. The figure of 5 μsec/mile is a useful guidance for transit time evaluation.

The line is fed from an infinite bus (with respect to the energised conductor) and is open-circuited at the receiving end. The bottom and top conductors of the circuit are each energised in turn and the resultant transient voltages are observed over a period of 2 msec and 10 msec respectively at the sending and receiving ends of the line.

2 msec Observation Time Study

Fig. (9.6) shows the results for the case of the bottom conductor being energised at voltage peak of a 400 KV-bus while the other two conductors are left floating. The input function as shown in the figure takes a few microseconds to develop, this is the rise time referred to earlier and for times greater than 90% of the observation period the instability in the input function is pronounced. This is a

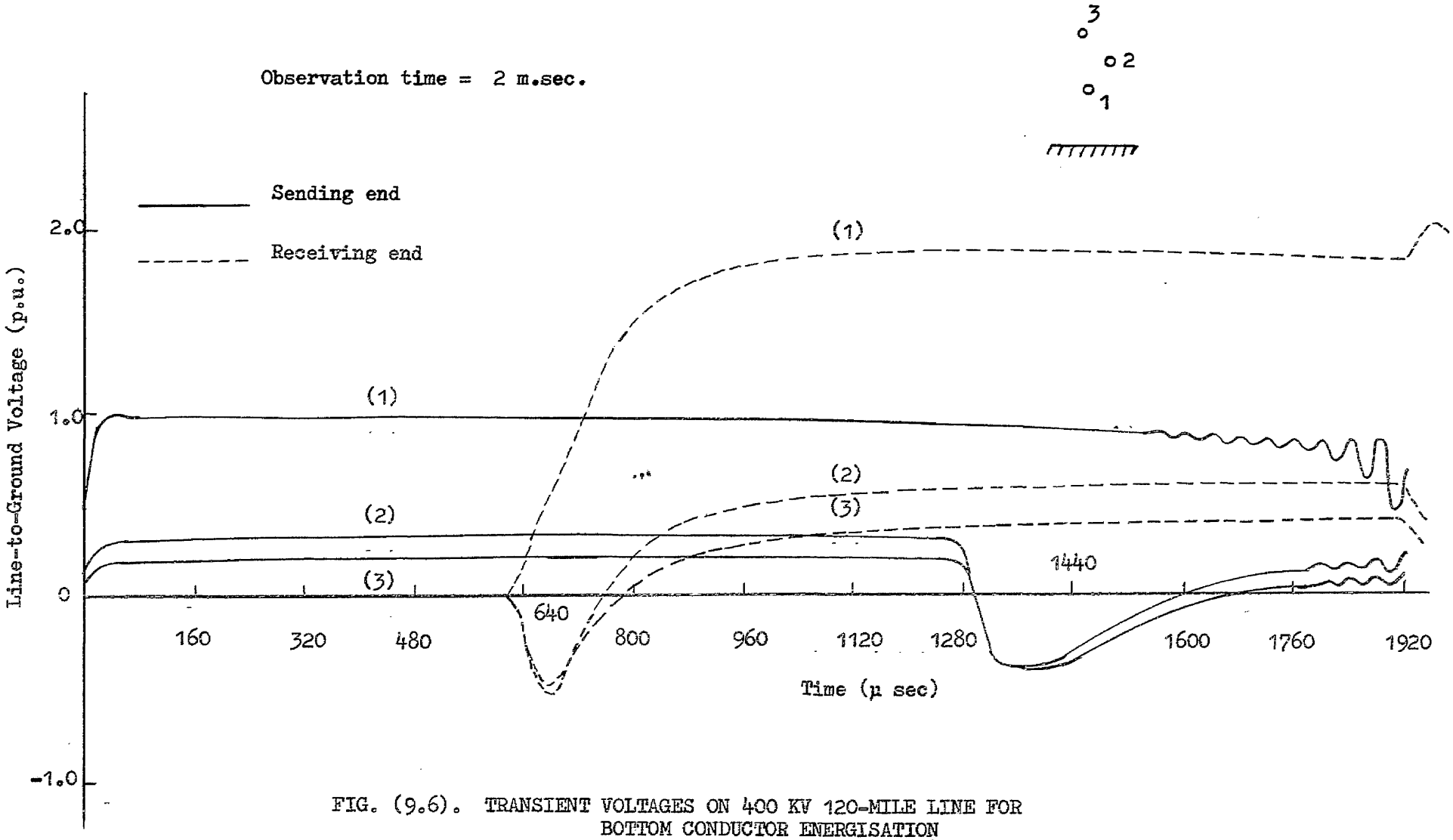

FIG. (9.6). TRANSIENT VOLTAGES ON 400 KV 120-MILE LINE FOR BOTTOM CONDUCTOR ENERGISATION

mathematical instability and is not a physical property of the system. At the receiving end of the line these oscillations are smoothed out and the line thus acts as a filter. The unenergised conductors acquire positive step voltage with respect to ground. These voltage steps before any reflection arrives at the sending end of the line can be calculated from a consideration of the surge impedance matrix of the line. As an approximation the surge impedance matrix calculated at 350 Hz has been used and induced voltages on the coupled conductors are obtained from

$$V_{in} = \frac{Z_{om}}{Z_{os}} \times V_{en} \qquad - (9.6)$$

where V_{in} and V_{en} are induced and energising voltages, Z_{os} and Z_{om} are the self and mutual surge impedance respectively. The results thus calculated are compared with these obtained from the curves of Fig. (9.6). These are tabulated below.

Phase Conductor	Bottom	Middle	Top
Voltage from Fig.(9.6) "KV"	326	106	68
Voltage from Equation (9.6) "KV"	326	101	63.4

It is seen that the agreement for the uncoupled conductors is favourable. The discrepancy between the two sets of result is due to the fact that surge impedance is taken at only one frequency. The time of transit down the line and the time between successive reflections is clearly seen from the curves for sending and receiving ends of the line with near doubling effect occurring at the receiving end.

The deviation from doubling is a result of attenuation due to ground and conductor losses. At the receiving end of the line the arrival of the ground wave travelling at a much lower velocity than the two aerial waves has resulted in a slow rising wave front at the receiving end of the phase that has closed. The initial positive steps appearing at the sending end of the coupled conductors are reflected as negative steps initially at the receiving end mainly due to the presence of the earth mode.

With the top phase closing first while the other two phase conductors are floating the arrival of the earth mode is more clearly marked at the receiving end of the line as shown by Fig. (9.7). There is a steep wave-front due to the arrival of aerial modes followed by a stationary condition around 680 μsec of observation time then a slow rise due to earth mode. The initial step rises induced on the unenergised phases at the sending end of the line are compared with those obtained from surge impedance evaluation. The agreement obtained is shown to be reasonable in the table below.

Phase Conductor	Bottom	Middle	Top
Voltage from Fig.(9.6) "KV"	65.7	98	326
Voltage from Equation (9.6) "KV"	60.7	94	326

10 Millisecond Observation Time

In Figs. (9.8) and (9.9) are shown sending and receiving end transient voltages observed over a long period of time for the case of top and bottom phase being energised

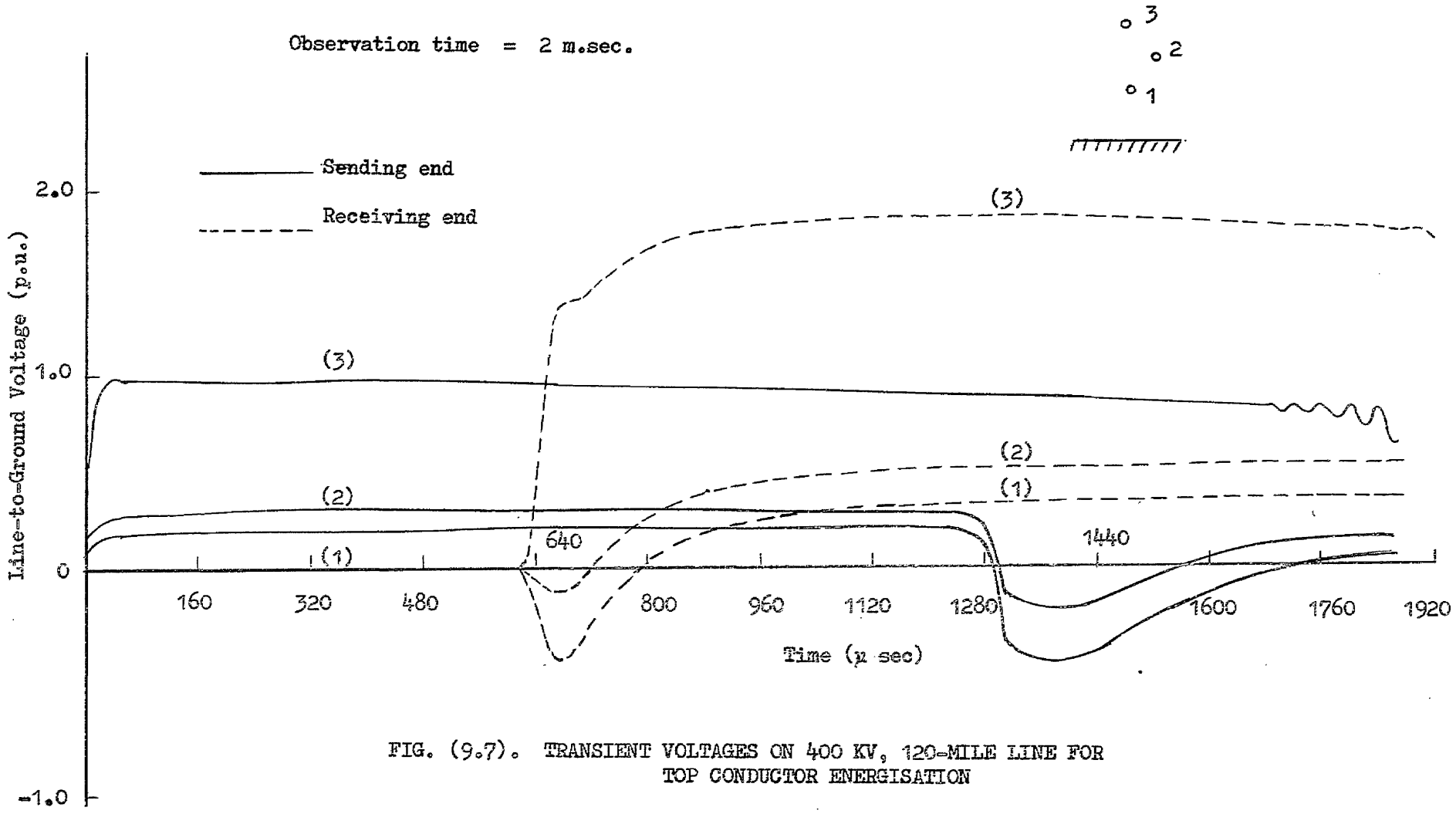

FIG. (9.7). TRANSIENT VOLTAGES ON 400 KV, 120-MILE LINE FOR TOP CONDUCTOR ENERGISATION

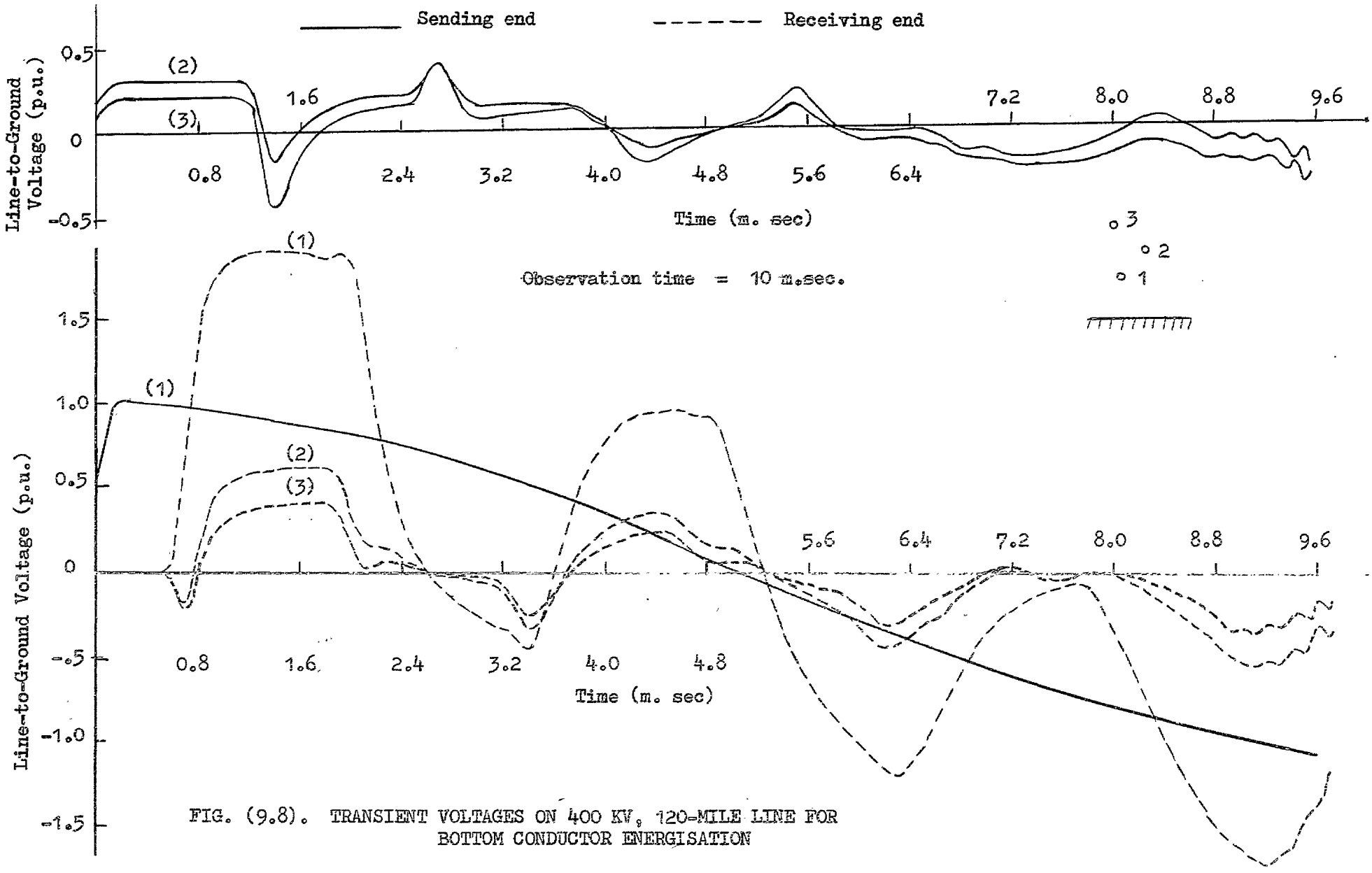

FIG. (9.8). TRANSIENT VOLTAGES ON 400 KV, 120-MILE LINE FOR BOTTOM CONDUCTOR ENERGISATION

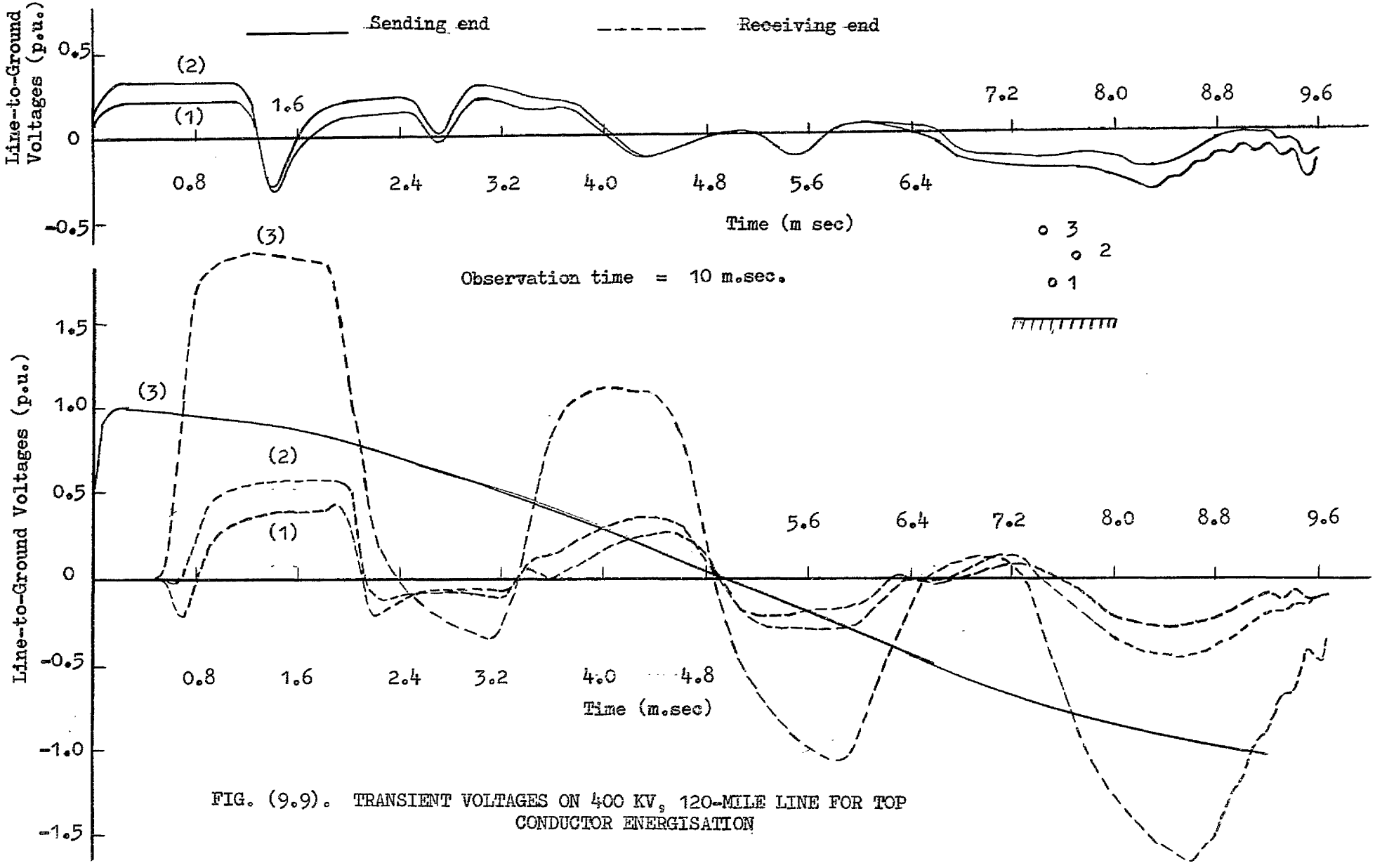

FIG. (9.9). TRANSIENT VOLTAGES ON 400 KV, 120-MILE LINE FOR TOP CONDUCTOR ENERGISATION

in turn at voltage peak of a sinusoidal input. There is general agreement up to 2 msec with the previously determined 2 msec response. The rise time of the input function is greater for the longer observation, 5 to 1 increase in comparison with shorter observation time. The reason for this is that as the total number of harmonics is fixed in both cases (50 odd harmonics) the increase in the observation time results in a decrease in the fundamental frequency which causes a loss of higher harmonics responsible for rise time definition; in this case therefore a poor definition of the input wave front. The effect of this on the rest of the system is that more optimistic values will be shown for the transient response than would be the case in practice. The line smoothing action on the oscillations that are inherent in the representation of the input function is apparent for both bottom and top conductor energisation.

The response of the line at the receiving end shows a kind of beat-effect. This is an indication of some form of modal interaction on the line. The voltage on the coupled conductors at the receiving end of the line tends to peak and trough with the main transient while at the sending end it varies in an irregular manner governed only by the arrival of reflected waves from the receiving end. This has been recognised in the analysis of sequential transients calculations. Both results of Fig. (9.8) and (9.9) clearly show 50 Hz component mounted on the line natural frequency response which is complicated for a multiconductor line by the fact that there are three line transit times for the

existing three modes of propagation, or at least two if the difference between the two approximately equal aerial modes is ignored.

9.7 Studies Relating to First Pole Closure Transients of a 600-Mile Line

9.7.1 Uncompensated Line

Transient overvoltages resulting from switching operations on long lines are greatly influenced by the Ferranti effects on these lines. In Fig. (9.10) the line response due to first pole closure is given at the sending end, mid-point and receiving end of the line. The line is energised from an infinite-bus source and the receiving end is open-circuited. The transient has been observed over a period of 30 msec. and this has revealed overvoltages of the order of four times normal peak line-to-ground voltages occurring at the receiving end of the line. This is far in excess of the normal doubling effect predicted by classical methods and such voltage magnitude can not be tolerated from practical points of view. The natural frequency response for this line is about 80 Hz. while the earth mode power frequency assuming the velocity of earth mode 2/3 the velocity of light is 75 Hz. These two frequencies are closely related to each other and may have resulted in some form of resonance that has given rise to the extreme transient overvoltages appearing on this line. To minimize these voltage rises, series and shunt compensation have been introduced at basically similar locations to the ones dealt with in steady-state analysis since those provide satisfactory operating conditions.

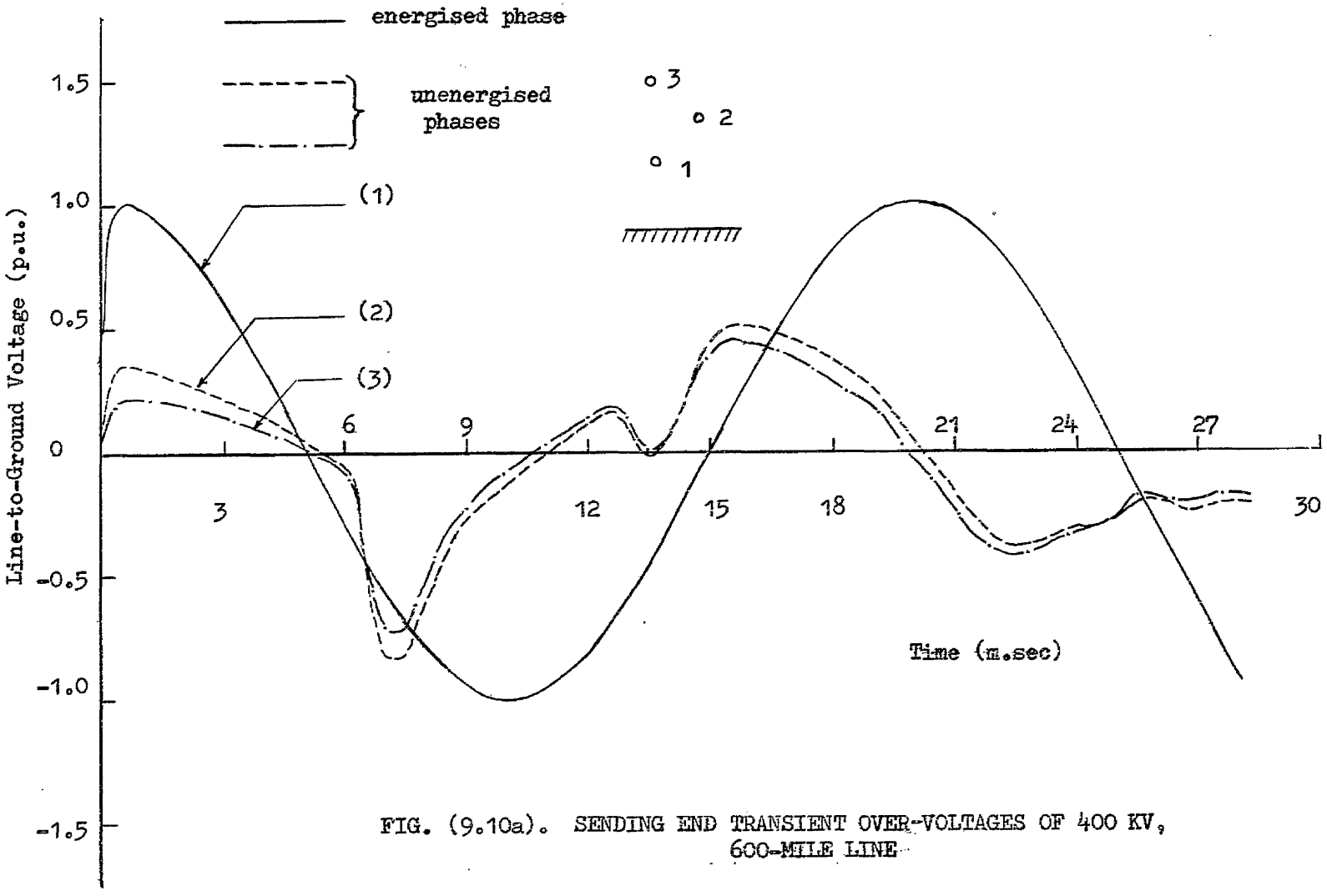

FIG. (9.10a). SENDING END TRANSIENT OVER-VOLTAGES OF 400 KV, 600-MILE LINE

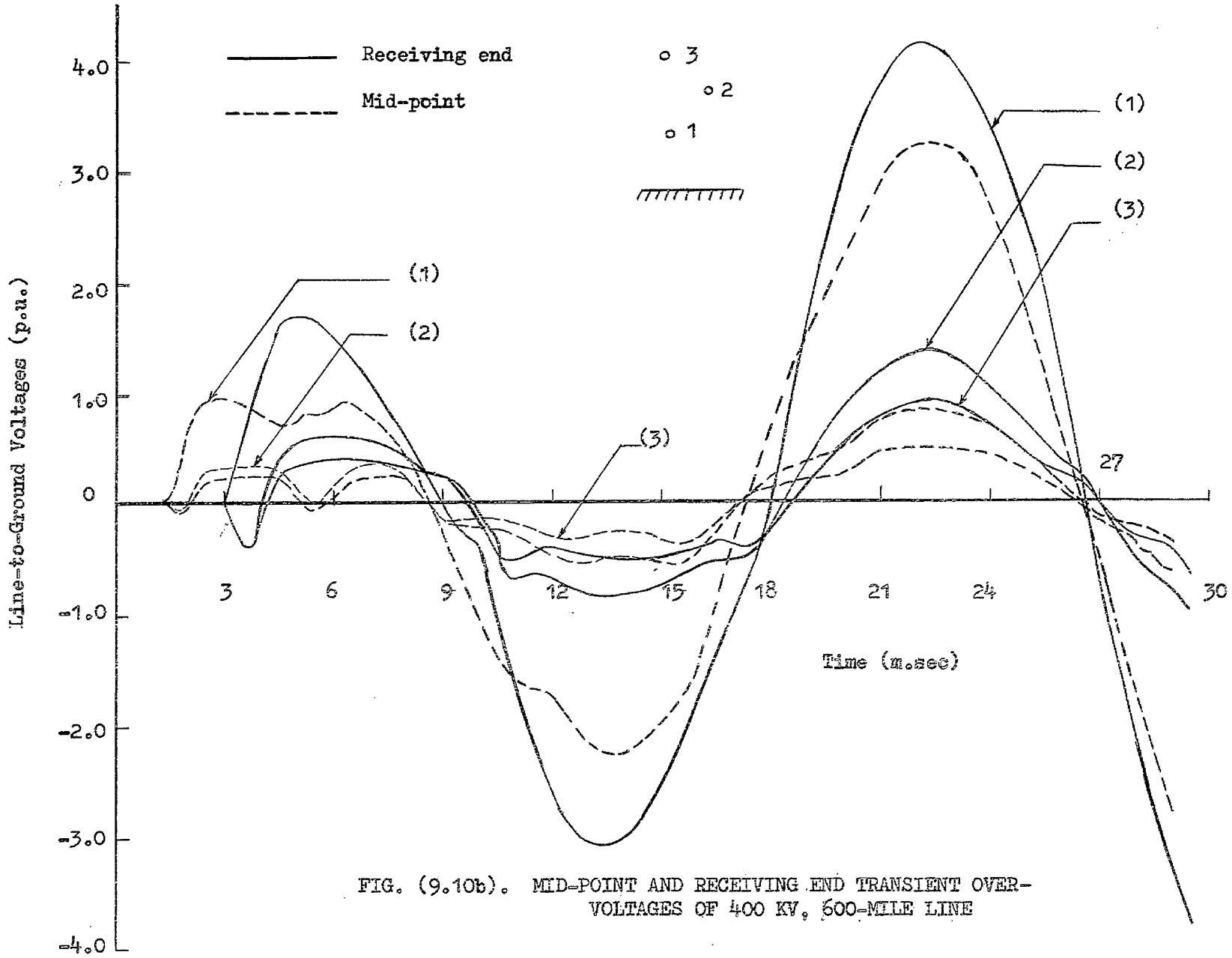

FIG. (9.10b). MID-POINT AND RECEIVING END TRANSIENT OVER-VOLTAGES OF 400 KV, 600-MILE LINE

9.7.2. Compensated Line

In the steady-state calculations the series capacitor and shunt reactor reactances are calculated from a knowledge of the positive sequence line inductive reactance or line positive admittance and depending on the degree of series or shunt compensation. These are introduced either at one location or distributed at various locations; they are 50 Hz reactances. For the transient calculations it is important to take into consideration the frequency dependence of these compensating elements and therefore the capacitor value in Farads and the inductor value in Henries are obtained before introduction in the program as lumped elements for the evaluation of their impedance (or admittances) at a general harmonic frequency.

With series compensation located at the centre of the line the reduction in the three voltage peaks appearing on the receiving end voltages of Fig. (9.10) are shown in Fig. (9.11) for different degrees of series compensations. This suggests that for further reduction in transient voltages shunt compensation has to be employed.

The effect of series and shunt compensation on the magnitude of the overvoltages is shown in Fig. (9.12) in which two series and shunt compensating stations located at 200 and 400 miles from the sending end of the line. A degree of 50 per cent for series and 30 per cent for shunt compensation have been considered. It is evident from these figures that substantial reductions in overvoltage have been produced. For the same degrees of series and shunt

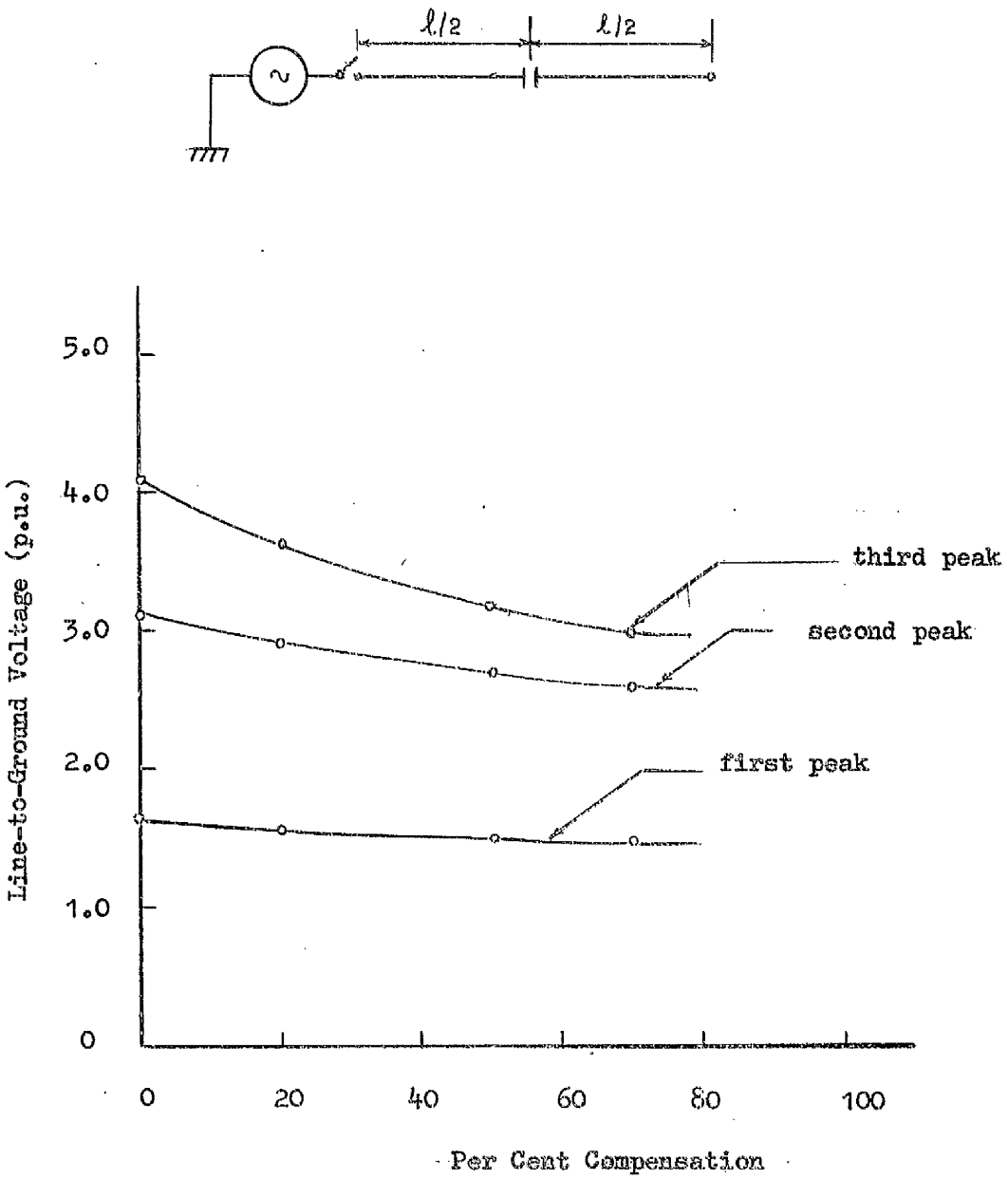

FIG. (9.11). EFFECT OF INCREASED SERIES COMPENSATION ON TRANSIENT OVER-VOLTAGES ON 400 KV, 600-MILE LINE

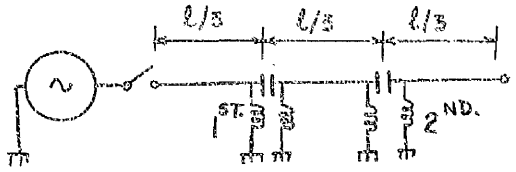

degree of series compensation = 50%

" " shunt " = 30%

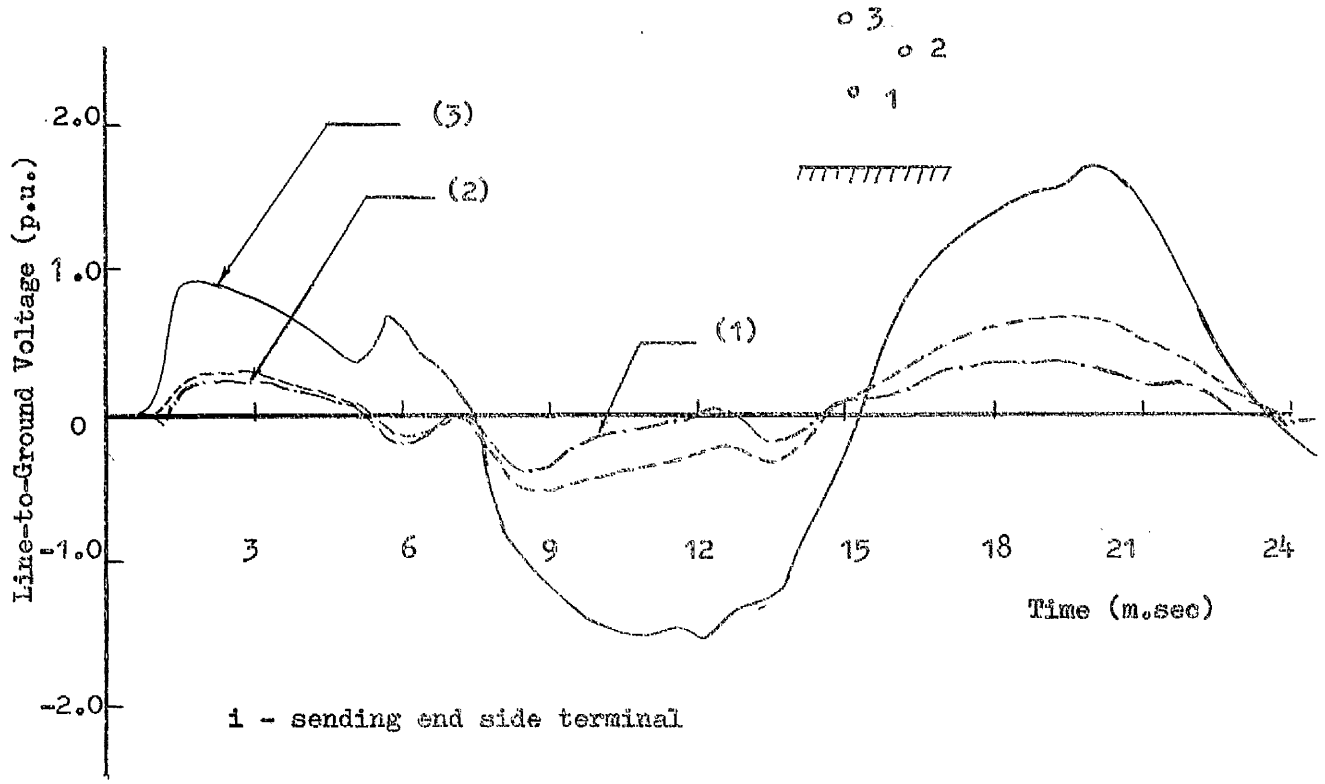

i - sending end side terminal

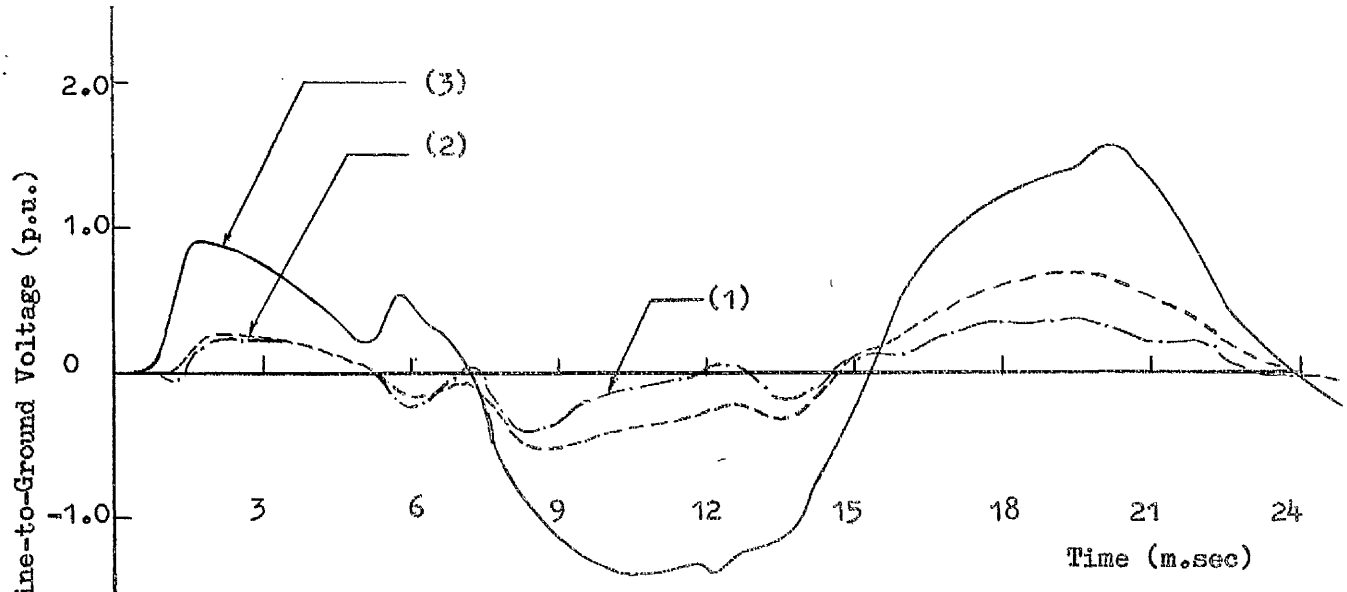

ii - receiving end side terminal

FIG. (9.12a). TRANSIENT OVER-VOLTAGES ON FIRST COMPENSATING STATION OF 400 KV, 600-MILE LINE

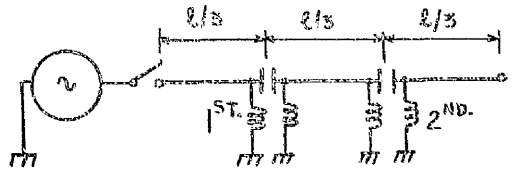

degree of series compensation = 50%

" " shunt " = 30%

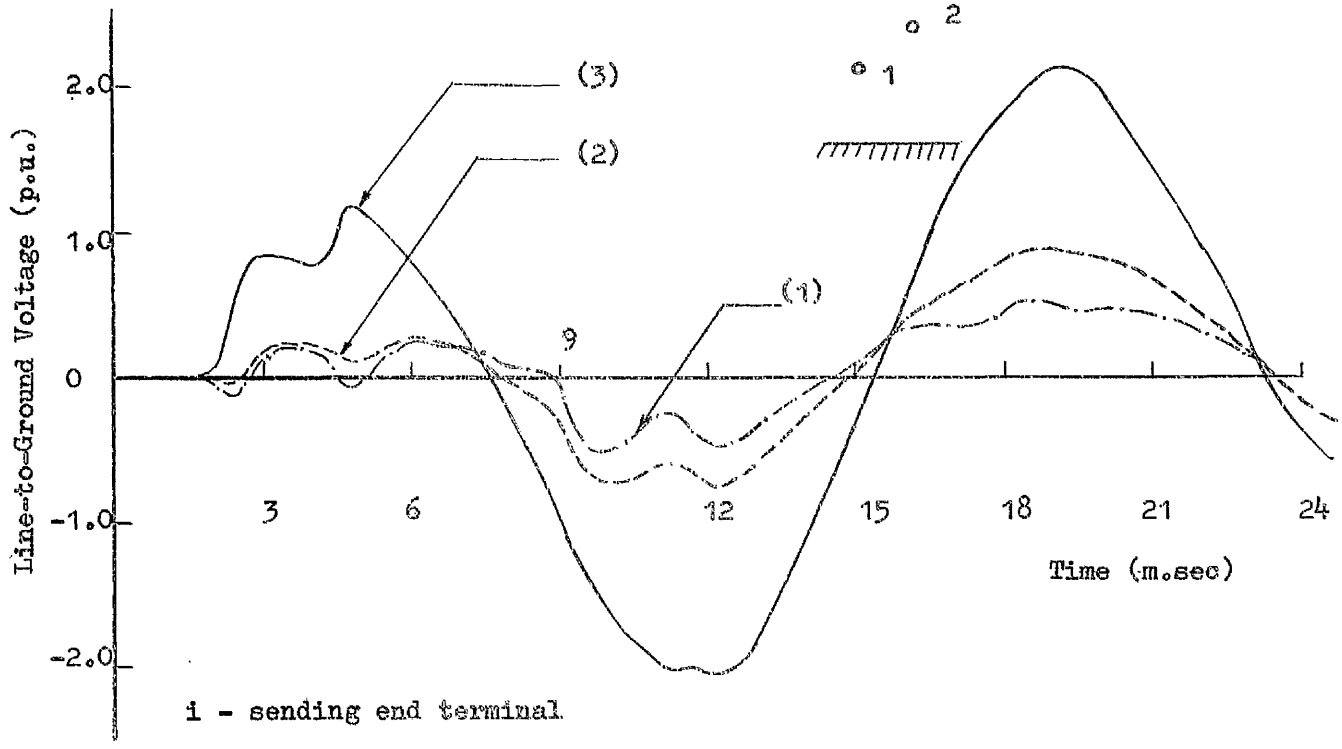

i - sending end terminal

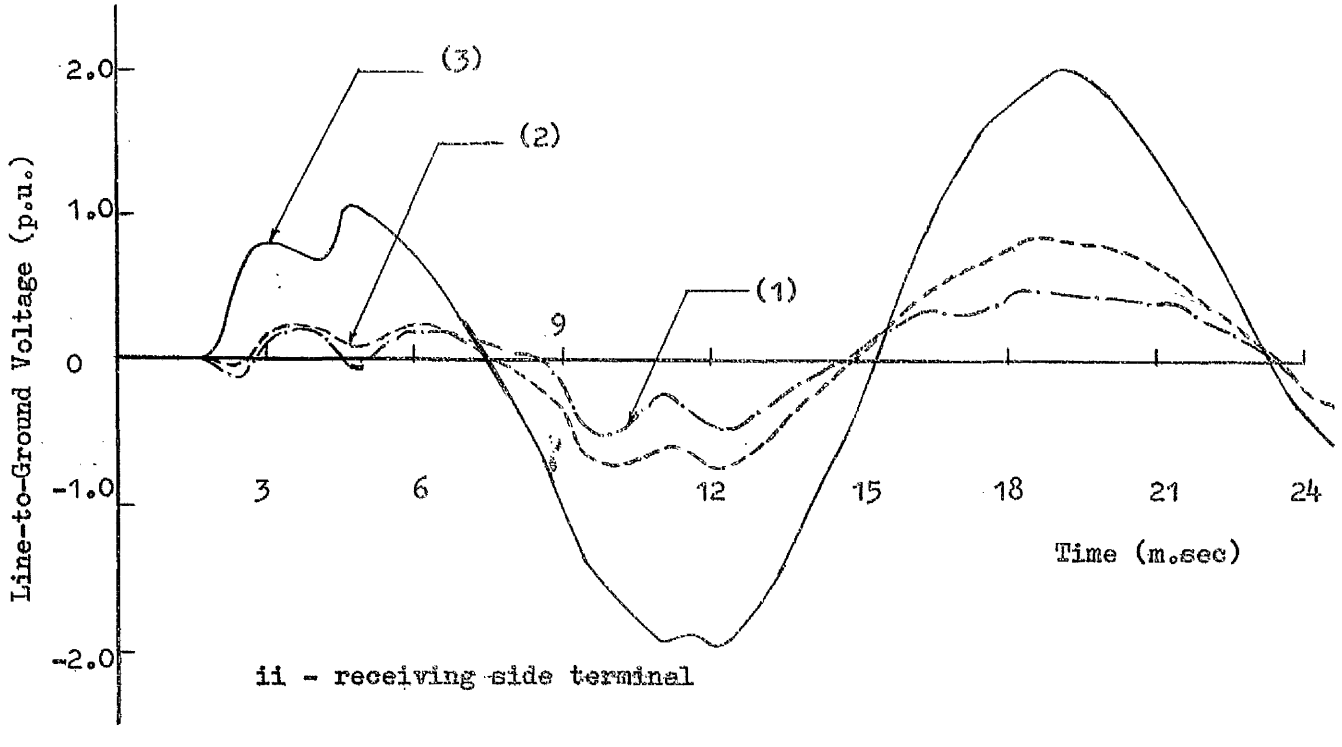

ii - receiving side terminal

FIG. (9.12b). TRANSIENT OVER-VOLTAGES ON SECOND COMPENSATING STATION OF 400 KV, 600-MILE LINE

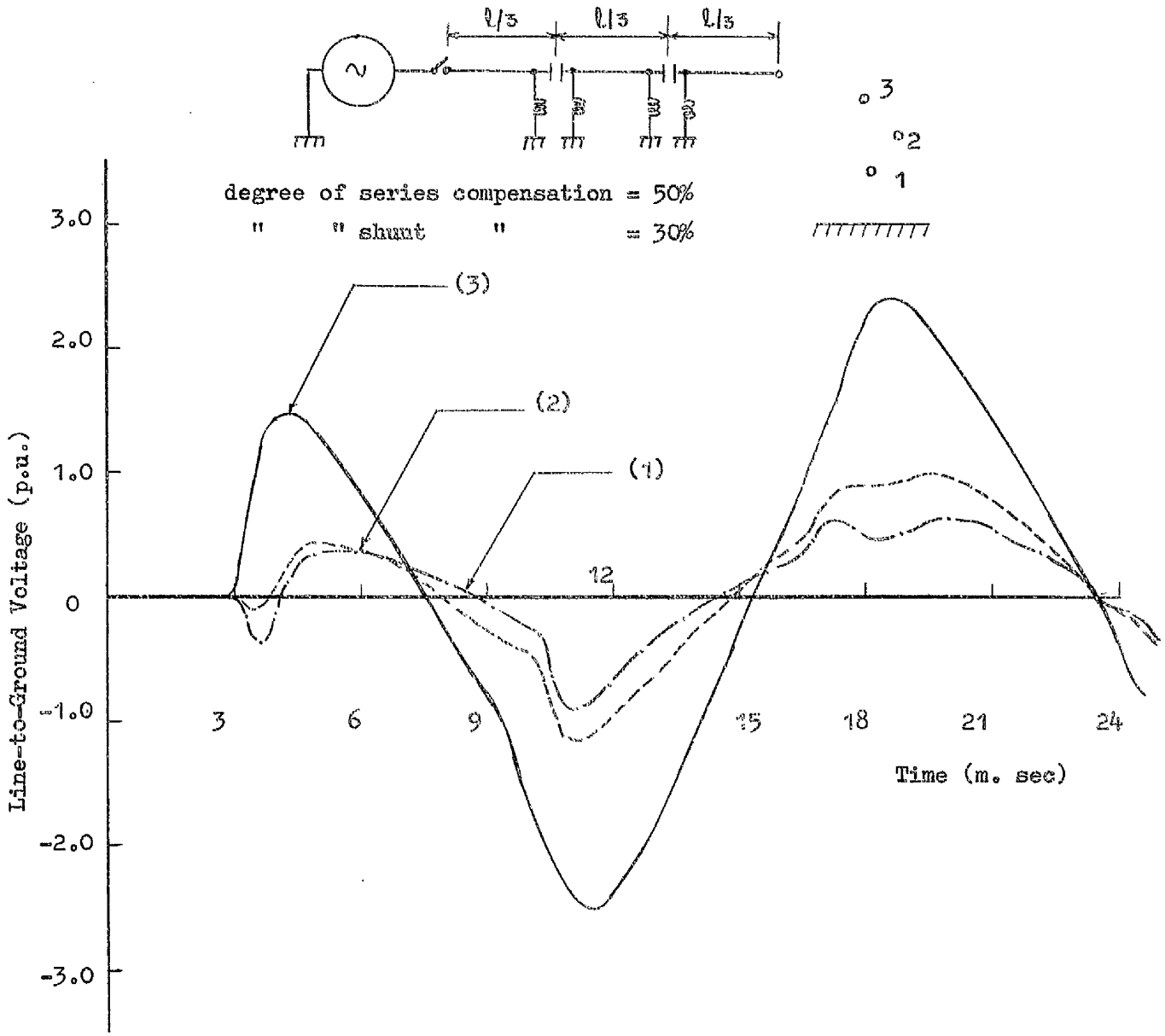

FIG. (9.12c). TRANSIENT OVER-VOLTAGES AT RECEIVING END OF 400 KV, 600-MILE COMPENSATED LINE

compensation a summary of results for maximum overvoltages occurring at the compensating stations terminals and also on the receiving end of the line is given in Table (9.3) when compensation is distributed among two and three stations. It has been found that combined series and shunt compensation produce in general good results and that when the top conductor is energised that lower overvoltages occur than for bottom conductor. This is in the main due to the dominance of earth mode on the bottom conductor of a vertical line with its amplified Ferranti effect due to the low phase velocity of the mode.

9.8 Simultaneous Pole Closure Transient Studies

A 50-mile line has been considered for the unrealistic case of simultaneous pole closure. The result is shown in Fig. (9.13) for the sending and receiving ends of the line when it has been energised from an infinite bus source. Since the second and third phase close onto lower voltages than the first phase as shown by the sending end result, the receiving end transients for these two phases prior to reflections are also lower. At the receiving end there is clearly a 50 Hz component riding on top of the line natural frequency components.

9.9 Sequential Pole Closure Transient Studies

Using the method proposed in section (9.3.3) for the sequential energisation of a transmission line, transient voltages at the sending and receiving ends of a 50-mile line of vertical arrangement have been evaluated over an observation period of 10 msec. The bottom phase conductor

TABLE (9.3). EFFECT OF SERIES AND SHUNT COMPENSATION ON LONG LINE OVER-VOLTAGES

1. Uncompensated Line

Uncompensated line. bottom conductor energised.	Maximum over-voltage (p.u.)	
	V_i	V_r
	3.20	4.15

2. Two compensating stations

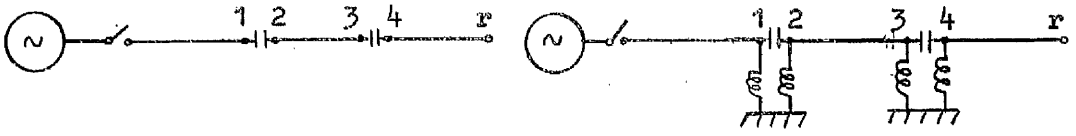

Type of Compensation	Maximum over-voltage (p.u)				
	V_1	V_2	V_3	V_4	V_5
series comp.	2.4	2.05	3.1	2.9	3.25
series & shunt: bottom conductor energised	1.8	1.58	2.4	2.28	2.73
series & shunt: top conductor energised	1.70	1.55	2.10	2.0	2.4

3. Three compensating stations

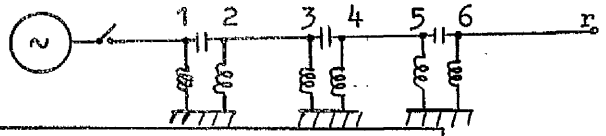

Type of Compensation	Maximum over-voltage (p.u.)						
	V_1	V_2	V_3	V_4	V_5	V_6	V_r
series and shunt: bottom conductor energised	1.58	1.4	1.9	1.8	2.4	2.3	2.6
series and shunt: top conductor energised	1.45	1.35	1.75	1.7	2.12	2.07	2.44

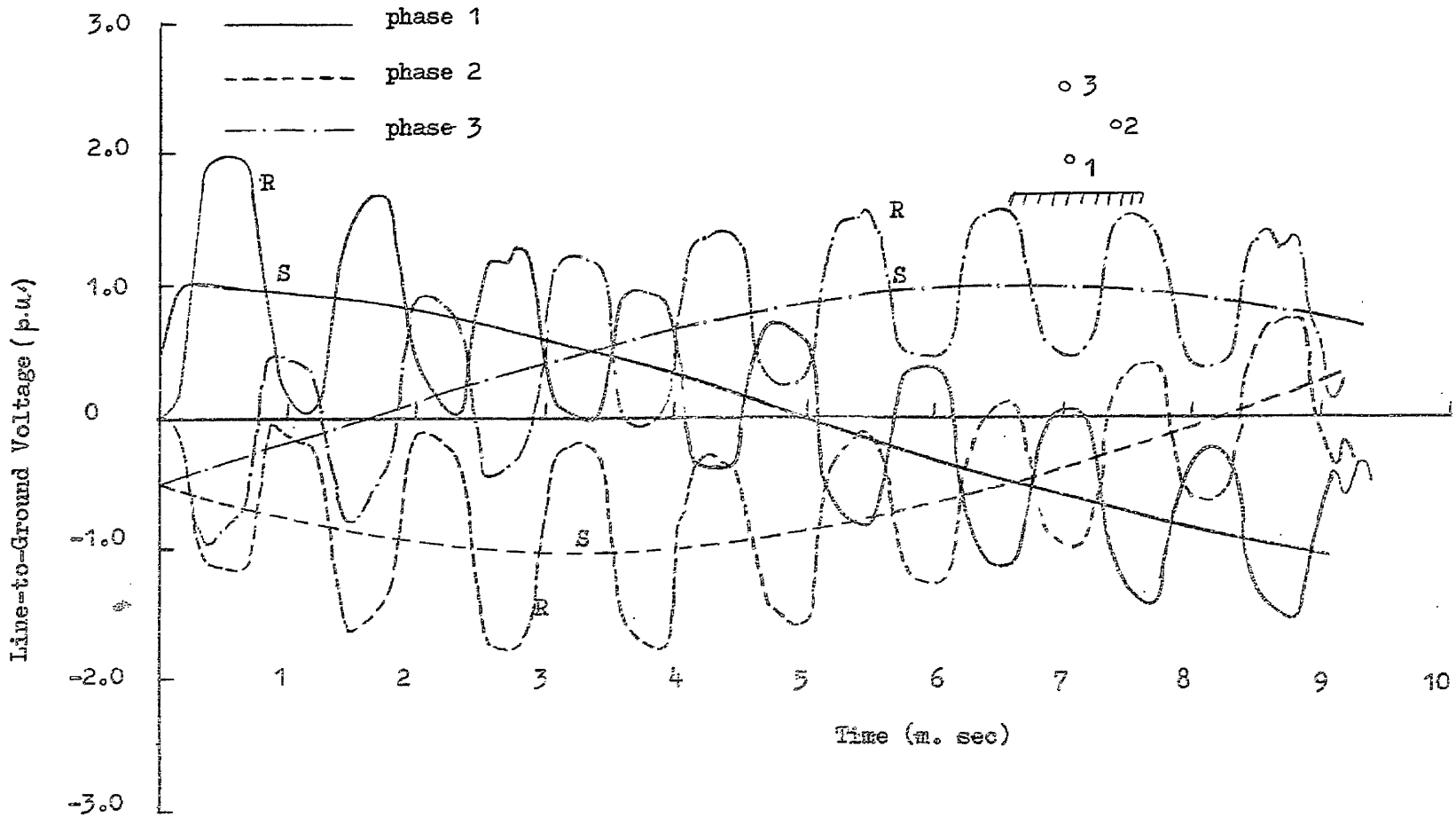

S ... sending end response

R ... receiving end response

FIG. (9.13). EFFECT OF SIMULTANEOUS POLE CLOSURE ON TRANSIENT RESPONSE OF 50-MILE LINE

breaker pole closes first at voltage peak followed by the middle and then the top phase 3.3 and 6.6 msec later, they both close at voltage peak too. The result is shown in Fig. (9.14.a) for the sending end and Fig. (9.14.b) for the receiving end. Source effect has been ignored. Immediately after the closure of the second phase the voltage appearing on that conductor at the sending end will be the voltage of the supply and similarly also when the third phase has been energised. This is confirmed from the result of Fig. (9.14.a).

At the sending end of the line since the second phase has closed at negative voltage peak then this sudden negative voltage step will have an influence on the voltage induced on the floating conductor of the third phase; it can have no effect on the already energised first phase. At exactly 3.3 msec, the time of the second phase closure, the voltage on the floating conductor has registered a negative step of voltage and has thus changed sign from a previous positive value 0.1 msec earlier. The voltage on the floating unenergised conductor is a contribution from the first phase and the second phase in proportion of the mutual surge impedances linking with those two phases. The voltage on this conductor shows a predominant influence from the second phase since there is a strong mutual effect between the top and middle conductors and a weak mutual between top and bottom conductors. When the third pole closes at 6.6 msec the voltage on that phase conductor jumps immediately to the positive peak value of the supply. Again this should have no influence on the voltages of the remaining two phases

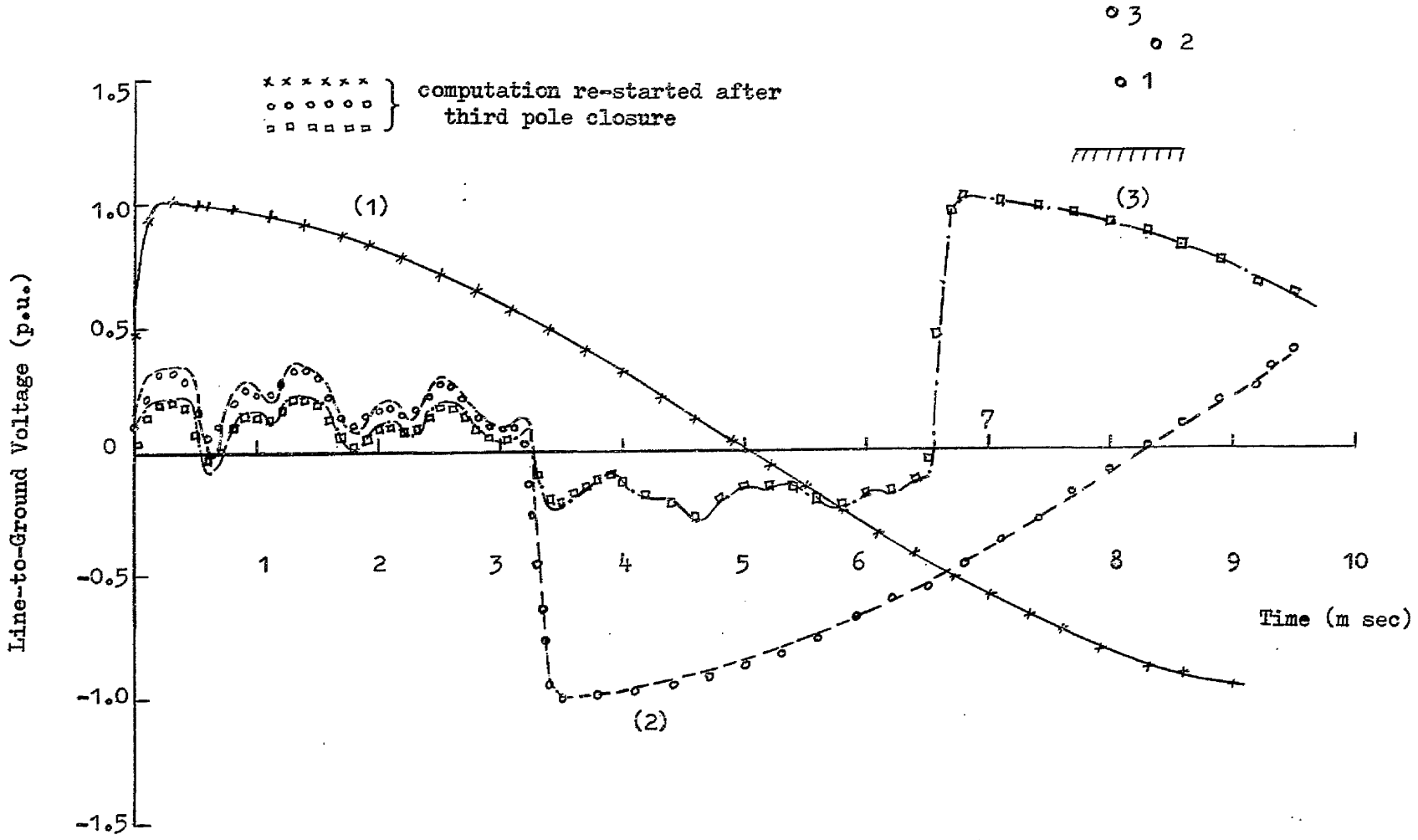

FIG. (9.14a). EFFECT OF SEQUENTIAL POLE CLOSURE ON SENDING END TRANSIENT RESPONSE OF 50-MILE LINE

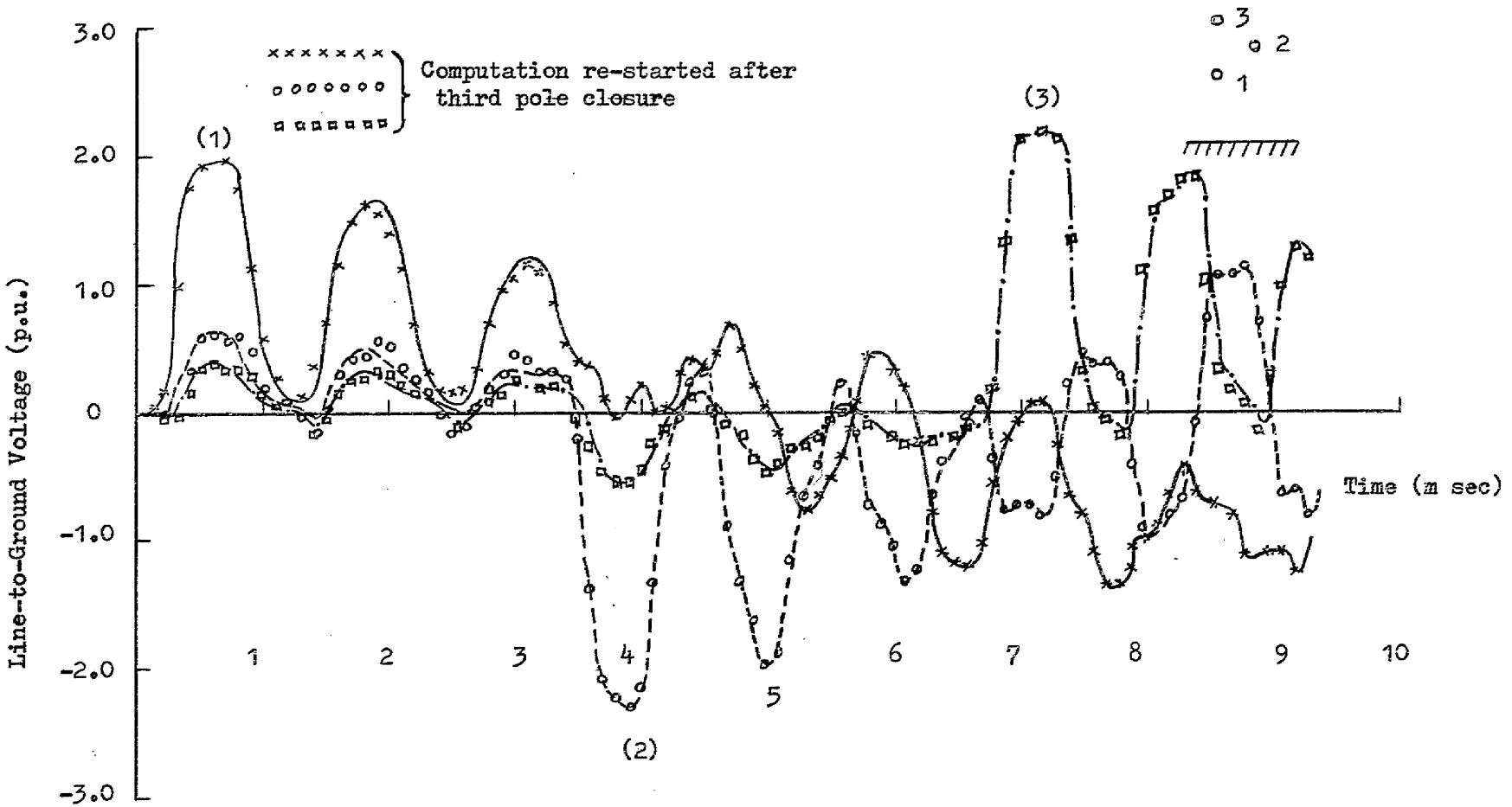

FIG. (9.14b). EFFECT OF SEQUENTIAL POLE CLOSURE ON RECEIVING END TRANSIENT RESPONSE OF 50-MILE LINE

at the sending end; this result is clear from the figure. Rise times are also apparent on the response of the second and third phase to close.

At the receiving end of the line, Fig. (9.14.b), there is near doubling effect on the first phase energised, and after the appropriate delay times on the second and third phases doubling effect also occurs there. The overvoltages on the second and third phase have maximum values of 2.3 and 2.2 p.u. of normal peak line-to-ground voltage in spite of reductions occurring due to line attenuation. This is primarily due to the fact that the voltages on these conductors at the closing instants have changed signs, and that these changes are reflected at the receiving end. The magnitude of overvoltage appearing, therefore, on the second and third phase would be dependent to a certain extent on the magnitude of the induced voltage existing on the phase conductor prior to the breaker pole closure. The arrival of the main surge at the receiving end of the line due to second pole closure is sensed by the remaining two phases and similarly for the main surge on the third phase. All transients are composed of 50 Hz component superimposed on the line natural frequency oscillations.

An additional means for checking the digital computer program used for sequential pole closure calculations and proving the validity of the results just described has been provided. First, second and third breaker poles have been closed, with the delay times mentioned above, and the computation restarted from time zero i.e. effectively

energising all poles simultaneously. The result is shown in Fig. (9.14.a) for the sending end and Fig. (9.14.b) for the receiving end. When compared with the same line response obtained in Fig. (9.14) the two results are nearly identical. In theory the two results should be truely identical; the apparent differences, however, are insignificant.

9.10 Recovery Voltage Transients Calculations

9.10.1 General

On the application of a sudden fault to a line oscillatory transients occur in a manner similar to that obtained due to line switching[73]. Studies relating to the evaluation of restriking transients across the breaker terminals or on the line side should take into consideration the transient nature of the fault current when the circuit is interrupted. It is very important in the design of circuit breakers for short line fault duty[74] to know precisely the rate of rise of the restriking transient and its magnitude for the first few natural frequency cycles following interruption.

In the following analysis interruption is assumed to take place at current zero after one-and- a half cycles of the normal system frequency from the occurrence of the fault. To simulate the breaker action the fault current is injected across the breaker terminals and the line transient response thus obtained since this fault current is produced by the steady-state voltage wavefrom then the resulting line response will give the line transient response superimposed directly on the line steady-state response.

For the transient response it is necessary to define precisely the front of the current wave just before interruption. Since the line recovery transient is often required over a very short period of time compared with the period of time between the occurrence and clearance of the fault, high frequency components of the fault current will be involved in the calculation of the restriking transients. The precise definition of this current for accurate determination of the restriking and recovery transient using this method of current injection will be described and its practical limitations pointed out before an alternative method is suggested. A digital computer program will then be given which is relevant to the case of the last pole to clear and an example of study presented.

9.10.2 Theoretical Developments

Since as mentioned the period of the restriking transients is much shorter compared with the period of fault current transient, the frequency of the fast transients may be in the range of 50 kHz. For precise calculations it is therefore essential that the high frequency components of the fault current be found before injection takes place through the switch terminals.

a. Method I

An observation period of time is chosen in the range of time for one and a half power frequency cycles. The determination of the fault current follows exactly the procedure described earlier for the first pole closure condition except that in this case the pole closes at

minimum voltage(giving the condition of maximum d.c. offset in fault current), of the sinusoidal wave form with a single line-to-earth fault on the phase under consideration, other phases are floating at the sending end,open-circuited at the receiving end. The system diagram is shown in Fig. (9.15.a). The determination of the line response is carried out at the regular intervals of time until the fault current response at the sending end of the line has passed through its third zero, detected by a change in sign. This time, after which the circuit is interrrupted, is then determined precisely. It is shown in Appendix (9.1) how this is to be determined on the assumption that the fault current varies linearly between the time interval $(n-1)t_0$ before interruption and the time interval nt_0 after interruption where n is the number of the n^{th} time step in the calculation and t_0 is such time step.

For the new observation time selected for the evaluation of the restriking voltage transients a new fundamental frequency is obtained which is different from the fundamental frequency on which the transient fault current calculations are based. The high frequency Fourier coefficients of the fault current wave up to the point of circuit interruption, third zero current, are then determined using the Fourier analytical piecewise synthesis method described in section (8.4.2). This moment in time is given in Appendix (9.1) as "T".

An important point to observe is that the piecewise synthesis method described earlier has been based on the

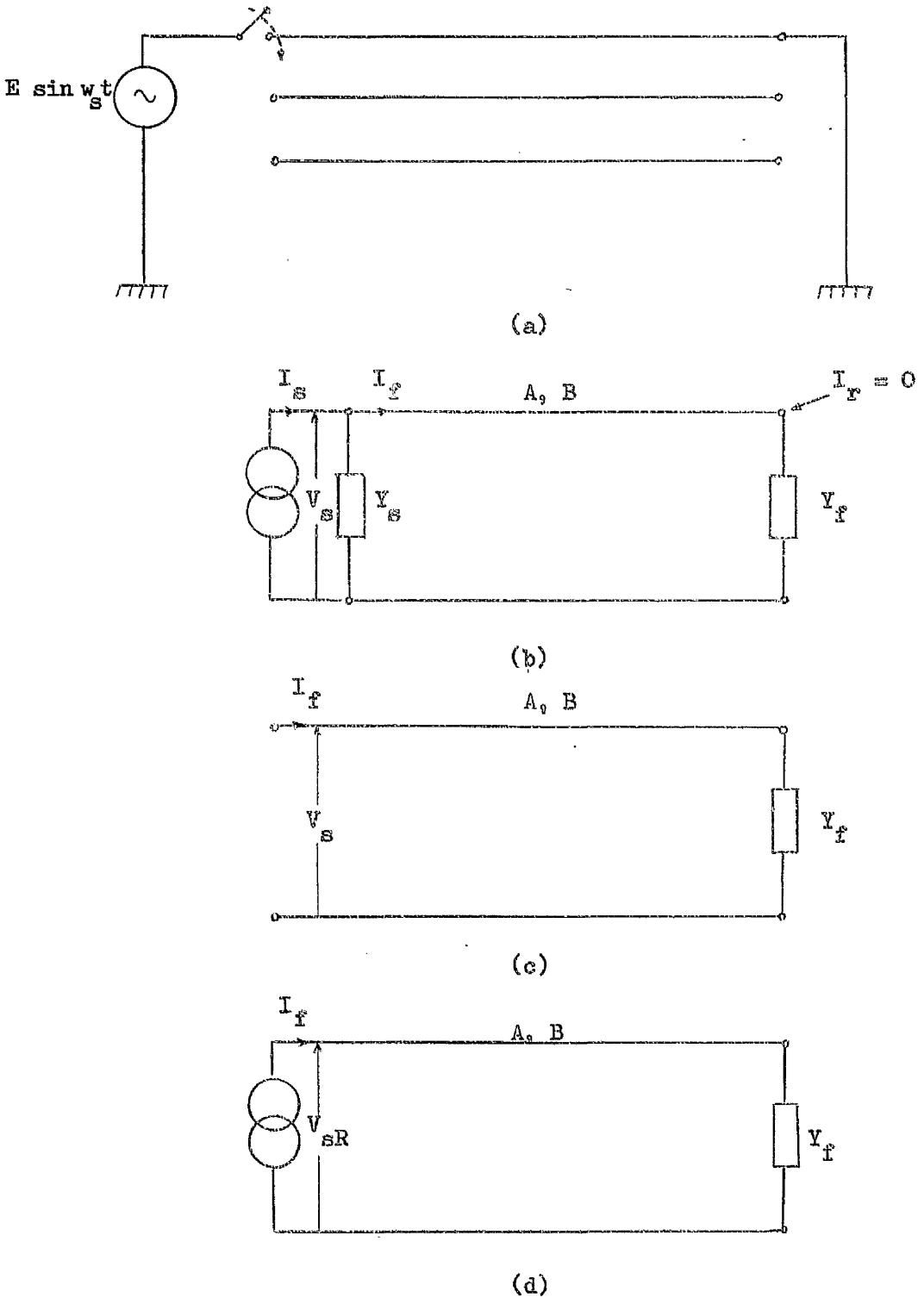

FIG. (9.15). SYSTEM DIAGRAM AND EQUIVALENT CIRCUIT MODELS FOR RESTRIKING TRANSIENTS CALCULATIONS

fact that we are dealing with linear time steps all the time. It is clear from Appendix (9.1) that a non-linear step is involved here and that account of this has to be taken and a modification made in the method described to incorporate this non-linear interval given as $[T-(n-1)t_0]$ in the appendix.

As soon as the high-frequency components have been evaluated the computation is re-started with this new current generator substituting the old voltage generator used in the earlier part of the calculation. The whole high-frequency components current wave is shifted back in time "T" seconds where its front is now on the origin of co-ordinates. This would thus involve a shift operator of a positive exponential function $\exp(j\omega T)$ being introduced. The voltage response obtained would therefore be the total recovery voltage transient appearing on the line side.

From a computational point of view, this method has failed primarily due to the positive exponential function $\exp(j\omega T)$ mentioned above. A computer exponential overflow rendered the computation impossible to obtain. Since ω is a complex frequency then $\exp(j\omega T)$ is in fact $\exp(j\omega T).\exp(aT)$. "T" is of the order of 36 msec but the shift constant "a" is based on an observation time of the order of a few hundred μsec. (dependent on the number of wave reflections required in the transient response) and effectively the product "aT" will be a large number and hence lead to an exponential overflow. This is the reason that it has not been possible to carry out numerically the method just proposed. This failure, however, has a physical meaning and it is the fact that the

back end of the displaced fault current wave has no direct bearing on the fast restriking voltage transient. An alternative method that encounters no such difficulty will now be presented.

b. Method II

The fault current response is calculated at the sending end of the short-circuited line and as time progresses a change in the sign of the fault current is recorded indicating that the current has passed through zero. When the third sign change has occurred, the time of circuit interruption is determined precisely by the method of Appendix (9.1). The calculation then commences for the evaluation the fault current response for two additional time intervals or more that would be adequate enough to cover the observation period for the restriking transient calculation. The fault current evaluated from the moment of interruption onwards (for two or more time steps) is then synthetised into its high frequency components and is injected into the faulted phase with an opposite sign to simulate current interruption by the principle of superposition.

The step, this time, between the time of interruption of the circuit "T" and the following time in the calculation "nt_0" (see Appendix (9.2)) constitutes a non-linear step and its transform must therefore be found separately and added to the general piecewise synthesis transform in order to find the overall transform of the injection current. The overall Fourier transform needed in the synthesis is given in Appendix (9.2).

The recovery voltage transients on the line-side are found by adding the steady-state component of voltage that existed before interruption to the transient component that appears across the breaker.

9.10.3 Mathematical Models

A 3-conductor system will be considered with a fault on phase 1. The admittance matrix for the representation of an infinite source is:-

$$[Y_s] = \begin{bmatrix} 10 & 0 & 0 \\ 0 & 0 & 0 \\ 0 & 0 & 0 \end{bmatrix}$$

and the fault admittance matrix Y_f is given by

$$[Y_f] = \begin{bmatrix} 10 & 0 & 0 \\ 0 & 0 & 0 \\ 0 & 0 & 0 \end{bmatrix}$$

(i) Obtain sending end voltage transform using Thévenin-Norton conversion theorem. The matrix equations with reference to Fig. (9.15.b) are

$$\begin{bmatrix} \bar{I}_s \\ 0 \end{bmatrix} = \begin{bmatrix} A+Y_s & B \\ B & A+Y_f \end{bmatrix} \cdot \begin{bmatrix} \bar{V}_s \\ \bar{V}_r \end{bmatrix}$$

from which $\bar{V}_s$ is obtained

$$\bar{V}_s = [A+Y_s - B(A+Y_f)^{-1}B]^{-1} \cdot \bar{I}_s \qquad - (9.7)$$

where $\bar{I}_s = [Y_s][\bar{e}]$

$\bar{e}$ is the transform of the supply wave of the phase energised.

(ii) Obtain fault current transform. Reference is made to Fig. (9.15.c)

$$\begin{bmatrix} \bar{I}_f \\ 0 \end{bmatrix} = \begin{bmatrix} A & B \\ B & A+Y_f \end{bmatrix} \cdot \begin{bmatrix} \bar{V}_s \\ \bar{V}_r \end{bmatrix}$$

from which $\bar{I}_f$ is obtained

$$\bar{I}_f = [A - B(A+Y_f)^{-1}B]\bar{V}_s \qquad - (9.8)$$

(iii) Obtain restriking voltage transient transform. Reference is made to Fig. (9.15.d).

$$\begin{bmatrix} \bar{I}_f \\ 0 \end{bmatrix} = \begin{bmatrix} A & B \\ B & A+Y_f \end{bmatrix} \cdot \begin{bmatrix} \bar{V}_{sR} \\ \bar{V}_r \end{bmatrix}$$

$$\bar{V}_{sR} = [A - B(A+Y_f)^{-1}B]^{-1} \cdot \bar{I}_f \qquad - (9.9)$$

Equation (9.9) is inverted by the usual methods to obtain the system response in the time domain.

9.10.4 Digital Computer Program

The flow diagram of the computer program for restriking transient voltage calculations is shown in Fig. (9.16). The line data is read and some basic calculations carried out as for all previous programs. The fundamental frequency of the longer observation time needed in determining fault current transient following the application of fault is obtained and so is the shift constant. Evaluation of line A,B constants then follows after determination of propagation properties i.e. surge impedance, propagation constants, etc. The selection of fault

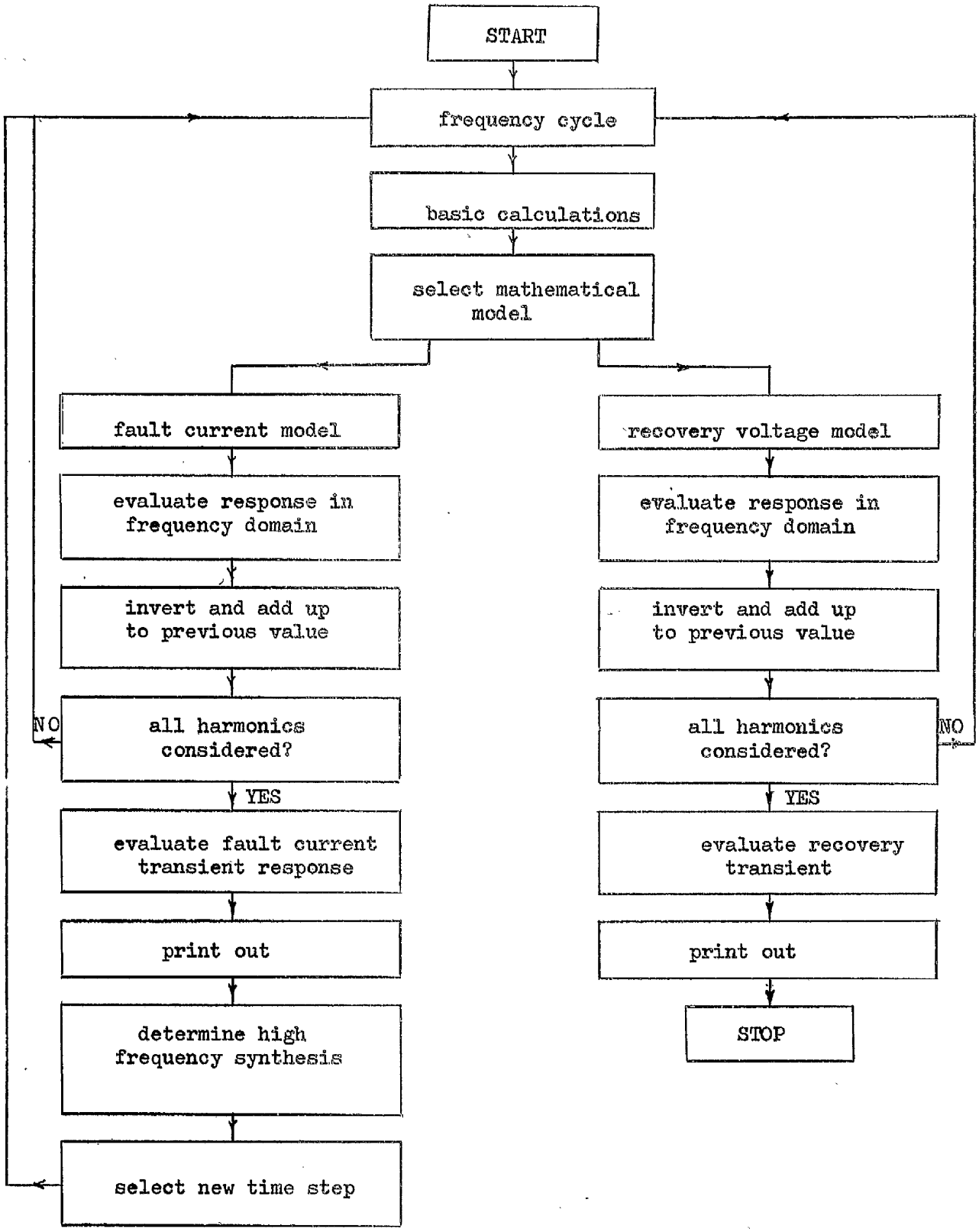

FIG. (9.16). FLOW DIAGRAM OF DIGITAL COMPUTER PROGRAM FOR RECOVERY TRANSIENTS CALCULATIONS

current mathematical model then follows to allow the calculation of the fault current transient to be made for all harmonics under consideration. Inside the high-frequency synthesis sub-routine the fault current wave-form is tested for its third zero indicated by a change in sign of two successive ordinates and when that happens the precise time of circuit interruption is calculated. Two or three additional current values are obtained for linear time steps "t_0". A new observation time for the restriking transient is chosen and both "ω_0" and "a" determined. The high frequency synthesis of the two linear steps together with the non-linear step is found. A new time interval t_0' is chosen and the calculation restarted to determine restriking transients due to circuit interruption this time selecting the model for the restriking transients calculation. When the computation is complete the result is printed out and the program comes to an end.

A small sub-routine has been included in this program to synthesise the fault current from its high frequency components and to compare this result with the result obtained in the early part of the program for the slow frequency fault transient calculations.

9.10.5 Computational Results

The vertical circuit line described in section (9.5) is chosen for this tudy. A 20 km line has been considered with the fault applied to the bottom phase only. The results are therefore valid for the case of the last pole to clear. The line is energised from a

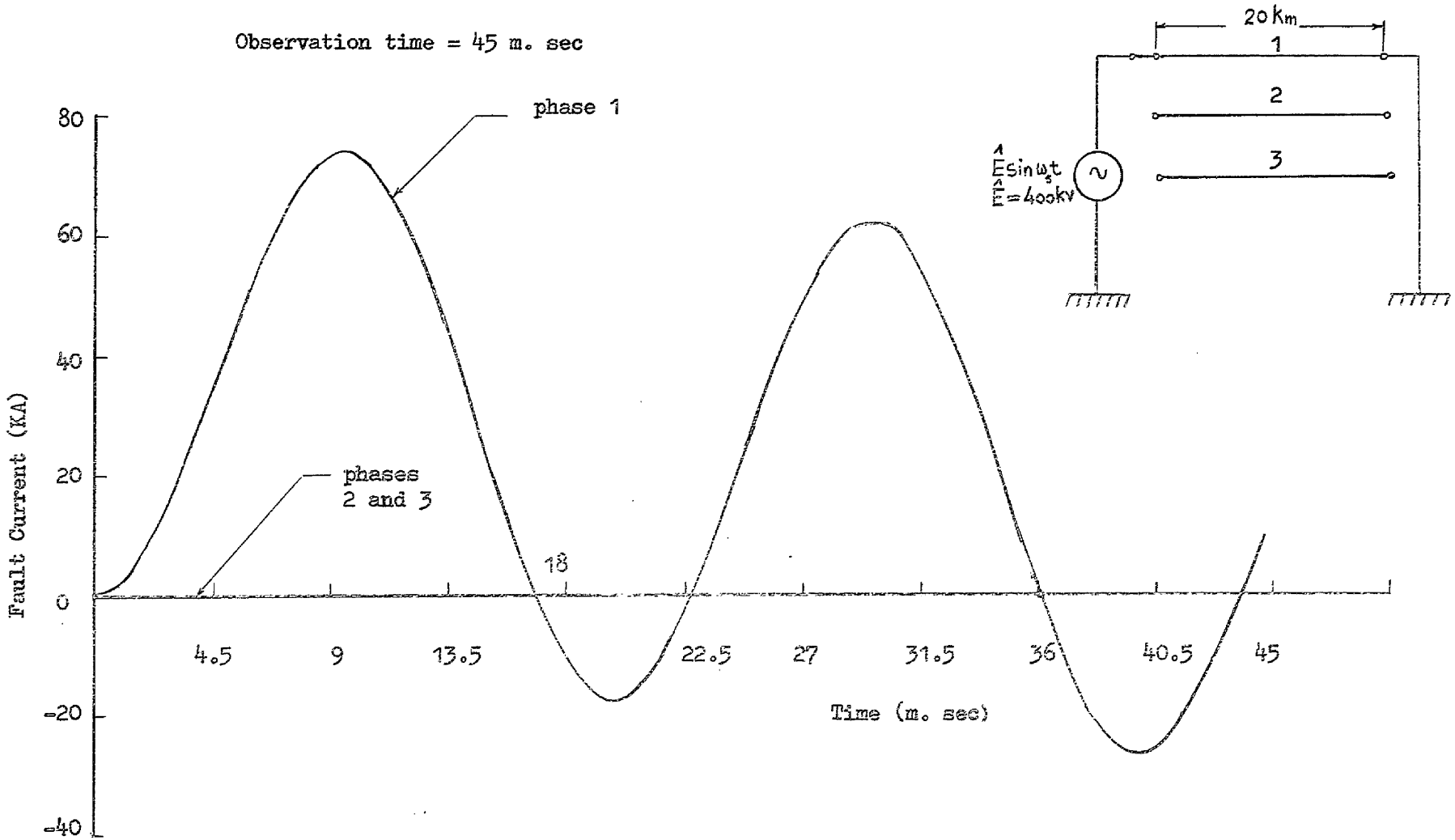

FIG. (9.17). SENDING END FAULT CURRENT TRANSIENT

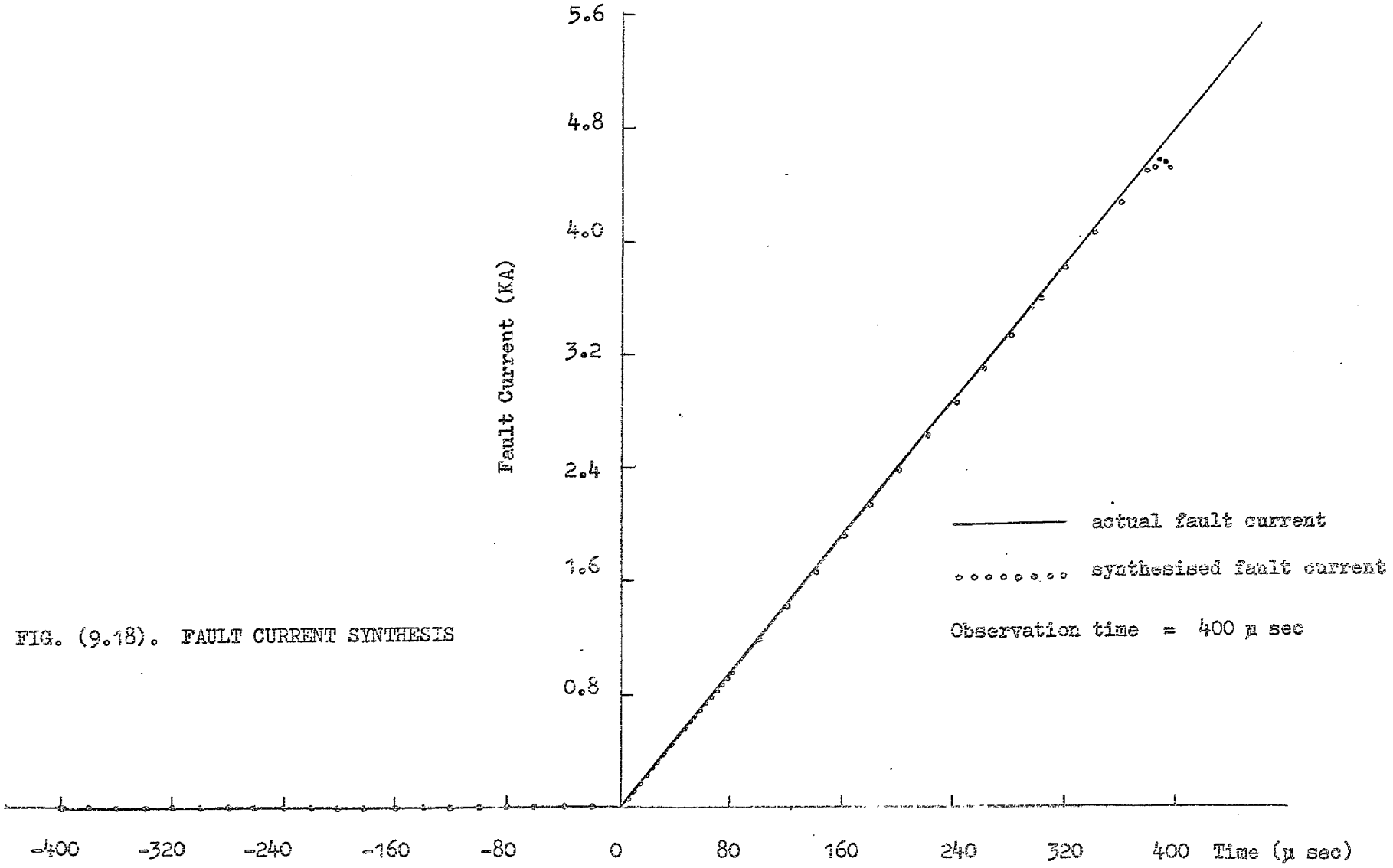

FIG. (9.18). FAULT CURRENT SYNTHESIS

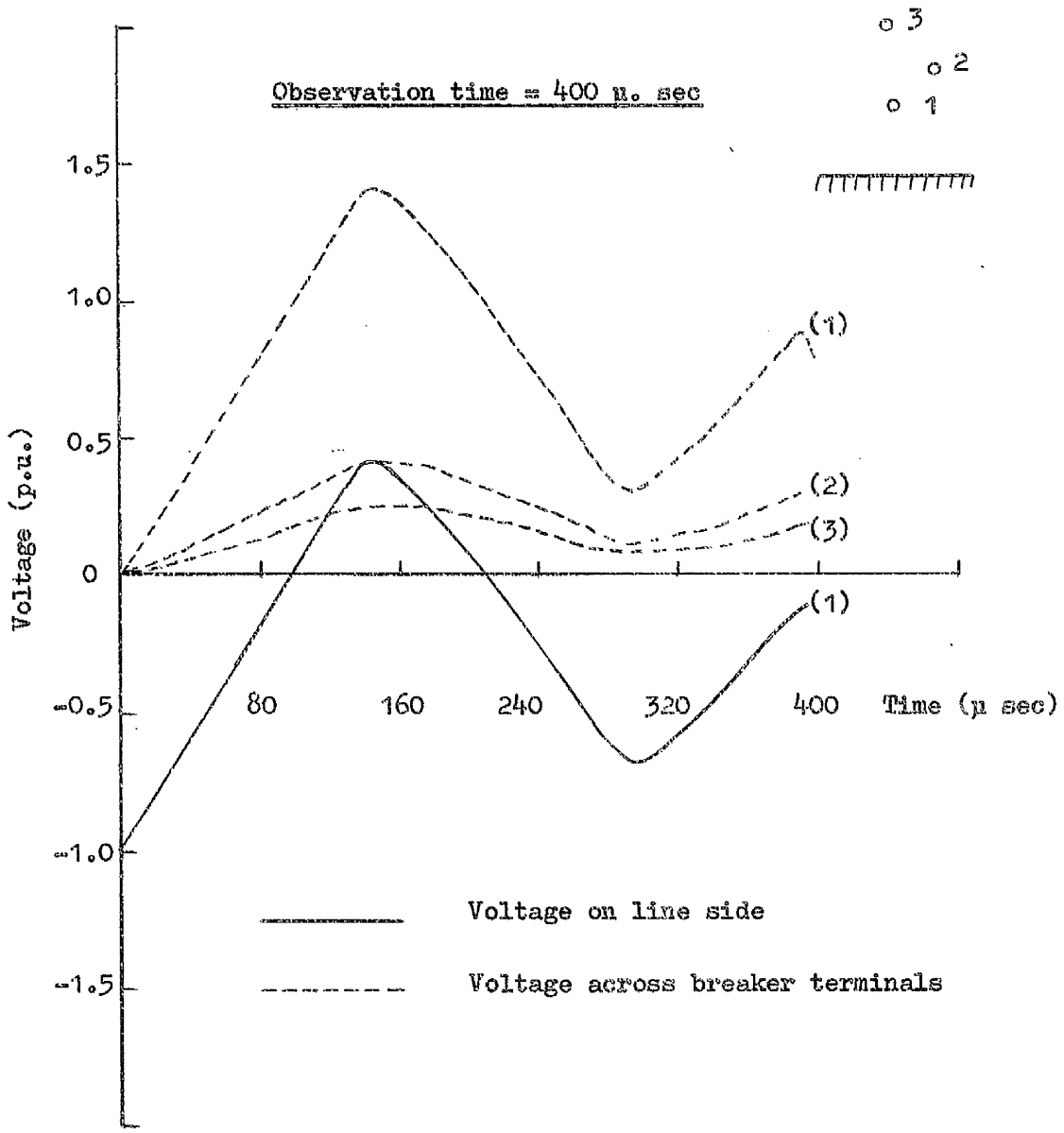

FIG. (9.19). RECOVERY VOLTAGE TRANSIENTS FOR 20 KM LINE

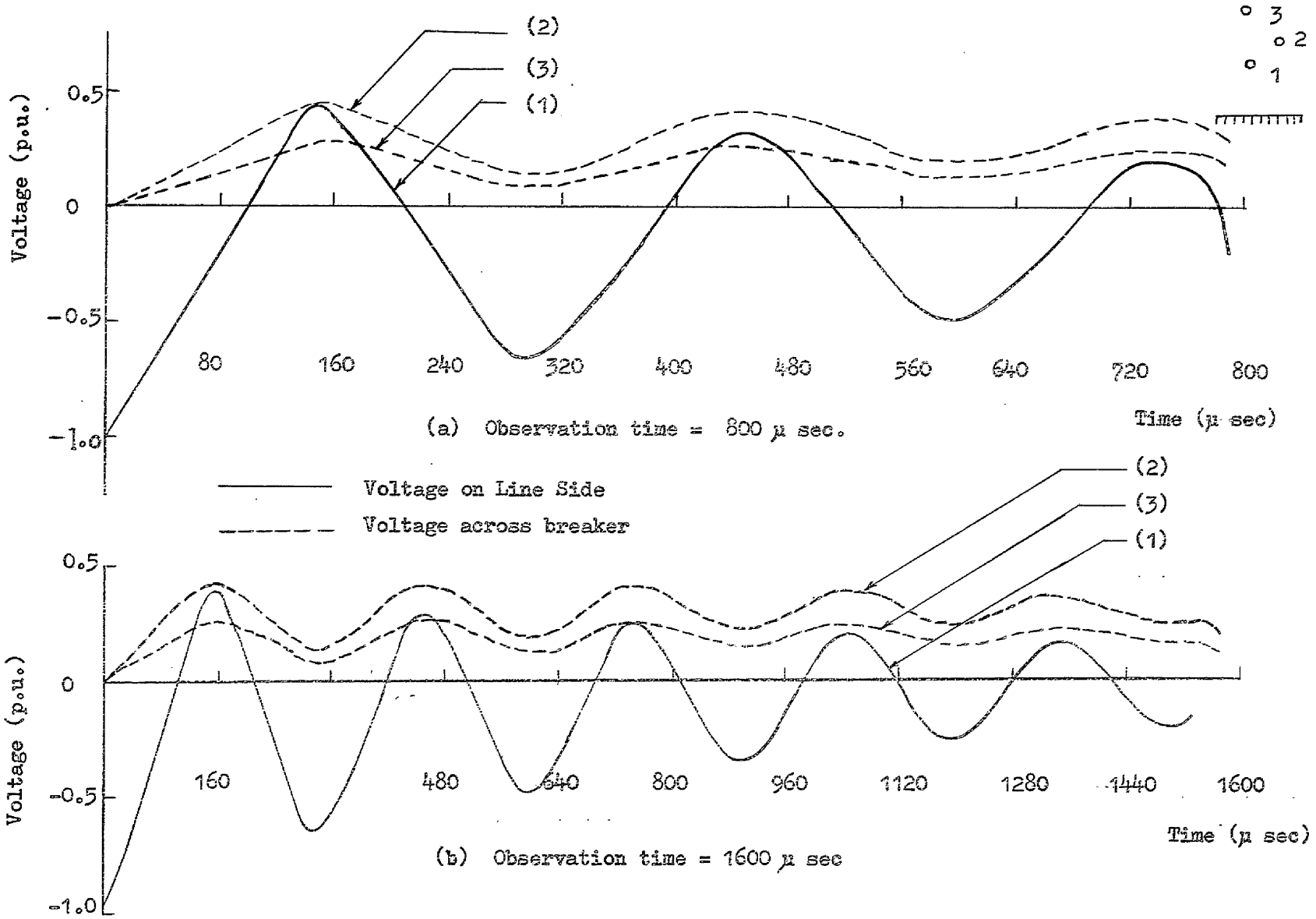

FIG. (9.20). RECOVERY VOLTAGE TRANSIENT FOR 20 KM LINE

400 KV bus and the fault current is observed for a period of 45 msec. Fig. (9.17) shows the sending end fault current in KA which turns out to be zero for the floating unfaulted conductors as is expected. The faulted phase fault current transient waveform reaches its third zero at 36 msec and with the method explained in Appendix (9.1) this time is found to be 35.99 msec indicating a very close agreement.

The computation is carried out for further steps after this time and from the high frequency Fourier components based on an observation time of 400 μsec for the restriking transient the synthesised current to be injected into the circuit to simulate circuit interruption is compared with the actual fault current. Computation has been carried out for $\pm$ 400 μsec. This serves as a good check since for $t < 0$ the synthetised current should be zero. This important result is shown in Fig. (9.18) and is a further indication of the power of the piecewise synthesis method.

The line-side recovery voltage transient is shown in Fig. (9.19) on all three phases for the 400 µsec observation period. Over longer periods of time the recovery transient is shown to die away exponentially in Fig. (9.20.a) for 800 µsec and Fig. (9.20.b) for 1600 µsec. There is also a noticeable asymmetry in the line-side recovery transient which has been observed also in field tests in this class of problem.

CHAPTER TEN

SOURCE SIMULATION

10.1 Introduction

The complexity of the source-side network terminating onto a bus from which a transmission line is energised has been recognized. This mainly is due to the fact that in general this source is not a localized generation source whose effective reactance can be derived from its short circuit MVA and the system voltage. Terminating at the bus-bar may be other transmission lines originating at some remote point in the network and these remote points may in turn be fed from other generating points. There is thus in fact no limit to the extent of such detailed source arrangement. In dealing with transient switching voltages the source side plays a very important role in the shape of the waveform and magnitudes of the transient and it is therefore rather important that source-side representation be considered very carefully when dealing with switching problems.

It is often not required to represent the entire network source configuration as from computation points of view this may not be economic. Sometimes it is not even necessary to consider the entire source side network as transit times to the distant points of such networks and back may exceed the observation time chosen for the problem and hence would be of no direct relevance to the study.

In this chapter some aspects of source side representation will be considered and the effect of source

side on transient voltages will be discussed with particular reference to first pole closure problems and sequential energisation problems.

The analysis presented earlier for sequential pole closure will be extended here to cover lines with precharge and a comparative study in this respect with results[75] obtained from a method using Bewley lattice diagram technique will be shown.

10.2 Method of Analysis

10.2.1 Simulation of Pole Closure

If the equivalent circuit of two general networks on either side of a switching station has been considered then before pole closure let there exist a voltage $V_{s\ell}$ on the line side of the breaker and a voltage V_{ss} on the source side of the breaker. Both $V_{s\ell}$ and V_{ss} arecolumn vectors whose elements represent the voltages of various phases to earth. Fig. (10.1.a) shows a hypothetical system and Fig. (10.1.b) is a schematic form of its equivalent. Before any of the breaker poles close the voltage existing across the switch terminals will be the difference between the two voltages on the line side and the source side. This is given as v below

$$v = V_{s\ell} - V_{ss}$$

To simulate switch closure it is necessary to inject across the breaker terminals a voltage -v in the manner shown in Fig. (10.1.b) so that the resultant voltage across the switch is zero indicating that the switch has been closed. To determine the voltage on the line side and on the source side

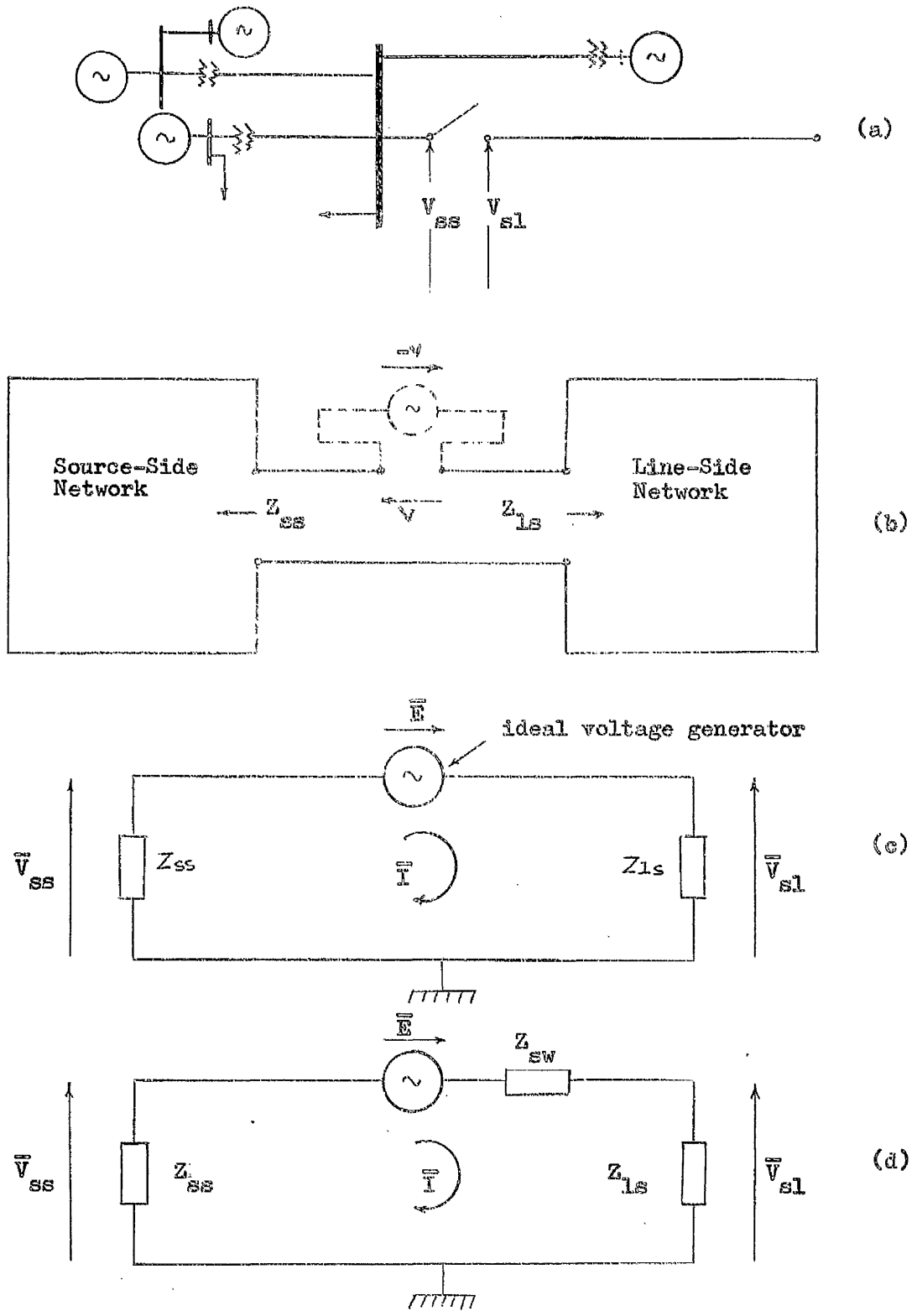

FIG. (10.1). SIMULATION OF SWITCH CLOSURE OF A POWER SYSTEM NETWORK

owing to switch closure let $Z_{\ell s}$ and Z_{ss} be the input impedance matrixes of the line side and source side networks viewed from the switching station location. Using the same notation as before for the line side and source side voltages and Fig. (10.1.c) the network equations will now be written.

Let $\bar{E}$ = the transform of the injected voltage across the switch terminals

$\bar{I}$ = the transform of the current flowing round the circuit

By Kirchoff's current law $\bar{I}$ can be determined

$$\bar{I} = (Z_{ss}+Z_{\ell s})^{-1}.\bar{E}$$

The flow of $\bar{I}$ causes a positive voltage drop with respect to earth on the line side and a negative voltage drop also with respect to earth on the source side.

$$\therefore \quad \bar{V}_{s\ell} = Z_{\ell s}(Z_{ss}+Z_{\ell s})^{-1}.\bar{E} \qquad - (10.1)$$

$$\bar{V}_{ss} = -Z_{ss}(Z_{ss}+Z_{\ell s})^{-1}.\bar{E} \qquad - (10.2)$$

Equations (10.1) and (10.2) provide the Fourier voltage transforms on the line and source sides which when inverted will give the transient response on either side of the breaker. The response of the system at other points in the network can be derived from equations (10.1) and (10.2) and the properties of the network. For example to find the receiving end voltage transient for the open-circuit transmission line shown in Fig. (10.1.a) the transform

of the input voltage is $\bar{V}_{s\ell}$, this voltage with the line A, B constants will be sufficient to determine the receiving end transform $\bar{V}_{r\ell}$ which when inverted will give the line response there.

In the example just considered the poles of the circuit breaker are considered to close simultaneously. The derivation is also valid for the case of single phase equivalent system in which only one pole exists and thus the equations simulate this, the matrixes now change into simple elements. When multiconductor lines and non-simultaneous pole closure is considered it is important that simulation of switching conditions should cover the fact that certain poles close while others do not, or the fact that poles close sequentially. This, however, is not a problem since at the switching station an impedance matrix can be introduced with all off-diagonal elements set to zero ohms and diagonal elements either zero ohms for breaker poles that are closed or 10^6 ohms which is sufficient to simulate poles that are still open. For first pole closure only of a three-phase system this impedance matrix is given below:-

$$Z_{sw} = \begin{array}{|c|c|c|} \hline 0 & 0 & 0 \\ \hline 0 & 10^6 & 0 \\ \hline 0 & 0 & 10^6 \\ \hline \end{array}$$

Equations (10.1) and (10.2) will therefore be modified by Z_{sw} now introduced in Fig. (10.1.d).

$$\bar{V}_{s\ell} = Z_{\ell s}(Z_{ss} + Z_{sw} + Z_{\ell s})^{-1}.\bar{E} \quad - (10.3)$$

$$\bar{V}_{ss} = -Z_{ss}(Z_{ss} + Z_{sw} + Z_{\ell s})^{-1}.\bar{E} \quad - (10.4)$$

When the second pole closes the appropriate diagonal element in the matrix Z'_{sw} is changed to zero and similarly also when the third pole closes; Z_{sw} will have all zero elements and equations (10.3) and (10.4) reduce to equations (10.1) and (10.2). The input impedances $Z_{\ell s}$ and Z_{ss} are obtained when all sources of the network except the energising one are short-circuited. Then by the principle of superposition the total system response is the sum of the steady-state response prior to circuit energisation plus the transient response obtained as a result of system energisation.

If an open-circuited line is considered then the steady-state voltage is zero for $t<0$ and the line total response will be the transient response only. On the source side and since for $t<0$ there a steady state voltage already exists, the total source side response will be the sum of this steady state voltage and the source side transient response.

10.2.2. Source Representation by Lumped Parameters

The source can be represented by lumped parameters, a lumped inductance to represent the short-circuit MVA of the source at the switching station and a lumped capacitance to represent any stray capacitance at the bus-bar to earth plus capacitance of voltage transformers for metering or relaying purposes. Such form of representation is shown in Fig. (10.2.a). For a 400 KV system the typical values of short-circuit MVA and bus-bar capacitance are 25,000 MVA and 2000 pf. The source inductance

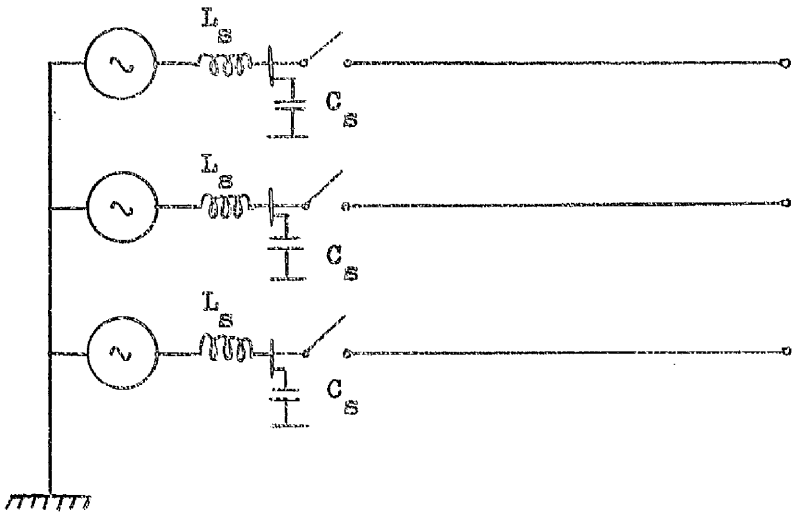

(a)

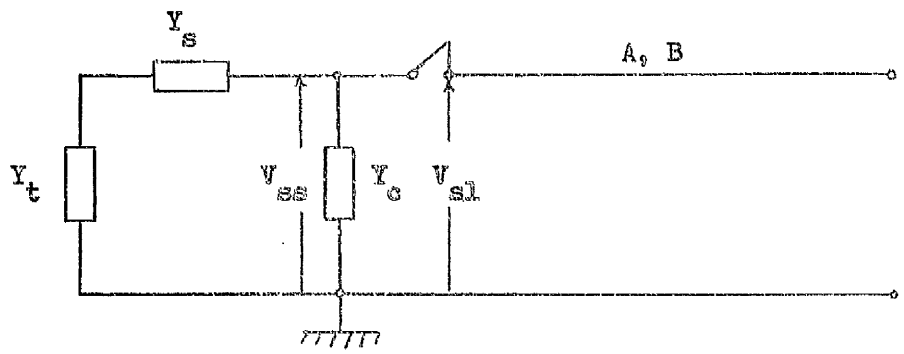

(b)

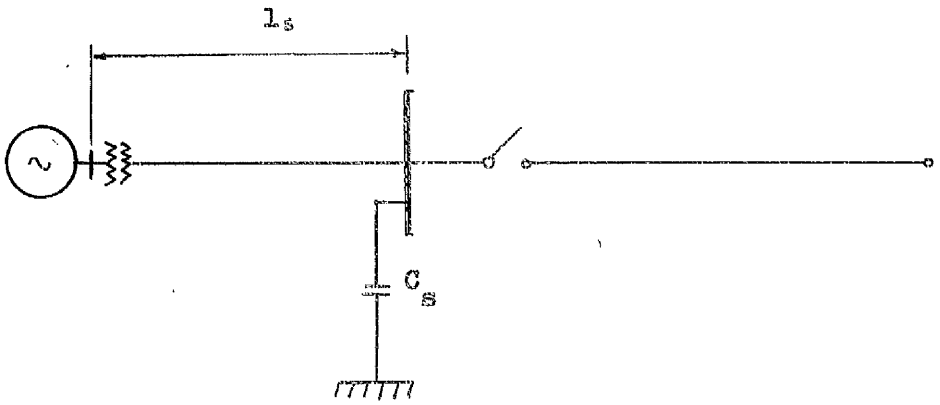

(c)

FIG. (10.2). SOURCE-SIDE REPRESENTATION

L_s is derived from

$$L_s = KV^2/(MVA \times \omega_s)$$

where ω_s is the angular frequency of the supply.

Using nodal analysis the equivalent source side admittance is found from the equivalent circuit of Fig.(10.2.b). Here the source is short-circuited by the terminal admittance matrix Y_t, where

$$Y_t = \begin{bmatrix} x & 0 & 0 \\ 0 & x & 0 \\ 0 & 0 & x \end{bmatrix} \quad ; \; x > 10 \text{ mhos}$$

The input admittance matrix on the source side is

$$Y_{ss} = [Y_c + Y_s - Y_s(Y_s + Y_t)^{-1} Y_s]^{-1}$$

and on the line side assuming A, B constants and an open-circuited line at its receiving end

$$Y_s = [A - BA^{-1}B]^{-1}$$

Since mutual effects are not represented then there will be no transient voltages induced on the unenergised conductors on the source side due to first pole closure. Due to coupling effects on the line side the unenergised phase conductors will acquire voltages in the usual manner. The piecewise transform of this voltage appearing across the breaker second pole is added on to the analytical transform of the injection voltage simulating the second pole closure.

In a similar manner the closure of the thirdbreaker pole is effected by adding on to the analytical injection transform of the voltage across the breaker the piecewise voltage transform of the induction transient voltage on the line side from the instant of first pole closure.

This form of source simulation assumes that the whole generation is localized at the switching station and ignores the fact that certain feeders are connected to the switching station bus-bar.

10.2.3 Source Representation by Distributed Parameter Networks

In practice several infeeds may terminate at the switching station bus-bar to which a transmission line has been connected. The equivalent source side input impedance would be made from a contribution of input impedances of all such infeeds. The infeed can be represented as a distributed parameter network and thus treated in exactly the same manner as the main circuit energised with its A, B constants derived from its propagation properties. At the end remote from the switching station the infeed may have a localized source of generation and this can be taken into consideration in the analysis by assuming a lumped parameter representation there, and the equivalent source impedance obtained from the short-circuit MVA and KV of the local station. Transformers can be represented by their equivalent circuits and again as lumped parameter networks, their leakage inductance can be added to the localized source inductance. The capacitance at the bus-bar can also be represented as discussed in section (10.2.2).

Though quite possible, the exact representation of the source infeed circuit - and there may be several infeeds - will be carried out at the expense of high costs in computation. This is not generally advisable from a practical point of view. Two forms of simplifications will now be presented which strike a good balance between economies in computation time and accuracy of source representation. In fact as will be illustrated later in studies carried out, the simplified nature of one of them is more attractive to choose since it has been found adequate enough for accurate source side simulation with one or more infeeds.

10.2.3.1 Simplified Representation

Assume one source infeed of length ℓ supplied from an infinite source and terminating at the switching station bus-bar shown in Fig. (10.2.c). In this simplification it also will be assumed that there is no coupling between the conductors of the infeed and that ground and conductor losses are ignored.

With a short-circuit at the generation point the input source-side admittance matrix at the switching station is obtained from the two-port current equations

$$Y_{ss} = Y_0 \coth \psi \ell_s$$

and ignoring ground and conductor losses

$$Y_{ss} = \begin{bmatrix} -j\, Y_{01}\cot(\omega \ell_s/c_0) & 0 & 0 \\ 0 & -j\, Y_{02}\cot(\omega \ell_s/c_0) & 0 \\ 0 & 0 & -j Y_{03}\cot(\omega \ell_s/c_0) \end{bmatrix}$$

where

$c_0 = 3\times10^8$ m/sec, velocity of light

$\omega = 2\pi f$

f = complex frequency used in transient calculations

ℓ_s = length of source infeed

Y_0 = characteristic admittance of conductor

$= 1/\sqrt{L/C}$ where L and C are the line constants

For a single conductor of radius r meters and mean height above perfect ground the line characteristic admittance is given by

$$Y_0 = 1/60 \log_e(2h/r)$$

To the source admittance Y_{ss} is added the capacitive admittance Y_c of the switching station bus-bar to give the total source side admittance or impedance matrixes. Though the source side infeed is fed from an infinite source the effect of the source inductance of a source of finite capacity can be easily included.

If the line is short the input impedance of a short-circuit lossless line is given by

$$\begin{aligned} Z_{s/c} &= Z_0 \tanh\gamma\ell \\ &\simeq Z_0\gamma\ell \text{ for small values of } \gamma\ell \\ &\simeq j\, Z_0\omega\ell/c_0 \simeq j\sqrt{L/C}.\omega\ell.\sqrt{LC} \simeq j\omega(L\ell) \end{aligned}$$

and the line appears effectively as a lumped inductance. As a matter of fact for short lengths of infeed the lumped parameter representation can easily be arrived at.

With this method the effect of several infeeds terminating at the switching station can also be considered. The total input admittance will be the summation of the individual infeeds input admittances.

The limitation of this form of representation stems from the fact that the effect of the different modes of propagation on the source side transient is not realizable since only one mode of propagation, namely positive sequence mode has been considered. It would appear that the results obtained from such type of representation are not truly representative of the actual source behaviour. To overcome this difficulty it is possible by the method of the following section to produce source side representation which takes into account the effect of different modes of propagation.

10.2.3.2 Representation by Symmetrical Circuit

In general the properties of the two aerial modes of propagation are not very different. The earth mode, however, has very different characteristics from the aerial modes. When making the assumption that the three-phase line is symmetrical the two aerial modes are made equal and as a result only slight errors may occur as a result of this approximation. The existence of the earth mode is still recognized by this assumption and this is important due to its different properties. By assuming a symmetrical circuit arrangement it is possible to obtain an analytical solution of the system characteristic equation and thus achieve savings in computation time due to numerical evaluation of the eigenvalues and eigenvectors of an otherwise non-

symmetrical circuit line. It is shown in Appendix (10) how the symmetrical circuit eigenvalues may be obtained. Having determined these and using one possible form of eigenvector matrix for the horizontal line as indicated in Appendix (10), the line A, B constants are readily obtained. The input impedance of the source side can then easily be determined.

If there are N such infeeds terminating at the switching station the total input admittance matrix on the source side is found by summing individual source infeed admittance matrixes and then adding to the sum total any capacitive admittance at the bus-bar of the switching station, thus

$$Y_{ss_{TOTAL}} = \sum_{n=1}^{N} [A_s - B_s(A_s+Y_t)^{-1}B_s] + j\,\omega\,C_s$$

A_s, B_s --- symmetrical system constants

Y_t --- is a diagonal matrix defined earlier.

When the first phase is energised owing to the coupling between phases on the source side terminals with this form of representation, transient voltages will be induced on the unenergised phases on the source side as well as on the line side. The voltage existing across the breaker pole from the moment of first pole closure will be the difference between the line side and source side transients. The transform of this voltage is added to the analytical transform of voltage injected across the switch

to simulate its closure; this is repeated when the third phase is energised.

10.2.4 Procedure for Calculation of Sequential Transients with Precharge

The calculation of transient voltages when the circuit breaker poles close on trapped charges on the line side is carried out in the following manner.

Let Ed_1, Ed_2 and Ed_3 be the trapped charges on the line side of a three-phase system and assume that there is no leakage path to ground. The system diagram is shown in Fig. (10.3).

Let v_1, v_2 and v_3 be the steady state voltages on the source side and $\bar{V}_1$, $\bar{V}_2$ and $\bar{V}_3$ be their transforms.

The voltage appearing across pole 1 before its closure is $Ed_1 - v_1$. Therefore $v_1 - Ed_1$ will be injected across the pole to simulate its closure.

Using Fourier transform method the voltage waveform $(\bar{V}_1 - Ed_1/j\omega)$ is injected across pole 1 and the system response then calculated. The total response on the line side will be the sum of the transient response due to the injection voltage plus the trapped charge voltage Ed_1 at all points on the line. On the source side the total response is the sum of the transient response plus the steady-state response v_1.

The induced transient voltage on the second and third phases is found. If mutual effects on the source side are not ignored then the transform of the voltage difference i.e.

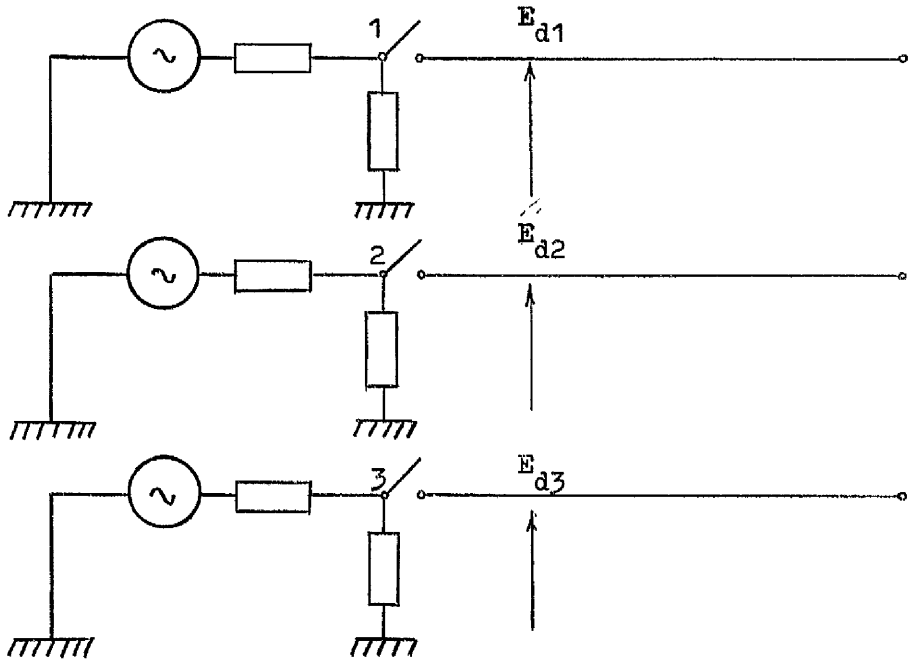

FIG. (10.3). SYSTEM DIAGRAM FOR SEQUENTIAL TRANSIENTS WITH PRECHARGE

induced voltage on the line side minus voltage on the source side is found using the synthesis method and this is added on to ($\bar{V}_2 - Ed_2/j\omega$) and injected across the second pole at the time of its closure. If there is no coupling among the source side phases then the voltage on the source side of the second phase automatically drops out. The transient response of the system is then evaluated and the total line side response is found from the sum of the transient response plus Ed_2. On the source side the total response is the transient component plus the steady state voltage v_2. Similarly the calculation is carried out due to third pole closure.

The terms ($\bar{V}_2 - Ed_2/j\omega$) for the second pole and ($\bar{V}_3 - Ed_3/j\omega$) for the third indirectly imply that these are modified by the shift-operator $\exp(-j\omega T)$ where $T = T_2$ and T_3 are the delay times for the second and third pole closures.

10.3 Description of Digital Computer Program

A flow diagram of a general computer program catering for source effects and perhaps line trapped charges is shown in Fig. (10.4) for non-simultaneous energisation of a three-phase system. The first part of the program is similar to most previous programs described earlier and deals with reading in the data of the line under consideration and performs some basic calculations needed in the problems. This is followed by a frequency cycle and calculation of eigenvalues, eigenvectors, surge impedance and admittance matrixes with the ultimate formation of the A, B constants of the main line to be energised all calculated at the particular frequency harmonic chosen. Then follows the setting of the first pole

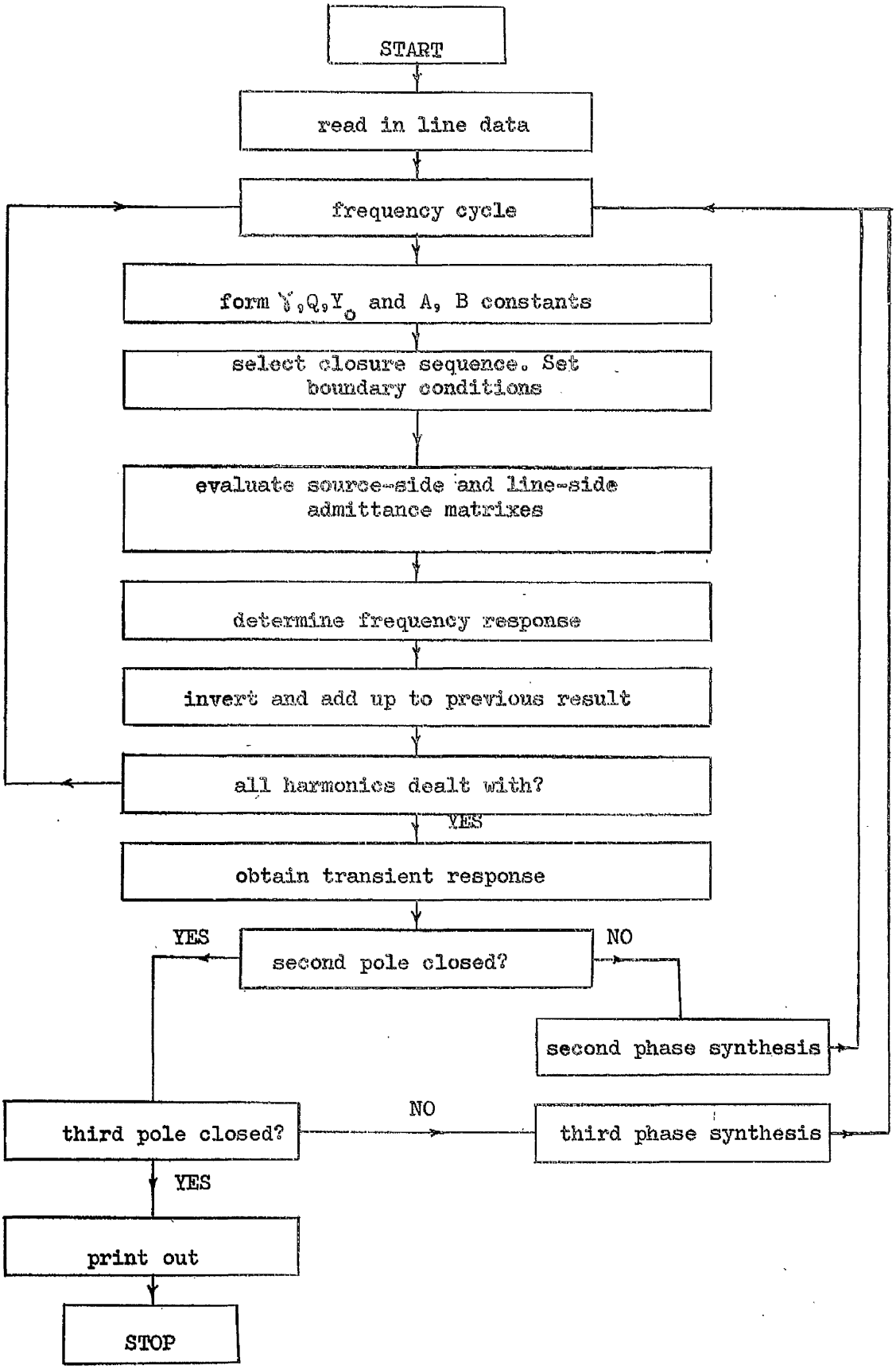

FIG. (10.4). FLOW DIAGRAM OF DIGITAL COMPUTER PROGRAM FOR SEQUENTIAL TRANSIENTS WITH SOURCE SIMULATION

closure conditions and if any trapped charges exist on the line prior to this phase closure these are taken into consideration, the switching station impedance matrix is included to describe the state of energised phases.

The input admittance or impedance matrixes on the source and line sides are then evaluated. These may take any of the various forms explained for source simulation and include any lumped capacitance at the switching station bus-bar. The computation proceeds and the line response due to first pole closure is determined adding the trapped charge voltage on to the line side transient response and the steady-state voltage on to the source side response for the overall system response. The Fourier coefficients of voltage appearing across the second pole are obtained using the synthesis sub-routine and added on to the analytical transform of the second phase, computation re-started and system response likewise determined. The program tests for third pole closure and when all poles have closed the final result is printed out.

10.4 Computational Results

Computational results presented in the following sections include system response due to first pole energisation only with different types of source side representation and sequential transients calculations with precharge and typical source side infeeds. The system configuration used for the main transmission line is the vertical circuit described in section(9.5) and the source side conductors have the same mean height above ground and the same equivalent radii as the main line energised.

10.4.1 First Pole Closure Transients

10.4.1.1 Simplified Source Representation

Fig. (10.5.a) shows the Bewley lattice diagram for the calculation of transient response of a lossless system. The system consists of one source infeed connected to a switching station from which an open-circuited transmission line is energised. The total source side response and the line side response at sending and receiving ends have been obtained and are shown in Fig. (10.5.b) for a step function input. In this calculation and for simplicity the line side and source side surge impedances are taken as equal and the response pattern obtained is classical.

Figs. (10.6.a) and (10.6.b) show the line side and source side response for a period of 2 msec of a vertical line 120 miles long energised at sinusoidal voltage peak from a switching station to which a 13.3-mile infeed has been connected for bottom conductor energisation. Mutual effects on the source side have been ignored and calculations have been carried out according to the methods described here. For comparitive purposes the results of the simplified model obtained using the Bewley lattice technique are included in the results of Fig. (10.6). It can be seen that the general trend of behaviour is similar in form for both types of approach though the results are not necessarily identical.

The closure of the breaker pole is followed by a dip in the magnitude of the transient on the source side and a sudden rise of voltage on the sending end line side, both of which depend on the relative surge impedances on source and

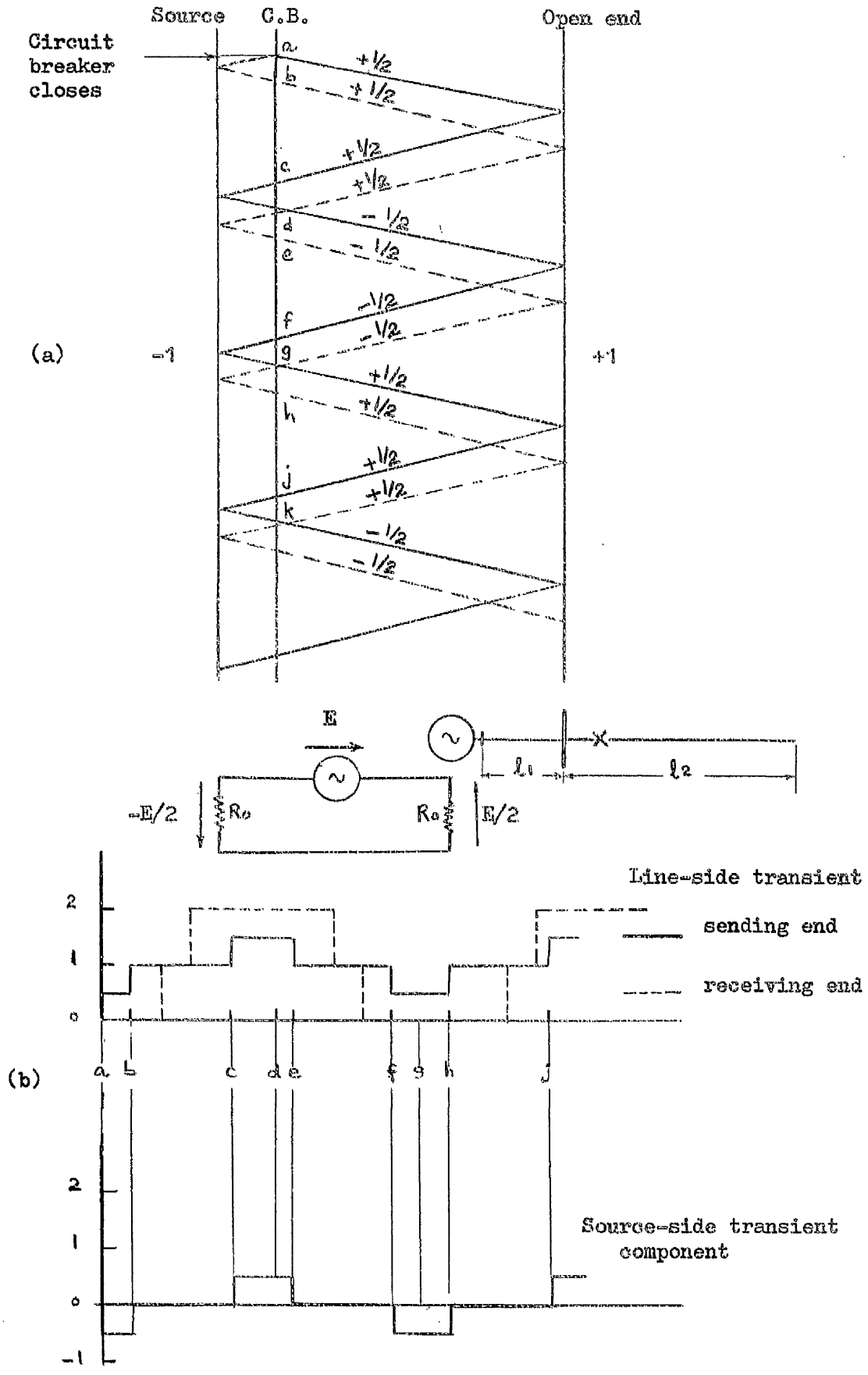

FIG. (10.5). LINE AND SOURCE-SIDE TRANSIENTS BY BEWLEY LATTICE METHOD

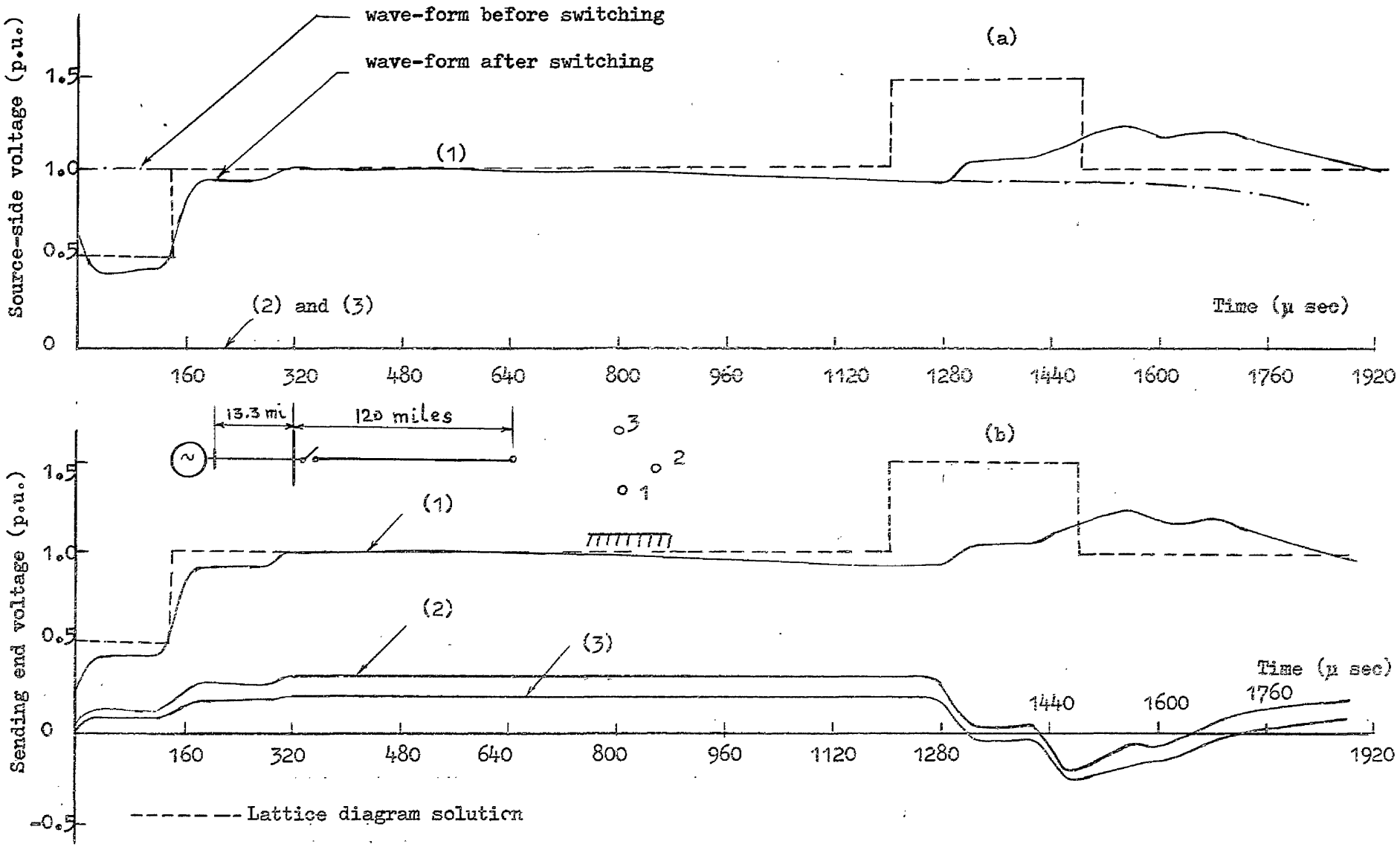

FIG. (10.6). SOURCE-SIDE AND SENDING END TRANSIENTS FOR SINGLE CIRCUIT 120-MILE WITH ONE SOURCE INFEED

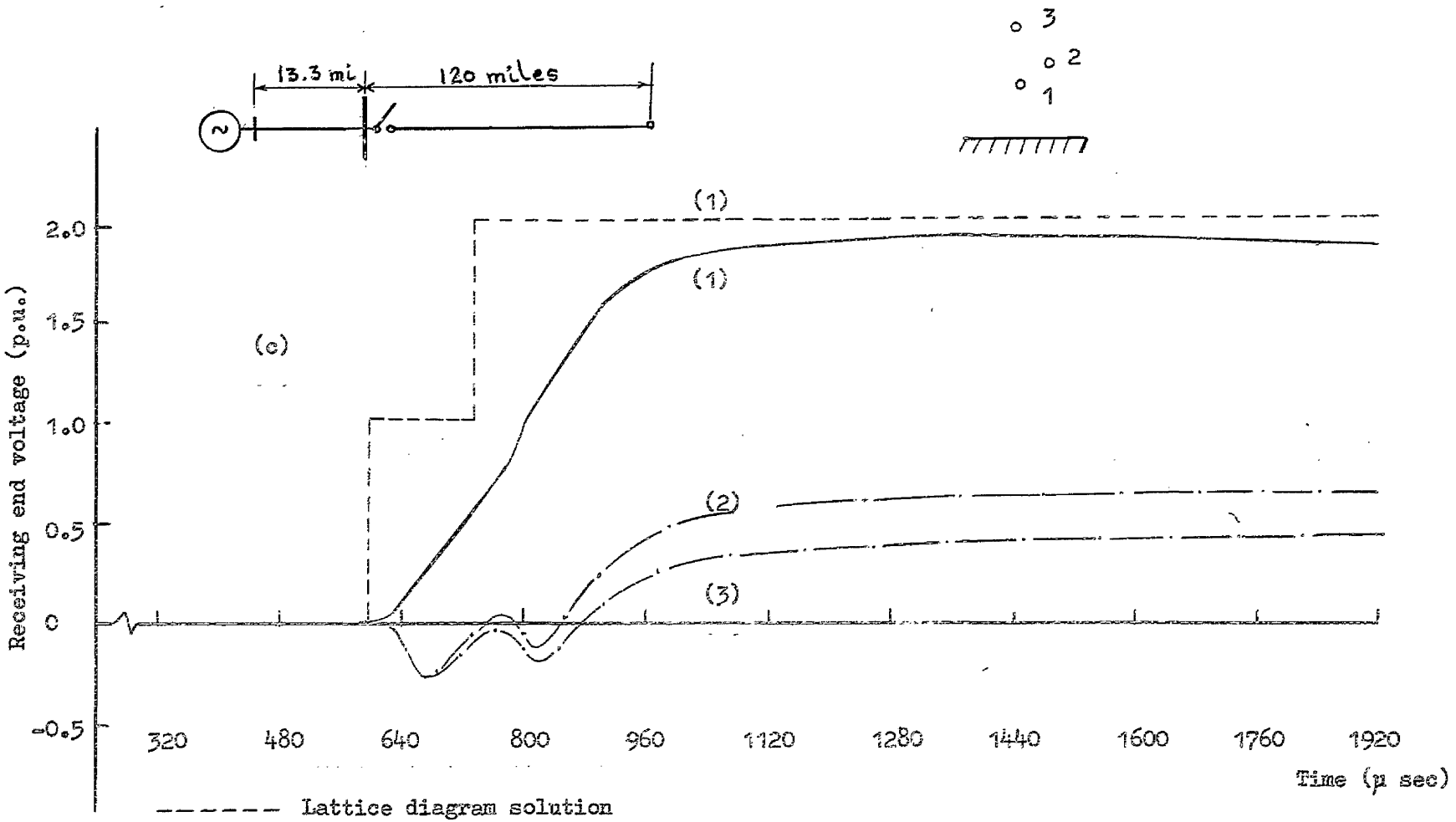

FIG. (10.6). RECEIVING END TRANSIENTS FOR SINGLE CIRCUIT 120-MILE LINE WITH ONE SOURCE INFEED

line sides of the conductor energised and for the system considered these are nearly equal and of magnitudes 351 ohms and 344 ohms for line side and source side respectively. These figures explain the identicality of the dip and rise at time zero. As soon as the pole closes the voltages on both sides of the breaker are equal and this is confirmed from the result. At twice the delay time of the source infeed circuit the arrival of the aerial waves from that short-circuited end causes the voltage at the breaker terminal to jump to the full voltage of the supply though in a gradual manner as opposed to the steep rise indicated by the response of the Bewley lattice method. This is due to the modification of the earth mode.

The voltage then stays constant with a slight drooping characteristic due to sinusoidal input wave until the arrival of the main surge from the open-circuited end of the energised line. At the breaker point the voltage starts rising again, this is mainly due to the fact that the source appears primarily as an inductance. It takes some time for the current to flow through an inductance and therefore this appears momentarily as an open circuit and hence the voltage rise. As time passes the inductance permits current flow and hence acts as short circuit and the voltage starts to decrease settling down to the voltage at the switching point.

Though not quite noticeable as with the Bewley lattice method mainly due to earth distortion effect, the main line receiving end transient response shows the conventional doubling effect, the difference being due to line attenuation.

This is brought about in two stages. First due to the arrival of the surge travelling down the main circuit followed later in time by the subsidiary surge which is being reflected from the short-circuited end of the source side circuit. Delayed times based on the velocity of light check reasonably well from these figures.

On the line side at both sending and receiving ends induced transient voltages appear on the coupled phases with an initial step rise at the sending end as expected. The double-kick of the induced transient is probably due to the effect of modal interaction resulting from the main and secondary surges of the source. The voltage response of the unenergised phases has also been computed in the program and the result has no transient component induced on those phases. This is a confirmation of the fact that coupling between conductors in this form of representation has been ignored.

A further example to illustrate the transient response calculation for bottom conductor energisation of overhead lines with this form of source representation is demonstrated in Fig. (10.7) which gives the transient response when the source side circuit is represented by a simplified three phase cable system with 20 ohm surge impedance. The response pattern obtained bears a close similarity to the result obtained from a Bewley lattice calculation which has been provided for purposes of comparison in the figure. Both overhead line and cable source infeed have equal length of 20 miles. The cable system has been formed from 1/2 in. radii overhead conductors whose

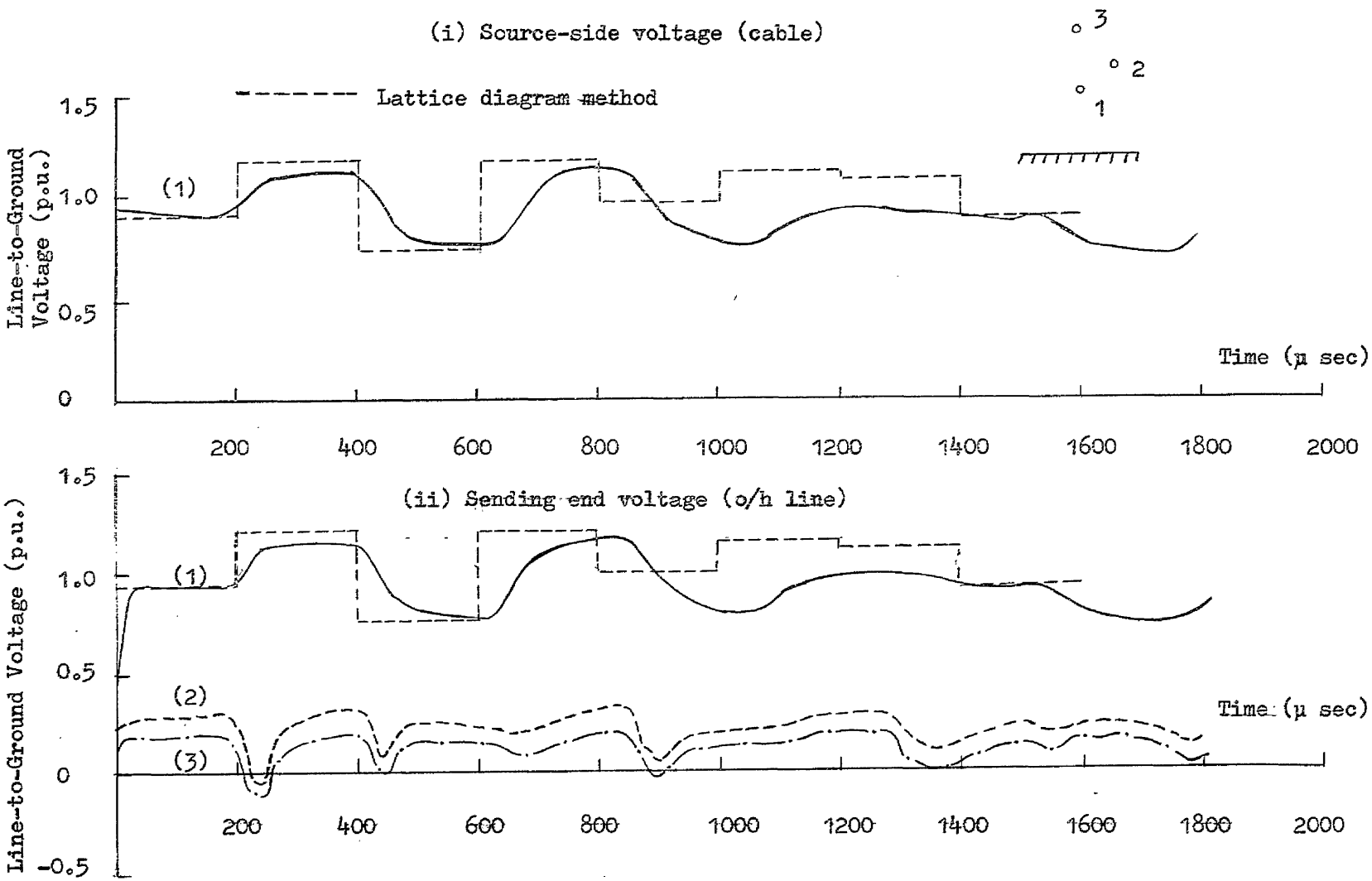

FIG. (10.7a). SOURCE-SIDE AND SENDING END TRANSIENT VOLTAGES FOR OVER-HEAD LINE/ CABLE SYSTEM

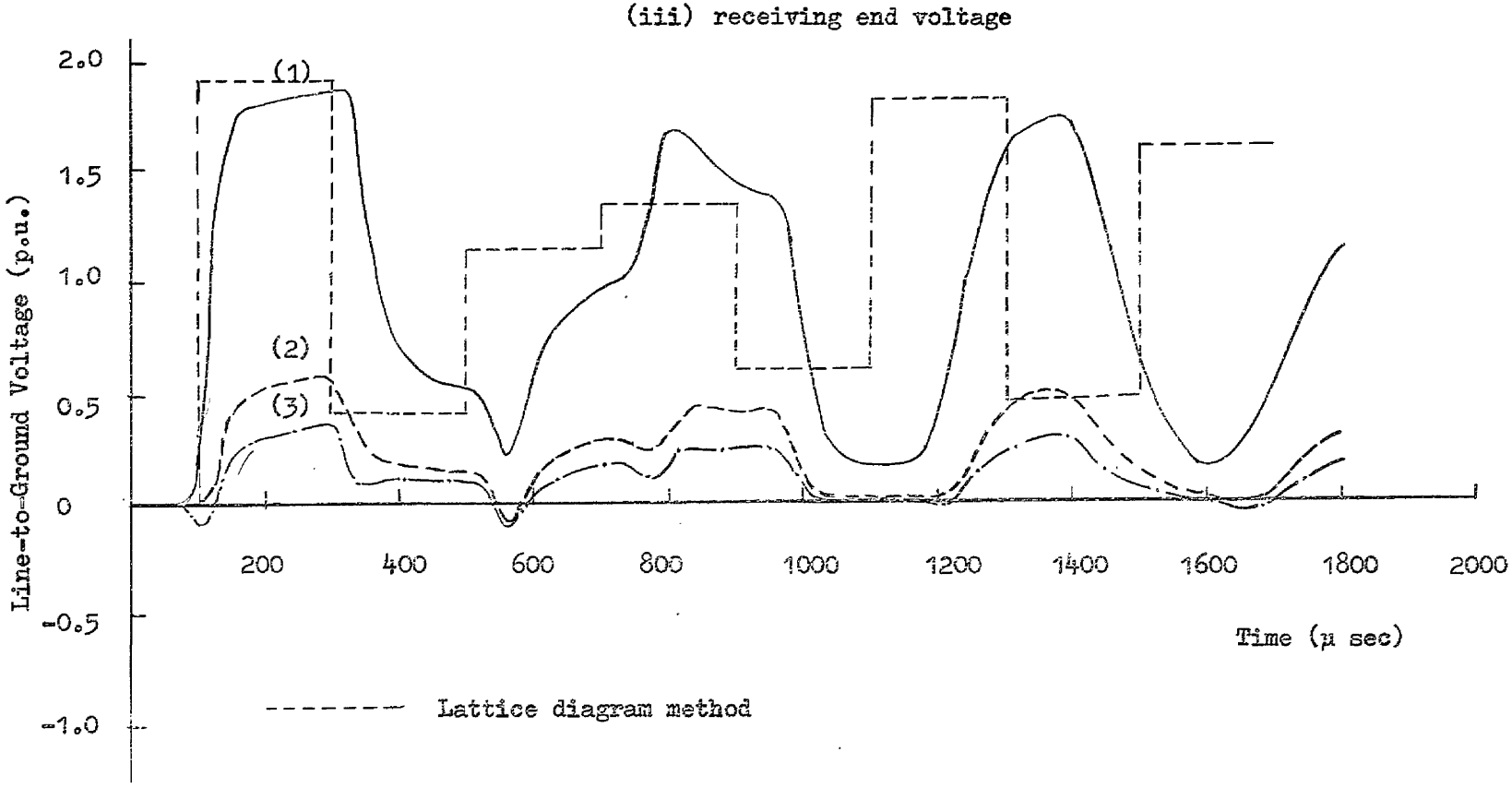

FIG. (10.7b). LINE-SIDE RECEIVING END TRANSIENT VOLTAGES FOR OVER-HEAD LINE/CABLE SYSTEM

height above ground is made so small; their effective surge impedance is 20 ohm. This height is 0.35 in. for all conductors. The velocity in this cable model is therefore equal to the velocity of light and hence the travel times for both cable source and main overlead line are identical. This is clearly shown from Fig. (10.7). The effect of 2000 p.f. bus-bar capacitance has not been included in the response assessment using Bewley lattice method; this contributes to some of the differences between the two types of result.

The magnitude and shape of the wave-fronts due to switching surges at any point on the system before any reflections arrive at the points concerned are independent of the source side circuit length. They are dependent only on the surge impedance of the circuits being energised. Fig. (10.8) is a study of the transient response of 120-mile vertical line. The source side circuit is also a line of the same configuration. Three different source lengths have been considered, these are 13.3, 20 and 30 miles in turn and the main transient response for a top conductor energisation is shown for these three infeed lengths for line and source sides. On the line side the secondary transients on the coupled phases are shown for the 13.3-mile source only, the trend for other source infeed lengths is not very different; these are excluded as they would distort the overall picture of the diagram. The arrival of the switching surges from the remote end of the source circuit is clearly indicated and these vary in almost direct proportion to the infeed length. A comparison of Fig. (10.8.a) with Fig. (10.6.c)

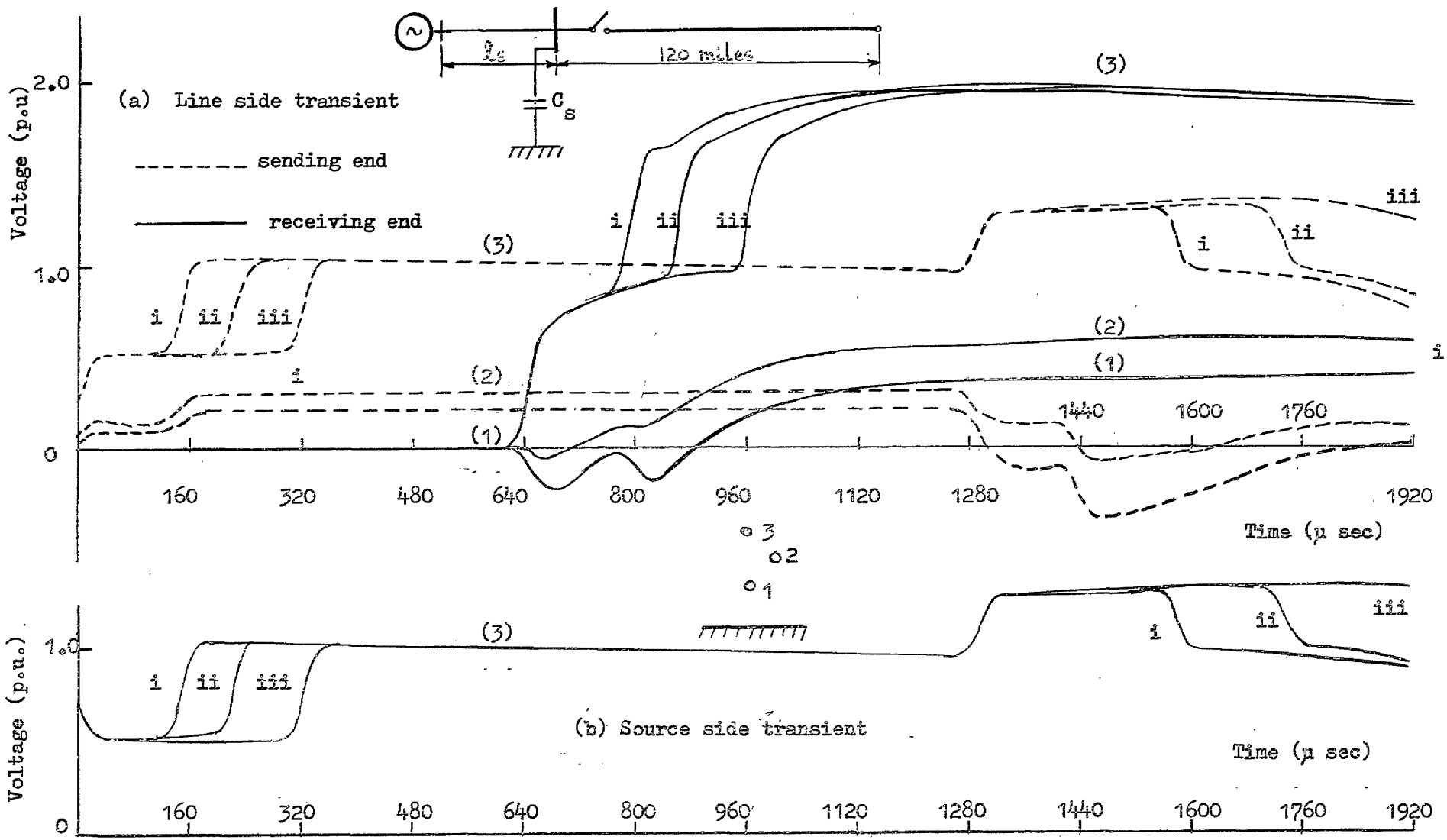

i - l_s = 13.3 miles. ii - l_s = 20 miles. iii - l_s = 30 miles. C_s = 2000 Pf

FIG (10.8.) EFFECT OF SOURCE INFEED LENGTH ON TRANSIENT VOLTAGES OF 120-MILE LINE FOR TOP CONDUCTOR ENERGISATION

shows that for the same source infeed length of 13.3 miles the arrival of the source side wave is clearly marked at the receiving end of the line when the top phase has been energised.

10.4.1.2 Source Representation by Symmetrical Model

As already mentioned, for economies in computation a symmetrical circuit arrangement can be used for source infeed representation. How best this does represent an actual non-symmetrical system is shown in Fig. (10.9) which gives the transient response of a horizontal circuit line the specifications of which are described in section (4.3). The response of the same line has also been included, on the grounds of symmetry, at both sending and receiving ends. The non-symmetrical circuit study has been carried out for an outer phase energisation and for first pole closure from an infinite bus system. The close similarities between the two results are a good justification for the choice of symmetrical representation. For longer observation times the deviation of the symmetrical arrangement from the true representation is expected to be pronounced because of the marked difference in the travel times of the two aerial modes. In any case this will not be of a serious nature.

The transient response of 120-mile line fed from 30-mile symmetrical circuit source is shown by the continuous curves in Fig. (10.10) for bottom phase energisation of the main circuit. Fig. (10.10.a) gives the source-side response which clearly shows the effect of successive reflections of

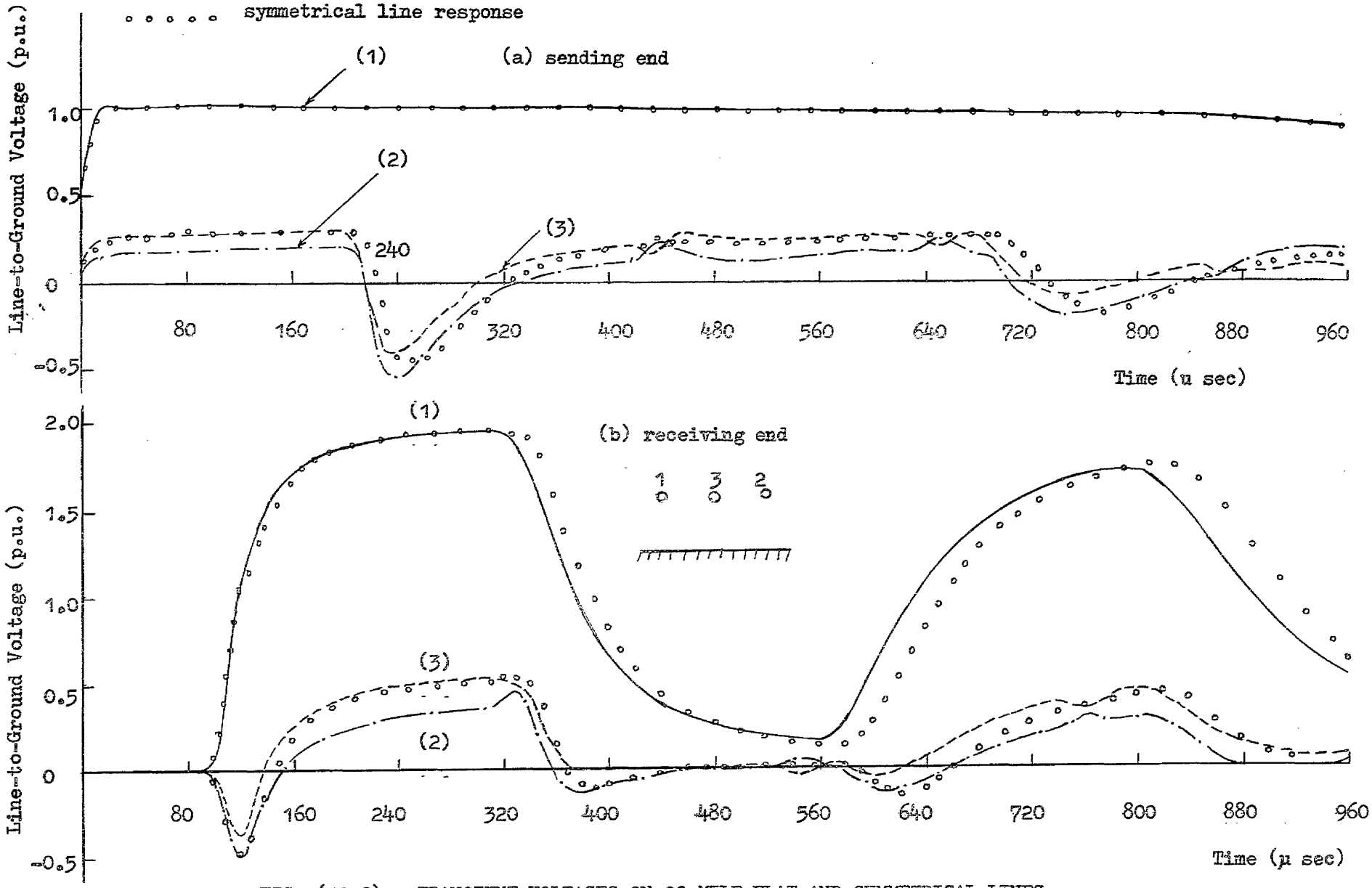

FIG. (10.9). TRANSIENT VOLTAGES ON 20-MILE FLAT AND SYMMETRICAL LINES

the waves travelling in both directions of the system. As opposed to the simplified form of representation described in the previous section the unenergised phases on the source side have transient voltages induced in them due to the mutual coupling to the energised phase hence the variation about the steady state source voltages of those phases. At the line side receiving end there is a considerable amount of attenuation and very pronounced distortion due to the added conductor and ground effects of the source side circuit. Ignoring minor details the general mode of behaviour marked in Fig. (10.10) is comparable to the behaviour of a similar system shown in Fig. (10.8.a) in which the source-side circuit takes the simplified form.

The complexity of the nature of the source and the effect this may have on the system transient response is clearly indicated by the curves of Fig. (10.10.c) for both source side and line side responses. The same main circuit has been considered but with infeed circuits to the switching station of lengths 13.3, 20 and 30 miles all of symmetrical configuration. The effect of more than one source circuit feeding at the switching station is an overall reduction in the surge impedance on the source. This causes a decrease in the magnitude of the travelling wave in the direction of the source-side and hence an increase in the magnitude of the initial wave travelling in the direction of the line side. This has been confirmed from the result of Fig. (10.10.c). With such types of system arrangement it would not be an easy matter to explain its behaviour in terms of the different modes of propagation due to the complications

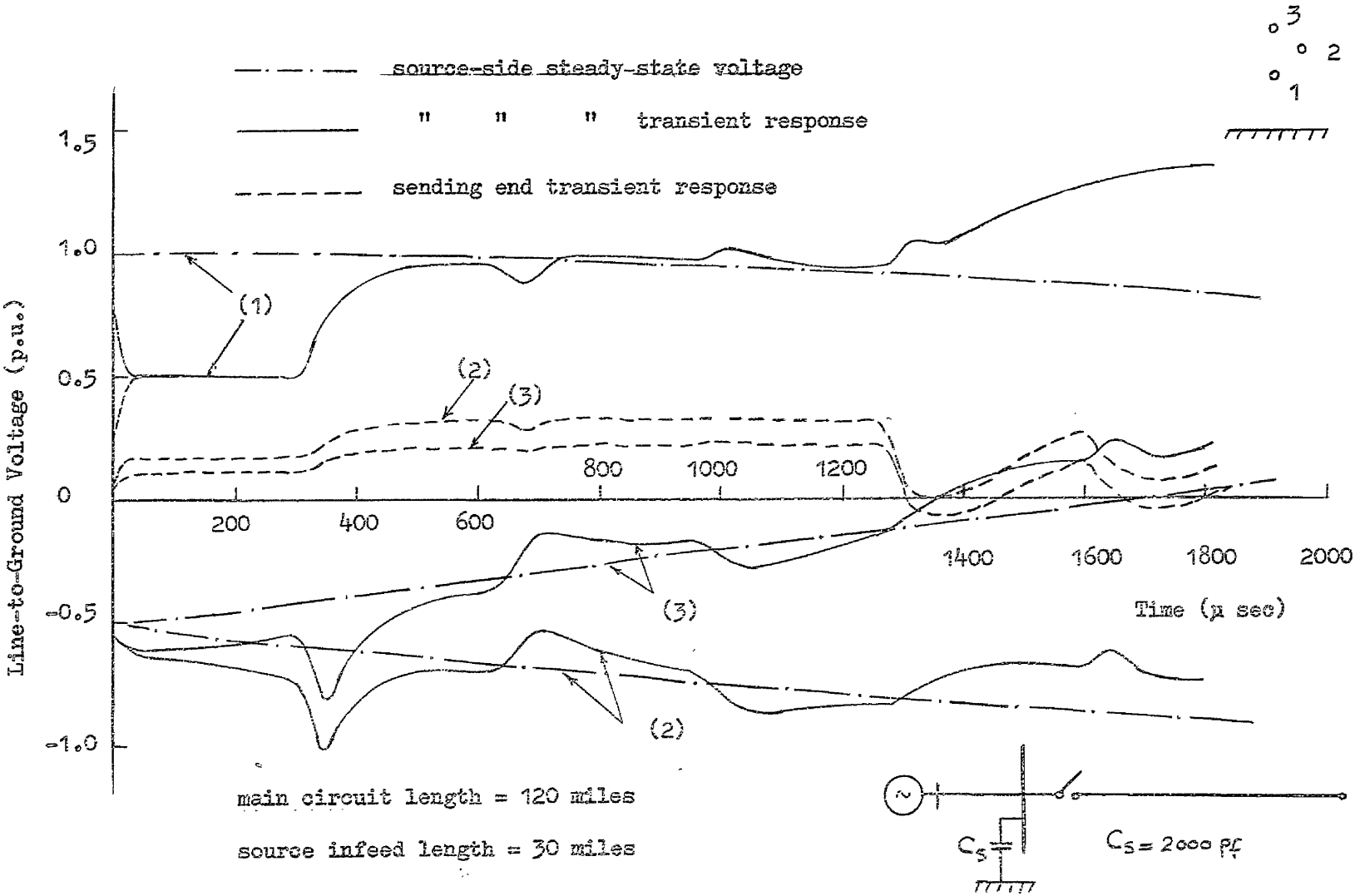

FIG. (10.10a). SOURCE-SIDE AND SENDING END TRANSIENT VOLTAGES OF 120-MILE LINE WITH ONE SYMMETRICAL SOURCE INFEED

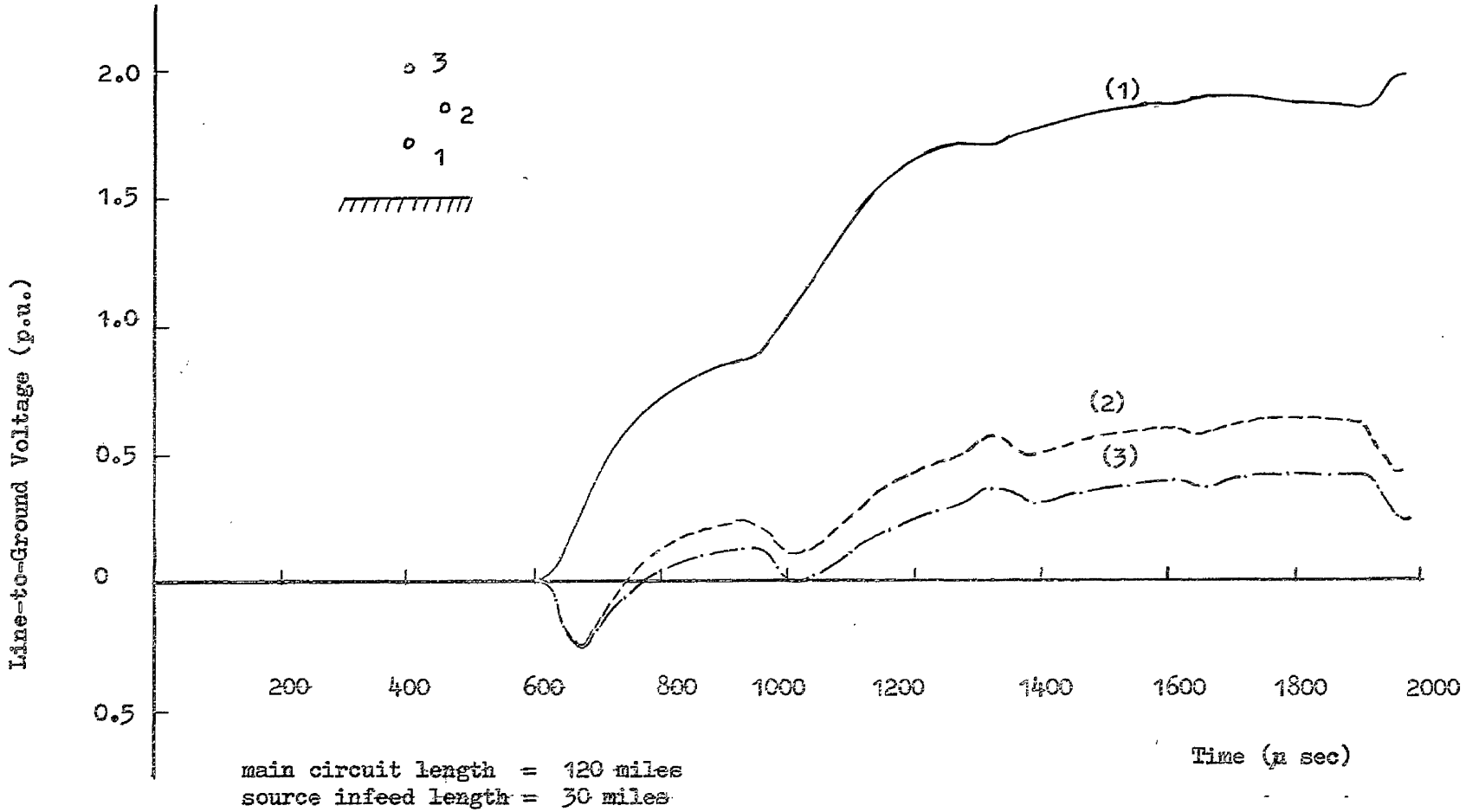

FIG. (10.10b). RECEIVING END TRANSIENT VOLTAGE OF 120-MILE LINE WITH ONE SYMMETRICAL SOURCE INFEED

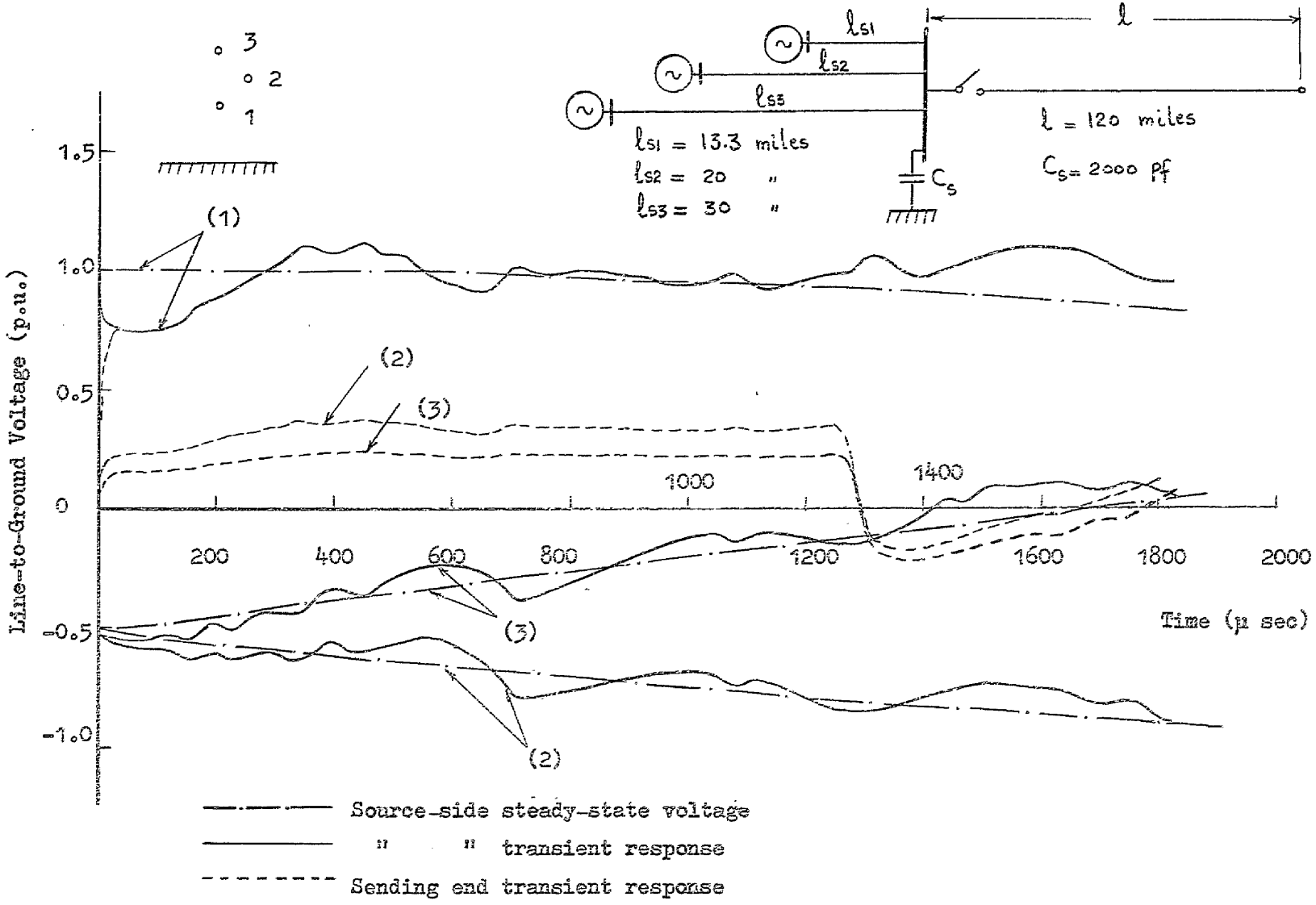

FIG. (10.10c). SOURCE-SIDE AND SENDING END TRANSIENT VOLTAGES OF 120-MILE LINE WITH THREE SYMMETRICAL INFEED CIRCUITS

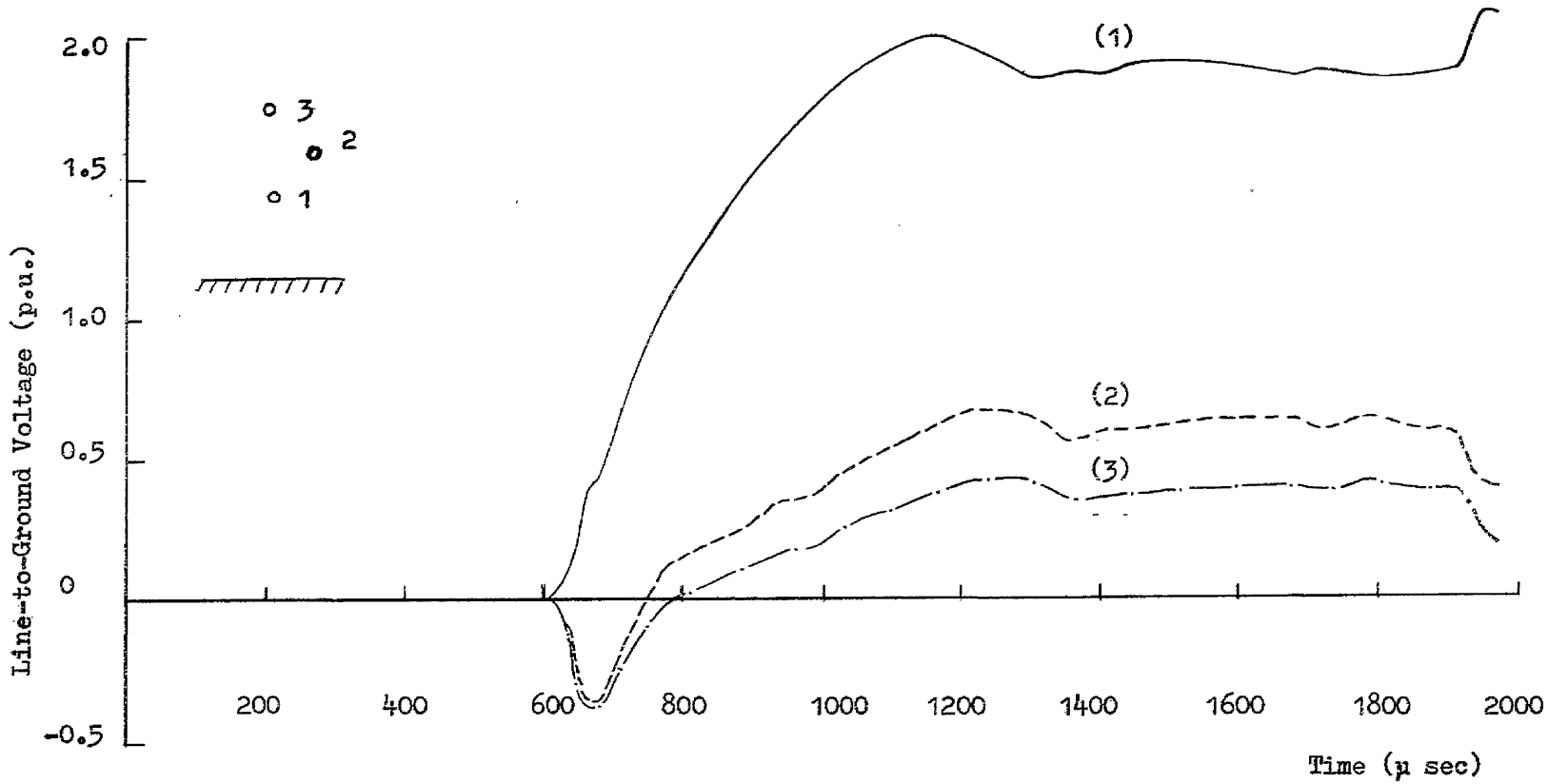

FIG. (10.10d). RECEIVING END TRANSIENT VOLTAGES OF 120-MILE LINE WITH THREE SYMMETRICAL INFEED CIRCUITS

introduced by the various lengths of the source infeed circuits. The result looks generally reasonable and is therefore acceptable as a realistic form of representation.

10.4.2 Sequential Transients with Precharge and Source Simulation

The results on the validity of the methods described for source simulation have demonstrated the effectiveness of these methods from a first pole closure point of view. More general types of study representing practical problems of sequential phase energisation with regard to source consideration and trapped charge effects are thought to be rather essential to prove the generality of the theoretical approach postulated when applied to such practical problems. Furthermore these studies will illustrate which of the various forms of source simulation would be most suitable from a practical point of view.

In Chapter 8 numerical calculations on sequential energisation of transmission lines have already verified the validity of the method of approach presented. It will now be demonstrated in a further comparative study of sequential transients calculations obtained from a method using the Bewley lattice technique that the general trend of both methods is the same. This will provide further grounds for judgement on the power of the new method.

10.4.2.1 Comparative Study with Bewley Lattice Techniques

Fig. (10.11) shows the transient response on the sending and receiving ends of the vertical line described in section(9.5). The line length is 100 miles and is fed

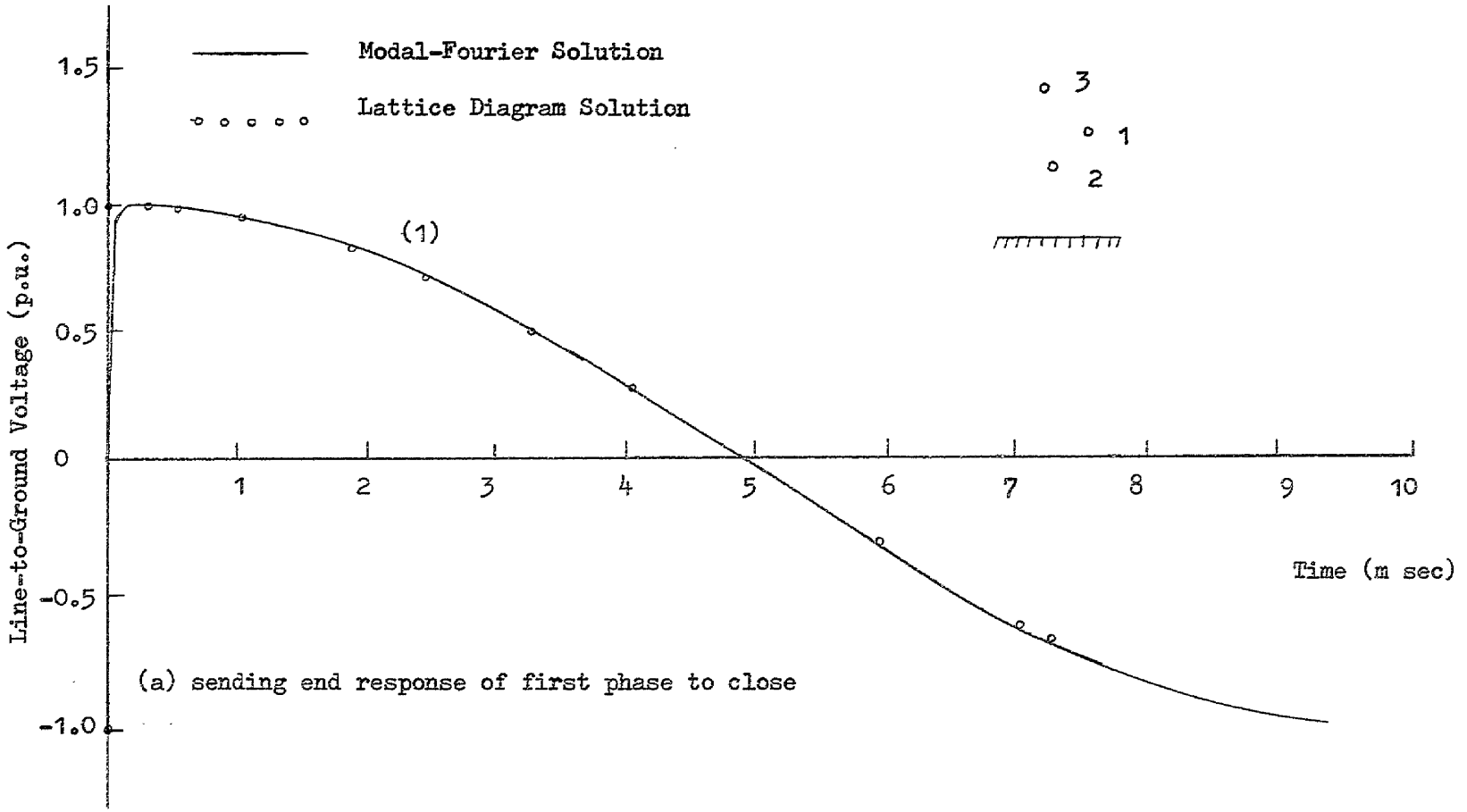

FIG. (10.11). COMPARATIVE STUDY ON SEQUENTIAL TRANSIENTS CALCULATION FOR A 100-MILE PRECHARGED LINE

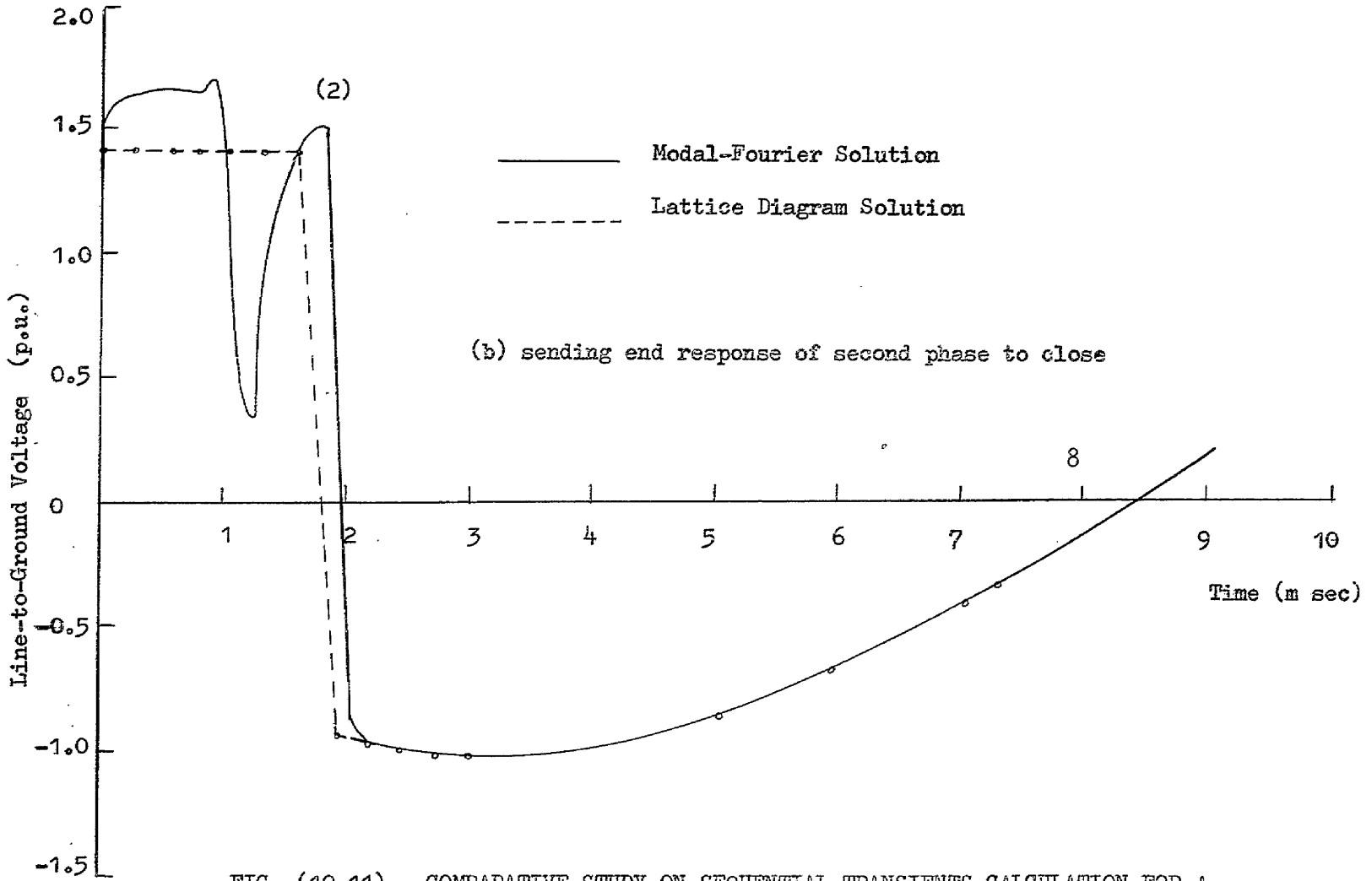

FIG. (10.11). COMPARATIVE STUDY ON SEQUENTIAL TRANSIENTS CALCULATION FOR A 100-MILE PRECHARGED LINE

(c) sending end response of last phase to close

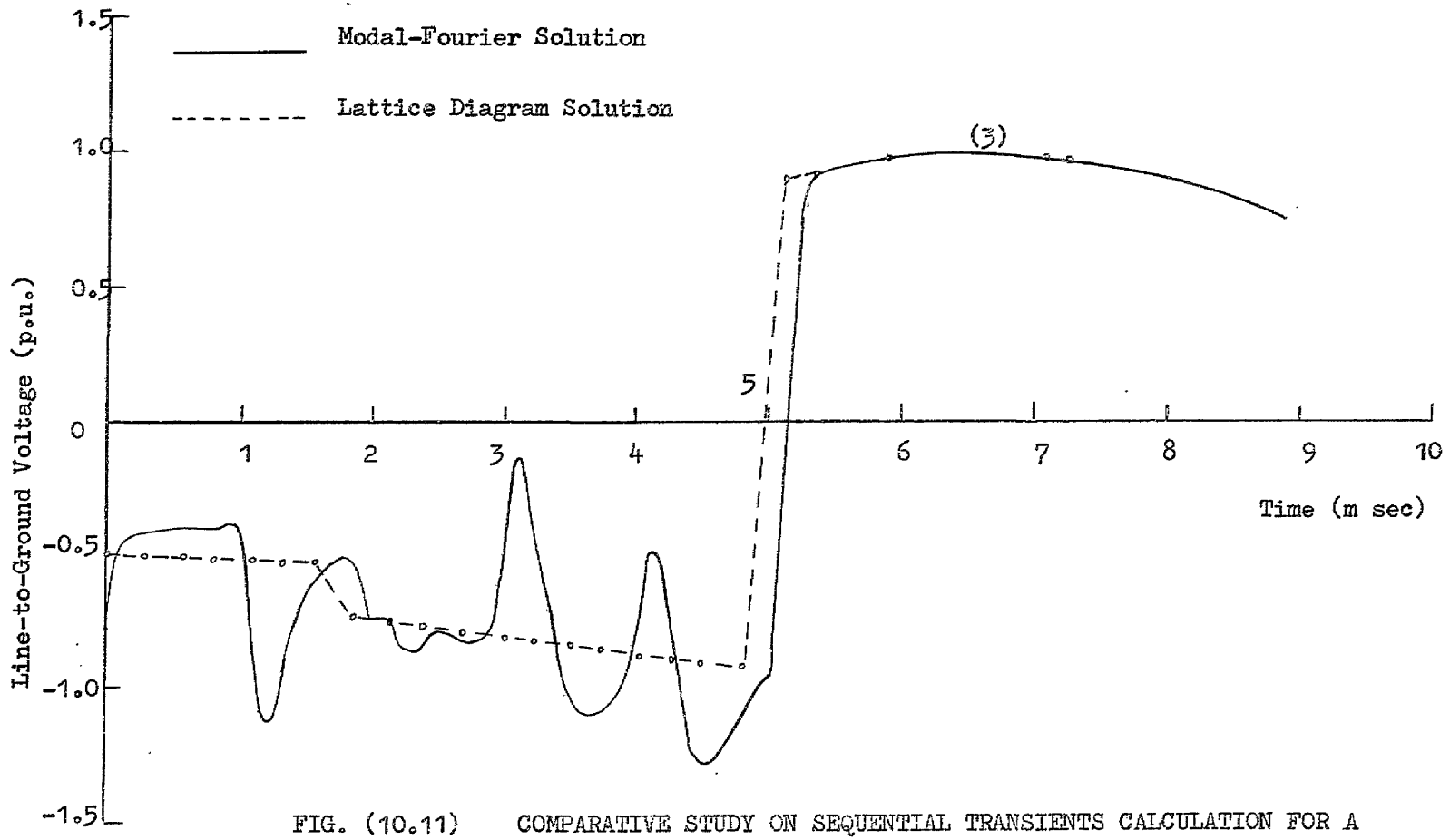

FIG. (10.11) COMPARATIVE STUDY ON SEQUENTIAL TRANSIENTS CALCULATION FOR A 100-MILE PRECHARGED LINE

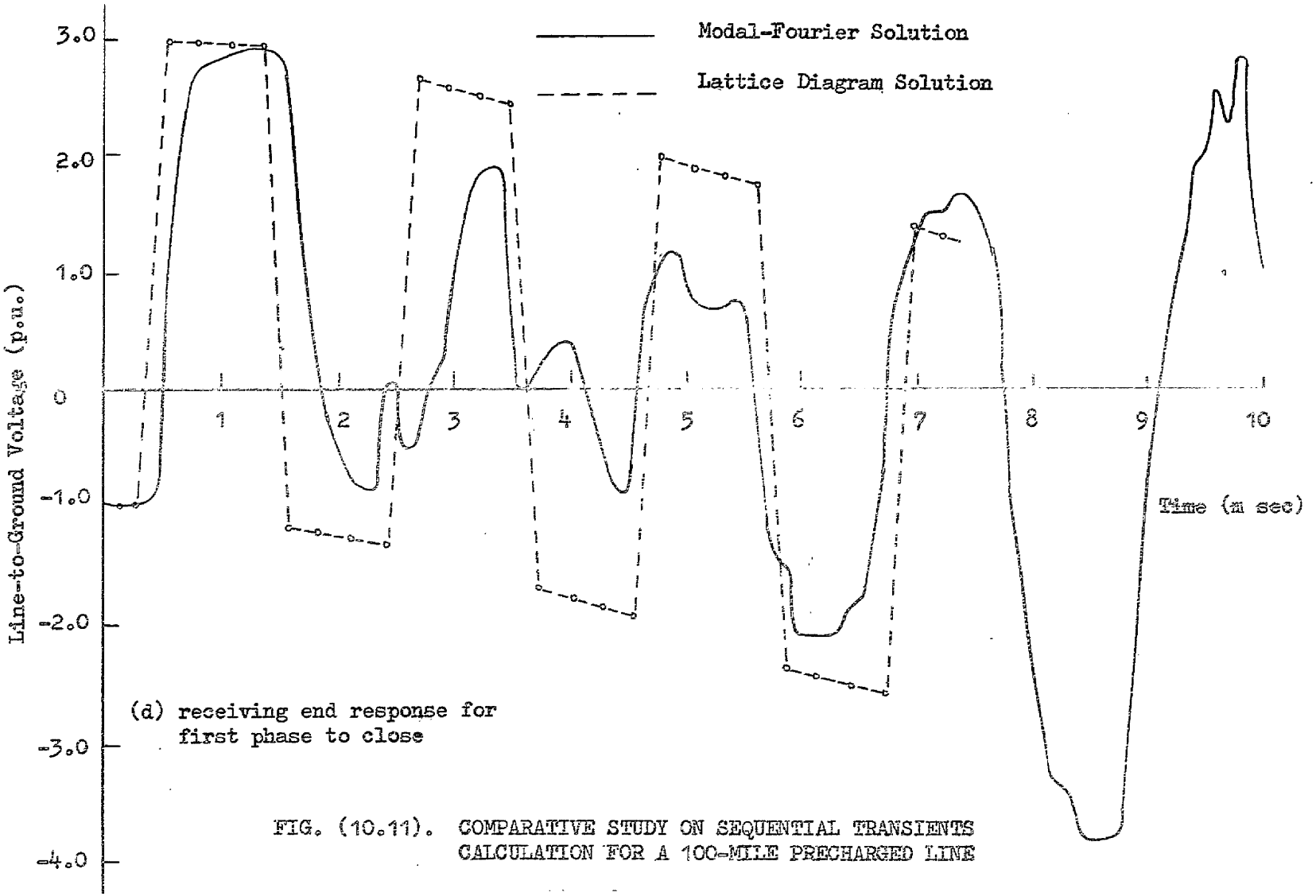

(d) receiving end response for first phase to close

FIG. (10.11). COMPARATIVE STUDY ON SEQUENTIAL TRANSIENTS CALCULATION FOR A 100-MILE PRECHARGED LINE

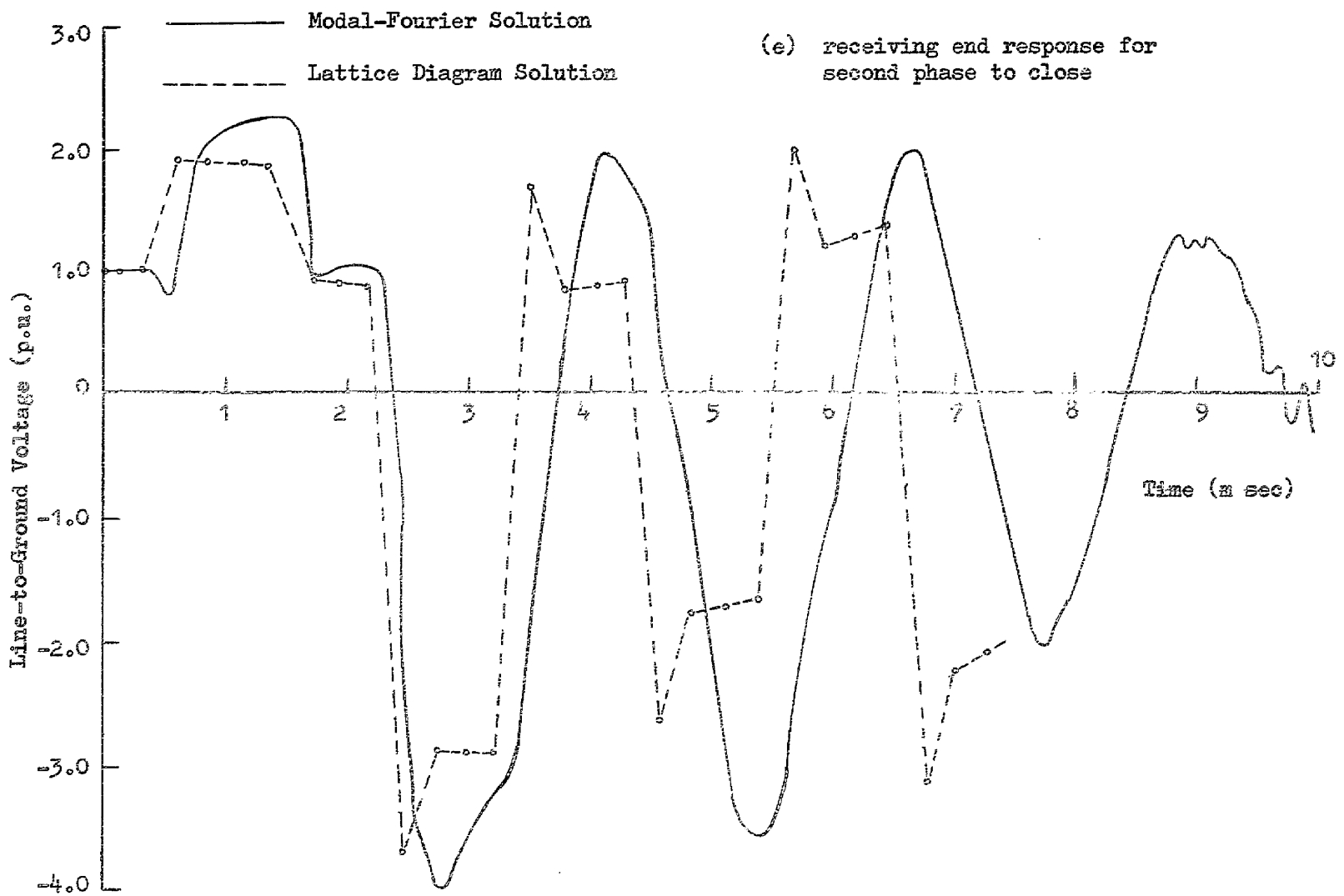

FIG. (10.11). COMPARATIVE STUDY ON SEQUENTIAL TRANSIENTS CALCULATION FOR A 100-MILE PRECHARGED LINE

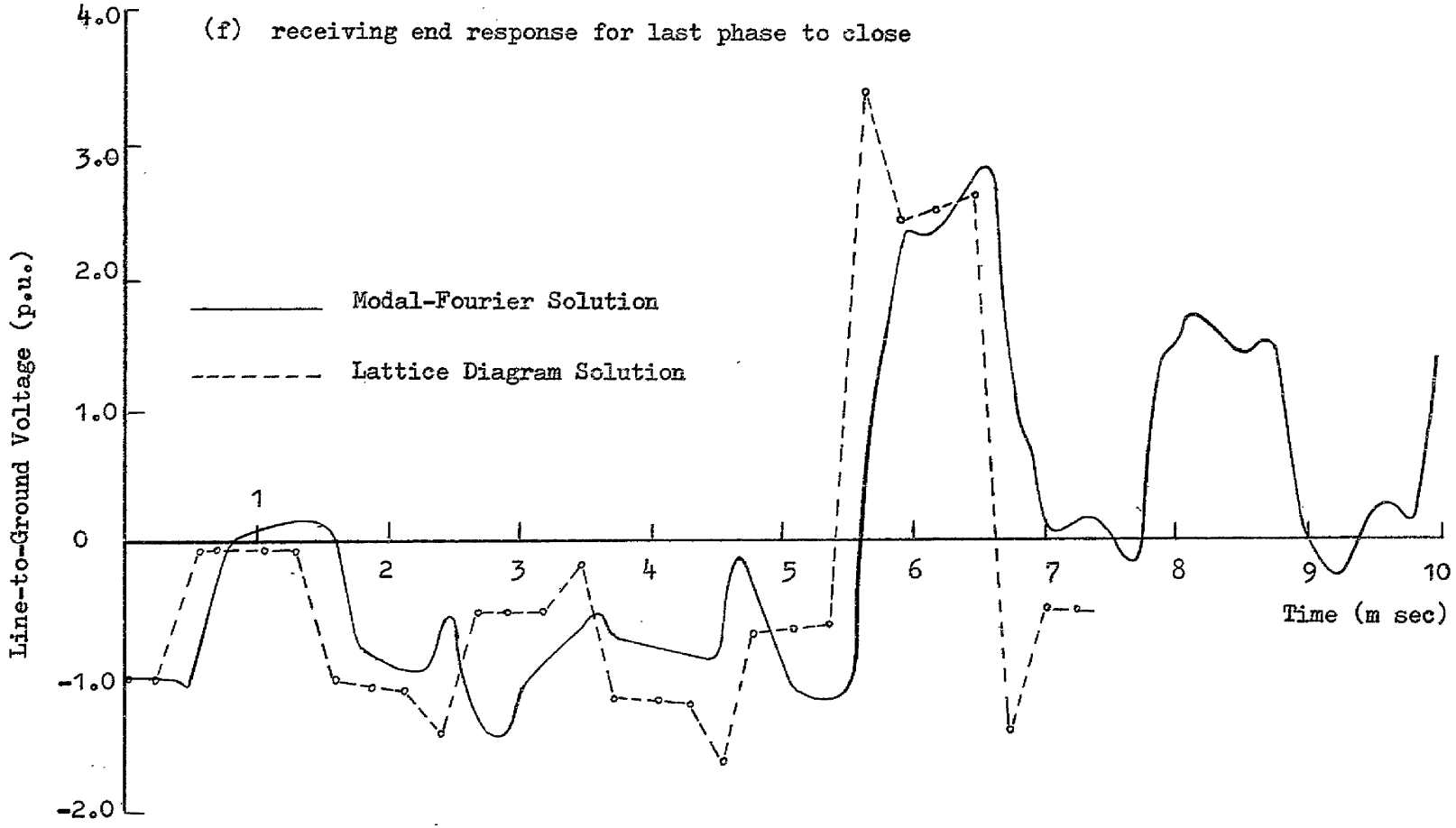

FIG. (10.11). COMPARATIVE STUDY ON SEQUENTIAL TRANSIENTS CALCULATION FOR A 100-MILE PRECHARGED LINE

from an infinite bus source. The line has negative trapped charge of -1.0 p.u. on the top and middle phase conductors and positive trapped charge of +1.0 p.u. on the bottom conductor. The middle phase (phase 1) closes first at voltage peak followed by the bottom phase (phase 2) 1.9 msec later and then the top phase closing at 5.1 msec. The Bewley lattice method results[75] are represented by broken lines. In the case of the Bewley lattice method system losses have been ignored.

At the sending end of the line, Fig. (10.11.), although the Bewley lattice method shows no greater details of the response pattern of the unenergised phases the general trend of the two results are closely identical. For the first phase the voltage changes from -1.0 p.u. to +1.0 p.u. - the peak value of the cosine wave at zero time. It takes a few microseconds for the voltage to reach that peak which is the normal rise time associated with the modified Fourier transform technique. This characteristic is also noticeable at the discontinuity points corresponding with the times of second and third pole closure.

At the receiving end of the line general agreement between the results of the two methods is apparent though there are significant differences in voltage magnitude and shape of the transient following successive reflections arriving at the receiving end of the line. For phase 1 the beat effect phenomenon is most clearly shown for this phase by the method used in this investigation and in particular substantial distortion effects revealed due to aerial and

earth modes interaction are well defined. For phase 2 the arrival of the switching surge at the receiving end due to second pole closure produces voltages of the order of 4.0 p.u. as shown by the two methods of evaluation. The deviation from the natural resonance frequency presented for the lossless system by the Bewley lattice calculation is due to the presence of the earth mode which is being considered in the case of modal analysis calculation.

10.4.2.2 Source and Line Trapped Charge Studies

i. Lumped Parameter Source

Fig. (10.12) shows the results of sequential transients calculations for a 100-mile line fed from a 400 KV bus. The middle phase closes first followed by the bottom and top phases 1.9 msec and 5.1 msec respectively. In one set of calculation the source effect is not taken into consideration and in the other the source is represented as a lumped inductance calculated on the basis of 25,000 MVA short-circuit level at the switching station bus-bar with a total lumped capacitance of 2000 pf between bus-bar and ground. Following the interpretation given in section (10.4.1) for first phase energisation only the result of Fig. (10.12) for source and line sides can similarly be explained with regard to variation about the mean value of the infinite bus sytem response for all three phases. It is belived in this respect that the results are self explanatory and no detailed discussion is intended. An important observation to be pointed out regarding Fig. (10.12.a) on the source side is that since no mutual effects are represented then the second and third phase responses prior to their energisation from the source

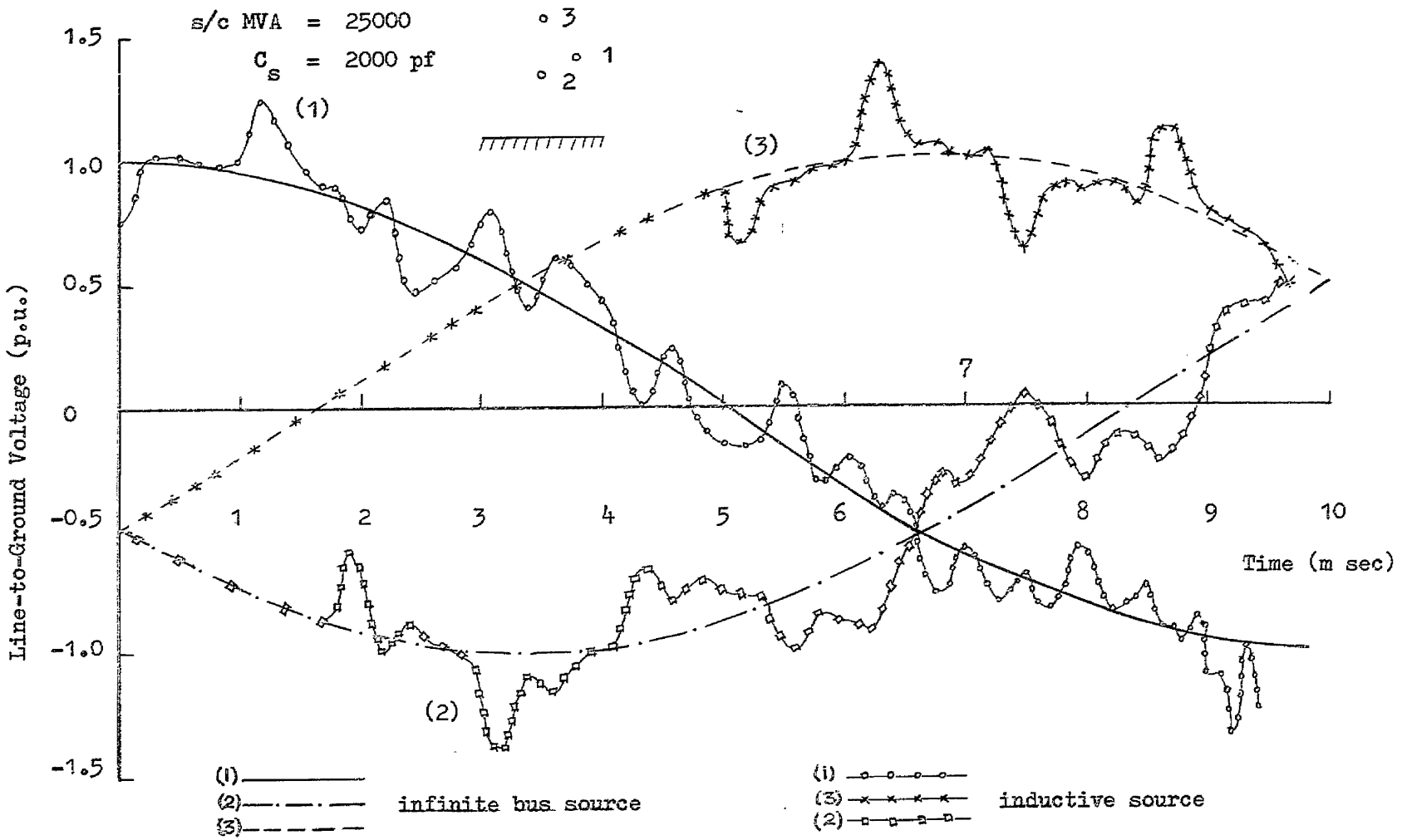

FIG. (10.12a). SOURCE-SIDE TRANSIENT VOLTAGES OF 400 KV, 100-MILE LINE FOR INFINITE BUS AND LUMPED INDUCTIVE SOURCES

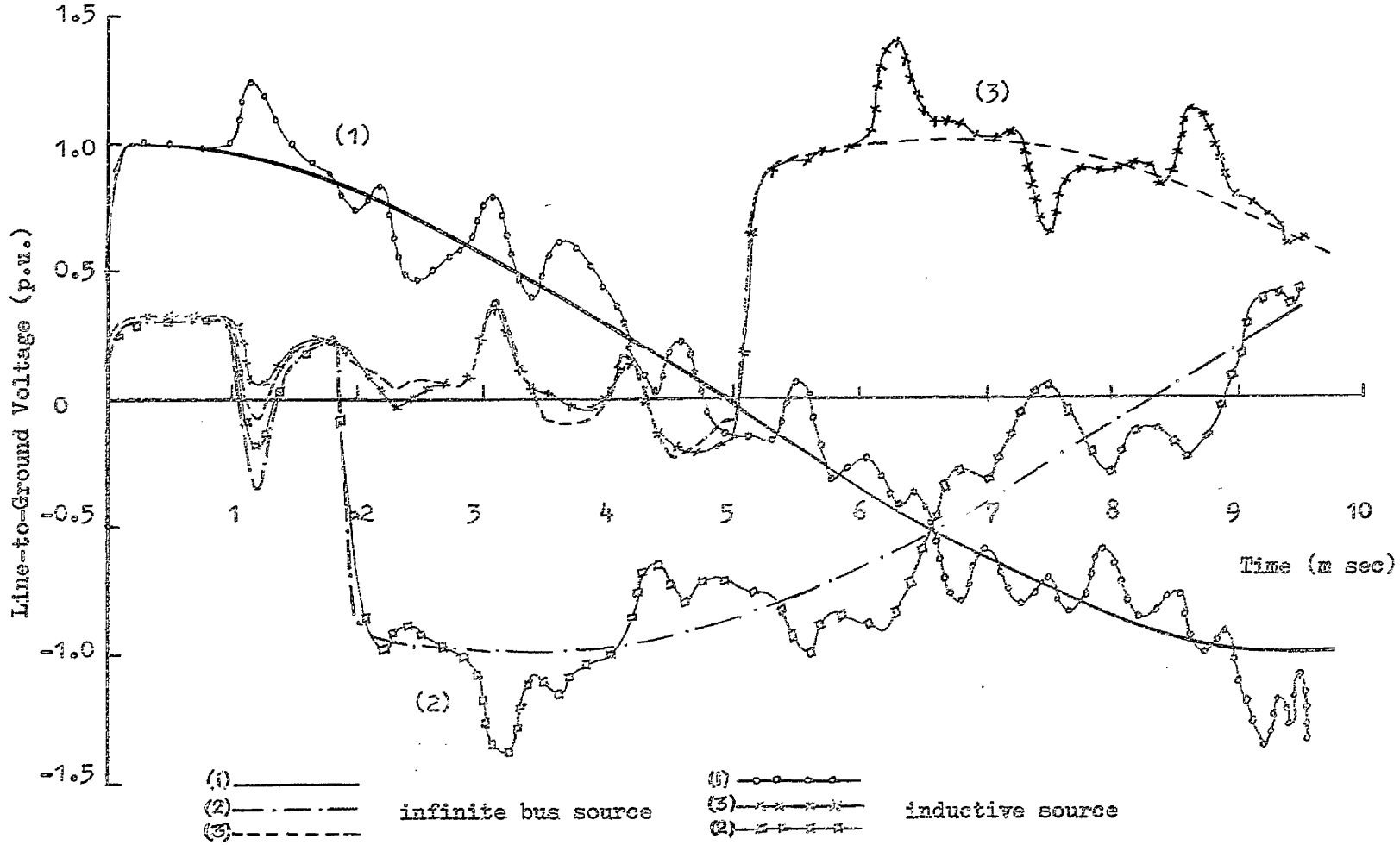

FIG.(10.12b). SENDING END TRANSIENT VOLTAGES OF 400 KV, 100-MILE LINE FOR INFINITE BUS AND LUMPED INDUCTIVE SOURCES

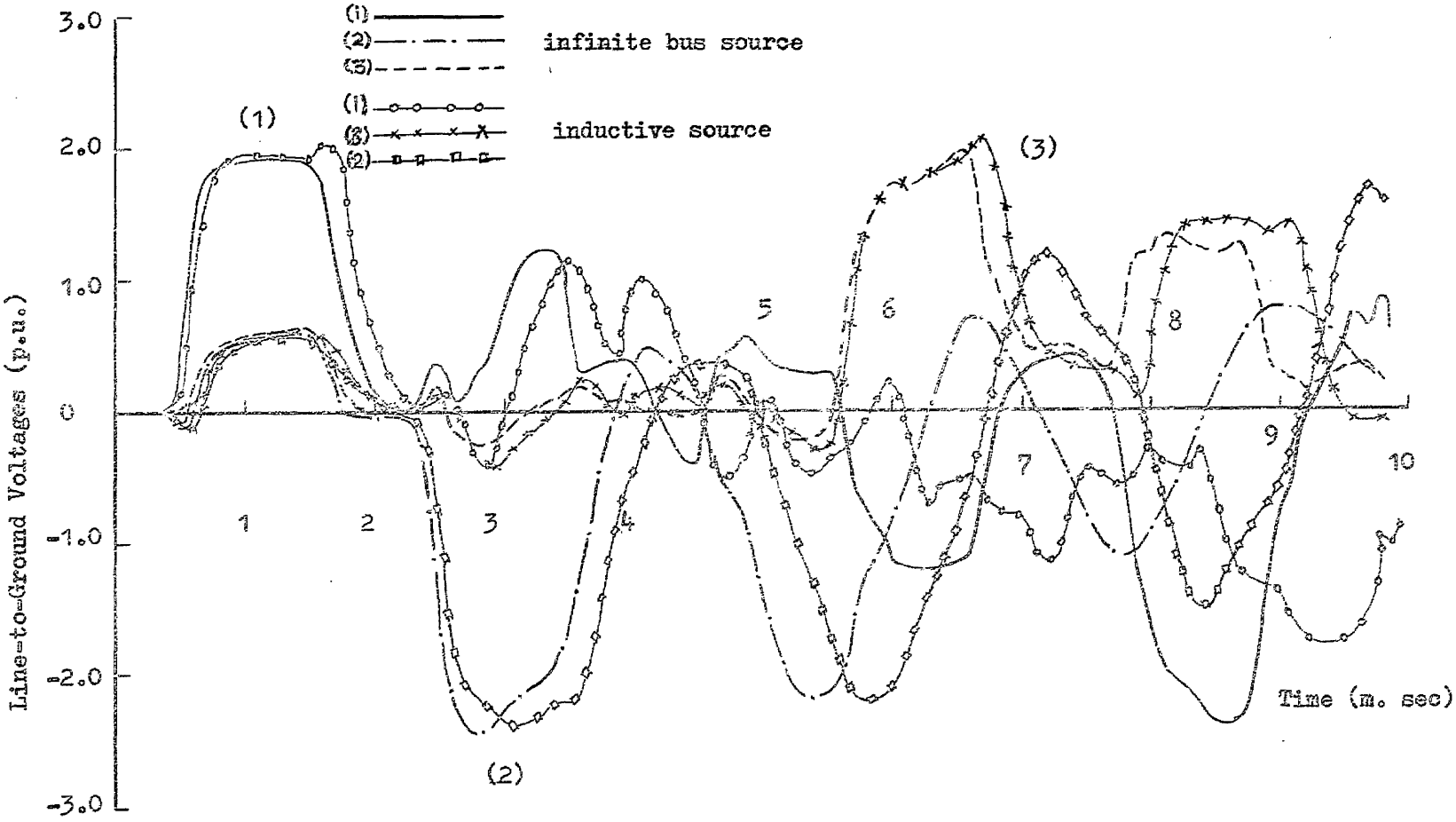

FIG. (10.12c). RECEIVING END TRANSIENT VOLTAGES OF 400 KV, 100-MILE LINE FOR INFINITE BUS AND LUMPED INDUCTIVE SOURCES

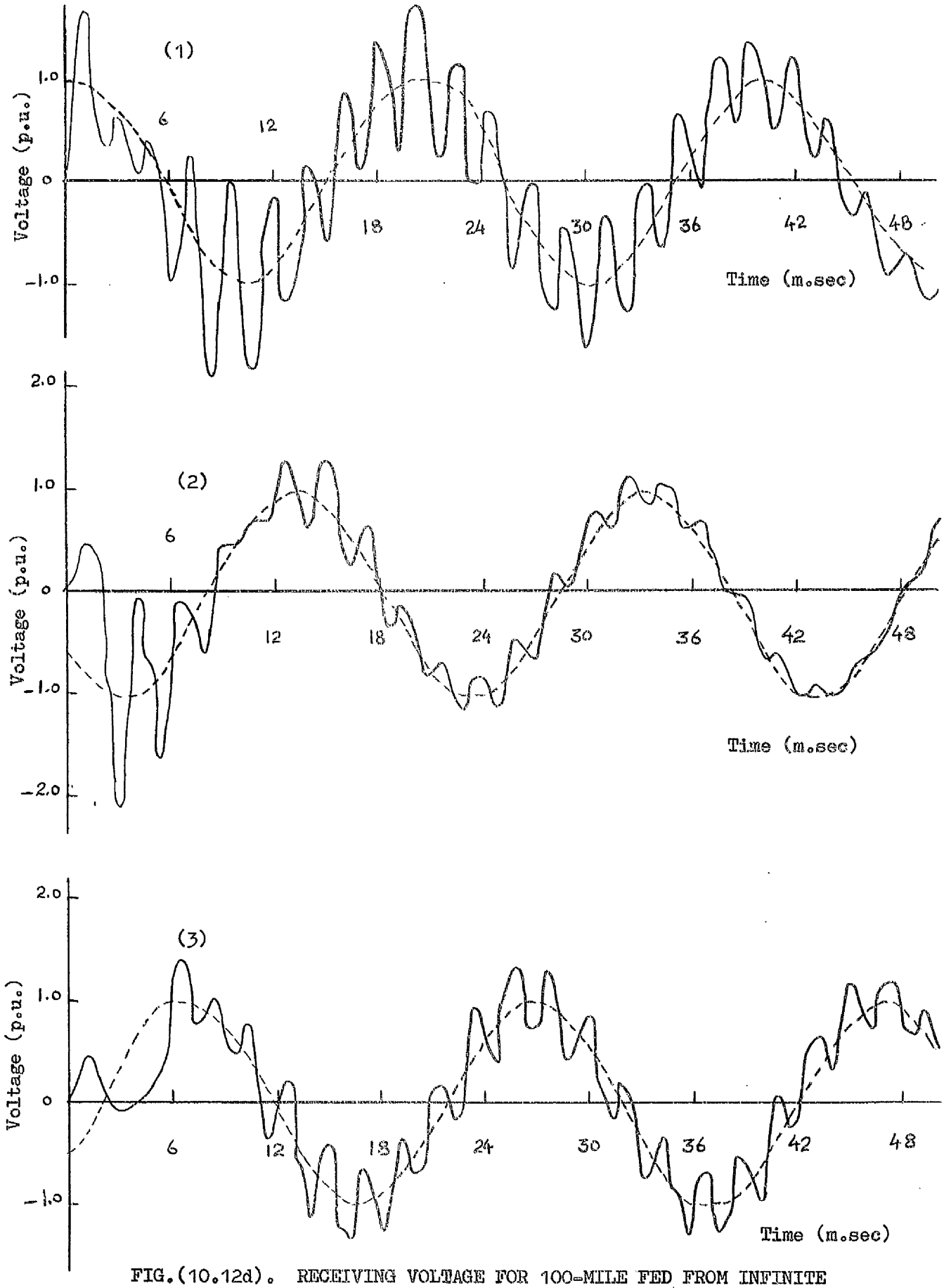

FIG.(10.12d). RECEIVING VOLTAGE FOR 100-MILE FED FROM INFINITE BUS SOURCE ON LONG OBSERVATION TIME BASIS

are the steady-state responses of those phases only.

Fig. (10.12.d) shows the transient response of the infinite bus sytem taken over a longer observation period of 60 msec superimposed on the source side steady-state response. It is interesting to note that the bottom phase response (second phase to close) reaches steady-state value more quickly than either top or middle phases.

ii. Distributed Parameter Source

Fig. (10.13) is the transient response of the same line above except that the source is represented as a distributed parameter infeed. The 100-mile line is fed from a 15-mile source infeed with an infinite bus at its remote end. The two forms of source representation described in the early paragraphs have been considered and a lumped capacitance of 2000 pf at the switching station bus-bar is included.

The system response for both source and line sides for these two forms of representation are generally agreeable. In the simplified form of source representation where mutual effects have been ignored the response is the steady-state response on the source side. With the symmetrical form of source representation transient voltages induced on the coupled unenergised phases modify the source side steady-state voltage and the total source side response varies about the mean steady-state value. The same is also true for the third phase. From results for the sending end side of the open-circuited line as well as source-side it appears that if

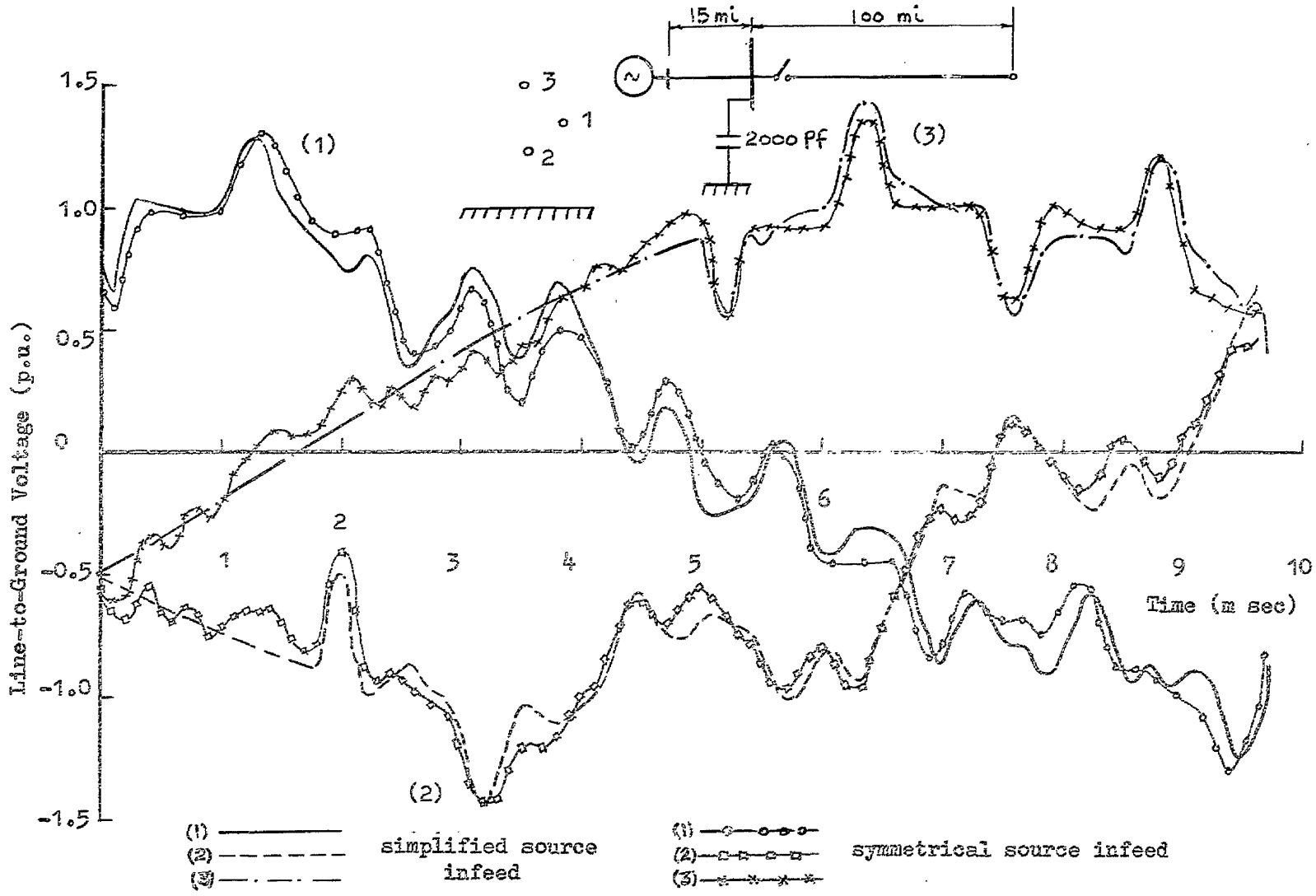

FIG. (10.13a). EFFECT OF SIMPLIFIED AND SYMMETRICAL SOURCE REPRESENTATION ON SOURCE-SIDE TRANSIENT VOLTAGES OF 400 KV, 100-MILE LINE

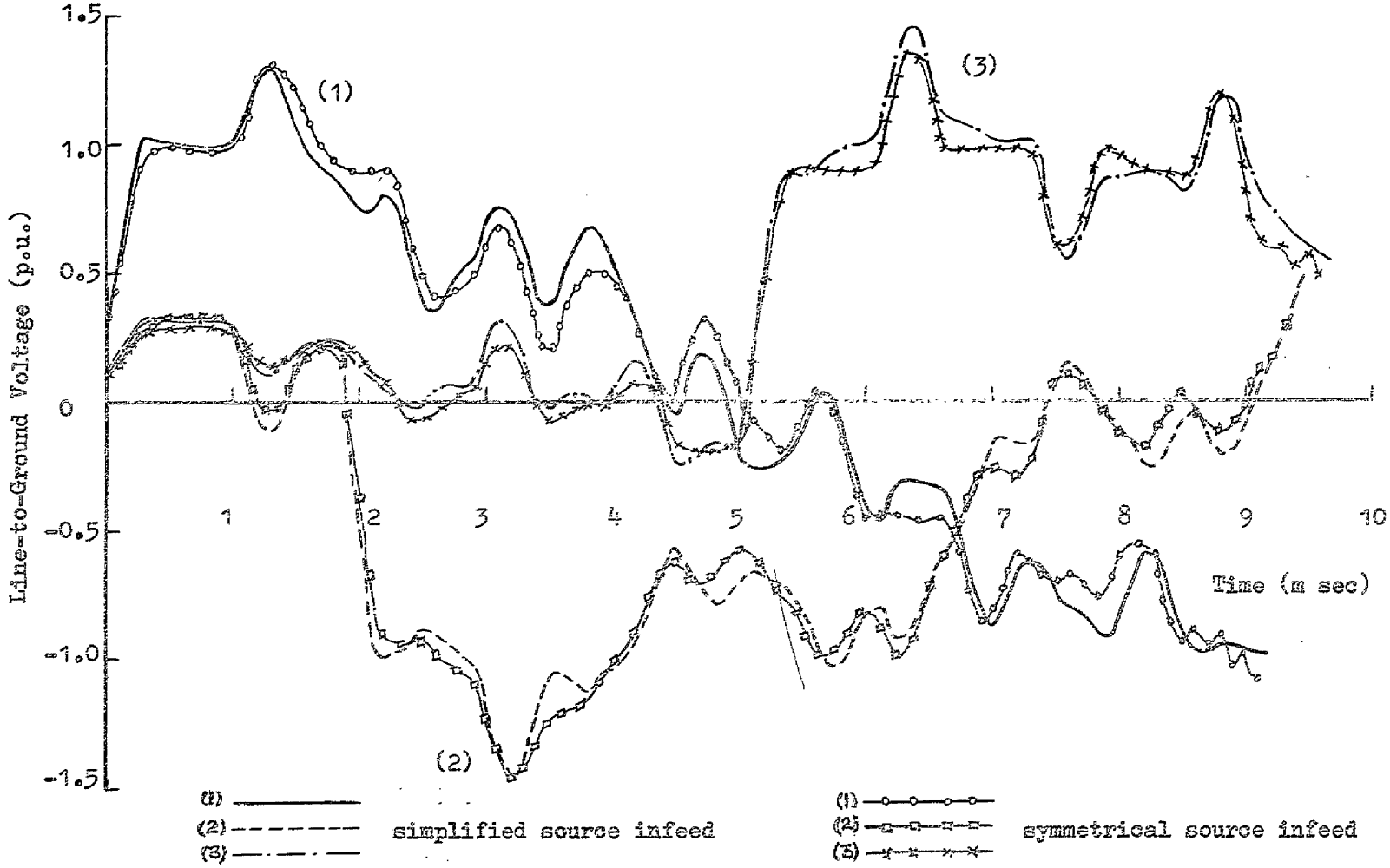

FIG. (10.13b). EFFECT OF SIMPLIFIED AND SYMMETRICAL SOURCE REPRESENTATION ON SENDING END TRANSIENT VOLTAGES OF 400 KV, 100-MILE LINE

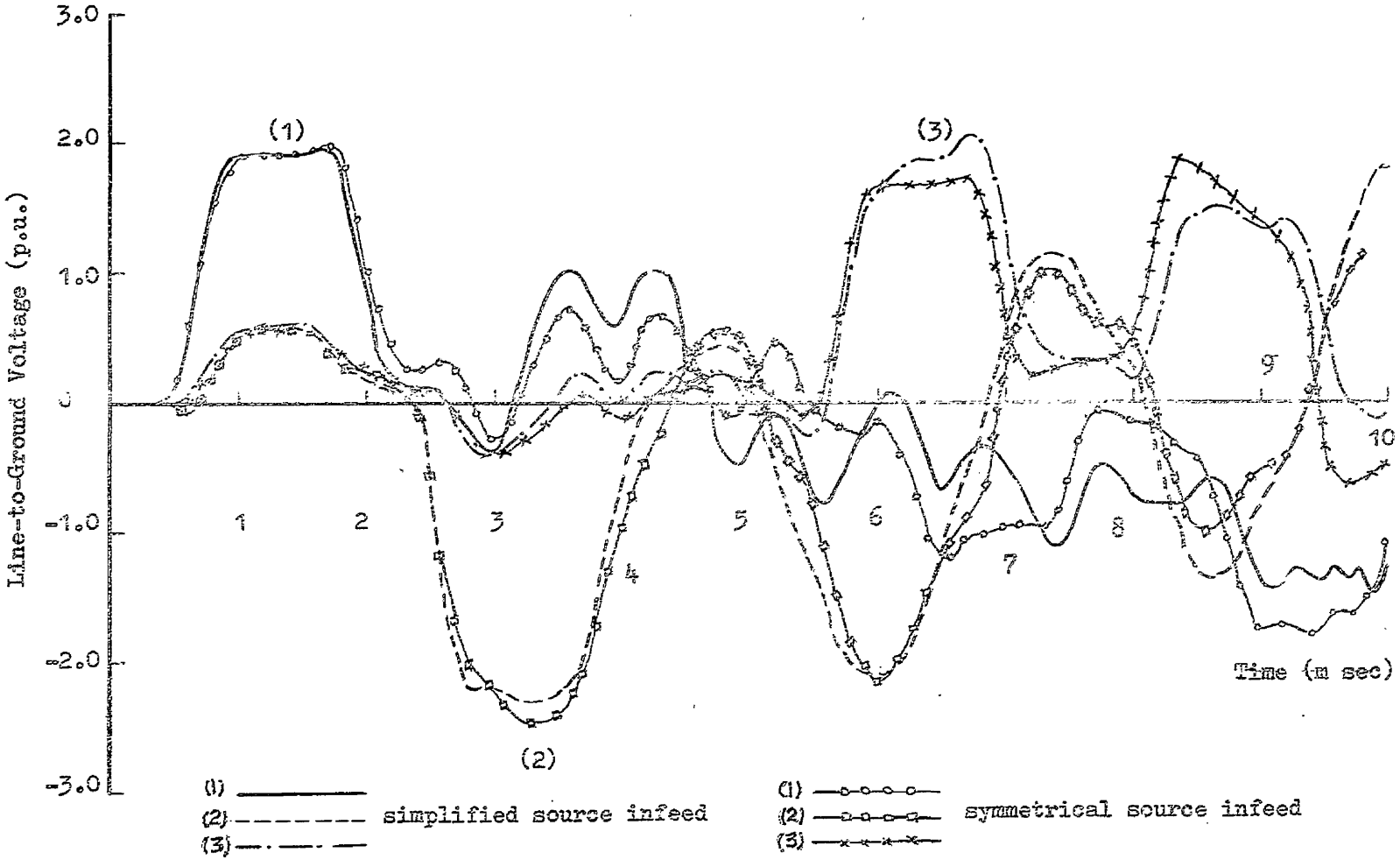

FIG. (10.13c). EFFECT OF SIMPLIFIED AND SYMMETRICAL SOURCE REPRESENTATION ON RECEIVING END TRANSIENT VOLTAGES OF 400 KV, 100-MILE LINE

greater details about the transient behaviour of the system are not required then the simplified form of representation for the source side is sufficient as in most practical cases. This has the advantage of further economies in computation costs.

On the receiving end of the line, the two forms of representation show noticeable differences particularly in the response pattern of phase 1, the first phase to be energised. Here the result of the symmetrical form of source circuit representation is to be accepted as more realistic to the actual system response. It is also noticed that the simplified form of representation offered yields optimistic values for the maximum voltage transients caused due to second pole closure at the open end of the line. Over a longer period of observation the differences may not be noticeable.

For shorter observation time studies where greater details are required it is advisable to use the more exact form of source representation, otherwise the simplified form can be relied on to give acceptable results within engineering accuracies and is very reliable for longer periods of observation time.

iii. Distributed Parameter Sources and Trapped Charge

Sequential switching transients with trapped charges on the line side are shown in Fig. (10.14) for both source and line sending and receiving ends. For eachphase of the vertical line two transient responses are given, one represents a

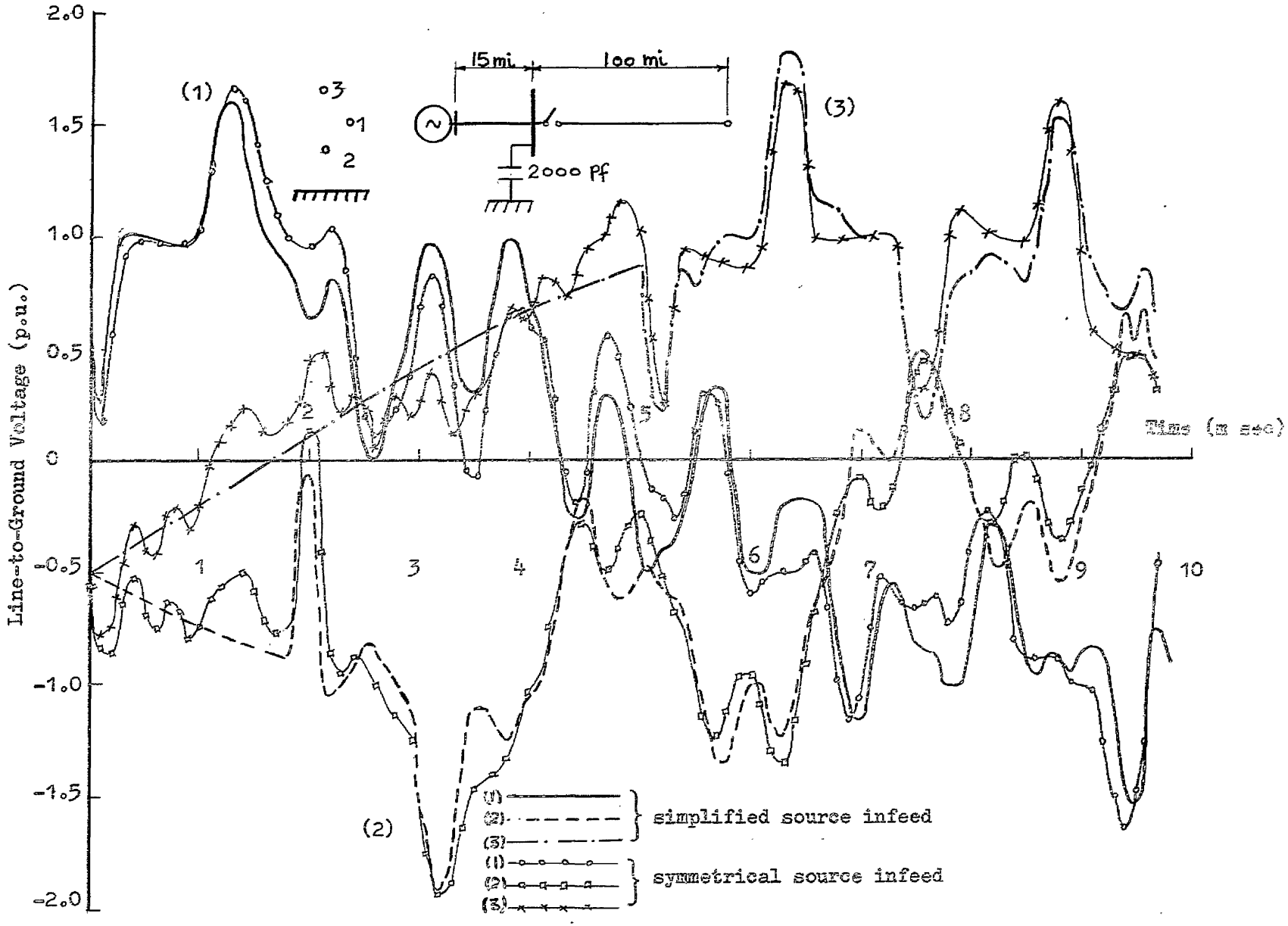

FIG. (10.14a). EFFECT OF SIMPLIFIED AND SYMMETRICAL SOURCE REPRESENTATION ON SOURCE-SIDE TRANSIENT VOLTAGES OF 100-MILE PRECHARGED LINE

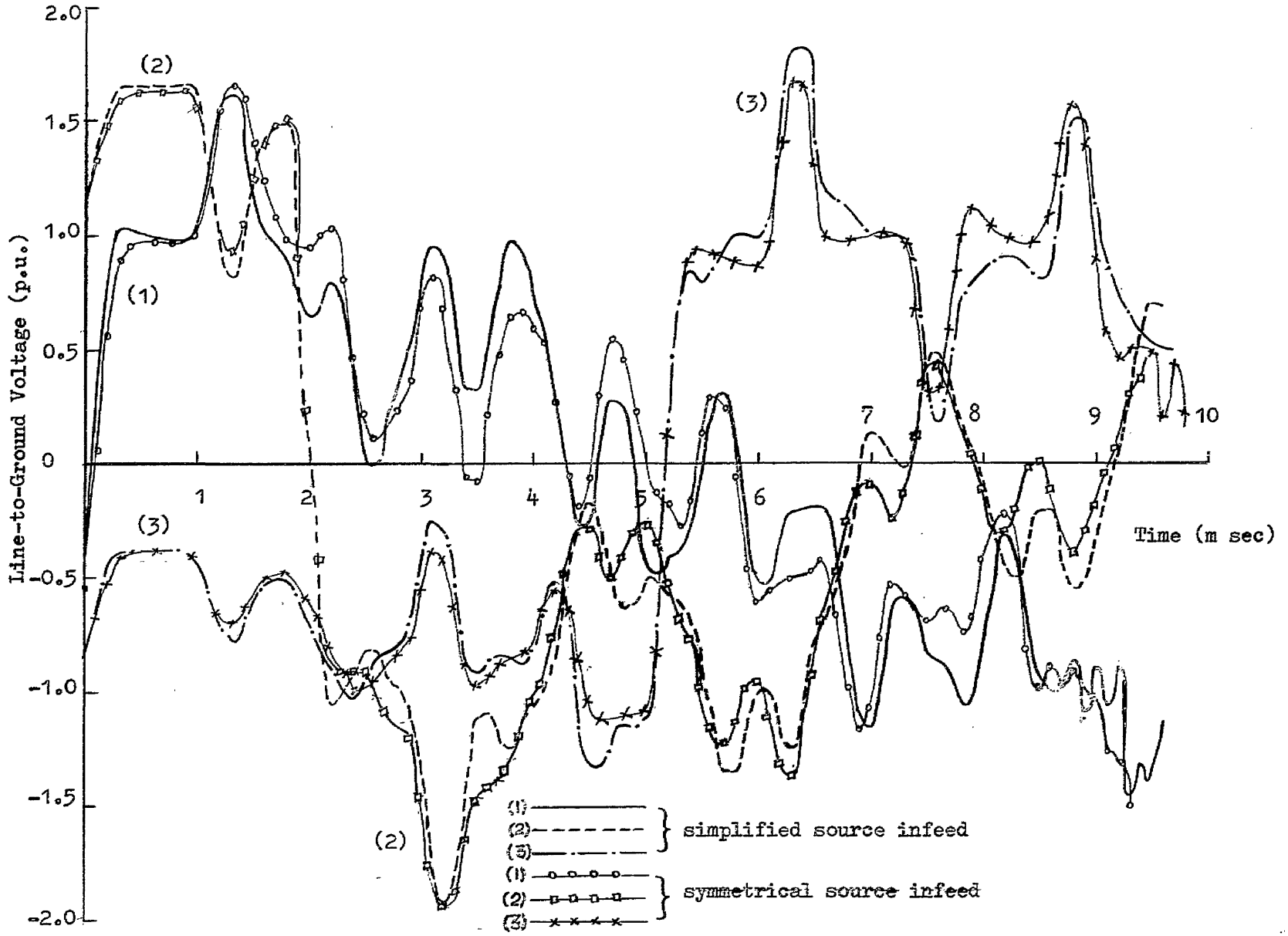

FIG. (10.14b). EFFECT OF SIMPLIFIED AND SYMMETRICAL SOURCE REPRESENTATION ON SENDING END TRANSIENT VOLTAGES OF 100-MILE PRECHARGED LINE

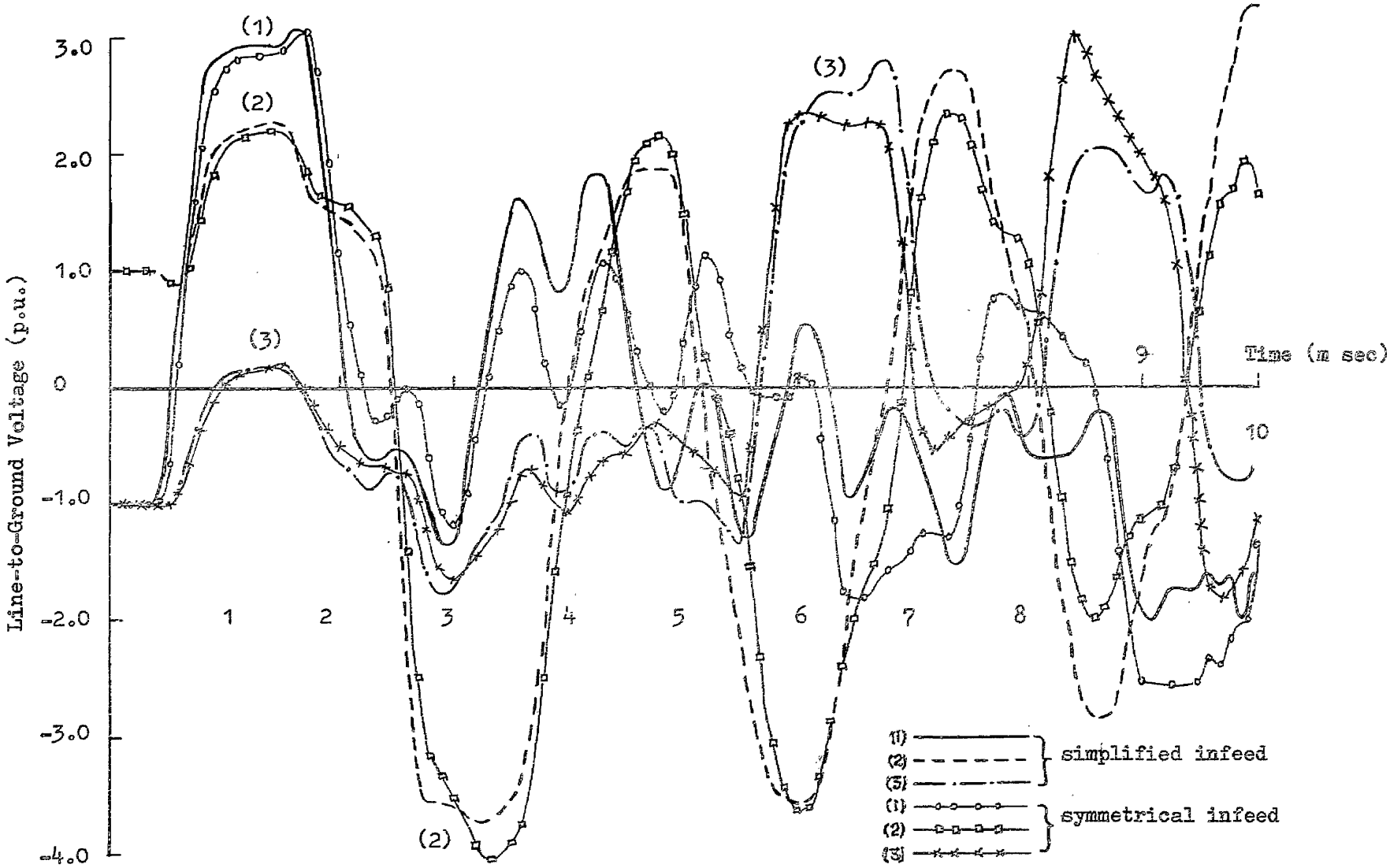

FIG. (10.14c). EFFECT OF SIMPLIFIED AND SYMMETRICAL SOURCE REPRESENTATION ON RECEIVING END TRANSIENT VOLTAGES OF 100-MILE PRECHARGED LINE

case in which a simplified source representation has been considered and the other a symmetrical circuit form of the source has been dealt with. Trapped charges of -1.0 p.u. exist on phases 2 and 3 and +1.0 p.u. on phase 2. The presence of trapped charges causes overvoltages of nearly 2.0 p.u. on the source side and about 4.0 p.u. on the line side receiving end. Such voltage magnitudes call for precautionary measures to be taken using reactor compensation and resistance switching [66].

The results again show the agreement of the response patterns obtained when the two source models are used. A detailed examination of these responses show that with trapped charges that the uncoupled source model provides a mean value of the source side response before second and third pole closure. For precise solutions it is important to use, therefore, the symmetrical form of representation though again from a practical point of view no greater advantages are gained unless shorter periods of observation are considered.

CHAPTER ELEVEN

CONCLUSIONS

11.1 General

Transmission of electrical power over long distances is of particular interest for countries where economic energy sources remote from centres of consumption are available. The wide knowledge and experience with high voltage A.C. systems in contrast with high voltage D.C. systems has justified the approach to the problem of very long-distance transmission from the A.C. point of view in the present investigation. Some fundamental steady-state properties of very long lines have been explored; these relate to methods of extending line lengths in relation to transfer of economic blocks of power at high voltages through the use of series and shunt compensation principles. Lines in the region of a quarter-to-half wavelength have been analysed for purposes of determining their fault characteristics and these have been extended to the study of apparent impedances seen by distance relays. The concern about the steady-state response of long-distance lines has led into investigations of problems of transient response for multiconductor transmission lines with reference to energising conditions.

The basic analytical tool used in this work has been the theory of modal analysis[18] derived from the concept of eigenvalue analysis. Through the use of this theory the identity of the system phase conductor has been retained and calculations have been carried out by representing each phase conductor individually. This has helped in revealing steady-state long line peculiarities that are up to the present time unknown; in this respect predictions of the classical line theory have been shown to be seriously misleading.

The analytical formulation of the multiconductor line transient problem has been developed from the steady-state equations formed through modal analysis and the application of Fourier transform technique which is recognized as a superior analytical method for the investigation of transient phenomena. The work presented in this thesis has extended the field of application of the Fourier transform technique, recently described for the handling of linear problems[21], to cover the analysis of non-linear problems of which the problem of sequential energisation of multiconductor lines is of particular interest.

A new approach to the analytical development of the system transient response using a Fourier series representation of the frequency function has been presented and its potential has been shown to be tremendous.

Systematic studies of multiconductor line transient response under energisation condition have been carried out and interpretation of the switching surge patterns through the concept of natural modes of propagation has been provided. The studies have included important effects such as source considerations and line trapped charges. The case of non-simultaneous pole closure of a circuit breaker has been dealt with. Precise estimations of restriking voltage calculations have been considered and attention has been given to the reduction of transient overvoltages of long lines through the use of reactive compensation.

The analysis has been carried out using the Manchester University Atlas Digital Computer.

11.2 Steady-state Long Line Response

The following conclusions are drawn for the section of the thesis dealing with the steady-state properties of very long lines:-

1. From a consideration of the general impedance loci of faulted multiconductor lines, it has been shown that for unbalanced-type faults that power frequency resonance occurs at approximately an eighth-wavelength and not a quarter-wavelength as predicted by classical transmission line theory. Due to the asymmetrical nature of the fault which is either earthed or isolated from earth, interaction takes place between the capacity currents of the floating conductor(s) and the inductive current of the faulted conductor(s). This interaction takes place between two quantities of opposite polarity and with the progressive increase in the fault distance the falling inductive current and the rising capacitive current eventually results in a minimum at a lower than a quarter-wave point and thus results in the "false" resonance shown by the eighth-wavelength point.

2. The classical pattern of the circular short-circuit loci with a quarter-wave resonance point has been confirmed for a balanced-type fault and in this respect is in full agreement with earlier predictions.

Peculiar phase impedance loci characteristics have been obtained for various fault combinations involving one or more phase conductors of horizontal or vertical circuit lines. These not only occupy the first and fourth quadrants of the R-X plane but are also contained in the second and third quadrants thus indicating a negative resistance component of the apparent impedance which has not up till now been considered in the design problems of distance relays. The reason for these peculiar loci shapes is primarily due to the aforementioned fault current and capacity current interaction. An additional complicating factor in the case of earth faults is due to the presence of a zero-sequence mode

travelling at a much lower velocity than the line aerial modes which travel at near the velocity of light.

4. The principles of distance protection schemes have previously been considered satisfactory for the identification of faults isolated from ground for all lengths of line. The results of studies carried out here have clearly shown the inadequacy of present distance protective equipment in coping with these types of fault in the case of very long lines. Extensive earth fault studies carried out on very long lines have revealed the limitations of sound-phase and residual compensated equipment in discriminating against faults on these lines. The relaying quantities obtained for sound-phase and zero-sequence relays are based on assumptions that the line is short in which case the line capacity current has justifiably been neglected. The uncompensated apparent impedance loci of long lines have shown the pronounced departure from the straight line impedance characteristic of a faulted short line and the reason is mainly due to the presence of long line capacitance current which has not been compensated for. Further work along these lines will be necessary for design modification of existing type protective schemes from the view-point of the line capacitance current for their satisfactory operation on very long lines

5. The steady-state performance studies carried out on very long lines have reaffirmed the effectiveness of the series capacitor in extending transmission distances and thus in coping with the problem of transfer of economic blocks of power over long lines. It has been shown in the thesis that the 50 Hz overvoltages across the series capacitor terminals can be minimized if the total series compensation of the line is divided among smaller groups and these then distributed along the line. Further reduction of these overvoltages and as a consequence of smoothing out of the long line voltage profiles can be successfully brought about by the application of shunt compensation. The object of shunt compensation being to cancel out certain proportions of the great capacitive power

generated by a long line which is responsible for the line internal voltage rises and is a direct cause of pronounced Ferranti effect voltage rises. The connection of the line shunt reactors at the series capacitor terminals has been shown to produce satisfactory service operating conditions, both for a smooth voltage profile and an ease on the demand of reactive power from either load of generation points for line charging purposes.

6. The optimum number and location of compensating stations can be determined according to the particular length of line and operating conditions under consideration. It has been shown, however, that one series/shunt compensating station at least will be needed for distance intervals of 200 miles on very long lines for the maintenance of satisfactory operating conditions.

7. Compensation studies have been carried out on a three-phase basis in order to investigate the pattern of power distribution on the asymmetrical phases of untransposed lines. In the past compensation studies were carried out on an equivalent single phase basis on the assumption that the line was fully transposed and hence that the power capability of the individual phases was the same; the findings were taken as applicable for untransposed lines. On the basis of the past methods heavier load transfer on very long lines were thought to be possible through the application of greater degrees of series compensation. Compensation degrees in the range of 80% to 90% were proposed[9] and in fact, up to 100% were believed to be possible[2]. With the methods of this thesis where the realistic case of a non-transposed line has been considered it is shown that the maximum degree of series compensation, assuming equal capacitors introduced in all phases, is governed entirely by the power carrying capacity of the individual phase conductors; this need not necessarily be

the same for all phases of a three-phase line. It is shown in a particular case of study that for degrees of series compensation greater than 80%, that certain phases show an increase in power transfer while others begin to show a decrease which will eventually lead to negative power transfer for extremely high degrees of compensation. From the series of studies carried out it may be suggested that for untransposed lines the maximum possible degree of series compensation is in the region of 80%. Exact values can only be determined from detailed examination of the particular cases of interest.

8. The effect on conductors asymmetry on the performance of an untransposed Line has been demonstrated from considerations of power transfer, this has reflected on the power unbalance of the separate phases. This unbalance property has already been shown to constrain the maximum possible degree of series compensation. A serious effect of the line unbalance is the production of undesirable negative-sequence currents that are hazards to machines, and also zero-sequence currents that could affect the operation of ground relays and result in interference to communication circuits[52]. Preliminary investigations carried out in the thesis have revealed considerable degrees of negative-sequence and zero-sequence unbalances in untransposed circuit lines. The conclusion arrived at here is that the problem of unbalance can not be ignored and that in the design stages of long untransposed lines extensive studies along this direction are necessary. No attempts have been made here to carry out studies relating to line balancing. It is possible, however, that the introduction of unequal compensating elements on the separate phases of an untransposed line may prove to be an effective means of balancing the line. This will justify further investigation in this direction because if positive results are achieved, substantial savings in transmission costs will be realized owing to the

elimination of the need for conductor transposition which is becoming more of a problem with the continual rise of system voltages and hence the inevitable use of multiple conductors.

11.3 Multiconductor Line Transient Response

A comprehensive analysis of the multiconductor Line transient response due to the effect of switching surges has been presented in this thesis and the following conclusions are drawn from the pattern of the investigation and the results of studies:-

1. The interest in switching phenomena has arisen as a result of the implementation of higher voltages and also due to the probability of their continual rise to as higher levels as 1000 KV^2. Consequently recent investigations have been concerned with studies pertaining to the propagation of switching surges on transmission systems rather than the propagation of lightning surges.

2. The review of the past methods for the analysis of the transient response of power systems presented in this thesis has pointed out to the limitation of the transient analyser approach in dealing with large complex networks. On these machines these complex networks can not be analysed for their transient response without making approximations and certain assumptions for example the lumped parameter representation of distributed parameter networks i.e. transmission lines and cable systems. The limitation of travelling wave methods has also been brought out, particularly their handling of lumped parameter elements by the method of transmission line stub representation and their ignoring of the frequency dependence of the system parameters and earth return path.

3. The advantages of the Fourier transform technique as a powerful tool for transient investigations have been indicated. The modified Fourier method[19,20] has been used in conjunction with the theory of modal

analysis[18] for the study of the propagation of switching surges on transmission lines. The results of studies carried out have shown the versatility of the theory of modal analysis reflected in the ease of obtaining the transient solutions from the network's steady-state equations. The same steady-state computer programs are applicable to the transient calculations and as a result efficiencies in computation are realized.

4. The Fourier transform technique used for the investigation of transmission line transient response has shown that the representation of the system response in the time domain has taken the form of a repetitive Fourier series. As a consequence the maximum possible observation time is limited to half the periodic time of this series; studies have revealed that the practical limits of the observation time of interest are in fact limited to about 80% to 90% of this periodic time due to an instability encountered in the inversion process of the complex Fourier integral. The choice of the shift constant "a" has been based on an engineering consideration whereby the magnitude of the repetitive stimulus is allowed, artificially, to decay exponentially to about a hundredth of its initial value at the end of the observation time before the following disturbance starts. This is done to avoid interference problems which will distort the result. The final result is readjusted by the rising exponential term. The choice of the step length "ω_o" is also based on the periodic time of the Fourier series.

It has been indicated in this thesis that a deeper understanding of the Fourier transform method is required for full appreciation of its power. The investigation has looked into some of the fundamental problems associated with the modified Fourier transform in an effort to remove the constraint of the theoretical maximum observation time

dictated by the Fourier series representation of the inversion integral. It has also been concerned with the provision of a more sound basis for the choice of the step length "ω_o" and the shift constant "a". It is believed, from a consideration of the results of the investigation, that these aims have been achieved. The new method of approach proposed and based on a Fourier series representation of the frequency function $f(\omega)$ over the truncation range has yielded a theoretical 4:1 improvement in the range of observation time for approximately a 6% increase in the total number of harmonics. This result is indicated in Fig. (7.1). It has also provided a rational basis for the choice of the factors concerned. It is important to note that the improvement is gained without impairing the rise time.

This new concept has made possible a clearer understanding of the inversion integral, namely that the longer observation times are associated with the low frequency regions of the "ω" function and that shorter observation times are associated with the high frequency regions. This has introduced the concept of a non-linear step "ω_o'". A shorter step length can be chosen for a precise definition of the frequency function in the regions where this varies rapidly which can be compensated for by the selection of a wider step length in the regions of slow variation.

Although not explored in full detail with regard to application problems for transient studies, it is believed that the theoretical foundation has been laid for a method which has a great potential. This approach opens a new scope for further investigation for its practical implementation. Apart from the gain in observation time limit which will allow a range of transient studies to be carried out in one computation process and hence yield efficiencies in computation,

instability problems of the older method type are non-existent. The Solodovnikov[71] sine integral which proved to be unstable by the older method has in fact yielded stable results by the new method.

3. In a recent work[21] the Fourier transform technique has been used for the study of switching transients on transmission systems. The technique has been applied to linear problems. The present investigation has also been concerned with a study of the propagation of switching surges on transmission lines using this technique, it has, however, gone beyond this existing work in analysing non-linear problems particularly the problem of sequential energisation of a transmission line which is faced in practice due to the non-simultaneous closure of the circuit breaker poles. The treatment of line trapped charges and the analysis of restriking voltage transients are other examples of non-linear problems that have been dealt with.

The piecewise technique developed in chapter (8) for the handling of non-linear problems has proved to be very successful from a consideration of the results for the particular examples quoted above. It is compatible with the Fourier transform technique since it forms the analytical transform of an arbitrary curve by breaking it down into a number of strips and linearizing the curve joining the two points on a strip. Linearization over the strip is only a first approximation which was found sufficient for the purposes of the present investigation. It is also possible to parabolize over the strip for further precision, this is a problem in practical application.

The range of non-linear problems open to investigation by this new method is wide. Resistance switching in three-phase systems, lightning arrester operation (Appendix 11), saturation effects in reactors and

transformers are typical practical problems that can now be looked into.

4. Transient studies carried out on simple systems through the use of a digital computer and by the methods of modal analysis and the modified Fourier transform have yielded results which compare favourably well with slide rule calculations using Bewley lattice diagram method. This check i.e. starting with the simplest of systems is a necessary confirmation on the correctness and validity of the digital computer program. The concept has been adopted throughout the investigation.

5. In the majority of studies carried out for first pole closure conditions, voltage doubling has occurred at the open-circuited end of the short and medium lines, the departure from exact doubling effect is due to attenuation of aerial and earth modes. The longer line investigations carried out with regard to this switching problem have shown that for the case of a 600-mile line a voltage of four times the peak line to ground voltage of the system has appeared at the open-circuited receiving end of the energised conductor. The reason for this is partly due to Ferranti effect of the longer line and partly due to resonance conditions between the earth mode frequency and the line natural frequency.

Methods of series and shunt compensation have been shown to yield substantial reductions on the magnitude of the overvoltage. The optimum number and location of the compensating stations has been carried out in accordance with the long line steady-state investigations and has confirmed the need of at least one compensating station every 200 miles for satisfactory operating conditions.

6. Practical sequential transient calculations that are carried out on a 50-mile line have demonstrated the power of the method used. The practical method of computation is substantiated by a computation check

in which calculations have been restarted from the instant of first pole closure after the third phase has been energised. Though as shown by Fig. (9.14) the two results are not exactly identical to each other it can be said that they are nearly identical to all intents and purposes. A further proof is demonstrated in Fig. (10.11) which is a comparative study of sequential transients on a precharged line. The comparison is carried out against results[75] obtained from a Bewley lattice diagram calculation. The validity of the method presented is clearly evident from this comparative study. A further point worthy of note from this demonstration is the ease with which line trapped charges have been handled.

The problem of severe overvoltages has been encountered in the case of long lines and reactive compensation has been suggested as a means of reducing these overvoltages. The severe overvoltages appearing as a result of energising a 100 mile line with trapped charges of opposite polarity to the energising wave also call for control. Whereas reactive compensation can be applied to yield positive results, resistance switching is also being recognized as an effective means of reducing the magnitude of the transient overvoltage. The problem of resistance switching calls for further investigation.

7. The present work has looked into the problem of source simulation and has proposed two methods whereby source feeders terminating at a switching station can be represented. The distributed parameter nature of the source is seen to be retained in both methods while reduction in computation time has been achieved by these methods of representation. Detailed studies have been carried out on these possible methods and the results compared with those obtained on the basis of fault MVA and system KV for the representation of the station in question.

Source effects and trapped charges have also been analysed and the results presented in chapter ten may be regarded as typical system studies. In this respect chapter ten may be regarded as a model for building up further studies on practical systems.

8. The recovery voltage transient study presented in the thesis is an additional proof of the versatility of the method described for handling non-linear problems. No claim can be made that the short line fault problem is dealt with here. Further work is needed along this direction and the method that has been proposed provides the facility for the investigation. The problem can be treated on a single-phase bases on the assumption of simultaneous pole tripping or on a three-phase basis for a more practical approach where sequential pole tripping occurs.

11.4 Comment

For the purposes of investigations carried out in this thesis a single circuit three-phase line of horizontal and vertical configuration has been chosen since this in fact forms the basis on which future power systems in the country are built. The computer programs have in fact been developed in a generalized manner to cope with multicircuit lines. The basic principles have been laid down and further work can be carried out for particular cases of interest in the field of long-distance transmission.

APPENDIX (2)

Formulation of Series Impedance and Shunt Admittance Matrixes

Consider a system of "N" conductors and their images below the earth plane. Fig. (a) shows three such conductors i, j, k and their images i', j', k'.

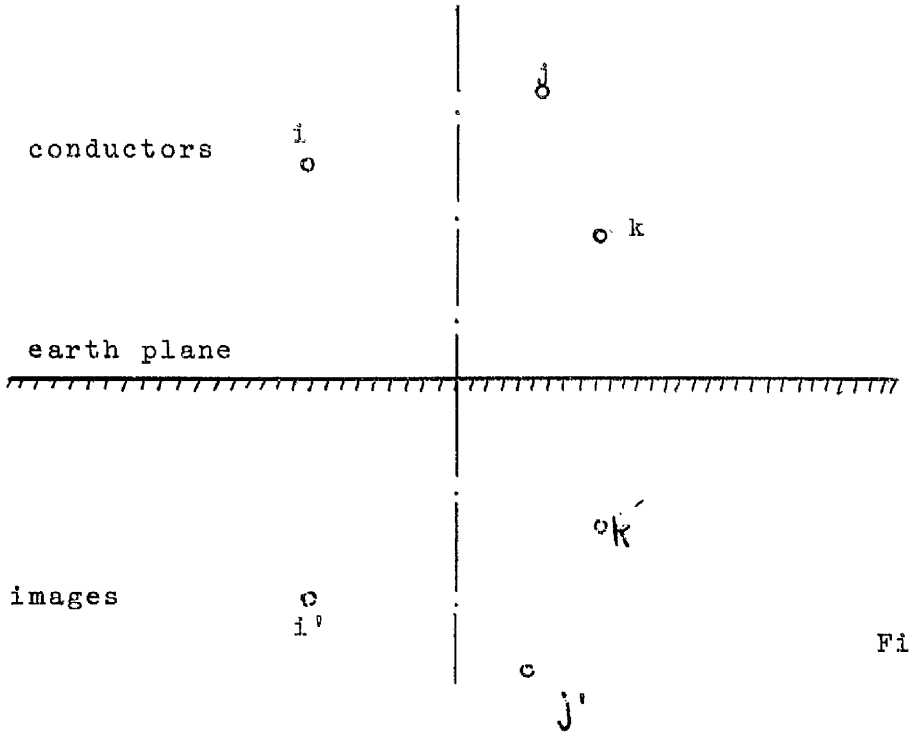

Fig. (a)

1. Shunt Admittance Matrix

This is given by the general expression:-

$$Y = j\ 2\pi\omega\varepsilon_0[\log_e\ (D/d)]^{-1}$$

The diagonal elements of the Y matrix are obtained by substituting the radius of the conductor in place of d and the distance between the conductor and its own image in place of D. For the off-diagonal elements D will now be the distance between the ith conductor and the jth

conductor image and d the distance between the ith and jth conductors. If a bundled conductor is considered then the corresponding radius for the self terms will be the radius of the bundle.

Two types of bundled conductors will be used and the equivalent phase bundle radii will now be given:-

i. Two-conductor bundle where the sub-conductors are separated by a distance s

$$d = \sqrt{r.s}$$

r being the radius of sub-conductor

ii. Quad-conductor bundle where the sub-conductors are situated on the corners of a square of side s

$$d = \sqrt[4]{2^{1/2}(r.s^3)}$$

These formulae for the equivalent bundle radius are derived on the assumption that the spacing s between the sub-conductors are small compared with their heights above ground; this is true in practice.

The matrix term $[\log_e(D/d)]^{-1}$ generally consists of Ne rows and Ne columns corresponding to the earth wires whose potentials may be assumed to be zero. Since propagation only on the phase conductors is of interest the "Ne" rows and columns of this matrix are removed.

2. Series Impedance Matrix

This consists of impedances due to geometrical configuration and earth return path and additional diagonal

terms representing the self impedance of the conductor. Each of these will be given in turn.

i. Impedance due to Geometry

This is purely reactive and is given by:-

$$Z_g = \frac{j\omega\mu_0}{2\pi} [\log_e(D/d)]$$

The matrix term $[\log_e(D/d)]$ is formed in the same way as in the formation of the system admittance matrix.

ii. Impedance due to Earth Return Path

$$Z_e = R_e + j X_e$$

where $R_e = 2P\omega\mu/2\pi$

$X_e = 2Q\omega\mu/2\pi$

The series for P and Q are given in reference (24). These are arranged in a manner suitable for power frequency and high frequency calculations.

iii. Self Impedance of Conductors

This is a diagonal matrix.

For power frequency problems

$$Z_c = \frac{\rho}{S_n \cdot S_r \cdot \pi} + j \frac{\omega\mu_0}{2\pi} \log_e (R/_{G.M.D.})$$

where

ρ = conductor resisitivity

S_n = conductor strands. In the case of steel reinforced conductors the presence of steel strands can be ignored since their contribution is small. In this case S_n will be the

total number of strands minus the steel strands

S_r = radius of individual strand

G.M.D. = geometric mean radius of conductor

R = overall radius of a concentric stranded conductor. For a stranded conductor the number of strands in each layer is an exact multiple of six and the total number of wires is then given by $\{1 + 3k(k+1)\}$ where k is an integer. The overall radius is given by $R = S_r(2k+1)$.

For high frequency problems or in the case of conductors with high permeability skin effect is pronounced; an alternative formula for the conductor internal impedance is:-

$$Z_c = R_c + j\ X_c$$

where:-

$$R_c = X_c = \frac{2.25\rho_m}{\sqrt{2}\ \pi\ S_r\ (S_{no}+2)}$$

S_{no} = number of conductor outer strands

$$m = \left(\frac{j\omega\mu}{\rho}\right)^{1/2}$$

μ = conductor permeability.

The empirical constant 2.25 caters for conductor stranding.

For the case of a bundled conductor it is important that

the internal impedance of the sub-concuductor be divided by the number of sub-conductors in a bundle in order to obtain the internal impedance of the multiple conductor.

iv. Total Series Impedance Matrix

$$Z = Z_g + Z_c + Z_e$$

Z includes terms corresponding to the phase conductors as well as earth wires. The removal of the earth wires from the system impedance matrix without disturbing their sheilding properties is effected by inverting Z, removing the rows and columns corresponding to the earth wires. The resultant matrix without the earth wires is reinverted to provide the system series impedance matrix. In so doing use has been made of the fact that the earth wires potential along their entire length is zero.

3. Normalized System Parameters

For practical considerations it has been found necessary to introduce a normalization factor $-\omega^2\mu_0\varepsilon_0$ obtained from the product of impedance and admittance coefficients $j\omega\mu_0$ and $j\omega 2\pi\varepsilon_0$ due to geometry. The division of the P matrix formed from the ZY product, by this normalization factor $\frac{}{2\pi}$ together with subtraction of a unit matrix from it eases the problem of convergence in the evaluation of system eigenvalues by the root-squaring technique. The actual system eigenvalues are obtained by addition of unity to the new computed eigenvalues with the proper adjustment effected by multiplication by the normalization factor.

APPENDIX (3)

Sound Phase and Zero-Sequence Compensation Principles of Distance Protection

(A) Phase-to-Ground Faults

Consider Fig. (1) which shows a single line to ground solid fault at a distance x miles from the sending end of a three phase transmission line.

The phase to earth voltage at the relaying point is given by:-

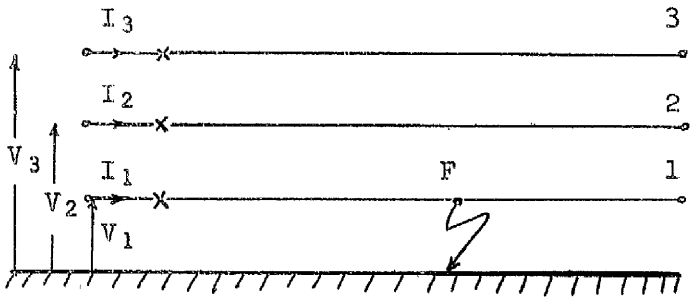

FIG. (1)

$$V_1 = x(Z_{11}I_1 + Z_{12}I_2 + Z_{13}I_3) \qquad - (1)$$

where Z_{11}, Z_{22} and Z_{33} are the self impedances of conductors, Z_{12}, Z_{23} and Z_{23} are the mutual impedances between the conductors.

The line is assumed to be short and untransposed with the impedances given in per mile length.

The earth-fault-loop impedance is given by:-

$$xZ_{11} = V_1/(I_1 + \frac{Z_{12}}{Z_{11}} \cdot I_2 + \frac{Z_{13}}{Z_{11}} \cdot I_3) \qquad - (2)$$

$$xZ_{11} = V_1/[I_1 + \{(Z_0-Z_1)/(2Z_1+Z_0)\}\{I_2+I_3\}] \quad - (8)$$

The relay in this case will also measure the earth-fault-loop impedance.

The zero sequence current for line to ground fault is defined by:-

$$i_0 = (I_1+I_2+I_3)/3$$

On substitution of this quantity equation (8) can be rearranged in another form

$$xZ_1 = V_1/[I_1 + \{(Z_0-Z_1)/Z_1\}i_0] \quad - (9)$$

The operation of the relay in this case is also a correct indication of the distance to the fault from the sending end except that the operating signal is now independent of the healthy phase currents as it is made up of the faulty phase current and a proportion of the residual current i_0. This form of compensation is known as residual or zero-sequence compensation and is derived on the assumption that the line is ideally transposed.

It is also possible to derive the residual compensation formula from a consideration of the positive, negative and zero sequence networks.

At the relay location

$$V_1 = x(Z_1i_1+Z_2i_2+Z_0i_0)$$

where i_1, i_2 and i_0 are the positive, negative and zero sequence currents of an earth fault

If the phase-to-ground relay on phase 1 is fed with a restraining signal equal to the phase-to-ground voltage on that phase and an operating signal which consists of a fault current on that phase plus a proportion of the healthy phase currents then the relay operation will give an indication of the fault position on that phase. The scheme is known as healthy-phase or sound-phase compensation.

When the line is transposed $Z_{12} = Z_{23} = Z_{13} = Z_m$ and $Z_{11} = Z_{22} = Z_{33} = Z_s$ where Z_s and Z_m are self and mutual impedances of the conductors.

$$\therefore \quad xZ_{11} = V_1/[I_1 + \frac{Z_m}{Z_s}(I_2+I_3)] \qquad - (3)$$

Equation (3) can be written in another form if use is made of the relationship between the self and mutual impedance terms of a transposed circuit and the positive, negative and zero sequence impedances of that circuit. These relationships are:

$$Z_1 = Z_s - Z_m \qquad - (4)$$

$$Z_0 = Z_s + 2Z_m \qquad - (5)$$

and since positive and negative sequence impedances are identical for transmission lines, (4) is also valid for the negative sequence impedance.

Solving (4) and (5) for Z_s and Z_m

$$Z_s = (2Z_1+Z_0)/3 \qquad - (6)$$

$$Z_m = (Z_0-Z_1)/3 \qquad - (7)$$

Subsitution of (6) and (7) in (3) yields:-

$$I_1 = i_0+i_1+i_2$$

$$\therefore \quad V_1 = xZ_{11}(i_1+i_2+(Z_0/Z_1).i_0)$$

$$xZ_1 = V_1/[I_1+((Z_0-Z_1)/Z_1)i_0] \qquad - (10)$$

(B) Phase-to-Phase Faults

The analysis of a double-phase fault on phases "1" and "2", and the method is applicable to three-phase faults, will now be considered

The voltages-to-neutral on phases 1 and 2 are given by:-

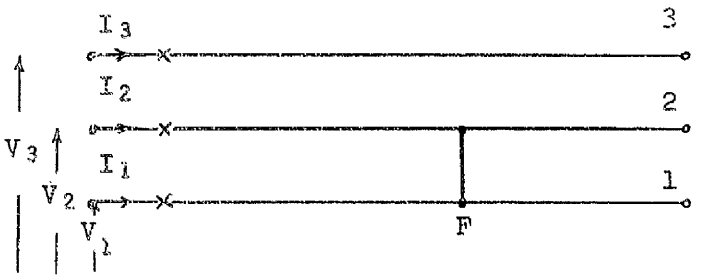

FIG. (2)

$$V_1 = x(Z_{11}I_1+Z_{12}I_2+Z_{13}I_3)$$

$$V_2 = x(Z_{22}I_2+Z_{12}I_1+Z_{23}I_3)$$

$$\therefore \quad V_1-V_2 = xZ_{11}(I_1-I_2) - xZ_{12}(I_1-I_2) + x(Z_{13}-Z_{23})I_3$$

$$(V_1-V_2)/(I_1-I_2) = x(Z_{11}-Z_{12}) + x(Z_{13}-Z_{23})I_3/(I_1-I_2) \qquad - (11)$$

In practice the phase-to-phase relaying quantities are determined on the assumption that the circuit is transpoed in which case equation (11) reduces to:

$$(V_1-V_2)/(I_1-I_2) = x(Z_s-Z_m)$$

and making the substitution that $Z_s-Z_m = Z_1$

$$(V_1-V_2)/(I_1-I_2) = xZ_1 \qquad - (13)$$

In this case it is clear that if the phase-to-phase relay is fed with a restraining signal proportional to the difference of phase-to-neutral voltages at the relay location and an operating signal proportional to the difference between the sending end fault currents that operation will occur if the apparent impedance xZ_1 seen falls below the minimum setting of this relay. The apparent impedance in this case is clearly proportional to the positive sequence impedance of the line with the distance to the fault as the constant of proportionality.

For faults through impedances the expressions of (A) and (B) will be modified by additional terms containing the impedance of the fault path.

APPENDIX (7)

Analytical Formulation of Time Response Using Sine and Cosine Transforms

Consider the Fourier Inverse Transform

$$f(t) = (1/2\pi) \int_{-\infty}^{+\infty} f(\omega)\exp(j\omega t)\, d\omega$$

$f(\omega)$ is complex.

Let $R(\omega)$ be real component of $f(\omega)$

and $I(\omega)$ be imaginary component of $f(\omega)$

$$f(t) = (1/2\pi) \int_{-\infty}^{+\infty} [R(\omega) + jI(\omega)][\cos\omega t + j \sin \omega t]d\omega$$

Noting that $R(\omega).\sin \omega t$ and $I(\omega).\cos \omega t$ are odd functions of ω

$$f(t) = (1/2\pi)\int_{-\infty}^{+\infty} [R(\omega)\cos\omega t - I(\omega)\sin\omega t]d\omega \qquad - (1)$$

For practical systems

$f(t) = 0$ for $t < 0$ and on substituting $t = -t$ in (1), we have

$$0 = (1/2\pi) \int_{-\infty}^{+\infty} [R(\omega)\cos\omega t + I(\omega)\sin\omega t]d\omega \qquad - (2)$$

since $\cos(-\omega t) = \cos \omega t$ and $\sin(-\omega t) = -\sin\omega t$ adding (1) + (2) we get :–

$$f(t) = (1/\pi) \int_{-\infty}^{+\infty} R(\omega) \cos \omega t\, d\omega$$

$R(\omega).\cos \omega t$ is an even function of ω

$$\therefore \quad f(t) = (2/\pi) \int_0^{\infty} R(\omega) \cos\omega t \, d\omega \qquad - (3)$$

Subtracting (1) - (2), we get

$$f(t) = -(1/\pi) \int_{-\infty}^{\infty} I(\omega) \sin\omega t \, d\omega$$

$I(\omega).\sin\omega t$ is an even function of ω

$$\therefore \quad f(t) = -(2/\pi) \int_0^{\infty} I(\omega) \sin\omega t \, d\omega \qquad - (4)$$

Equations (3) and (4) are the sine and cosine transforms due to Solodovnikov and others[71].

If a truncation frequency W is taken then the limits of integration change accordingly.

Consider equation (4) and let $I(\omega)$ be represented as a Fourier series of the form

$$I(\omega) = (\pi/W) \sum_{-\infty}^{+\infty} b_n \sin(n\omega\pi/W)$$

Substitute $\pi/W = t_0$

$$\therefore \quad I(\omega) = t_0 \sum_{-\infty}^{+\infty} b_n \sin(\omega n t_0)$$

Substituting for $I(\omega)$ given in (4) the above expression for the representation of $I(\omega)$ we get

$$f(t) = -\sum_{-\infty}^{+\infty} t_0 . b_n \, (2/\pi) \int_0^{\pi/t_0} \sin \omega n t_0 \sin\omega t \, d\omega$$

$$f(t) = -\sum_{-\infty}^{+\infty} t_0 . b_n . (2/\pi) . (1/2) \int_0^{\pi/t_0} \{\cos\omega(t-nt_0) - \cos\omega(t+nt_0)\} d\omega$$

or

$$f(t) = -\sum_{-\infty}^{+\infty} b_n \left[\frac{\sin\pi(t/t_0-n)}{\pi(t/t_0-n)} - \frac{\sin\pi(t/t_0+n)}{\pi(t/t_0+n)}\right] \qquad - (5)$$

If $t = rt_0$ where r is an integer

$$\frac{\sin\ \pi(t/t_0-n)}{\pi(t/t_0-n)} = 0 \text{ for all values of r.}$$

A similar expression under this condition to the one obtained using the exponential form of the integral is thus found.

$$f(t) = -\sum_{-\infty}^{+\infty} b_n \frac{\sin\pi(t/t_0-n)}{\pi(t/t_0-n)} \qquad - (6)$$

It can similarly be shown using form (3) of the inversion integral and a cosine series representation for $R(\omega)$ with Fourier coefficients a_n as

$$R(\omega) = t_0 \sum_{-\infty}^{+\infty} a_n \cos(\omega n t_0)$$

that f(t) is given by

$$f(t) = \sum_{-\infty}^{+\infty} a_n \frac{\sin\ \pi(t/t_0-n)}{\pi(t/t_0-n)} \qquad - (7)$$

APPENDIX (9.1)

Determination of Time for Circuit Interruption

Assume linear variation of fault current in the neighbourhood of current zero i.e. HIK in the figure shown.

Let f_{n-1} be the magnitude of fault current obtained numerically at the $(n-1)^{th}$ time interval.

Let f_n be the magnitude at the n^{th} time interval.

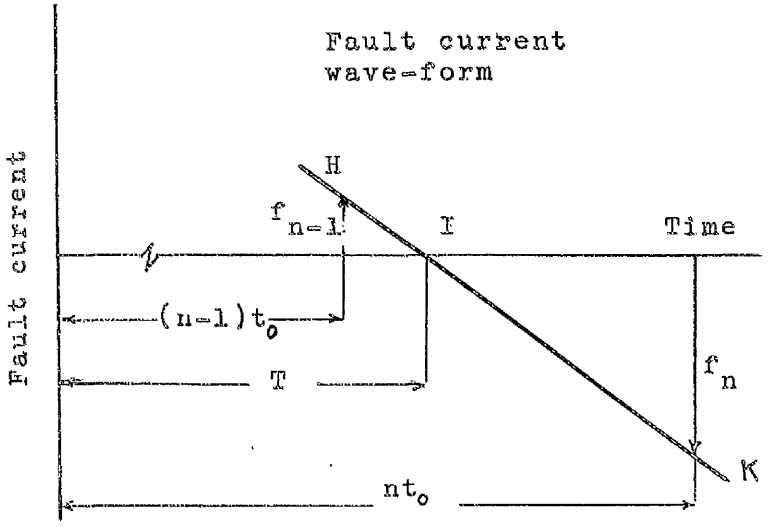

t_0 --- the time interval used in the calculation

T --- the time at which the circuit is interrupted.

From the geometry of the figure

$$\frac{f_{n-1}}{T-(n-1)t_0} = \frac{-f_n}{nt_0-T}$$

$$f_{n-1}\ (nt_0-T) = -\ f_n\{T - (n-1)t_0\}$$

giving

$$T = nt_0 - (f_n/f_n-f_{n-1}).t_0$$

The interval of time $\{T - (n-1)t_0\}$ is in fact a non-linear time interval which becomes the normal step "t_0" if f_n is made equal to f_{n-1}.

There would be a certain error involved in making the assumption that this sinusoidal current wave varies linearly in the vicinity of T but the error for the sort of angle involved is small and can be neglected.

APPENDIX (9.2)

Fourier Transform of Injected Current for Restriking Transients Calculation

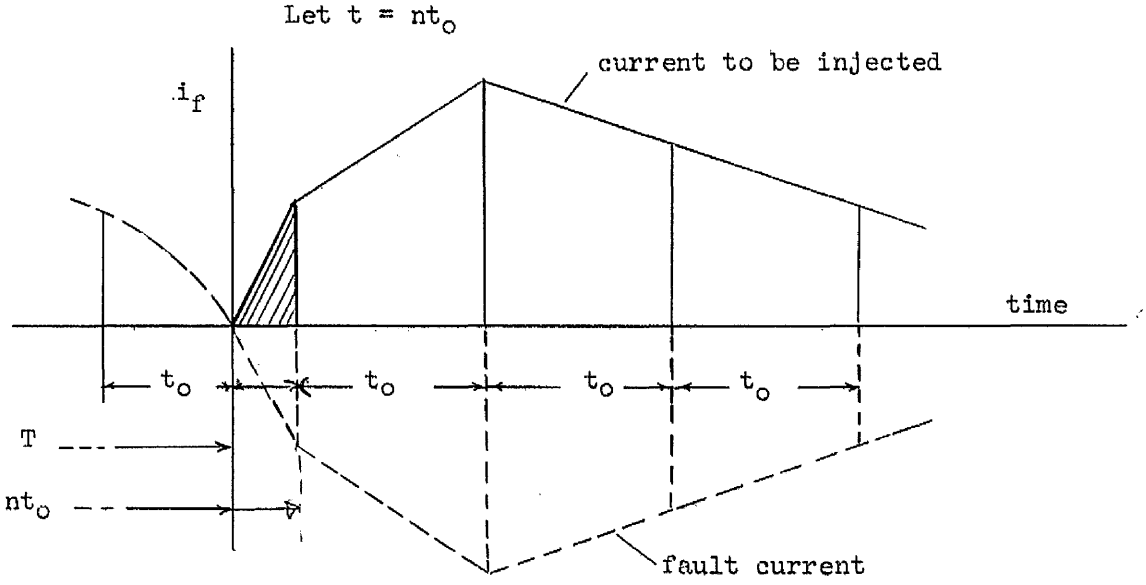

FIG. (1)

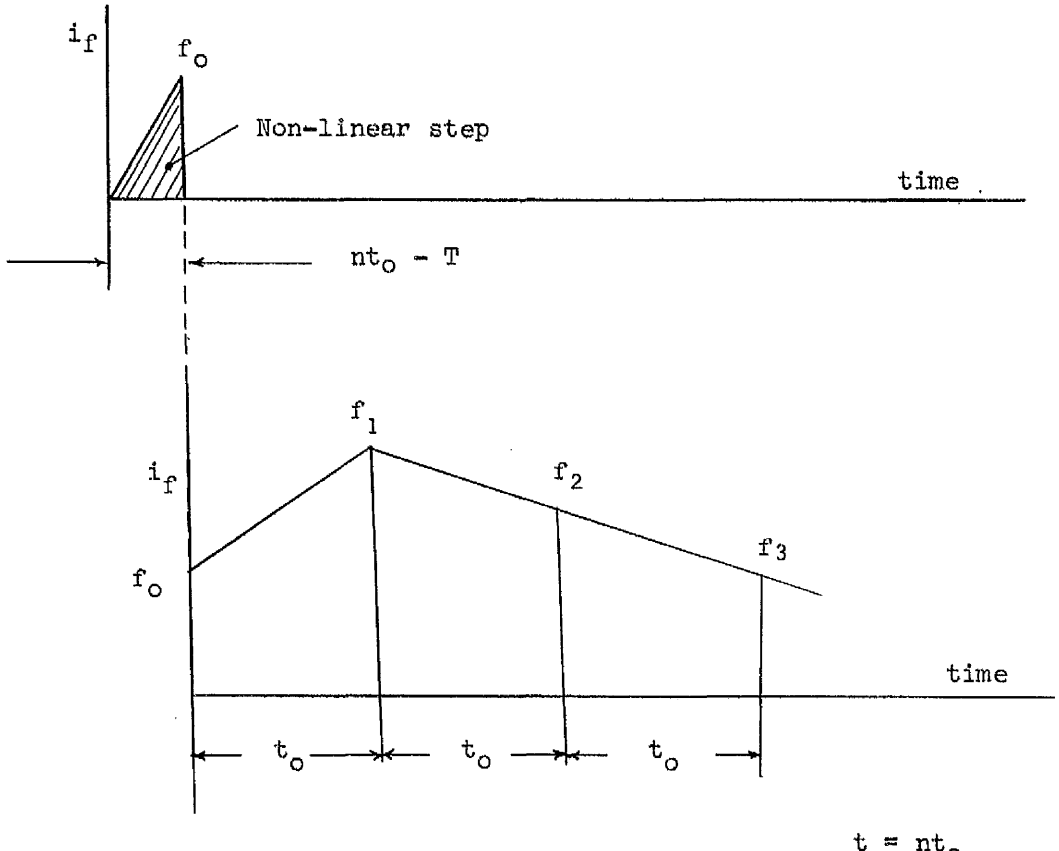

FIG. (2)

Transform of non-linear step:-

$$f(\omega) = (1/j\omega)\left[\{f_0/j\omega(t-T)\} - \{f_0/j\omega(t-T)\}.\exp(-j\omega t) - f_0[\exp(-j\omega t)]\right]$$

Transform of "N" linear steps

This is the same general transform given by equation(8.5) but modified by the shift operator $\exp[-j\omega(t-T)]$ where $(t-T)$ is the time delay of all linear steps as shown in Fig. (2) of this appendix.

Complete Transform

The complete transform of the injected current wave is the combination of the non-linear step transform and the transform of the "N" linear steps. This is given by:-

$$f(\omega) = \frac{1}{j\omega}\left[\begin{array}{l} f_0(1-1/j\omega t_0) + f_1/j\omega t_0 \\ + [f_{N-1}/j\omega t_0 - f_N(1+1/j\omega t_0)]\exp(-jN\omega t_0) \\ + 1/j\omega t_0 \sum_{n=1}^{N} (f_{n+1}-2f_n+f_{n-1})\exp(-jn\omega t_0).\exp[-j\omega(t-T)] \\ + f_0/j\omega(t-T) - f_0[1+1/j\omega(t-T)]\exp[-j\omega(t-T)] \end{array}\right]$$

APPENDIX (9.3)

Fourier Transform of Energising Voltages

The three phase voltages energising a line are given by

$$v_1 = \hat{V} \cos(\omega_s t + \phi_1) \quad - (1)$$

$$v_2 = \hat{V} \cos(\omega_s t + \phi_2) \quad - (2)$$

$$v_3 = \hat{V} \cos(\omega_s t + \phi_3) \quad - (3)$$

If the breaker poles close simultaneously then:

$$\phi_1 = 0°$$

$$\phi_2 = 120°$$

$$\phi_3 = 240°,$$

whereas for sequential pole closure the phase angle displacements include the general delay angles of closure.

Expanding (1), we have:-

$$v_1 = \hat{V}(\cos\omega_s t \cos\phi_1 - \sin\omega_s t \sin\phi_1)$$

and its Fourier transform is given by:-

$$\bar{v}_1 = \hat{V} \cos\phi_1 . \frac{j\omega}{\omega_s^2 - \omega^2} - \hat{V} \sin\phi_1 . \frac{\omega_s}{\omega_s^2 - \omega^2} \quad - (4)$$

Similarly the transforms of (2) and (3) can be found.

APPENDIX (10)

Eigenvalues and Eigenvectors of a Symmetrical Circuit

After eliminating the earth wires the basic impedance and admittance matrixes of a three phase symmetrical circuit are:-

$$Z = \begin{bmatrix} Z_s & Z_m & Z_m \\ Z_m & Z_s & Z_m \\ Z_m & Z_m & Z_s \end{bmatrix} \quad ; \quad Y = \begin{bmatrix} Y_s & Y_m & Y_m \\ Y_m & Y_s & Y_m \\ Y_m & Y_m & Y_s \end{bmatrix}$$

where Z_s, Y_s are average sum of all conductors self impedance and admittance terms.

Z_m, Y_m are average sum of all conductors mutual terms.

The "P" matrix is obtained from the product ZY.

Solving the characteristic equation to obtain the eigenvalues

$$P = ZY = \det \begin{bmatrix} P_s-\lambda & P_m & P_m \\ P_m & P_s-\lambda & P_m \\ P_m & P_m & P_s-\lambda \end{bmatrix} \cdot \begin{bmatrix} Q_{11} \\ Q_{21} \\ Q_{31} \end{bmatrix} = 0$$

where Q is a column of eigenvector matrix.

and $$P_s = Z_{ss} - 2Z_mY_m$$

$$P_m = -Z_sY_m + Z_mY_s - Z_mY_m$$

Factorizing the determinant

$$\begin{vmatrix} 0 & P_s+P_m-\lambda & 2P_m \\ -(P_s-P_m-\lambda) & P_s-\lambda & P_m \\ 0 & P_m & P_s-\lambda \end{vmatrix} = 0$$

i.e. $(P_s-P_m-\lambda)\ \{(P_s-\lambda)(P_s+P_m-\lambda) - 2P_m^2\} = 0$

This equation gives two identical roots P_s-P_m and a third root (P_s+2P_m)

$$\therefore \qquad \lambda_1 = \lambda_2 = P_s-P_m$$
$$\lambda_3 = P_s+2P_m$$

There are thus two propagation constants

$$\gamma_1 = \gamma_2 = \sqrt{P_s-P_m} \qquad \text{and } \gamma_3 = \sqrt{P_s+2P_m}$$

One possible form of eigenvector matrix to use is

$$\begin{bmatrix} 1 & 1 & -1 \\ -1 & 1 & -1 \\ 0 & 1 & 2 \end{bmatrix}$$

The characteristic impedance matrix is given by

$$Z_o = \begin{bmatrix} Z_{os} & Z_{om} & Z_{om} \\ Z_{om} & Z_{os} & Z_{om} \\ Z_{om} & Z_{om} & Z_{os} \end{bmatrix}$$

But $Z_o = Q\gamma^{-1}Q^{-1}Z$

$$Z_o = \begin{bmatrix} 1 & 1 & -1 \\ -1 & 1 & -1 \\ 0 & 1 & 2 \end{bmatrix} \cdot \begin{bmatrix} \frac{1}{\gamma_1} & 0 & 0 \\ 0 & \frac{1}{\gamma_3} & 0 \\ 0 & 0 & \frac{1}{\gamma_1} \end{bmatrix} \cdot \begin{bmatrix} 1/2 & -1/2 & 0 \\ 1/3 & 1/3 & 1/3 \\ -1/6 & -1/6 & 1/3 \end{bmatrix} \cdot \begin{bmatrix} Z_s & Z_m & Z_m \\ Z_m & Z_s & Z_m \\ Z_m & Z_m & Z_s \end{bmatrix}$$

from which

$$Z_{os} = \{(2/\gamma_1+\tfrac{1}{\gamma_3})Z_s + 2(\tfrac{1}{\gamma_3}-\tfrac{1}{\gamma_1})Z_m\}/3$$

and $$Z_{om} = \{(\tfrac{1}{\gamma_3}-\tfrac{1}{\gamma_1})Z_s + (2/\gamma_3+\tfrac{1}{\gamma_1})Z_m\}/3$$

Similarly the characteristic admittance can be found from

$$Y_0 = YQ\gamma Q^{-1}$$

APPENDIX (11)

Procedure for Handling Resistance Switching and Lightning Arrester Operation

1. Resistance Switching

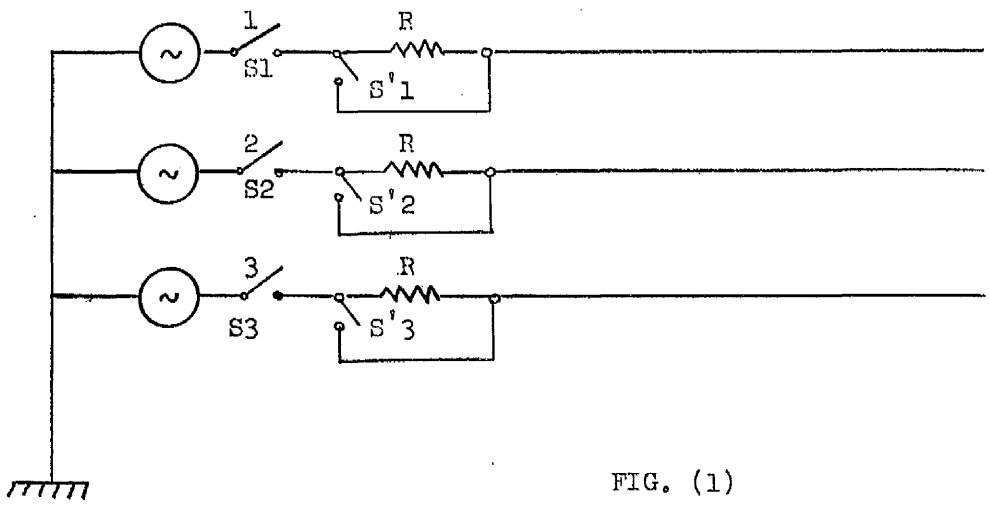

FIG. (1)

Consider Fig. (1) in which a three-phase line is energised through resistance R inserted in all three phases at the sending end of the line.

In practice Switches S1, S2 and S3 close sequentially thus energising the line through the switching resistance R. Later in time switches S1', S2' and S3' short out the resistors in a sequential manner too. In order to solve this problem digitally using the Fourier transform method the following procedure may be followed:-

i - Switch S1 is closed and the system response obtained as usual and with all three siwtching resistors in circuit. The induced voltage appearing across the second and third poles is stored.

ii - From the synthesis routine the transform of induced voltage across the second pole is determined; this is added to the analytical transform of the energising voltage of the second phase. Switch S2 is then closed (S1 remains closed and all resistors R stay in circuit). The system response is evaluated.

iii - In a similar manner the synthesis transform appearing across the third pole is obtained and added to the corresponding analytical transform after which S3 is closed. Now all three switches are closed and the line is being energised through the three resistors. The system response is evaluated up to the moment in time when all three resistances are to be shorted out. At this moment the computation is then stopped.

iv - The computation is restarted with all three phases energised simultaneously through zero resistance in phase 1 i.e. resistor of phase 1 shorted out, and resistors R in phases 2 and 3 i.e. their corresponding resistors still in circuit. The transform of voltage across pole 1 is purely analytical and that across poles 2 and 3 partly analytical and partly synthesis. The system response is obtained from this new time and up to the moment in time when the resistor in the second phase is shorted out.

v - Process (iv) is repeated but now with only resistor R in phase 3. System response is evaluated.

vi - Lastly the resistor in phase 3 is shorted out and the system response obtained.

2. Lightning Arrester Operation

Mechanism of Operation

Fig. (2) shows one phase of a three phase system consisting of an

overhead line and a lightning arrester connected at some intermediate point on the line for purposes of protecting some apparatus there from switching surges.

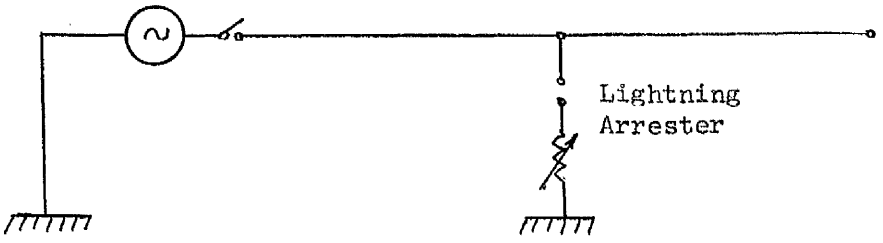

FIG (2)

The arrester consists of a spark gap which flashes over and thus shorts the line temporarily as soon as the magnitude of the switching surge between its live conductor terminal and neutral exceeds the normal system voltage but is below the insulation breakdown voltage[76]. A non-linear resistor is provided and connected in series with the gap to prevent the flow of power current to ground after the switching surge current has been discharged.

The non-linear relationship between voltage and current of a lightning arrester is given by what is known as its characteristic. As the discharge level is reached current flows and can be determined from this characteristic. The current drops to a minimum at a voltage level below the discharge level. The curve shown in Fig. (3) is a typical lightning arrester characteristic.

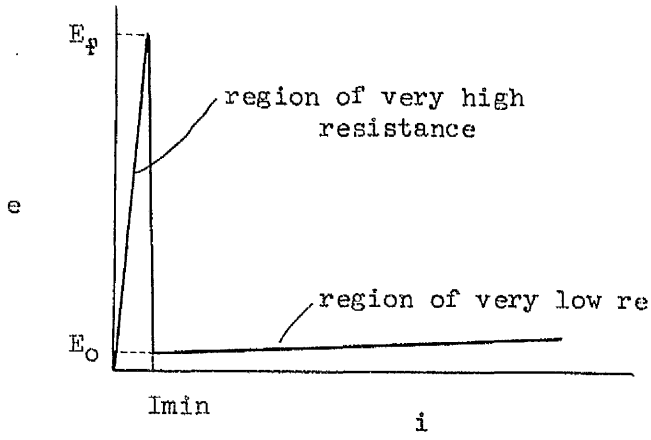

E_o - arc drop voltage

E_1 - flashover voltage

FIG. (3)

Procedure for Handling Operation

i The transient voltage $v_1(t)$ across the arrester terminals and current $i_1(t)$ flowing through it and given by $v_1(t)/R_1$ are obtained.

ii The modulus of $v_1(t)$ obtained from i is compared with the arrester flashover voltage E_f and if this is greater than E_f the computation is stopped signifying arrester operation at time τ_1. See Fig. (4.a).

iii At τ_1 two voltage generators are introduced as shown in Fig. (4.b) E_o represents the arc drop voltage and its Fourier transform is modified by the delay operator $\exp(-j\omega\tau_1)$. $e_1(t)$ derived from $v_1(t)$, $i_1(t)$ and the change of conditions, owing to arrester operation, from the region of very high resistance to the region of very low resistance is given by:

$$e_1(t) = v_1(t) - R_2 i_1(t)$$

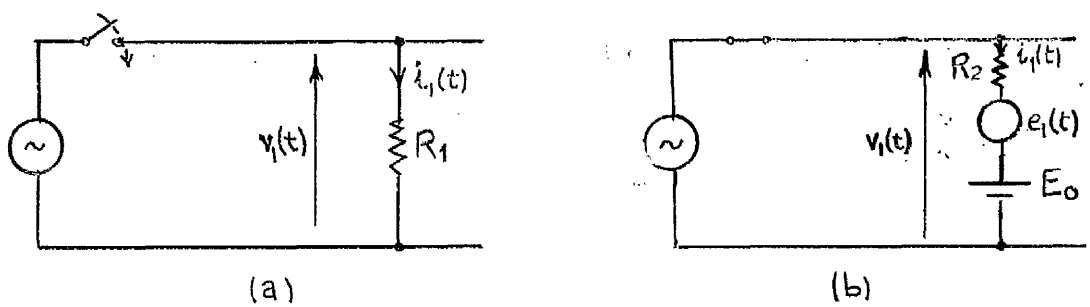

FIG. (4)

iv The system response is further determined for times greater than τ_1 and the arrester voltage $v_2(t)$ and current $i_2(t)$ obtained. From τ_1 onwards the arrester current is compared against I_{min}. When $i_2(t) < I_{min}$ the arrester extinguishes at τ_2 and operation is transferred again to the region of R_1. In this case a voltage generator $e_2(t)$ must be included in series with R_1 in order to take care of conditions between the limits $0 \leq t \leq \tau_2$. Over this interval $e_2(t)$ is given by the expression

$$e_2(t) = v_1(t) - R_1 i_1(t) \quad [0 < t < \tau_1]$$

$$e_2(t) = v_2(t) - R_1 i_2(t) \quad [\tau_1 < t < \tau_2]$$

In fact $e_2(t) = 0$, and therefore only the second component needs to be taken into account. Due consideration here must be given to the change of arrester current slope in order to prevent occurrence of false operating conditions.

v The procedure is repeated cyclically according to the state of the arrestor.

It is important to note that between τ_2 and the time of next flashover, τ_3, when $-(E_o/j\omega).\exp(-j\omega\tau_3)$ is introduced operation occurs for reverse arrester characteristics and hence the need for $-E_o$.

BIBLIOGRAPHY

1. CORY, B. J. 'Long Distance Transmission of Electrical Energy', British Power Engineering, Vol. 4, December, 1961, p.45.

2. DILLARD, J. K. 'What's Ahead in Transmission Systems?', IEEE Internat. Convention Record (U.S.A.), Vol. 12, Pt. 3, 1964, P.113.

3. ADAMSON, C., HINGORANI, N. G. 'High Voltage Direct Current Power Transmission', (Book) GARRAWAY Ltd., London.

4. CORY, B. J., editor. 'High Voltage Direct Current Converters and Systems', MacDONALD, London.

5. BARNES, H.C., PRICE, W. A. 'D.C. Has Drawbacks for U.S. Power Systems', Electrical World, December 17, 1962, p. 47.

6. BAXHENOV, S. A. 'The 220 KV Cable Line of Kashira - Moscow D.C. Transmission System,' U.S.S.R. Direct Current Research. Reports of the Leningrad Current Research Institute.

7. BENNETT, N. B. ROSE, C. L. 'Considerations Leading to the Selection of High Voltage Direct-Current Lines for System Interties', IEE High Voltage D.C. Power Conference, Sept. 1966.

8. HUBERT, F. J. GENT, M. R. 'Half-Wavelength Power Transmission Lines', IEEE Trans. PAS-84, No. 10, 1965, p. 965.

9. DuBOIS, E. W., et al. "Extra-Long-Distance Transmission', TRANS. AIEE, PAS, 1962, p. 1108.

10. WAGNER, W., "Technical and Economic Aspects of the transmission of Electrical Energy Over Long Distances," JIEE, 95, 1948, p.340.

11. CLARKE, Edith, CRARY, S.B. "Stability Limitations of Long-Distance A-C Power Transmission Systems," Trans. AIEE, 1941, Vol. 60, p.1051.

12. SCHURIG, O. R. 'A Miniature A-C Transmission System for the Practical Solution of Network and Transmission Problems,' Trans. AIEE, Vol. 42, 1923, p.831

13. WAGNER, C.F., EVANS, R. D. "Symmetrical Components," Electric Journal, 1928, 25, pp. 151-157, 194-197, 307-311 and 359-362.

14. ADAMS, G. E. 'Wave Propagation Along Unbalanced High Voltage Transmission Lines', AIEE, Pt. III - PAS, 1959, p. 639.

15. PERZ, M. C. 'Natural Modes of Power-Line Carrier on Horizontal 3-phase Lines,' Trans. IEEE, PAS, 1964, p. 679.

16. HEDMAN, D. E. 'Propagation on Overhead Transmission Lines, Pt. I - Theory of Modal Analysis', Trans. IEEE, PAS, 1965, p. 200.

17. BOWMAN, W. I. McNAMEE, J. M. 'Development of Equivalent Pi and T Matrix Circuits for Long Untransposed Transmission Lines,' IEEE Trans., PAS, 1964, p. 625.

18. WEDEPOHL, L. M. "Application of Matrix Methods to the Solution of Travelling-Wave Phenomena in Polyphase Systems," Proc. IEE, Vol. 110, No. 12, 1963, p. 2200.

19. MULLINEUX, N., DAY, Sylvia, J. and REED, J. R. "Developments in Obtaining Transient Response Using Fourier Transforms: Gibbs Phenomena and Fourier Integrals," I.J.E.E.E., Vol. 3, No. 4, 1965, p. 501.

20. MULLINEUX, N, DAY, Sylvia, J. and REED, J. R. "Developments in Obtaining Transient Response Using Fourier Transforms: Use of the Modified Fourier Transform," I.J.E.E.E., Vol. 4, No. 1, 1966, p. 31.

21. MULLINEUX, N., et al. "Calculation of Switching, Phenomena in Power Systems," Proc. IEE, Vol. 114, No. 4, 1967, p. 478.

22. PIPES, L. A. "Matrix Methods for Engineering," Prentice-Hall, Inc.

23. WEDEPOHL, L. M. "Electrical Characteristics of Polyphase Transmission Systems With Special Reference to Boundary-Value Calculations at Power-Line Carrier Frequencies," Proc. IEE, Vol. 112, No. 11, 1965, P. 2103.

24. WEDEPOHL, L. M. SHORROCKS, W. B., GALLOWAY, R. H. "Calculation of Electrical Parameters for Short and Long Polyphase Transmission Lines," Proc. IEE, Vol. 111, No. 12, 1964.

25. BUTTERWORTH, S. "Electrical Characteristics of Overhead Lines," E.R.A. Report, 1954.

26. WEDEPOHL, L. M. WASLEY, R. G. "Wave Propagation in Polyphase Transmission Systems: Resonance Effects Due to Discretely Bonded Earth Wires," Proc. IEEE, Vol. 112, No. 11, p.1965.

27. WASLEY, R. G. "The Natural Mode Theory of High Frequency Tower Resonance Effects in Multiconductor Lines," M.Sc. Thesis, The Victoria University of Manchester, 1965.

28. STEVENSON, W. D., Jr. "Elements of Power System Analysis," McGraw-Hill Book Company, Inc., 1962.

29. WARRINGTON, A. R. Van C. "Protective Relays, their theory and Practice," Chapman and Hall, 1962.

30. ATABEKOV, G. I. "The Relay Protection of H.V. Networks," Pergamon Press.

31. NEHER, J. H. "A Comprehensive Method of Determining the Performance of Distance Relays," A.I.E.E. Trans., Vol. 56, 1937, p. 833.

32. GOLDSBOROUGH, S. L. "A Distance Relay with Adjustable Phase-Angle Discrimination," A.I.E.E., Vol. 63, 1944, p. 835.

33. HUTCHINSON, R. M. "The Mho Distance Relay", Trans. A.I.E.E., Vol. 65, 1946, p. 353.

34. WARRINGTON, A. R. Van C. "Application of the Ohm and Mho Principles to Protective Relays," Trans. A.I.E.E., 65, 1946, p. 378.

35. LEWIS, W. A. and TIPPET, L. S. "Fundamental Basis For Distance Relaying," Trans. A.I.E.E., 1931, 50, p. 420.

36. WRIGHT, A. "Limitations of Distance Type Protective Equipment When Applied to Extremely-High-Voltage Power Lines," Proc. I.E.E., 1961, 108C, p. 271.

37. DAVISON, E. B. and WRIGHT, A. "Some Factors Affecting the Accuracy of Distance-Type Protective Equipment Under Earth-Fault Conditions," Proc. I.E.E., Vol. 110, No. 9, 1963, p. 1678.

38. ADAMSON, C. and TÜRELI, A. "Errors of Sound-Phase Compensation and Residual Compensation Systems in Earth-Fault Distance Relaying", Proc. I.E.E., Vol. 112, No. 7, 1965, p. 1369.

39. PROTECTIVE RELAYS APPLICATION GUIDE, "Principles and Practice of Distance Relaying Applied to MV and HV Feeders," Chapter 8. The English Elect. Comp. Ltd., 1967.

40. CLARKE, Edith "Three-Phase Multiple-Conductor Circuits," Trans. A.I.E.E., Vol. 51, 1932, p. 809.

41. CRARY, S. B. "Long-Distance Power Transmission", A.I.E.E. Transactions, 1950, Vol. 69, II, p. 834.

42. ———— "The Swedish 380 KV System", Published by the Swedish State Power Board.

43. ———— "Long-Distance Electrical Transmission Between the V.I. Lenin Hydroelectric Station and Moscow," by NEKRASOV, A. M. and ROKOTYAN, S. S., Editors. Israel Program for Scientific Translations, 1965.

44. CHAMBERS, F. et al. "Tennese Valley Authorities 500 KV System - System Plans and Considerations," I.E.E.E. Power Apparatus and Syst., 1966, PAS-85, No. 1, p. 22.

45. JOHNSON, A. A. , BARKLE, J. E. and POVEJSIL, D. J. "Fundamental Effects of Series Capacitors in High-Voltage Transmission Lines," A.I.E.E. Trans. Vol. 70, 1951, p. 526.

46. STARR, E. C. and EVANS, R. D. "Series Capacitors For Transmission Circuits", A.I.E.E. Transactions, Vol. 61, 1942, p. 963.

47. HOARD, B. V. "Characteristics of 400-MILE, 230-KV Series Capacitors", A.I.E.E., Transactions, Vol. 65, 1946, p. 1102.

48. BREUER, G. D., RUSTEBAKKE, H. M., GIBLEY, R. A. and SIMMONS, H. O. Jr., "The Use of Series Capacitors to Obtain Maximum EHV Transmission Capability," I.E.E.E., Trans. Vol.83, 1964, p. 1090.

49. BERDY, J. "Protection of Circuits with Series Capacitors," I.E.E.E. Transactions, Pt. III, Vol. 81, 1963, p. 929.

50. JANCKE, G. JENKINS, R., NORDSTRÖM, B.and NORLIN, L. "The Choice of Shunt Reactors For the Swedish 400 KV System," CIGRE, 1962, No. 412.

51. CLARKE, Edith "Circuit Analysis of A.C. Power Systems, II", John Wiley & Sons, Inc.

52. LAWRENCE, R. F. and POVEJSIL, D. J. "Determination of Inductive and Capacitive Unbalance for Untransposed Transmission Lines", Trans. A.I.E.E., Vol. 71, Pt. III, 1952, p. 547.

53. CLAIR, H. P. ST. "Practical Concepts in Capability and Performance of Transmission Lines," Trans. A.I.E.E., Pt. III, 1953, p. 1152.

54. WAGNER, C. F. and EVANS, R. D. "Symmetrical Components", Electrical Journal, 1928, 25 pp. 151-157, 194-197, 307-311 and 359-362.

55. SCHROEDER, T. W. "The Cause and Control of Some Types of Switching Surges", Trans. A.I.E.E., 66, p. 696, 1943.

56. PETERSON, H. A. and CONORDIA, C. "Analysers ... For Use in Engineering and Scientific Problems," Gen. Elect. Review, 48, p. 29, 1945.

57. EVANS, R. D., MONTEITH, A. C. "System Recovery Voltage Determination by Analytical and A.C. Calculating Board Methods," A.I.E.E., Trans. 56, 1937, p. 695.

58. URAM, R. and FEERO, W. E. "Mathematical Analysis and Solution of Transmission Line Transients, Pt. 2. Applications, I.E.E.E., Trans. PAS, 83, 1964. p. 1123.

59. GALIYANO, M. C. et al. "Field Tests of Lightning Arrester Voltage and Current Caused by Switching a 220KV Line," A.I.E.E. PAS, 80, Pt. III, 1961, p. 128.

60. McELROY, A. J. et al. "Field Measurements of Switching Surges on Unterminated 345-KV Transmission Lines," I.E.E.E. Trans., Power Apparatus and Syst. 82, 1963, p. 465.

61. BURGER, U. ELMIGER, E., GLAVITSCH, H. "Transient Phenomena Measured and Computed for the Swiss, 420 KV System Tavanasa - Sils - Breite," CIGRE, Vol. III, 1966 , No. 409.

62. McELROY, A. J., SMITH, H. M. 'Propagation of Switching-Surge-Wave-Fronts on EHV Transmission Lines,' A.I.E.E., PAS, 81, Pt. III, 1962, p. 983.

63. BEWLEY, L. V. "Travelling Waves on Transmission Systems", Dover Publication.

64. BARTHOLD, L. O and CARTER, G. K. 'Digital Travelling-Wave Solutions", A.I.E.E., Trans. PAS, 80, Pt. III, 1961, p. 812.

65. McELROY, A. J., PORTER, R. M. "Digital Computer Calculations of Transients in Electric Networks," I.E.E.E. Trans., PAS, 82, 1963, p. 88.

66. BICKFORD, J. P.,DOEPEL, P. S. "Calculation of Switching Transients With Particular Reference to Line Energisation," Proc. I.E.E. Vol. 114, No. 4, 1967, p. 465.

67. PIPES, L. A. "Matrix Methods for Engineering," Prentice-Hall, Inc. 1963.

68. URAM, R., MILLER, R. W. "Mathematical Analysis and Solution of Transmission-Line Transients, Pt. I - Theory," I.E.E.E. Transactions, PAS, 83, 1964, p. 1116.

69. LANCZOS, C. "Applied Analysis", Pitman.

70. WEDEPOHL, L. M. "Discussion on Calculation of Switching Phenomena in Power Systems and Calculation of Switching Transients With Particular Reference to Line Energisation," Proc. I.E.E., Vol. 11e, No. 10, 1967, p. 1457.

71. SOLODOVNIKOV, V. V., TOPCHEEV, Yu. I. and KRUTIKOVA, G. V., "Procedure for Obtaining Transient Response From Frequency Response," Infosearch.

72. WEDEPOHL, L. M. "Discussion on Induced Voltages in the Sheaths of Crossbonded A.C. Cables," Proc. I.E.E., Vol. 113, No. 12, 1966, p. 1990.

73. PETERSON, H. A., "Transients in Power Systems," Dover Publications.

74. AMERASINGHE, S. N. "Transient Analysis of Multiconductor Transmission Lines With Special Reference to The Short Line Fault Problem," M.Sc. Thesis. University of Manchester, 1965.

75. BICKFORD, J. P. - Private Communcation.

76. BARTHOLD, L. O., JOHNSON, I. B., SCHULTZ, A. J. "Switching Surges and Arrester Performance on High-Voltage Stations," A.I.E.E., Trans. Pt. III, Vol. 75. 1956, p. 481.

ACKNOWLEDGEMENTS

The author wishes to express his gratitude to Professor C. Adamson, M.Sc. (Eng.), D.Sc., C.Eng., FIEE., for his support and for the provision of research facilities in the Power Systems Centre, Department of Electrical and Electronics Engineering in the Faculty of Technology.

The author is extremely indebted to his supervisor Professor L. M. Wedepohl, B.Sc. (Eng.), Ph.D., C.Eng., M.I.E.E., without whose stimulating ideas, active interest and very generous help and encouragement at all times this work would not have been realized.

The author would like to express sincere thanks to Mr. A. E. Efthymiadis, B.Sc., M.Sc.Tech., for his kind help and advice and to his colleagues Mr. R. G. Wasley and Mr. D. J. Wilcox with whom he had very useful discussions.

The author wishes to thank Dr. J. P. Bickford of A.E.I., for providing the lattice diagram solution given in the section on comparative study of sequential transients calculations. He would also like to thank the University of Manchester Computing Service for running his computer programs.

Finally the author is grateful to the University of Khartoum - Sudan, for the award of a Scholarship enabling him to carry out this research work.